Physics Lib.

ITHACA MEETING—JUNE 18-21, 1930

VOLUME 35 SECOND SERIES NUMBER 10

MAY 28 1930

THE PHYSICAL REVIEW

A JOURNAL OF EXPERIMENTAL AND THEORETICAL PHYSICS

CONDUCTED BY

THE AMERICAN PHYSICAL SOCIETY

BOARD OF EDITORS

Managing Editor JOHN T. TATE, University of Minnesota

I. S. BOWEN, R. S. MULLIKEN, H. D. SMYTH, E. U. CONDON, C. J. DAVISSON, F. K. RICHTMYER, K. F. HERZFELD, A. W. HULL, F. W. LOOMIS

MAY 15, 1930

Space-Distribution of X-Ray Photoelectrons Ejected from the *K* and *L* Atomic Energy-Levels — CARL D. ANDERSON 1139

Hyperfine Structure in Neutral Manganese. Mn I — H. E. WHITE AND R. RITSCHL 1146

Mean Lives of Lines of Mercury Triple: $2^3P_{012}-2^3S_1$ — ROBERT H. RANDALL 1161

Hydrogen Atom in the Stark Effect — FRANCIS G. SLACK 1170

A Possible Origin of the Band at 2540 in the Spectrum of Mercury Vapor — R. ROLLEFSON 1177

Ionization of Hydrogen by Single Electron Impact — WALKER BLEAKNEY 1180

Electron Energy Losses in Mercury Vapor — CASTLE W. FOARD 1187

Motion of Slow Positive Ions in Gases — JAMES S. THOMPSON 1196

Absorption Coefficient for Slow Electrons in Gases — C. E. NORMAND 1217

On the Concentration of Metastable Mercury Atoms — E. GAVIOLA 1226

Most Probable 1930 Values of the Electron and Related Constants — ROBERT A. MILLIKAN 1231

Uniform Positive Column of an Electric Discharge in Mercury Vapor — THOMAS J. KILLIAN 1238

Absorption of Resonance Radiation in Mercury Vapor — ANCIL R. THOMAS 1253

Dispersion Formula and Raman Effect for the Symmetrical Top — MORRIS MUSKAT 1262

Location of the Electromotive Force in the Photovoltaic Cell — W. NORWOOD LOWRY 1270

Viscosity of Compressed Gases — JAMES H. BOYD, JR. 1284

Letters to the Editor — 1298

Book Reviews — 1301

PUBLISHED BY THE AMERICAN PHYSICAL SOCIETY

PUBLICATION OFFICES: 450-454 AHNAIP STREET, MENASHA, WIS.

EDITORIAL OFFICES: MINNEAPOLIS, MINN.

THE AMERICAN PHYSICAL SOCIETY

OFFICERS OF THE SOCIETY

President:	HENRY G. GALE	University of Chicago, Chicago, Ill.
Vice-President:	W. F. G. SWANN	Bartol Research Foundation, Philadelphia, Pa.
Secretary:	W. L. SEVERINGHAUS	Columbia University, New York City
Treasurer:	G. B. PEGRAM	Columbia University, New York City
Editor:	JOHN T. TATE	University of Minnesota, Minneapolis, Minn.
Local Secretary for the Pacific Coast:	L. B. LOEB	University of California, Berkeley, Calif.

THE PHYSICAL REVIEW

Published by the American Physical Society at 450 Ahnaip St., Menasha, Wis. Executive office: University of Minnesota, Minneapolis, Minn. Two volumes annually, twelve issues per volume.

First series. From July 1, 1893, to January 1, 1913, the REVIEW was conducted by Edward L. Nichols, Ernest Merritt and Frederick Bedell, with the financial support of Cornell University. The first four volumes were issued annually; subsequent volumes, semi-annually; thirty-five volumes in all.

Second series. On January 1, 1913, the REVIEW was transferred to the American Physical Society as announced on the first page of the new series which was then begun. Since then it has been conducted by a Board of Editors elected by the Society. Semi-annual volumes begin in January and July. Since July 1, 1929, the REVIEW has been issued twice a month.

Contributors are referred to page 2 of the advertisements for further information.

Annual Subscription, throughout the Postal Union, $10.00 in advance.

Single copies of current volume, $.60.

General index, 1893-1920, $4.00, in advance.

Back Volumes, $6.00 per volume; Back Numbers, $1.00 per copy for issues prior to July 1, 1929 (Vols. 1-33), $.60 per copy for issues subsequent thereto. Postage is free if remittance accompanies order; otherwise postage is extra. No bound volumes can be supplied. The REVIEW offers to purchase a limited number of First Series, Vol. 1, No. 1 (at $2.00 each); Second Series, Vol. 7, No. 1, January 1916; Vol. 7, No. 2, February 1916; Vol. 7, No. 4, April 1916; and Vol. 7, No. 5, May 1916 (at $2.00 each).

Advertisements. Rates will be supplied by the Editor on request. Copy for each number must be received at Minneapolis two weeks prior to the dates of issue; old copy is used until new copy is received. Send electrotypes direct to the printers, George Banta Publishing Co., Menasha, Wis.

Discount of ten percent is allowed subscription agencies and members of the American Physical Society.

Changes of address and Complaints of failure to receive the REVIEW, in the case of members of the Physical Society, should be addressed to the Treasurer; in the case of other subscribers to 450 Ahnaip St., Menasha, Wis.; or to the Editor. New copies can be sent free in response to complaint of non-delivery only if notice of non-delivery is received within three months of date of issue.

Editorial Correspondence should be addressed to the PHYSICAL REVIEW, University of Minnesota, Minneapolis, Minn.

Entered at the postoffice at Menasha, Wis., as second class matter.
Acceptance for mailing at special rate of postage provided for in section 1103, Act of October 3, 1917, authorized September 6, 1926.

Second Series *May 15, 1930* *Vol. 35, No. 10*

THE

PHYSICAL REVIEW

SPACE-DISTRIBUTION OF X-RAY PHOTOELECTRONS EJECTED FROM THE *K* AND *L* ATOMIC ENERGY-LEVELS

By Carl D. Anderson

California Institute of Technology, Pasadena, California

(Received April 2, 1930)

Abstract

A C.T.R. Wilson expansion-chamber was used to study the space-distribution of photoelectrons ejected from a gas by monochromatic x-rays. In agreement with Auger, and Watson and Van den Akker a more isotropic space-distribution was found for electrons ejected from the *L* energy-levels than for those ejected from the *K* energy-level. The distribution of the electrons from the *L* energy-levels became less isotropic with an increase in frequency of the incident radiation. For a given radiation, the average forward momentum of the electrons from the *K* energy-level was found to decrease with an increase in the binding energy of the parent atom. Within experimental error, however, for electrons from the *K* energy level, even for different binding energies, the average forward momentum remained the same for a given velocity of ejection of the electron. The average forward momentum of electrons from the *L* energy-level was greater than that for electrons from the *K* energy-level for a given velocity of ejection. The space-distribution of electrons from the *K* energy-level was in fair accord with the recent results of quantum mechanics.

THE longitudinal space-distribution of photoelectrons ejected from a gas by x-rays has been extensively studied by means of the C. T. R. Wilson expansion-chamber by several investigators.[1,2] The general shape of the distribution curve for electrons ejected from the *K* energy-level and the dependence on the frequency of the incident radiation has been determined, and are in approximate agreement with the recent quantum mechanical expressions.[3,4,5,6] Results so far published for the space-distribution of electrons ejected from the *L* energy-levels are rather meager. Auger[7] and Watson and Van den Akker[8] have shown, however, that a more isotropic

[1] E. J. Williams, J. M. Nuttal and H. S. Barlow, Proc. Roy. Soc. **A121,** 611 (1928).
[2] M. P. Auger, C.R. **187,** 1141 (1928).
[3] A. Sommerfeld, Atombau und Spektrallinien, Wellenmechanischer Erganzungsband.
[4] G. Wentzel. (Communicated in Lecture Series of Norman Bridge Laboratory.)
[5] A. Carrelli, Zeits. f. Physik **56,** 694 (1929).
[6] S. E. Szczeniowski, Phys. Rev. **35,** 374 (1930).
[7] M. P. Auger, C.R. **188,** 447 (1929).
[8] E. C. Watson and J. A. Van den Akker, Proc. Roy. Soc. **A126,** 138 (1929).

space-distribution exists in this case. In the present work, the distribution of electrons ejected from the L energy-levels is found to become less isotropic as the frequency of the incident radiation is increased.

The C. T. R. Wilson expansion-chamber employed in this investigation was essentially that described by Simon and Loughridge.[9,10] Only minor refinements were effected to insure greater accuracy in the data obtained.

Simple filtering of the general radiation obtained from an x-ray tube was found to produce radiation not sufficiently monochromatic so other means of monochromatizing the x-rays were employed. Monochromatism

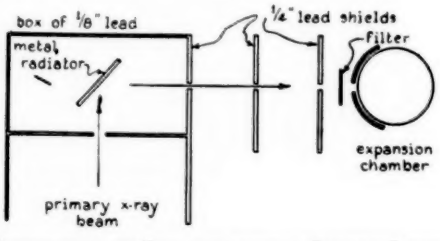

Fig. 1. Fluorescence radiator as source of monochromatic x-rays.

was insured, in one instance, by the selection of the $K\alpha$ line of molybdenum by means of a calcite crystal spectrometer. For the other frequencies, the secondary fluorescence radiation from a metal plate, irradiated by primary x-rays from a tungsten-target Coolidge type tube, was collimated to a narrow beam and passed into the expansion chamber (Fig. 1). A. H. Compton[11] has shown the fluorescence radiation obtained in this manner to be very homogeneous, having 99 percent of its energy in the characteristic K line-radiation of the metal radiator.

The wave-lengths of the x-rays used in this investigation are given in Table I together with the metal radiator employed in three cases.

TABLE I.

Source	Monochromatizer	λ
M_o target tube	Calcite spectrometer	0.71 A
W " "	Silver radiator	0.56 A
W " "	Palladium radiator	0.59 A
W " "	Tin radiator	0.49 A

The relatively faint $K\beta$ lines of palladium were filtered out by means of a ruthenium filter. The presence of the $K\beta$ lines in the other cases was not objectionable.

The longitudinal space-distribution curves, representing the density of emission per unit angle of the photoelectrons as a function of the angle between the direction of ejection and the forward direction of the x-ray beam, were plotted in a number of cases to show the effect of the energy level from

[9] A. W. Simon and D. H. Loughridge, Jour. Opt. Soc. **13,** 679 (1926).
[10] D. H. Loughridge, Phys. Rev. **30,** 488 (1927).
[11] A. H. Compton, Proc. Nat. Acad. **14,** 549 (1928).

which the electron is taken, and also the effect of a change in the frequency of the incident radiation.

In Figs. 2 and 3 are plotted the results obtained respectively from measurements on 272 tracks in air produced by radiation of 0.71A and on 200 tracks in air produced by radiation of 0.56A. Each small circle represents the number of electrons ejected in a 15° interval the point being plotted at an angle corresponding to the center of the interval. Points are plotted every 5° and therefore represent overlapping intervals.

In order to study the distribution where the binding energy was of appreciable magnitude, C_2H_5Br was introduced into the expansion-chamber in an atmosphere of hydrogen. The photoelectrons were produced by radiation of 0.59A, most of them being ejected from the K shell of the bromine

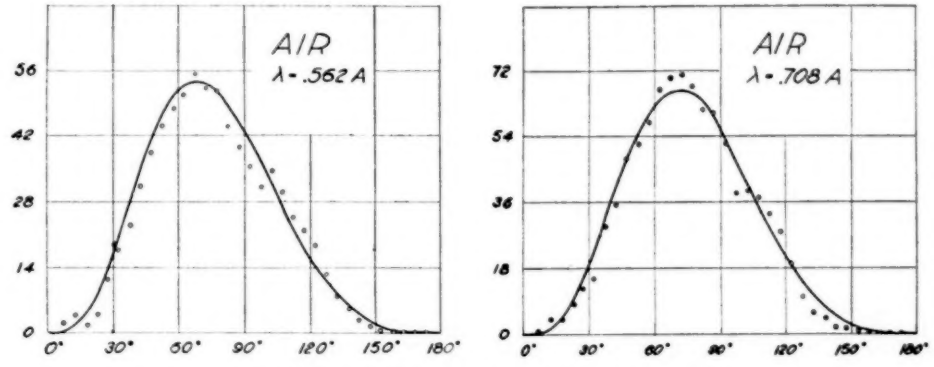

Figs. 2 and 3. Space distribution of photoelectrons ejected from air.

atom. About 64 percent of the energy of the incident radiation was required to remove the electron from the atom, the remaining 36 percent appearing as kinetic energy. The secondary and tertiary photoelectrons could easily be distinguished from one another due to the difference in path length.* Photoelectrons ejected from levels other than the K level of bromine or from light atoms could be distinguished by their long path length and hence omitted in the measurements. Thus, only the photoelectrons having their origin in the K shell of bromine were included. Fig. 4 represents the distribution curve plotted as before for 233 tracks of electrons ejected from the K level of bromine by radiation of 0.59A.[12]

For the study of the distribution of electrons ejected from the L energy levels, CH_3I was introduced into the chamber in an atmosphere of hydrogen and photoelectrons produced by radiation of 0.71A and 0.49A emission, being from the L levels of iodine. The results of measurements on 200 tracks formed by radiation of 0.71A are shown in Fig. 5. In agreement with the work of Auger the curve is broader than that found for the K electrons indicating a

* The ratio of the number of secondary to tertiary photoelectrons was found to be 2.5 in agreement with Auger [Ann. de Physique **6**, 229 (1926)] and Wentzel [Zeits. f. Physik **43**, 524 (1927)].

[12] C. D. Anderson, Phys. Rev. **34**, 547 (1929).

more isotropic distribution. The small circles as before represent the experimental points. Fig. 6 represents the distribution of 264 photoelectrons ejected from the L levels of iodine by radiation of 0.49A. The curve here is narrower

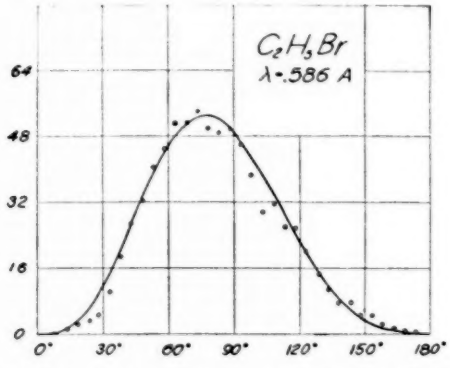

Fig. 4. Space distribution of photoelectrons ejected from K energy-level of bromine.

than in Fig. 5, indicating a decrease in the isotropy of the distribution with an increase in the frequency of the incident radiation. Watson and Van den Akker[8] have shown that photoelectrons ejected from the L_{II} and L_{III} energy levels have a space-distribution more isotropic than those from the K and L_I energy levels, and Robinson and Cassie[13] have found the relative number of

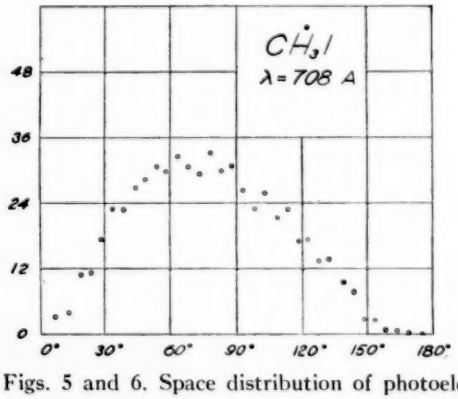

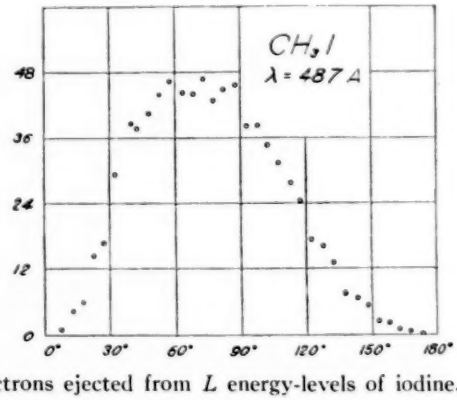

Figs. 5 and 6. Space distribution of photoelectrons ejected from L energy-levels of iodine.

L_I electrons ejected to increase with an increase in the frequency of the incident radiation. The narrower distribution curve of Fig. 6 may then be explained by the presence of a greater proportion of L_I electrons than is the case for the curve of Fig. 6.

A theoretical expression derived recently by Wentzel[14] on the basis of quantum mechanics,

$$P(\theta) \alpha \frac{\sin^3 \theta}{\left[1 - \frac{v}{c}\cos\theta + \frac{h\nu}{2mc^2}\right]^4} \tag{1}$$

[13] H. R. Robinson and A. M. Cassie, Proc. Roy. Soc. **A113,** 296 (1926–27).
[14] G. Wentzel, reference 4.

gives the probability of ejection per unit angle of a photoelectron from the K energy level as a function of the angle, θ, between the direction of ejection and the forward direction of the x-ray beam, where v represents the velocity of ejection, ν the frequency of the incident radiation, and h, m, and c are the customary physical constants.

The solid-line curves of Figs. 2, 3 and 4 represent $P(\theta)$ with the proper values of v and ν inserted, the curves being plotted on a scale to conform to the experimental points. No analogous theoretical expression has as yet been published for the probability of ejection of a photoelectron from the L levels.

The observed asymmetry of the distribution about a plane normal to the x-ray beam may be compared with the theory in several ways.[15] The value of cos θ averaged over all the photoelectron tracks, a quantity proportional to the average forward momentum of the photoelectrons may be computed as follows

$$\overline{\cos\theta} = \frac{\int_0^\pi P(\theta)\cos\theta d\theta}{\int_0^\pi P(\theta)d\theta} = \frac{4}{5}\frac{v}{c} + \cdots \qquad (2)$$

if only first order terms in v/c are retained. The observed and calculated values of the mean of cos θ are listed in Table II.

TABLE II.

Energy Level	Gas	λ	$\overline{\cos\theta}$ (obs.)	$\overline{\cos\theta}$ (calc.)
K	Air	0.71 A	0.182	0.210
K	Air	0.56 A	0.210	0.235
K	C_2H_5Br	0.59 A	0.133	0.138
L	CH_3I	0.71 A	0.230	
L	CH_3I	0.49 A	0.255	

The average forward momentum of the K electrons for a given radiation decreases with an increase of the binding energy of the parent atom. Within experimental error, however, K electrons of the same initial velocity have the same average forward momentum. It is to be noted, moreover, that in accord with the results of Auger and Watson and Van den Akker for a given velocity of ejection, the L electrons have an average forward momentum greater than that of the K electrons. The difference in behavior of the K and L electrons is more marked for the lower frequencies of incident radiation. The asymmetry to be expected on theoretical grounds for the L electrons has not as yet been brought to light.

The bi-partition angle, θ_b, the half-angle at the apex of a cone which divides the photoelectrons into two groups of equal numbers, is defined by Eq. (3). Calculation of cos θ_b shows it to be equal to v/c to a first approximation. The experimental and calculated values of cos θ_b are given in Table III.

[15] Williams, Nuttall and Barlow, reference 1.

$$\int_0^{\theta_b} P(\theta)d\theta = \int_{\theta_b}^{\pi} P(\theta)d\theta. \tag{3}$$

TABLE III.

Energy Level	Gas	λ	cos θ_b (obs.)	cos θ_b (calc.)
K	Air	0.71 A	0.242	0.262
K	Air	0.56 A	0.292	0.294
K	C_2H_5Br	0.59 A	0.191	0.173
L	CH_3I	0.71 A	0.174	
L	CH_3I	0.49 A	0.242	

For a given value of v/c the bi-partition angle for electrons ejected from the L energy-levels seems to occur nearer 90° than for those from the K energy-level, in agreement with the conclusions of Auger.[2,7]

The ratio, of the number of electrons ejected forward of the plane normal to the x-ray beam, to the number ejected backward, ρ, is given by Eq. (4):

$$\rho = \frac{\int_0^{\pi/2} P(\theta)d\theta}{\int_{\pi/2}^{\pi} P(\theta)d\theta} = \frac{2+3\frac{v}{c}}{2-3\frac{v}{c}} + \cdots. \tag{4}$$

The observed and calculated values of ρ are given in Table IV.

It is to be noted that no marked difference was found in the behavior of ρ for the K and L electrons.

TABLE IV.

Energy Level	Gas	λ	ρ (obs.)	ρ (calc.)
K	Air	0.71 A	2.17	2.30
K	Air	0.56 A	2.39	2.58
K	C_2H_5Br	0.59 A	1.74	1.70
L	CH_3I	0.71 A	2.00	
L	CH_3I	0.49 A	2.30	

In conclusion I wish to express my gratitude to Professor R. A. Millikan and Professor E. C. Watson for their interest in this work.

Note added in proof:

Since this article was written, G. Schur [Ann. d. Physik, **4**, 441, (1930)] has published a theoretical expression for the space-distribution of photo-electrons ejected from the L energy-levels of an atom. For the longitudinal space-distribution he finds,

$$P(\theta)\alpha \sin^3\theta + \frac{4v}{c}\sin^3\theta\cos\theta\left(1-\frac{I_L}{h\nu}\right) + \frac{I_L\sin\theta}{h\nu+3I_L}\left\{1+\frac{8I_L}{h\nu}\sin^2\theta + \frac{2v}{c}\cos\theta\left(1+2\sin^2\theta\left(1+\frac{11I_L}{h\nu}\right)\right)\right\} \tag{5}$$

where I_L represents the mean value of the binding energy of the $\angle$ energy-levels, and the other quantities remain as defined above.

Calculation of the average value of cos θ for L electrons, in the manner carried out above for K electrons, leads to the following results:

TABLE V.

Energy level	Gas	λ	$\overline{\cos\theta}$ (obs.)	$\overline{\cos\theta}$ (calc.)
L	CH_3I	0.71 A	.23	.17
L	CH_3I	0.49 A	.25	.22

The agreement here is not satisfactory, the observations seeming to indicate a greater average forward momentum of the photoelectrons than the theory.

Calculation of ρ, defined as above, leads to the following results:

TABLE VI.

Energy level	Gas	λ	ρ (obs.)	ρ (calc.)
L	CH_3I	0.71 A	2.0	1.9
L	CH_3I	0.49 A	2.3	2.4

With regard to ρ, experiment and theory are in fair accord.

A decrease in the isotropy of the space-distribution curve for L electrons, with an increase in the frequency of the incident radiation, as was found above, is also to be expected from the theory. The ratio of the number of L_{II} and L_{III} electrons to the L_I electrons is given by

$$\frac{L_{II} + L_{III}}{L_I} = \frac{I_L}{h\nu + 3I_L}\left(3 + 8\frac{I_L}{h\nu}\right) \tag{6}$$

which for this case, leads to:

TABLE VII.

Energy level	Gas	λ	Relative proportion of	
			L_I Electrons	L_{II} and L_{III} Electrons
L	CH_3I	0.71 A	67%	33%
L	CH_3I	0.49 A	72%	28%

For the harder radiation then, due to the greater proportion of L_I electrons ejected, a slightly less isotropic distribution is to be expected.

HYPERFINE STRUCTURE IN NEUTRAL MANGANESE, Mn I.

By H. E. White* and R. Ritschl
Physikalisch-Technische Reichsanstalt, Berlin

(Received March 5, 1930)

Abstract

Observations. The hyperfine structure patterns of some 30 or 40 lines in the spectrum of Mn I have been photographed by means of a prism spectrograph and silvered Fabry-Perot etalons. A tube, designed by Schüler, and operated at liquid air temperatures, has been used as a light source for most of the lines and a king vacuum furnace for the others. Patterns of from 2 to 6 components are found, some degrading in intensity and intervals toward low frequencies and others toward higher frequencies.

Interpretation. The strictly *LS* coupling in the well-known multiplet structure of Mn I, and *Ji* coupling in the hyperfine structure enable vector diagrams to be drawn for the space quantization of each valence electron with respect to the nucleus. Some of the hyperfine structure terms are computed directly from observed term differences while others are computed from the observed diagonal components. The normal state $^6S_{2\frac{1}{2}}(3d^54s^2)$ is found to be quite narrow, whereas the metastable $^6D(3d^54s)$ terms show the widest separations. While the hyperfine structure intervals for any given term are proportional to cos (Ji), the total separations are approximately determined by cos (Si), the l values of the electrons contributing but very little.

Theoretical computations. A study of the vector diagrams for the different multiplet terms shows quite definitely that while the hyperfine structure is determined primarily by the coupling between the 4*s* electron and the nucleus, the remaining valence electrons must also be taken into account. The hyperfine structure formula given by Goudsmit and Bacher for the interaction between an *s* electron spin and the nuclear spin is extended so as to include not only the spins of all of the valence electrons but their l values as well. From the derived general formula and the observed hyperfine structure term separations, coupling constants to be associated with each electron have been computed. While the energy of interaction between electron spin s and nuclear spin i is given by $ais\cos(is)$ the energy of interaction between electron l value and nuclear spin i is given by $ail\cos(il)$.

THE hyperfine structure in the spectral lines of neutral manganese was investigated in this laboratory by Janicki[1] some twenty years ago and later verified by Wali-Mohammed.[2] An analysis of the gross or multiplet structure of Mn I was first given by Catalan,[3] some of the terms being later assigned to definite electron configurations by Hund.[4] A more complete analysis of the gross structure has been given by Russell[5] and by McLennan,

* National Research Fellow.
[1] Janicki, Ann. d. Physik **29,** 833 (1909).
[2] Wali-Mohammed, Astrophys. J. **39,** 198 (1914).
[3] Catalan, Phil. Trans. Roy. Soc. London **223,** 127 (1923).
[4] Hund, Linienspektren, p. 161, 1927.
[5] Russell, Astrophys, J. **66,** 184 (1927).

McLay and Crawford.[6] Since the *hfs*[7] of many of the lines is observed to have the same general appearance as that found in a number of other elements (for example, praseodymium, lanthanum, iodine, and bromine) it was hoped that an analysis of the *hfs*, at the expense of the well-known *gs*, would not only verify the interpretation of *hfs* given previously by one of the authors,[8] but at the same time to lead to some conclusions concerning *hfs* in general.

Apparatus and Measurements

A Zeiss three-prism constant deviation spectrograph, with a large glass optical system specially constructed for fine-structure work, was used in conjunction with quartz Fabry-Perot etalons for photographing the *hfs*. In order to eliminate self-reversal of resonance lines and at the same time to

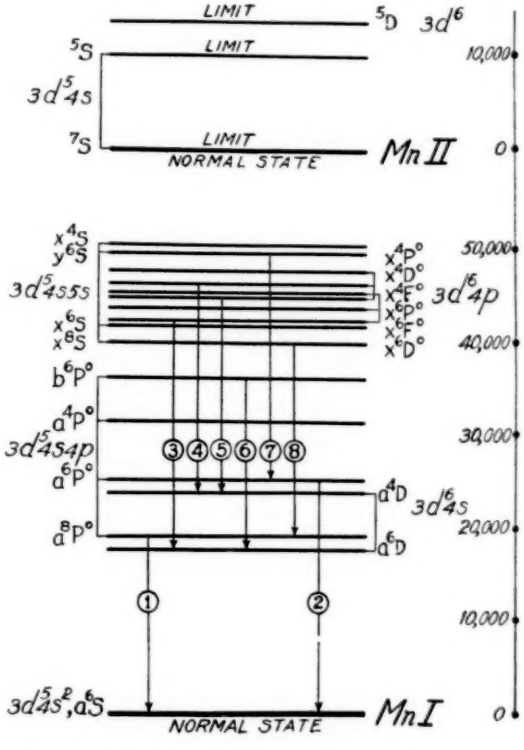

Fig. 1. Term scheme of neutral manganese, Mn I.

produce very sharp lines, a metal discharge tube, operated at liquid air temperatures, has been used. Prior to publication, the design and operation of this tube was very kindly submitted to the authors by Dr. Schüler.[9] The manganese lines were excited in a discharge of argon by placing small pieces

[6] McLennan, McLay and Crawford, Trans. Roy. Soc. Canada **20,** 15 (1926).

[7] The words hyperfine structure and gross structure will be abbreviated by *hfs* and *gs* respectively.

[8] White, Phys. Rev. **34,** 1404 (1929); Proc. Nat. Acad. Sci. **16,** 68 (1930).

[9] Schüler, Zeits. f. Physik **59,** 149 (1930).

TABLE I. *Measured hfs-components in Mn I.*

Mult. No.	Design.	λ ν	$\Delta\lambda_1$ $\Delta\nu_1$	$\Delta\lambda_2$ $\Delta\nu_2$	$\Delta\lambda_3$ $\Delta\nu_3$	$\Delta\lambda_4$ $\Delta\nu_4$	$\Delta\lambda_5$ $\Delta\nu_5$	Total $\Delta\lambda$ Total $\Delta\nu$
	$^6S_{2\frac{1}{2}}-{}^8P_{3\frac{1}{2}}{}^0$	5394.677 18531.65	+.0325 −.1116	+.0285 −.0979	+.0230 −.0790	+.0200 −.0687	+.0111 −.0381	+.1151 −.3953
1	$^6S_{2\frac{1}{2}}-{}^8P_{2\frac{1}{2}}{}^0$	5432.555 18402.45	+.0306 −.1036	+.0247 −.0836	+.0198 −.0671	+.0133 −.0450		+.0884 −.2993
	$^6S_{2\frac{1}{2}}-{}^6P_{3\frac{1}{2}}{}^0$	4030.760 24802.23	+.0155 −.0930	+.0133 −.0798	+.0104 −.0624	+.0079 −.0474	+.0052 −.0312	+.0523 −.3138
2	$^6S_{2\frac{1}{2}}-{}^6P_{2\frac{1}{2}}{}^0$	4033.074 24788.01	+.0142 −.0873	+.0127 −.0781	+.0090 −.0553	+.0060 −.0369		+.0419 −.2576
	$^6S_{2\frac{1}{2}}-{}^6P_{1\frac{1}{2}}{}^0$	4034.489 24779.31	+.0145 −.0891	+.0117 −.0719	+.0077 −.0473			+.0339 −.2083
	$^6D_{4\frac{1}{2}}-{}^6D_{3\frac{1}{2}}{}^0$	4018.108 24880.32	−.0192 +.1188	−.0155 +.0959	−.0129 +.0799	−.0100 +.0619		−.0651 +.4029
	$^6D_{3\frac{1}{2}}-{}^6D_{2\frac{1}{2}}{}^0$	4035.730 24771.69	−.0159 +.0976	−.0135 +.0829	−.0107 +.0657			−.0507 +.3113
	$^6D_{4\frac{1}{2}}-{}^6D_{4\frac{1}{2}}{}^0$	4041.366 24737.15	−.0165 +.1010	−.0140 +.0857	−.0116 +.0710	−.0093 +.0569	−.0060 +.0367	−.0574 +.3513
	$^6D_{2\frac{1}{2}}-{}^6D_{1\frac{1}{2}}{}^0$	4048.760 24691.97	−.0146 +.0890	−.0125 +.0763	−.0098 +.0598			−.0369 +.2251
	$^6D_{3\frac{1}{2}}-{}^6D_{3\frac{1}{2}}{}^0$	4055.553 24650.62	−.0142 +.0863	−.0122 +.0742	−.0099 +.0602	−.0070 +.0426		−.0481 +.2925
3	$^6D_{2\frac{1}{2}}-{}^6D_{2\frac{1}{2}}{}^0$	4063.533 24602.18	−.0133 +.0807	−.0102 +.0619				−.0364 +.2209
	$^6D_{3\frac{1}{2}}-{}^6D_{4\frac{1}{2}}{}^0$	4079.245 24507.44	−.0139 +.0834	−.0110 +.0660	−.0082 +.0492			−.0436 +.2616
	$^6D_{\frac{1}{2}}-{}^6D_{1\frac{1}{2}}{}^0$	4079.428 24506.34	−.0197 +.1182					−.0197 +.1182
	$^6D_{1\frac{1}{2}}-{}^6D_{2\frac{1}{2}}{}^0$	4082.947 24485.22	−.0112 +.0672	−.0091 +.0546	−.0070 +.0420			−.0273 +.1638
	$^6D_{2\frac{1}{2}}-{}^6D_{3\frac{1}{2}}{}^0$	4083.639 24481.07	−.0109 +.0654					−.0326 +.1956

TABLE I (*continued*).

4	$^4D_{1\frac{1}{2}}-{}^4D_{\frac{1}{2}}^0$	4453.013 22450.42	+.0172 −.0867				+.0172 −.0867
	$^4D_{\frac{1}{2}}-{}^4D_{\frac{1}{2}}^0$	4472.793 22351.14	−.0229 +.1145	−.0162 +.0810			−.0391 +.1955
	$^4D_{\frac{1}{2}}-{}^4D_{1\frac{1}{2}}^0$	4490.078 22265.10	−.0235 +.1165				−.0235 +.1165
5	$^4D_{3\frac{1}{2}}-{}^4F_{3\frac{1}{2}}^0$	4709.704 21226.83	+.0133 −.0599				+.0420 −.1893
	$^4D_{2\frac{1}{2}}-{}^4F_{2\frac{1}{2}}^0$	4727.462 21147.10	+.0152 −.0697				+.0421 −.1883
6	$^6D_{4\frac{1}{2}}-{}^6P_{3\frac{1}{2}}^0$	5341.070 18717.64	−.0628 +.2201	−.0530 +.1857	−.0438 +.1535	−.0342 +.1199	−.0232 +.0813	−.2170 +.7605
	$^6D_{3\frac{1}{2}}-{}^6P_{3\frac{1}{2}}^0$	5407.432 18487.97	−.0552 +.1888	−.0445 +.1522				−.1627 +.5564
	$^6D_{3\frac{1}{2}}-{}^6P_{2\frac{1}{2}}^0$	5420.368 18443.82	−.0581 +.1976	−.0467 +.1589	−.0348 +.1184			−.1846 +.6279
	$^6D_{2\frac{1}{2}}-{}^6P_{3\frac{1}{2}}^0$	5457.468 18318.44	−.0508 +.1705	−.0408 +.1369				−.1423 +.4777
	$^6D_{2\frac{1}{2}}-{}^6P_{2\frac{1}{2}}^0$	5470.640 18274.33	−.0545 +.1821	−.0435 +.1453				−.1484 +.4958
	$^6D_{2\frac{1}{2}}-{}^6P_{1\frac{1}{2}}^0$	5481.395 18238.48	−.0662 +.2203	−.0512 +.1704	−.0365 +.1215			−.1539 +.5122
	$^6D_{1\frac{1}{2}}-{}^6P_{2\frac{1}{2}}^0$	5505.877 18157.38	−.0484 +.1597	−.0413 +.1362				−.1189 +.3922
	$^6D_{1\frac{1}{2}}-{}^6P_{1\frac{1}{2}}^0$	5516.773 18121.52	−.0748 +.2458	−.0498 +.1636				−.1246 +.4094
	$^6D_{\frac{1}{2}}-{}^6P_{1\frac{1}{2}}^0$	5537.749 18052.88	−.1116 +.3640					−.1116 +.3640
7	$^6P_{3\frac{1}{2}}^0-{}^6S_{2\frac{1}{2}}^0$	4061.744 24613.03	−.0326 +.1975	*−.0290* *+.1757*	*−.0210?* *+.1272?*			−.1066? +.6458?

of manganese metal in the tube, the discharge itself taking place in a small cylinder, 2 cm long and 1 cm in diameter, working as a Paschen hollow cathode, in the bottom of the tube. The light from the discharge was reflected into a horizontal position by a plane mirror and then brought to focus on the slit of the spectrograph. With a current of 100 to 200 m.a. at about 2500 volts d.c., exposure times at 4000A ranged from 1 to 5 minutes. In the absence of hydrogen, and at the right pressure, the manganese lines were stronger than those of argon. With silvered quartz mirrors, separated by invar rings 5, 7.5, 10, 12, and 15 mm in thickness, placed between the colimmating lens and the prisms, a resolving power of nearly one million at 4000A has been obtained. The mirrors were silvered in vacuum by evaporation from electrically heated silver filaments, a method developed previously by one of the authors.[10] While the lines photographed have the same appearance as those found in praseodymium,[11] they are in general about one-fifth to one tenth as wide and vary in number from one to six components.

An energy level diagram of Mn I is given in Fig. 1. Each *gs*-multiplet, for which the *hfs* has been studied, is shown by a transition arrow and assigned a number for reference in Tables I and II. All of the lines except those in multiplets numbered six and seven, have been photographed with the light source at liquid air temperatures, thus enabling the *hfs* $\Delta\lambda$'s in Tables I and II to be given to four decimal places. The last two multiplets, numbers six and

TABLE II. *Measured hfs-components in Mn I.*

Mult. No.	Design	λ / ν	Total $\Delta\lambda$ / Total $\Delta\nu$	Mult. No.	Design	λ / ν	Total $\Delta\lambda$ / Total $\Delta\nu$
	$^4D_{3\frac{1}{2}}-{}^4D_{2\frac{1}{2}}{}^0$	4414.887 22644.29	+.0264? −.1352?		$^4D_{1\frac{1}{2}}-{}^4D_{2\frac{1}{2}}{}^0$	4498.897 22221.45	sharp
	$^4D_{2\frac{1}{2}}-{}^4D_{1\frac{1}{2}}{}^0$	4436.358 22534.70	+.0226 −.1148	4	$^4D_{2\frac{1}{2}}-{}^4D_{3\frac{1}{2}}{}^0$	4502.223 22205.01	+.0244 −.1204
4	$^4D_{3\frac{1}{2}}-{}^4D_{3\frac{1}{2}}{}^0$	4451.578 22457.66	+.0274 −.1383	7	$^6P_{1\frac{1}{2}}{}^0-{}^6S_{2\frac{1}{2}}$	4057.959 24635.99	−.0792 +.4810
	$^4D_{2\frac{1}{2}}-{}^4D_{2\frac{1}{2}}{}^0$	4464.679 22391.76	+.0236 −.1184		$^6P_{2\frac{1}{2}}{}^0-{}^6S_{2\frac{1}{2}}$	4059.399 24627.26	−.0850 +.5160
	$^4D_{1\frac{1}{2}}-{}^4D_{1\frac{1}{2}}{}^0$	4470.142 22364.40	sharp				

seven, were photographed using as a light source a King vacuum furnace operated at about 2000°C. Fortunately these two multiplets show the widest *hfs* in Mn I, thus making it possible to resolve some of the patterns at this temperature. The manganese lines were brought out much stronger than is usually obtained from such a furnace by applying a potential of 120 volts d.c. between a small anode and the heating element of the furnace.[12] The anode is

[10] Ritschl, Verhand. d. Deutsch. Phys. Ges. (3), **10**, 33 (1929).
[11] White, Phys. Rev. **34**, 1397 (1929).
[12] Schüler, Zeits. f. Physik **37**, 728 (1926).

here placed coaxial with and extends half way through the heated graphite tube of the furnace.[10] Since the relative intensities of the components in each pattern are always found to decrease regularly toward longer or shorter wave-lengths, the wave-length and frequency number of only the strongest component in each pattern is given in column three. The wave-lengths and frequency numbers of the other components may be obtained by adding or subtracting, as the case may be, the $\Delta\lambda$'s and $\Delta\nu$'s given in columns four, five, six, seven and eight. Where only the first two, three, or four components of a group are resolved, the end of the group has been measured. The total

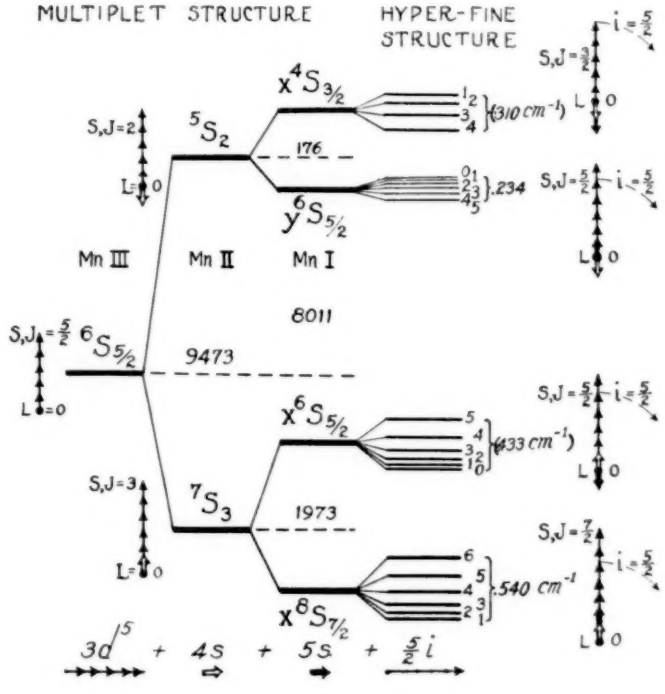

Fig. 2. Hyperfine structure terms and space quantization vectors for the electron configuration $3d^5 4s5s$.

width of each pattern is given in the last column. In general the measurements given by Janicki[1] are in good agreement with those in Tables I and II. The additional component which Janicki found on the short wave-length side of λλ4030, 4033 and 4034 is very probably a self-reversal effect of each *hfs*-component, and, is not found on any of our plates. At liquid air temperatures very sharp and well-resolved patterns of these three lines have been photographed. As reported by Janicki, λλ6021, 6016, and 6013 appear sharp. Although these lines are quite strongly excited at liquid air temperatures and are visually seen to be quite narrow, they have not been photographed due to the extremely long exposures necessary at this wave-length.

Owing to an early mistake in the width of an etalon ring, the computations reported in a brief note, "Letters to the Editor" in the Physical Review,[13] are

[13] White and Ritschl, Phys. Rev. **35**, 208 (1930).

in error. The $\Delta\lambda$'s and $\Delta\nu$'s for the two lines there given may be corrected by multiplying by a factor of 1.25.

THE COMPUTATION AND INTERPRETATION OF THE *HFS*-TERM SEPARATIONS

There are two distinct and characteristic systems of multiplet terms in the arc spectrum of manganese, as may be seen from Fig. 1; (a) a system of *normal* multiplet terms built upon the ^5S and ^7S ($3d^5 4s$) terms of Mn II, which in turn are built upon the ^6S ($3d^5$) term of Mn III, and (b) a system of inverted multiplet terms built upon the inverted ^5D ($3d^6$) term of Mn II. It has been indicated previously[8] that the *hfs* of manganese is in good agreement with the

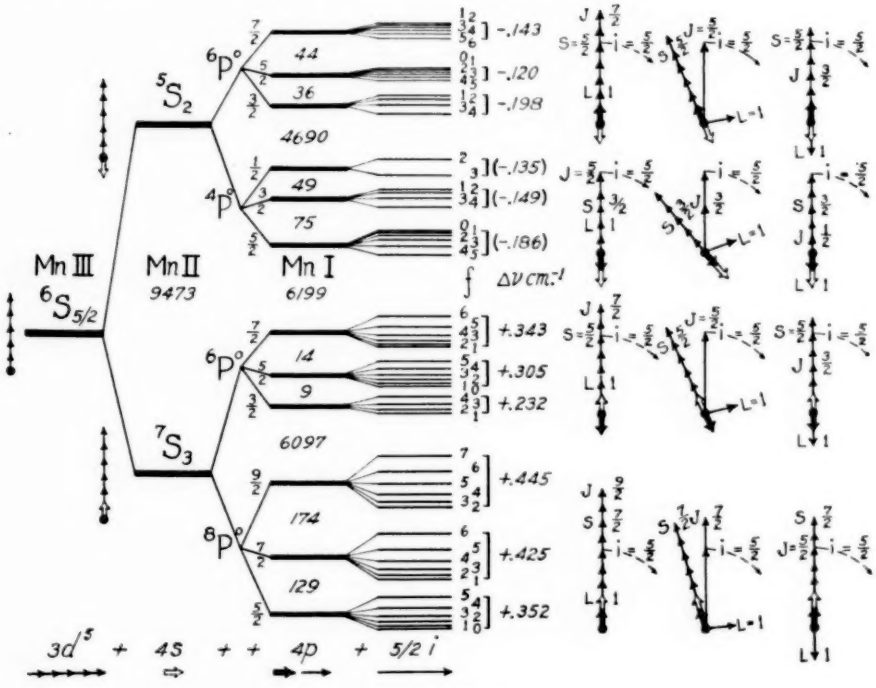

Fig. 3. Multiplet structure terms, *hfs*-terms, and space quantization vectors for the electron configuration $3d^5 4s4p$.

interpretation of *hfs* in other elements. Here in manganese, as in many other elements, the deep penetrating and tightly bound *s* electron is found to play an important role. The coupling of a 4*s* electron with the resultant of six other valence electrons is observed to give the widest *gs*-separations while its strong coupling with the nucleus gives rise to the widest *hfs*-separations. Fortunately, *LS* coupling in the *gs* and *Ji* coupling in the *hfs* is quite rigidly held to, thus enabling vector diagrams for the space quantization of the *s* and *l* values for each valence electron to be quite accurately drawn. It has also been previously shown[8] that the total *hfs*-separation of a *gs*-term should be approximately proportional to $\cos(is)$, where *s* is the spin of the deeply penetrating and tightly bound *s* electron, and *i* is the nuclear spin momentum. Since this proportionality is taken for the vector position $\cos(Ji) = 1$, where

cos (is) = cos (Js), it may be stated that for each gs-term where cos (Js) is *positive*, the *hfs*-terms are *normal*, and where cos (Js) is *negative* the *hfs*-terms are *inverted*.

At the left in Fig. 2 the building up of the x^4S, x^6S, y^6S, and x^8S $(3d^5 4s5s)$ terms of Mn I is shown starting with the parent term ^6S $(3d^5)$ of Mn III. This is done in order to show the direction taken on by the spins of the $4s$ and $5s$ electrons in each gs-term and to show the shift in energy due to the inversion (with respect to the electron resultant J) of either the $4s$ or $5s$ electron. At the right in Fig. 2, it may be seen that when the $4s$ electron spin is parallel with J, cos (Js_{4s}) positive, the *hfs*-terms are *normal*, and when oppositely directed, cos (Js_{4s}) negative, the *hfs*-terms are *inverted*. Space quantization of i with J and s is only shown for the position of largest f value.

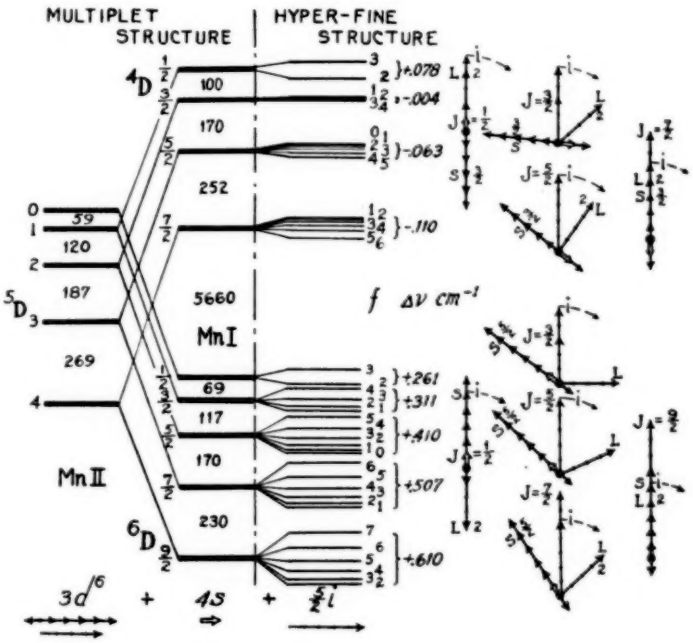

Fig. 4. Hyperfine structure terms and space quantization vectors for the electron configuration $3d^6 4s$.

The building up of the a^4P^0, a^6P^0, b^6P^0, and a^8P^0 $(3d^5 4s4p)$ terms in Fig. 3 is quite similar to that of the x^4S, x^6S, y^6S and x^8S terms in Fig. 2. The addition of a $4p$ electron, with quantum number $s=\frac{1}{2}$ and $l=1$, in place of a $5s$ electron, with $s=\frac{1}{2}$ and $l=0$, however, splits both ^5S and ^7S $(3d^5 4s)$ of Mn II into six levels in place of two. The vector diagrams for each level are given at the right in Fig. 3. For each gs-level of a^4P^0 and b^6P^0, cos (Js_{4s}) negative, the *hfs*-terms are *inverted*, whereas, for a^6P^0 and a^8P^0, cos (Js_{4s}) positive, the *hfs*-terms are *normal*.

Starting with the inverted ^5D $(3d^6)$ term of Mn II at the left in Fig. 4, the addition of a $4s$ electron splits each level into two levels resulting in the *inverted* multiplet terms a^4D and a^6D $(3d^6 4s)$. Here again for cos (Js_{4s}) negative, the *hfs*-terms are *inverted*, while for cos (Js_{4s}) positive they are *normal*.

The stepwise inversion of the *hfs* in the four terms of a^4D follows directly from the stepwise change from positive cos (Js_{4s}) in $a^4D_{\frac{1}{2}}$ to negative cos (Js_{4s}) in $a^4D_{3\frac{1}{2}}$.

Each spectral line in manganese is in reality a tiny multiplet. Several characteristic types of these *hfs*-multiplets are shown in Figs. 5 and 6. A new Zeiss microphotometer, having variable magnification, has been used to obtain density curves from the best plates, copies of which are shown at the bottom of the figures. From the total width of lines of the type shown in Fig. 5, it is obvious why only the *diagonal* lines have been resolved and measured. The intervals between the *diagonal* lines give only the difference between the

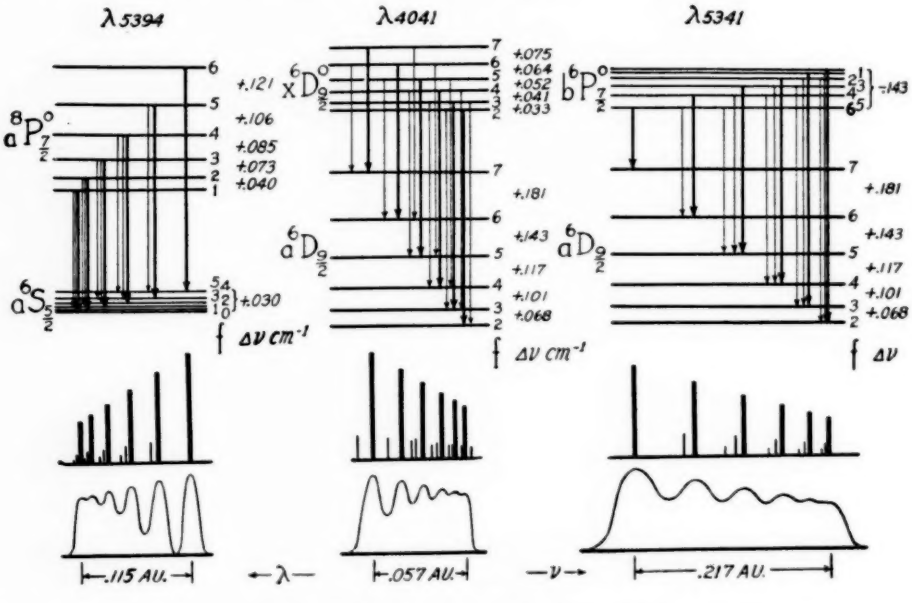

Fig. 5. Hyperfine structure patterns in neutral manganese. λλ5394 and 4041 taken at liquid air temperatures and λ5341 taken from a vacuum furnace.

set of levels above and the set below. It should here be pointed out that the total width of λ4041 is only 0.057A. It was hoped, therefore, in a wide pattern of lines like λ5341, Fig. 5, that the *off diagonal*, or faint lines, could be observed. Since the *gs*-multiplet to which this line belongs was so weakly excited in the Schüler tube, and at the same time lies in a region of the spectrum where photographic plates are rather insensitive, the vacuum furnace was resorted to. The only trace of the *off diagonal*, or faint lines, in any of the *hfs*-multiplets has been found in the lines $a^8P^0_{4\frac{1}{2}, 3\frac{1}{2}, 2\frac{1}{2}}, -x^8S_{3\frac{1}{2}}$. All three lines of this *gs*-multiplet, λλ4823, 4783, and 4754, are shown in Fig. 6. Even though the extremely narrow patterns of these lines have not been completely resolved, their interpretation is quite unambiguous since their general appearance verifies the order and magnitude of the *hfs*-term separations of a^8P^0 and x^8S arrived at from other considerations. What has actually been measured is indicated at the bottom of the figure. The five *off diagonal* lines on the low frequency side of λ4783 fortunately fall almost together and can be

measured as a single strong component. With the measured separations between this component and the first two diagonal components and, making the valid assumption that the Landé interval rule is in operation, the x^8S, and in turn the a^8P^0, *hfs*-term separations can be approximately computed. With this as a start, the total separation of the normal state $^6S_{2\frac{1}{2}}$ $(3d^54s^2)$ is determined from the two resonance lines λλ5394 and 5432 to be about 0.030 cm^{-1}. The separations for $a^6P^0_{3\frac{1}{2}, 2\frac{1}{2}, 1\frac{1}{2}}$ are then determined from λλ4030, 4033, and 4034. While the *hfs*-patterns of $^6D-{}^6D^0$ and $^4D-{}^4D^0$ $(3d^64s-3d^64p)$

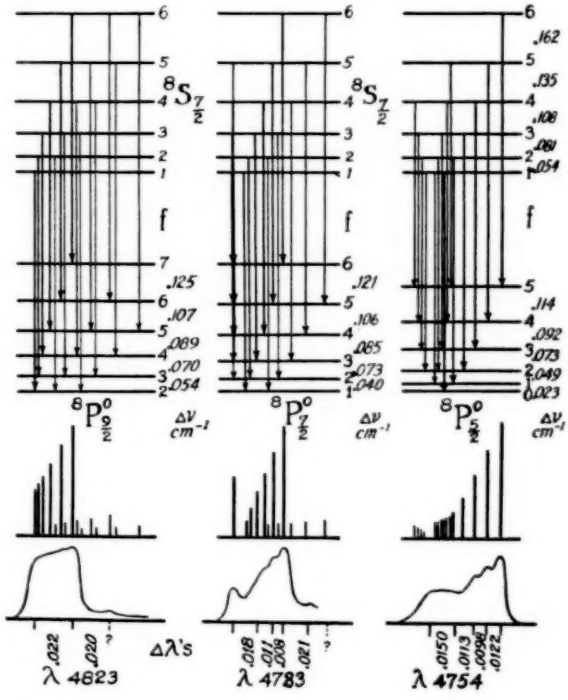

Fig. 6. Very narrow hyperfine structure patterns in the octet system of manganese taken at liquid air temperatures.

have been obtained at liquid air temperatures, none of them resolve the *off diagonal* components that must certainly be there. From the measured differences between the different patterns of a multiplet, however, a clue to the *hfs*-separations is obtained. The successive differences, for example, between the $\Delta\nu$'s of λλ4018, 4055 and 4083 as compared with the successive differences between the $\Delta\nu$'s of λλ4079, 4055 and 4035 show that the a^6D $(3d^64s)$ separations are about two and one-half times as wide as those of x^6D^0 $(3d^64p)$. Even though relations of this kind can only give, at best, an approximation to the true separations, it has been necessary to use such relations to compute the separations for a^6D, b^6P^0, a^4D, x^6D^0 and x^4D^0. The *gs*-terms and *hfs*-term intervals are given in Table III.

Theoretical Interpretation

It has quite generally been observed that the widest *hfs*-separations are due to the strong coupling between the spin of a single *s* electron and the nu-

TABLE III. *hfs-term intervals, Mn I.*

Term	Value	$\Delta\nu_1$	$\Delta\nu_2$	$\Delta\nu_3$	$\Delta\nu_4$	$\Delta\nu_5$	Total $\Delta\nu$
$a^6S_{2\frac{1}{2}}$	59937.47	+.010	+.008	+.006	+.004	+.002	+.030
$x^8S_{3\frac{1}{2}}$	20506.13	+.162	+.135	+.108	+.081	+.054	+.540
$x^6S_{2\frac{1}{2}}$	18533.50	+.144	+.115	+.087	+.058	+.029	+.433
$y^6S_{2\frac{1}{2}}$	10524.27	−.078	−.062	−.047	−.031	−.016	−.234
$x^4S_{1\frac{1}{2}}$	10346.03	−.138	−.103	−.069			−.310
$a^8P_{4\frac{1}{2}}{}^0$	41232.09	+.125	+.107	+.089	+.070	+.054	+.445
$a_8P_{3\frac{1}{2}}{}^0$	41405.80	+.121	+.106	+.085	+.073	+.040	+.425
$a_8P_{2\frac{1}{2}}{}^0$	41534.98	+.114	+.092	+.073	+.049	+.023	+.352
$a^6P_{3\frac{1}{2}}{}^0$	35135.24	+.103	+.088	+.068	+.051	+.033	+.343
$a^6P_{2\frac{1}{2}}{}^0$	35149.46	+.097	+.086	+.061	+.041	+.020	+.305
$a^6P_{1\frac{1}{2}}{}^0$	35158.16	+.099	+.080	+.053			+.232
$b^6P_{3\frac{1}{2}}{}^0$	24167.53	−.044	−.037	−.030	−.019	−.013	−.143
$b^6P_{2\frac{1}{2}}{}^0$	24211.65	−.040	−.032	−.022	−.008		−.120
$b^6P_{1\frac{1}{2}}{}^0$	24247.40	−.100	−.060	−.038			−.198
$a^4P_{2\frac{1}{2}}{}^0$	28936.41	−.062	−.050	−.037	−.025	−.012	−.186
$a^4P_{1\frac{1}{2}}{}^0$	28861.11	−.066	−.050	−.033			−.149
$a^4P_{\frac{1}{2}}{}^0$	28812.58	−.135					−.135
$a^6D_{4\frac{1}{2}}$	42885.17	+.181	+.143	+.117	+.101	+.068	+.610
$a^6D_{3\frac{1}{2}}$	42655.50	+.160	+.123	+.103	+.073	+.048	+.507
$a^6D_{2\frac{1}{2}}$	42485.96	+.142	+.111	+.083	+.053	+.021	+.410
$a^6D_{1\frac{1}{2}}$	42368.98	+.128	+.104	+.079			+.311
$a^6D_{\frac{1}{2}}$	42300.28	+.261					+.261
$a^4D_{3\frac{1}{2}}$	36640.81	−.033	−.028	−.022	−.016	−.011	−.110
$a^4D_{2\frac{1}{2}}$	36388.29	−.021	−.017	−.013	−.008	−.004	−.063
$a^4D_{1\frac{1}{2}}$	36217.00	−.002	−.001	−.001			−.004
$a^4D_{\frac{1}{2}}$	36118.69	+.078					+.078
$x^6D_{4\frac{1}{2}}{}^0$	18148.04	+.075	+.064	+.052	+.041	+.033	+.265
$x^6D_{3\frac{1}{2}}{}^0$	18004.88	+.065	+.052	+.042	+.034	+.022	+.216
$x^6D_{2\frac{1}{2}}{}^0$	17883.78	+.062	+.050	+.037	+.025	+.012	+.186
$x^6D_{1\frac{1}{2}}{}^0$	17793.97	+.057	+.043	+.028			+.128
$x^6D_{\frac{1}{2}}{}^0$	17738.89	+.092					+.092

clear spin i, and also that the observed intervals follow the Landé interval rule. Since the classical quantum mechanics have yielded interval rules which agree so well with observations in *gs*-multiplets, Goudsmit and Bacher[14] have extended them to some of the simpler cases in *hfs*. The Landé interval rule for separations between two states f and $(f+1)$ is, as in *gs*, given by $\Delta\nu = A(f+1)$, where f is the resultant of i and J, and A is an observed proportionality constant. The total separation of a multiplet term is given by

$$\Delta\nu = mA \tag{1}$$

where $m = \sum f$'s minus the smallest f.

Assuming the cosine law for the interaction energy of any two electronic angular momentum vectors, the energy of interaction between an s electron spin and the nuclear spin, i, as shown by Goudsmit and Bacher and others, may be written

$$ais\cos(is). \tag{2}$$

Since i and s are constants, a is a constant to be associated with the electron, its value depending upon how strongly the electron spin is coupled with the nucleus spin.

[14] Goudsmit and Bacher, Phys. Rev. **34**, 1501 (1929).

In the case of an s electron and an arbitrary other electron, in LS coupling,

$$a_1 is \overline{\cos(is_1)} = a_1 is_1 \cos(ij)\cos(js)\cos(ss_1) = A\, ij \cos(ij) \tag{3}$$

where in terms of the quantum mechanics cosines

$$A = a_1 \frac{s(s+1) + s_1(s_1+1) - s_2(s_2+1)}{2s(s+1)} \cdot \frac{j(j+1) + s(s+1) - l_2(l_2+1)}{2j(j+1)} \tag{4}$$

and is the A of Eq. (1). The subscripts denote the s and arbitrary electron respectively. As pointed out by Goudsmit and Bacher, this expression for A, which is also applicable in the case where an s electron is added to a more general electron configuration, takes into account only the interaction between the s electron and the nucleus and neglects the interaction of the other valence electrons. A study of the vector diagrams and *hfs* shown in Figs. 2, 3, and 4 shows quite definitely that while the total *hfs*-separations depend primarily upon the 4s electron, the remaining valence electrons also make some contribution, and in some cases almost equal the contribution of the 4s electron. We may extend Eq. (4) in such a way that it is applicable to p, d, and f electrons as well as to s electrons. This is done by assuming that the electron has only a spin s and that its l vector is associated with the remaining valence electrons. This total *remainder* is then thought of as a parent term R_1 to which an electron spin S_1 alone is added to give the resultant multiplet term under consideration. Eq. (4) is then written

$$A = a_1 \frac{S(S+1) + S_1(S_1+1) - S_{R_1}(S_{R_1}+1)}{2S(S+1)} \cdot \frac{J(J+1) + S(S+1) - L_{R_1}(L_{R_1}+1)}{2J(J+1)} \tag{5}$$

Here S_1 may represent the spin of one or more electrons and a_1 the coupling constant associated with S_1. Making the valid assumption that the energy of interaction between an l vector and the nuclear spin i is given by

$$ail \cos(il) \tag{6}$$

the l vectors of each valence electron may be taken into account by replacing each S and L of Eq. (5) by L and S respectively. Taking into account all of the electrons we get the general expression

$$\begin{aligned} A = {} & \sum_n a_n \frac{S(S+1) + S_n(S_n+1) - S_{R_n}(S_{R_n}+1)}{2S(S+1)} \cdot \frac{J(J+1) + S(S+1) - L_{R_n}(L_{R_n}+1)}{2J(J+1)} \\ & + \sum_n a_n \frac{L(L+1) + L_n(L_n+1) - L_{R_n}(L_{Rn}+1)}{2L(L+1)} \cdot \frac{J(J+1) + L(L+1) - S_{R_n}(S_{R_n}+1)}{2J(J+1)} \end{aligned} \tag{7}$$

For n valence electrons this gives A in terms of $2n$ constants. With seven valence electrons in manganese the fourteen constants are readily reduced to

TABLE IV. *hfs-coupling constants. Electron configurations $3d^5 4s4p$ and $3d^5 rs^2$.*

Term	Total $\Delta\nu$	$R_1\,R_2\,R_3\,R_4$	mA	A				a_1 $4s_s$	a_2 $4p_s$	a_3 $4p_l$	a_4 $3d_s{}^5$
$a^8P_{4\frac{1}{2}}{}^0$	+.445	$^7P\,^7P\,^8S\,^3P$	25A	$+a_1$ 1/9	$+a_2$ 1/9	$+a_3$ 2/9	$+a_4$ 5/9	.120	.019	*.006*	*.002*
$a^8P_{3\frac{1}{2}}{}^0$	+.425	$^7P\,^7P\,^8S\,^3P$	20A	$+a_1$ 59/441	$+a_2$ 59/441	$+a_3$ 4/63	$+a_4$ 295/441	.124	.021	*.006*	*.002*
$a^8P_{2\frac{1}{2}}{}^0$	+.352	$^7P\,^7P\,^8S\,^3P$	15A	$+a_1$ 9/49	$+a_2$ 9/49	$-a_3$ 2/7	$+a_4$ 45/49	.110	.018	*.006*	*.002*
$a^6P_{3\frac{1}{2}}{}^0$	+.343	$^5P\,^7P\,^6S\,^1P$	20A	$+a_1$ 1/7	$-a_2$ 5/49	$+a_3$ 2/7	$+a_4$ 5/7	.112	.020	*.006*	*.002*
$a^6P_{2\frac{1}{2}}{}^0$	+.305	$^5P\,^7P\,^6S\,^1P$	15A	$+a_1$ 31/175	$-a_2$ 31/245	$+a_3$ 4/35	$+a_4$ 31/35	.113	.018	*.006*	*.002*
$a^6P_{1\frac{1}{2}}{}^0$	+.232	$^5P\,^7P\,^6S\,^1P$	9A	$+a_1$ 7/25	$-a_2$ 1/5	$-a_3$ 2/5	$+a_4$ 7/5	.105	.020	*.006*	*.002*
$b^6P_{3\frac{1}{2}}{}^0$	−.143	$^7P\,^5P\,^6S\,^1P$	20A	$-a_1$ 5/49	$+a_2$ 1/7	$+a_3$ 2/7	$+a_4$ 5/7	.125	.018	*.006*	*.002*
$b^6P_{2\frac{1}{2}}{}^0$	−.120	$^7P\,^5P\,^6S\,^1P$	15A	$-a_1$ 31/245	$+a_2$ 31/175	$+a_3$ 4/35	$+a_4$ 31/35	.112	.021	*.006*	*.002*
$b^6P_{1\frac{1}{2}}{}^0$	−.198	$^7P\,^5P\,^6S\,^1P$	9A	$-a_1$ 1/5	$+a_2$ 7/25	$-a_3$ 2/5	$+a_4$ 7/5	.137	.018	*.006*	*.002*
$a^4P_{2\frac{1}{2}}{}^0$	*−.186*	$^5P\,^5P\,^4S\,^3P$	15A	$-a_1$ 3/25	$-a_2$ 3/25	$+a_3$ 2/5	$+a_4$ 21/25	*.118*	*.019*	*.006*	*.002*
$a^4P_{1\frac{1}{2}}{}^0$	*−.149*	$^5P\,^5P\,^4S\,^3P$	9A	$-a_1$ 11/75	$-a_2$ 11/75	$+a_3$ 4/15	$+a_4$ 77/75	*.118*	*.019*	*.006*	*.002*
$a^4P_{\frac{1}{2}}{}^0$	*−.135*	$^5P\,^5P\,^4S\,^3P$	3A	$-a_1$ 1/3	$-a_2$ 1/3	$-a_3$ 2/3	$+a_4$ 7/3	*.118*	*.019*	*.006*	*.002*
$a^6S_{2\frac{1}{2}}$	+.030	^1S_d	15A				$+a_4$				.002

TABLE V. *hfs-coupling constants. Electron configuration $3d^5 4s5s$.*

Term	Total $\Delta\nu$	R_1 R_2 R_3	mA	A			a_1 $4s_s$	a_2 $5s_s$	a_3 $3d^5{}_s$
$x^6S_{3\frac{1}{2}}$	+.540	$^7S\,^7S\,^3S$	20A	$+a_1$ 1/7	$+a_2$ 1/7	$+a_3$ 5/7	.149	.030	.002
$x^6S_{2\frac{1}{2}}$	+.433	$^5S\,^7S\,^1S$	15A	$+a_1$ 1/5	$-a_2$ 1/7	$+a_3$ 1	.156	.030	.002
$y^6S_{2\frac{1}{2}}$	−.234	$^7S\,^5S\,^1S$	15A	$-a_1$ 1/7	$+a_2$ 1/5	$+a_3$ 1	.165	.030	.002
$x^4S_{1\frac{1}{2}}$	−.310	$^5S\,^5S\,^3S$	9A	$-a_1$ 1/5	$-a_2$ 1/5	$+a_3$ 7/5	.156	.030	.002

TABLE VI. *hfs-coupling constants. Electron configuration $3d^6 4s$.*

Term	Total $\Delta\nu$	R_1 R_2 R_3	mA	A			a_1 $4s_s$	a_2 $3d^6{}_s$	a_3 $3d^6{}_l$
$a^6D_{4\frac{1}{2}}$	+.610	$^5D\,^2D\,^6S$	25A	$+a_1$ 1/9	$+a_2$ 4/9	$+a_3$ 4/9	.159	.011	.004
$a^6D_{3\frac{1}{2}}$	+.507	$^5D\,^2D\,^6S$	20A	$+a_1$ 37/315	$+a_2$ 148/315	$+a_3$ 26/63	.158	.011	.004
$a^6D_{2\frac{1}{2}}$	+.410	$^5D\,^2D\,^6S$	15A	$+a_1$ 23/175	$+a_2$ 92/175	$+a_3$ 12/35	.153	.011	.004
$a^6D_{1\frac{1}{2}}$	+.311	$^5D\,^2D\,^6S$	9A	$+a_1$ 13/75	$+a_2$ 52/75	$+a_3$ 2/15	.153	.011	.004
$a^6D_{\frac{1}{2}}$	+.261	$^5D\,^2D\,^6S$	3A	$+a_1$ 7/15	$+a_2$ 28/15	$-a_3$ 4/3	.154	.011	.004
$a^4D_{3\frac{1}{2}}$	−.110	$^5D\,^2D\,^4S$	20A	$-a_1$ 3/35	$+a_2$ 18/35	$+a_3$ 4/7	.156	.011	.004
$a^4D_{2\frac{1}{2}}$	−.063	$^5D\,^2D\,^4S$	15A	$-a_1$ 13/175	$+a_2$ 78/175	$+a_3$ 22/35	.156	.011	.004
$a^4D_{1\frac{1}{2}}$	−.004	$^5D\,^2D\,^4S$	9A	$-a_1$ 1/25	$+a_2$ 6/25	$+a_3$ 4/5	.156	.011	.004
$a^4D_{\frac{1}{2}}$	+.078	$^5D\,^2D\,^4S$	3A	$+a_1$ 1/5	$-a_2$ 6/5	$+a_3$ 2	.156	.011	.004

three or four since five $3d$ electrons may be treated as a unit. The electron configuration $3d^5 4s4p$, for the terms shown in Fig. 3, will here be used as an example. For the $4s$ electron with l value 0, only one constant, a_1 of Table IV, is to be determined. The contribution of a $4p$ electron with s value $\frac{1}{2}$ and l value 1 is represented by two constants, a_2 and a_3 respectively. The five $3d$ electrons, considered as a unit, have a spin value $2\frac{1}{2}$ and an l value 0 and may therefore be treated as a single s electron with spin $2\frac{1}{2}$ and represented by one constant, a_4, Table IV.

The values of the a's in the last four columns of Table IV may be computed from the $\Delta\nu$'s of Table III in the following manner. From Eqs. (1) and (7) and the total $\Delta\nu$'s we get for

$$a^6S_{2\frac{1}{2}}, \quad +0.030 = 15(\qquad\qquad\qquad\qquad + a_4 \quad) \tag{8}$$

$$a^8P_{4\frac{1}{2}}^0, \quad +0.445 = 25(a_1 1/9 + a_2 1/9 + a_3 2/9 + a_4 5/9) \tag{9}$$

$$a^8P_{2\frac{1}{2}}^0, \quad +0.352 = 15(a_1 9/49 + a_2 9/49 - a_3 2/7 + a_4 45/49) \tag{10}$$

$$a^6P_{3\frac{1}{2}}^0, \quad +0.343 = 20(a_1 1/7 - a_2 5/49 + a_3 2/7 + a_4 5/7). \tag{11}$$

From the four simultaneous equations the four constants a_1, a_2, a_3, and a_4 can be determined. Since a_3 and a_4 are small as compared with a_1 and a_2 they are assumed the same for all of the terms in Table IV and are set in italics. The constant a_3 for $^8P_{4\frac{1}{2}}^0$ for example, is the mean of six values, taking each time Eq. (9) and one of the six equations from the $^6P^0$ terms. The a_1's for the $4s$ electron are then computed independently for each term, so that the four constants following each term give the total $\Delta\nu$ in column two. Since the $\Delta\nu$'s for the a^4P^0 terms have not been observed they have been computed from the mean values of the a's of the other nine P^0 terms. A method similar to that used for the P^0 terms has been used to determine the a's for the D and S terms of the electron configurations $3d^5 4s5s$ and $3d^6 4s$ respectively. The results are shown in Tables V and VI.

It is to be expected that the value of a_1 for the $4s$ electron obtained from each term of each electron configuration would be nearly the same. It is likewise to be expected that a_4 of Table IV and a_3 of Table VI would have nearly the same value. Attempts to alter any one set of a's or $\Delta\nu$'s is found to alter other sets of a's or $\Delta\nu$'s in such a way as to make conditions worse. Just how much, from the theoretical standpoint, a_1 ($4s$) should be changed by a change in the electron configuration, for example from $3d^5 4s4p$ to $3d^6 4s$, is difficult to determine. The agreement between the a_1's within each of the elec tron configurations is as good as can be expected.

The narrow *hfs*-separations in the ^4D terms of Fig. 4 and the wide separations in the ^6D terms show that the coupling of the six $3d$ electrons with the nucleus almost neutralizes that of the $4s$ electron. This same effect is also found in the b^6P^0 terms of Fig. 3. It should here be stated that preliminary calculations of a_1, a_2, and a_4 for the first nine terms of Table IV, omitting the l value of the $4p$ electron a_3, indicated that the inclusion of the l value would give more constant values of a_1 and a_2.

A study of Figs. 2, 3, and 4 and a comparison of these figures with Tables IV, V, and VI shows that only a few of the interesting relations to be found between the *hfs* and the *gs* of manganese have been pointed out above. This investigation has been carried on at Professor Paschen's laboratory at the Physikalisch-Technische Reichsanstalt, Berlin.

MEAN LIVES OF LINES OF MERCURY TRIPLET $2^3P_{012}-2^3S_1$

By Robert H. Randall
Physics Laboratories, Columbia University

(Received April 4, 1930)

Abstract

The mean life of each of three lines coming from the same upper level in the mercury atom has been measured. The triplet $2^3P_{012}-2^3S_1$ was excited by electron impact under conditions involving negligible ionization and concentration of excited atoms. The method was that previously described by Webb, in which high frequency voltages are applied in phase to the excitation and detecting systems. The lines were excited in a sealed-off tube with mercury pressures between 0.004 and 0.03 mm. The exciting voltage was less than ten volts. The excitation was such that there was no appreciable concentration in the $2P$ states. A specially designed potassium-hydride photoelectric cell was used as the detecting system. Optical filters were used to isolate the line measured. The results agree with the assumption that the radiation decays exponentially after impact. For the lines λ4047 and λ4358 the lives were found to be the same within the experimental error (0.75 percent) viz. $\tau=5.75\times10^{-8}$ secs. The value for λ5461 was four times greater, $\tau=2.37\times10^{-7}$ secs. The agreement between the lives of λ4047 and λ4358 supports the quantum assumption that lines coming from the same level in the atom have the same life. Collins has found that under certain exciting conditions the fine-structure of λ5461 is anomalous as compared to λλ4047 and 4358. It is suggested that the longer life found for λ5461 may be explained by considering the fine structure of the 2^3S_1 level. The results are then consistent with the above assumption.

Introduction

FROM the relation between the mean life, τ_n, of an excited atomic state and the Einstein probabilities for transitions to all possible lower states,

$$\tau_n=\left(\sum_m A_m^n\right)^{-1}$$

it is generally assumed that all spectral lines originating in the same upper level in the atom have the same life.[1] Direct experimental evidence on this point is scarce.

While Kerschbaum[2] has measured τ for a number of spectral lines, using Wien's canal-ray method, and has found equal lives for lines originating in the same upper level, in agreement with the Einstein assumptions, he also found, in general, equal lives for *all* the arc lines of any one element. This last is hardly to be expected, as Maxwell[3] has pointed out, since the sum of the transition probabilities, upon which the lives depend, is not necessarily the same for every level in the atom.

The present investigation was undertaken to test further the validity of the Einstein assumptions by measuring the mean lives of each of several

[1] Pauli, Handbuch der Physik, V. 23, p. 11.
[2] H. Kerschbaum, Ann. d. Physik **83**, 287 (1927).
[3] L. R. Maxwell, Phys. Rev. **34**, 199 (1929).

lines coming from the same upper level, but under simpler excitation conditions than obtained in Kerschbaum's measurements. The lines were excited by simple electron impact at voltages below ionization. The mercury $2^3P_{012} - 2^3S_1$ triplet, λλ5461, 4358 and 4047, was chosen because the intensity of the lines and their wide wave-length separation favored the application of the particular method of measurement used. Since levels higher than the 2^3S_1 were not excited to any appreciable extent, the conditions were less complicated than where high voltage excitation is used, as in Wien's canal-ray method. Voltage and pressure conditions were such as to make it unlikely that absorption and re-emission played any part in the persistence of the radiation.

Method

The method of measurement employed was a modification of that previously used in this laboratory.[4] The excitation was produced by electron impact excited by alternating voltages in such a way that there was excitation during only the positive half cycle. A voltage of the same frequency and phase was applied to a photoelectric detecting system, so that only radiation reaching the photoelectric surface in the positive half cycle was effective; during the negative half cycle the photoelectrons were held in the surface. As the frequency was increased, the total excitation being held constant, the photoelectric current decreased, owing to the persistence of the radiation, some of which then reached the photoelectric surface in the negative half cycle. From the form of the curve, the value of the mean life τ of the radiation was calculated, assuming that radiation excited at the time $t=0$ falls off acording to the law e^{-kt}.

Apparatus

The details of the apparatus are shown in Fig. 1. The excitation was produced in an evacuated vessel of Pyrex, containing electrodes C, G, G' and O. The hot cathode C, for which we are indebted to Dr. A. W. Hull of the General Electric Company, was equipotential, consisting of an oxide-coated nickel cylinder with an internal tungsten heater. Electrodes G and G', comprising the accelerating system, were in the form of two concentric cylinders of 1.6 mm mesh nickel gauze, with a difference in radius of 2.0 mm. For most of the measurements grids G and G' were connected together just outside the cell and used as a single electrode which we shall call GG'. The outer cylindrical electrode O, of sheet nickel, had a window covered with gauze to allow the passage of the radiation.

All metal parts were pre-outgassed. Before sealing off, the excitation cell was baked for several hours at 450°C, the filament sensitized and a strong arc operated for an hour. Later tests indicated that accumulated gas did not exceed 10^{-4} mm of mercury.

The mercury vapor pressure in the excitation cell was controlled by a mercury well at the bottom, kept in a water-bath whose temperature was

[4] H. W. Webb, Phys. Rev. **24,** 113 (1924); F. G. Slack, Phys. Rev. **28,** 1, (1926); H. W. Webb and H. A. Messenger, Phys. Rev. **33,** 319 (1929).

held constant to 0.1°C. The body of the tube was superheated to about 80°C.

The detecting system, containing electrodes *P*, *H* and *W*, was a specially constructed photoelectric cell placed at a distance of 8 cm from the excitation cell. The potassium-covered electrode *P* was a nickel cylinder, supported on a long re-entrant glass tube to increase the electrical leakage path. Surrounding *P* was a cylindrical nickel gauze electrode *H*. Against the walls was a third cylindrical grid, which in addition to removing the photoelectrons quickly, served as a flashing electrode in forming the sensitive potassium-hydride surface. During the flashing process electrode *H* was slid to one end of the cell, allowing a more uniform discharge between *W* and *P* and preventing the formation of a light sensitive surface on *H*.

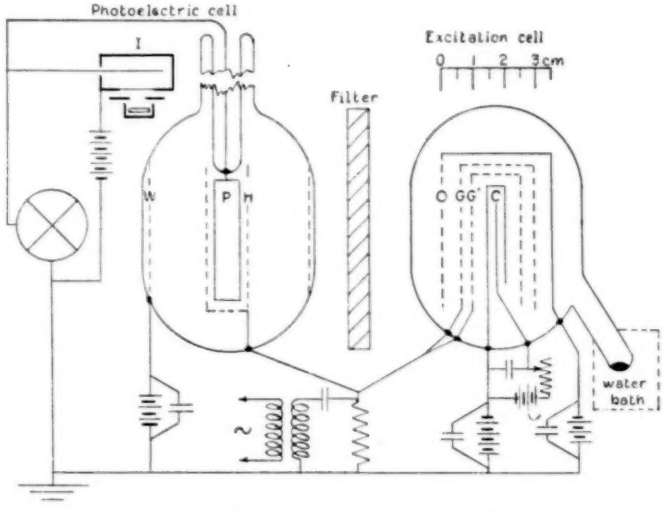

Fig. 1. Schematic diagram of apparatus and electrical circuits.

The metal parts were pre-outgassed and the cell which was of Pyrex, was baked out before distilling in the potassium. The hydrogen necessary for the flashing process was thoroughly pumped out before sealing off. The gas pressure in the cell after sealing off was below 10^{-4} mm mercury.

An electric heater on the electrometer lead prevented internal electrical leakage due to the formation of a film of potassium. Occasionally, after standing, a strong reverse photoelectric current from the grid *H* was found, due probably to a thin potassium film. This effect soon disappeared, however, after exposure to the heat of the excitation cell.

Corning glass filters were used between the excitation cell and the photoelectric cell to isolate each of the three lines; filters nos. G 555-Q and G 34-Y for λ5461; nos. G585-L and G-38 for λ4358; and nos. G586-A and G38-L for λ4047.

Photographs of a mercury arc taken through the filter for λ5461 and for λ4358, made certain that under the conditions of excitation of this experiment, the transmission of one filter for either of the other two lines, or for any other line likely to be excited, was less than 1 percent of the transmission

for the desired line. The radiation transmitted by the filter for λ4047 also included the line λ4078, but was otherwise monochromatic. White[5] and Crozier[6] have found that under excitation conditions similar to those of this experiment, λ4078 was considerably weaker than λ4047. A study of the results of the present investigation showed that the presence of the small quantity of λ4078 did not affect the measurement of the life of λ4047.

There was always a considerable steady photoelectric current, due to the light from the hot cathode of the excitation cell. This was balanced out by means of a radio-active leak, *I*, Fig. 1, controlled by a variable lead shutter over the opening of the metal box containing the active material.

The filament was heated by an 8 volt storage battery while all other d.c. voltages were furnished by small dry cells. The alternating voltages were supplied by air-core transformers coupled to the 60 cycle lighting circuit

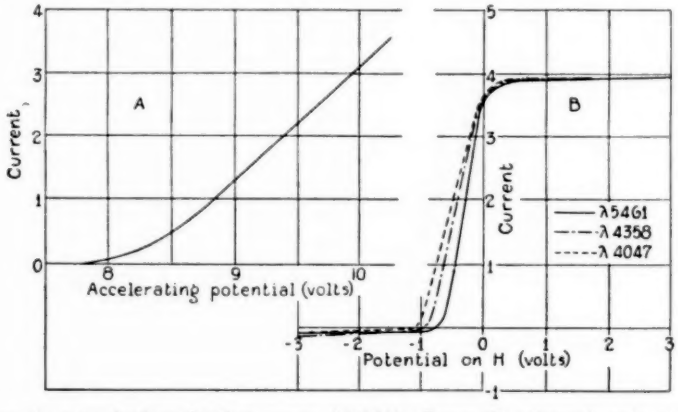

Fig. 2. Curve *A*, a typical excitation curve (λ4358). Curve *B*, photoelectric characteristics.

or to a vacuum-tube oscillator of variable frequency. The voltages were applied to the experimental cells across a nearly non-inductive resistance of about 45 ohms, one end of which was connected directly to the grids *II* and *GG'*. In the case of the high frequencies supplied by the oscillator this resistance formed part of a tuned circuit which helped to insure a pure impressed sine wave. The alternating voltages were measured with a vacuum-tube voltmeter. The frequencies were measured with a wave-meter.

A Compton quadrant electrometer with a sensitivity of about 3000 mm per volt was used to measure the photoelectric current.

Experimental and Results

Fig. 2 shows the steady current characteristics of the exciting and of the detecting systems which it was necessary to know in calculating the lives of the radiations. The excitation curve (*A*) was taken with the filter for λ4358 in place, and shows how the photoelectric current varied with the accelerating voltage between *GG'* and *C*, the voltage between *II* and *P* being held constant. The voltage conditions were $P=0.0$, $II=2.0$, $W=6.0$, $GG'=0.0$, $O=-3.0$, and *C* variable between 0.0 and -10.5 volts.

[5] D. R. White, Phys. Rev. **28**, 1125 (1926).
[6] W. D. Crozier, Phys. Rev. **31**, 800 (1928).

The curve for λ4358 shows that this radiation appeared at about the theoretical voltage 7.7 and that the variation of the photoelectric current was roughly linear for higher voltages up to 10.5 volts. Excitation curves taken with each of the other two filters were found to have exactly the same shape as that shown for λ4358, agreeing with the results of White[5] and Crozier.[6] The line λ4078 should theoretically come in at 7.9 volts. There was, however, no evidence of complexity in the excitation curve found for λ4047, indicating that λ4078 was considerably weaker than λ4047.

The photoelectric characteristics Fig. 2 (*B*) were taken with each of the three filters separately, maintaining a constant voltage between *GG'* and *C*

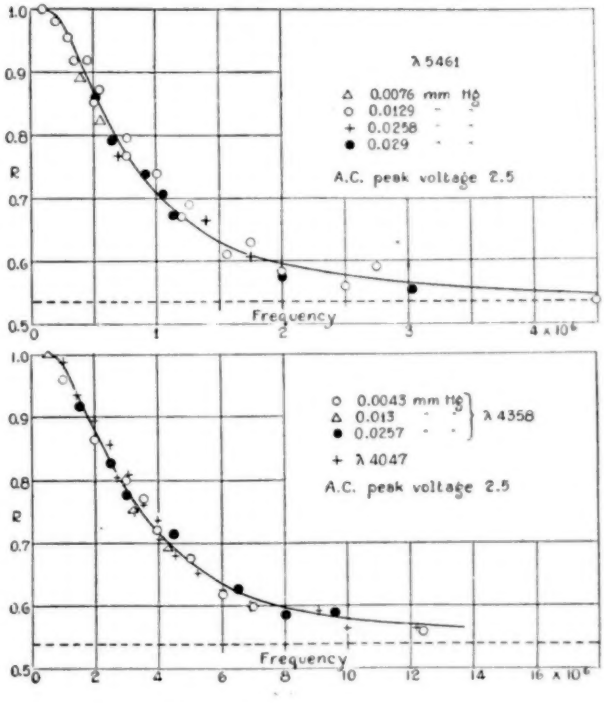

Fig. 3. *R*-frequency curves.

and varying the voltage between *H* and *P*. The ordinates are proportional to the photoelectric currents in each case and have been reduced to the same saturation current for comparison. The voltage conditions for the curves shown were $GG'=0.0$, $C=-9.0$, $O=-3.0$, $P=0.0$, and *H* variable between -3.0 and 3.0 volts. The three curves show that for these wave-lengths the cell was practically unidirectional and that a change of only a volt in the potential on *H* was sufficient to produce saturation. The shift in the stopping voltage is the only marked variation of the photoelectric characteristic with wave-length.

The curves from which the lives of the radiations were determined were obtained by applying alternating voltages, of the same peak value and phase, to *GG'* and *H* simultaneously and measuring the photoelectric current at different frequencies. The curves in Fig. 3 are typical of those obtained.

The abscissas are the frequencies. The ordinates are proportional to the photoelectric currents and represent in each case the ratio R of the current obtained with a high frequency to that obtained with a low frequency, 60 cycles, for which the effect of the persistence of the radiation was negligible. The ratio R was used instead of the actual photoelectric current to avoid error due to changes in the sensitivity of the photoelectric cell.

The d.c. voltage conditions for the curves shown were $GG'=0.0$, $C=-7.5$, $O=-3.0$, $P=0.0$, $II=0.0$ and $W=6.0$. The peak value of the alternating voltage applied to GG' and II was 2.5, so that the accelerating voltage varied between 5 and 10 volts. Measurements were taken at several different pressures, varying between 0.004 and 0.03 mm of mercury, as indicated in the figure. In the case of λ4047 the different pressures are not specified on the graph, for the sake of clearness, but the points for this line were taken over the same pressure range as for λ4358. Pressures below 0.004 mm in the case of λλ4047 and 4358, and below 0.007 mm in the case of λ5461, could not be used since there was then insufficient energy to give a measurable photoelectric current, while with pressures much above 0.03 mm trouble was experienced with the arc striking.

It is important for this method of measurement that the impressed alternating voltages be of approximately sine form. The tests for wave-form described in earlier papers, were made for each frequency and indicated that up to the highest frequency it was possible to use, 1.2×10^7 cycles, no error was introduced due to faulty wave-form.

The solid lines shown with the experimental points in Fig. 3 were calculated in a manner similar to that discussed in earlier papers. It was assumed that the radiation excited at any time $t=0$ falls off according to the exponential law e^{-kt}. Since the excitation was approximately linear with the voltage, the excitation during the positive half cycle approximated the form of the positive half of a sine curve. Also the photoelectric cell was nearly unidirectional and saturated quickly with a reversal of the voltage. It was therefore possible to find a simple approximate analytic expression for R as a function of the frequency f

$$R=\frac{K^2+2\pi^2f^2}{K^2+4\pi^2f^2}.$$

To this approximate expression certain correction terms, amounting to about 10 percent had to be added to take care of the fact that the photoelectric cell did not saturate instantaneously with a reversal of the voltage, and also the fact that excitation did not begin immediately with positive values of the alternating voltage. Since these correction terms were complicated and involved quantities determined empirically from the excitation and photoelectric characteristics, they are of no special interest here. With very high frequencies R approached a limiting value determined by the photoelectric characteristics and the amplitude of the applied alternating voltages. This is shown in Fig. 3 (a) and (b) by a horizontal dotted line.

By trial, a value of K was found such that the calculated curve best fitted the experimental points. The agreement was such as to justify the assumption of an exponential decay. For λ5461, K was found to be 4.23×10^{6} secs.$^{-1}$; the mean life of the radiation, τ, was then $1/K$ or 2.37×10^{-7} secs. The same K was found for λ4358 and for λ4047, viz. 1.74×10^{7} secs.$^{-1}$, giving a mean life for each of these lines of 5.75×10^{-8} secs. The life of λ5461 was therefore closely four times that of λλ4358 and 4047.

The precision of measurement for τ was about 4 percent. In order to see how closely the lives of λ4358 and λ4047 agreed, a fixed frequency of 3×10^{6} cycles was used and a large number of alternate measurements of R were taken by simply interchanging the filters, the electrical conditions remaining the same. The same value of R was found for both lines to within the experimental error 0.75 percent, indicating the same value of K for the two lines to within that precision.

Measurements were taken using a peak value for the alternating voltage of 1.1 instead of 2.5. This resulted in a slightly different form for the calculated $R-$ frequency curve. The experimental points lay on the calculated curve, however, and the values of K which best fitted the data agreed in every case with those found using a peak voltage of 2.5, to within the experimental error.

Using Corning glass filter no. G-586-AW, measurements were made on the mean life of another group of lines, which included the singlet $2^{3}P_{1}-3^{1}D_{2}$, λ3663, and the triplet $2^{3}P_{1}-3^{3}D_{123}$, λλ3650, 3654 and 3662. These lines could not be separated optically and the life measured was for the composite radiation. It was found impossible to obtain a complete R-frequency curve, since the radiation was apparently short-lived and it was necessary to go to very high frequencies before the photoelectric current began to decrease. Enough of the curve was obtained from which to estimate a value for the mean life of the radiation of 2.4×10^{-8} secs., certain to within 10 percent. The curve was too incomplete, however, to be able to determine whether there were different lives for the different components of the radiation.

Discussion

There was some question as to the purity of the radiation reaching the photoelectric cell when using the filter for λ4047. The theoretical voltages at which λ4047 and λ4078 come in are 7.7 and 7.9 respectively. Both White[5] and Crozier,[6] however, found no appreciable intensity for λ4078 under 8.4 volts. From a study of their voltage-intensity curves for these lines, the change in the peak value of the alternating voltage from 1.1 to 2.5 volts which changed the peak of the excitation voltage from 8.6 to 10.0 volts, would be expected to increase the average intensity of λ4078, as compared to that of λ4047, several times. If the intensity of λ4078 were comparable to that of λ4047, a change in the peak voltage should result in different R-frequency curves, providing the life of λ4078 were appreciably different from that of λ4047. No such change was noted, indicating either that the intensity of λ4078 was too low to give a measurable photoelectric current; or that if λ4078 were present to any considerable extent, its life was very

nearly that of λ4047. In either case the measured life must be approximately the true life of λ4047.

A study of the results for all three lines, λλ5461, 4358 and 4047, leads to the conclusion that the results were not affected by absorption and re-emission of the radiation, but that the lives measured are actually those of the single atomic processes. It has been shown that for λ2537 these absorption and re-emission processes play an important part in the persistence of the radiation emitted by excited mercury vapor, even down to pressures of 0.0002 mm of mercury.[7] It is also known that under certain conditions large concentrations of excited atoms in the 2^3P_1 and the metastable 2^3P_0 state exist in the vapor and considerable absorption of λ4358 and λ4047 results.[8] The subsequent re-emission of all three lines, λλ4047, 4358 and 5461 by atoms so excited to the 2^3S_1 level would cause persistence of the radiation in the vapor, beyond the mean life of the single atomic processes.

That such absorption processes did not occur to any measurable extent in the present experiment is evident from the fact that no change in the mean life resulted from varying the pressure and the exciting alternating voltages. Increasing the pressure should increase the concentration of atoms excited to the 2^3P_1 and 2^3P_0 states and as a consequence there should be greater persistence of the lines under study, if absorption processes were playing a part. The concentration of atoms in the 2^3P_1 and 2^3P_0 states would also be greater when the peak voltage of 2.5 was used than with the peak voltage of 1.1, since in the former case the population in these states would be augmented by the return of electrons from upper states excited by the higher accelerating voltages.

A further test for effects due to absorption was made by varying the voltage on the outer electrode *O* in the excitation cell between the limits −8.0 and 0.0 volts. This had the result of increasing the total number of excited atoms produced in the positive half cycle, as *O* was made less negative, and this change should have increased the probability of any quantum of radiation being absorbed by an excited atom before escaping from the vapor. Again, some of the curves were taken with the two accelerating grids, *G* and *G'* connected together; for other curves only the inner grid served as an accelerating grid, the outer of the pair being connected to the electrode *O*. This change also affected the total concentration of excited atoms and should therefore have affected any persistence due to absorption.

The lives measured were, however, found to be independent of any of these pressure or voltage changes, indicating that they are the true mean lives of the corresponding single atomic processes.

The results show identical lives for λλ4047 and 4358. This is strong evidence in support of the assumption that lines coming from the same upper level in the atom have the same life. While the fact that λ5461 was found to have quite a different life than the other two lines may be interpreted as evidence that the Einstein relation is not valid, it is believed that a much more reasonable explanation will be found in the fine-structure of the lines.

[7] H. W. Webb and H. A. Messenger, Phys. Rev. **33,** 319 (1929).

[8] C. Füchtbauer, Phys. Zeits. **21,** 635 (1920); R. W. Wood, Proc. Roy. Soc. **A106,** 679, (1924), Phil. Mag. **50,** 774 (1925), Phil. Mag. **4,** 406 (1927).

These fine-structure components have been carefully studied. Under the conditions obtaining in a strong arc λ5461 has at least twelve distinct components; λ4358 at least twenty; and λ4047 at least nine. Ruark[9] has proposed a fine-structure energy level scheme which supposes a triple fine structure for the 2^3S_1 level as well as a triple fine structure for each of the $2P$ levels, and which accounts for about $\frac{2}{3}$ of the components found in the arc. Some experiments of Collins,[10] however, have shown that the fine structure of these lines is much simpler when the lines are optically excited than in the strong arc. He excited the lines in a resonance tube placed next to a mercury arc. Atoms were excited to the 2^3S_1 level by the successive absorption of λ2537 and λ4358. About half the components found in a strong arc appeared in the case of λλ4358 and 4047, while only *one* of the many arc components of λ5461 appeared. When nitrogen was introduced into the resonance tube little change was noted in the fine structures of λλ4358 and 4047, but to the single component of λ5461 was added one other equally strong component.

These results indicate a certain anomalous character for λ5461 as compared to the other two lines. It suggests that under certain excitation conditions, quite different upper fine-structure levels may be involved in the case of λ5461 than in the case of λλ4047 and 4358, and that the lives measured in the present investigation may therefore be the lives characteristic of these different sub-levels. It is, however, not possible to say whether a single one of these sub-levels is involved in the case of each of the lines or whether the result, in each case, is the average life of lines coming from a group of sub-levels. The precision of the method is such that if a radiation were made up of two components of about equal intensity, the complexity could be detected if their lives differed by more than 30 percent. Again, if there were two components of widely different lives, the complexity could be detected as long as the intensity of one component was not less than 10 percent that of the other. Since there was no evidence of complexity from the curves, it was concluded either that one fine-structure component predominated in the case of each of the three lines, or that if several strong components were excited in each case, they had about equal lives.

A study of the fine structure of these lines under conditions of excitation somewhat similar to those of this investigation is being undertaken in this laboratory.

It is interesting to note that Wien,[11] using his canal-ray method, found a value for the mean life of λ4358 of 1.82×10^{-8} secs. No explanation can be offered for the difference between the value of the mean life found here and Wien's result. It should be pointed out, however, that the type of excitation was quite different for the two experiments, Wien using high voltages, while here the exciting voltage was always below ionization.

The author wishes to express his thanks to Professor H. W. Webb, who suggested this problem, for his continued help and advice throughout the experiment.

[9] A. E. Ruark, Phil. Mag. **1,** 977 (1926).
[10] E. H. Collins, Phys. Rev. **32,** 753 (1928).
[11] W. Wien, Ann. d. Physik **73,** 483 (1924).

THE HYDROGEN ATOM IN THE STARK EFFECT

By Francis G. Slack
Department of Physics, Vanderbilt University

(Received April 4, 1930)

Abstract

Characteristics of the hydrogen atom wave function, which show the statistical distribution of electronic charge with respect to the nucleus and electric field, are computed for the first five quantum states. The results are tabulated and are represented graphically for one state as an example. The average coordinates of the electronic charge are also computed and included in the tabulation.

EXPERIMENTS[1] with hydrogen canal rays in an electric field show phenomena apparently dependent upon the statistical distribution of the electronic charge with respect to the nucleus and to the electric field.[2] This statistical "distribution of charge" or "electronic configuration" is dependent on the wave functions of the various states of the hydrogen atom, as indicated by Schrödinger.[3]

In the following paper we compute and present in tabular and graphical form certain characteristics of the electronic configuration of the hydrogen atom wave function, namely, the statistical total charge in certain regions between which this charge reduces to zero, and the average coordinates of the total electronic charge with respect to the nucleus. These are computed from Schrödinger's[3] expressions for the Stark effect, using unperturbed wave functions in the case of a vanishingly small field.[4] No attempt is made to place any special significance or meaning on the computed values further than has been done[5] and it is unnecessary to choose from among the several points of view already expressed by various authors.[6]

We start with the Schrödinger wave equation for the hydrogen atom in an electric field of strength F:

$$\Delta\psi + \frac{8\pi^2 m}{h^2}\left(E + \frac{e^2}{r} - eFz\right)\psi = 0$$

and insert the parabolic coordinates λ_1, λ_2, ϕ where: $x=(\lambda_1\,\lambda_2)^{1/2}\cos\phi$, $y=(\lambda_1\,\lambda_2)^{1/2}\sin\phi$, and $z=1/2(\lambda_1-\lambda_2)$. The field has the direction of $+z$,

[1] J. Stark, Berliner Berichte 20 (1913); H. Lunelund, Ann. d. Physik **45**, 517 (1914); R. Wierl, Ann. d. Physik **82**, 563 (1927).

[2] F. G. Slack, Ann. d. Physik **82**, 576 (1927).

[3] E. Schrödinger, Ann. d. Physik **80**, 437 (1926).

[4] Condon and Morse, "Quantum Mechanics" p. 125.

[5] Condon and Morse, "Quantum Mechanics" p. 28.

[6] Ruark and Urey "Atoms, Molecules, and Quanta" p. 537; A. Sommerfeld, Phys. Zeits. **30**, 866 (1929).

i.e. the direction of the axis of the λ_2 parabolas. The wave function (ψ) satisfying this equation under these conditions is given by Schrödinger as:

$$\psi_{k_1 k_2 m} = \lambda_1{}^{m/2}\lambda_2{}^{m/2}e^{-(\lambda_2+\lambda_1)/2na_0}L^m_{m+k_1}\left(\frac{\lambda_1}{na_0}\right)L^m_{m+k_2}\left(\frac{\lambda_2}{na_0}\right)e^{\pm im\phi}$$

where $n=(k_1+k_2+m+1)$ is the total quantum number, k_1 and k_2 are parabolic quantum numbers and $(m+1)$ is the equatorial quantum number. L^m_{m+k} is the mth derivative of the $(m+k)$th Laguerre polynomial. $a_0=h^2/4\pi^2me^2$ the radius of the first Bohr orbit of the hydrogen atom. Forming the product of the wave function (ψ) with its conjugate ($\bar{\psi}$) we obtain the "electronic charge density" or "electronic probability"

$$\rho = \psi\bar{\psi} = \lambda_1{}^m\lambda_2{}^m e^{-(\lambda_1+\lambda_2)/na_0}\left[L^m_{m+k_1}\left(\frac{\lambda_1}{na_0}\right)\right]^2\left[L^m_{m+k_2}\left(\frac{\lambda_2}{na_0}\right)\right]^2.$$

For normalization[2] we introduce the factor C so that $\int_{\phi=0}^{2\pi}\int_{\lambda_1=0}^{\infty}\int_{\lambda_2=0}^{\infty}C\rho dv=e$ where $dv=1/4(\lambda_1+\lambda_2)d\lambda_1 d\lambda_2 d\phi$ is the volume element and e is the total extra-nuclear or electronic charge. We determine

$$C = \frac{k_1!k_2!e}{\pi(na_0)^{2m+3}[(m+k_1)!]^3[(m+k_2)!]^3n}.$$

Thus we obtain a final normalized expression for the integral of ρdv where we may evaluate over any set of limits to determine $e_{\text{limits}}=\iiint C\rho dv$ within their boundary. This being the integral of "charge density" multiplied by volume element we designate it by e_{limits} and have:

$$e_{\text{limits}} = \iiint \frac{C}{4}(\lambda_1+\lambda_2)\lambda_1{}^m\lambda_2{}^m e^{-(\lambda_1+\lambda_2)/na_0}\left[L^m_{m+k_1}\left(\frac{\lambda_1}{na_0}\right)\right]^2\left[L^m_{m+k_2}\left(\frac{\lambda_2}{na_0}\right)\right]^2 d\lambda_1 d\lambda_2 d\phi$$

where the limits $\int_{\phi=0}^{2\pi}\int_{\lambda_1=0}^{\infty}\int_{\lambda_2=0}^{\infty}$ will give a total electronic charge e. However on substituting concrete values of the quantum numbers and evaluating the Laguerre polynomials it is seen that for certain values of λ_1 and λ_2 the expression for ρ vanishes. Along these parabolas the "charge density" and hence the charge is zero. This gives us natural limits or boundaries within which we shall evaluate the integral. (The expression is degenerate in regard to the angular coordinate (ϕ) and thus has axial symmetry about an axis parallel to the impressed field. Integration over this coordinate then always introduces the factor 2π.)

As an example we introduce the quantum numbers for one substate and carry through the integration. Thus for the state $2-1-2$, $n=5$, $k_1=2$, $k_2=1$ and $m=1$ we have:

$$e_{2-1-2\text{ limits}} = \int_{\lambda_1}\int_{\lambda_2}\frac{C\pi}{2}(\lambda_1+\lambda_2)\lambda_1\lambda_2 e^{-(\lambda_1+\lambda_2)/5a_0}\left[L_3{}^1\left(\frac{\lambda_1}{5a_0}\right)\right]^2\left[L_2{}^1\left(\frac{\lambda_2}{5a_0}\right)\right]^2 d\lambda_1 d\lambda_2$$

$$= \frac{C\pi}{2}\int_{\lambda_1}\int_{\lambda_2}(\lambda_1+\lambda_2)\lambda_1\lambda_2 e^{-(\lambda_1+\lambda_2)/5a_0}\left[-3\left(\frac{\lambda_1}{5a_0}\right)^2+18\left(\frac{\lambda_1}{5a_0}\right)-18\right]^2\left[2\left(\frac{\lambda_2}{5a_0}\right)-4\right]^2 d\lambda_1 d\lambda_2.$$

The roots of $[-(\lambda_1/5a_0)^2+6(\lambda_1/5a_0)-6]$ are $\lambda_1=6.34a_0$ and $\lambda_1=23.66a_0$, and the root of $[(\lambda_2/5a_0)-2]$ is $\lambda_2=10a_0$ and thus the expression under the integral will vanish along the three parabolas fixed by these values of λ_1 and λ_2 as well as for $\lambda_1=0$ or $\lambda_2=0$ and for $\lambda_1=\infty$ or $\lambda_2=\infty$. These four λ_1 parabolas intersected by the three λ_2 parabolas will divide the region surrounding the nucleus into six regions[7] bounded by the limits:

$$e_1=\int_{\lambda_1=0}^{6.34a_0}\int_{\lambda_2=0}^{10a_0};\quad e_2=\int_{\lambda_1=0}^{6.34a_0}\int_{\lambda_2=10a_0}^{\infty};\quad e_3=\int_{\lambda_1=6.34a_0}^{23.66a_0}\int_{\lambda_2=0}^{10a_0};$$

$$e_4=\int_{\lambda_1=6.34a_0}^{23.66a_0}\int_{\lambda_2=10a_0}^{\infty};\quad e_5=\int_{\lambda_1=23.66a_0}^{\infty}\int_{\lambda_2=0}^{10a_0};$$

$$e_6=\int_{\lambda_1=23.66a_0}^{\infty}\int_{\lambda_2=10a_0}^{\infty}.$$

Substituting its values as given for C and integrating in this particular case we have:

$$e_{2-1-2\text{ limits}}=\frac{e}{2^3\cdot 5^6\cdot 6a_0^5}\left\{\left[-\frac{\lambda_1^6}{125a_0^3}e^{-\lambda_1/5a_0}+\frac{6}{25a_0}\lambda_1^5e^{-\lambda_1/5a_0}-\frac{18}{5a_0}\lambda_1^4e^{-\lambda_1/5a_0}-180a_0\lambda_1^2e^{-\lambda_1/5a_0}-1800a_0^2\lambda_1e^{-\lambda_1/5a_0}-9000a_0^3e^{-\lambda_1/5a_0}\right]^{\text{limits}}\left[-\frac{\lambda_2^3}{5a_0}e^{-\lambda_2/5a_0}+\lambda_2^2e^{-\lambda_2/5a_0}-10a_0\lambda_2e^{-\lambda_2/5a_0}-50a_0^2e^{-\lambda_2/5a_0}\right]^{\text{limits}}+\left[-\frac{\lambda_1^5}{125a_0^3}e^{-\lambda_1/5a_0}+\frac{7}{25a_0^2}\lambda_1^4e^{-\lambda_1/5a_0}-\frac{20}{5a_0}\lambda_1^3e^{-\lambda_1/5a_0}+12\lambda_1^2e^{-\lambda_1/5a_0}-60a_0\lambda_1e^{-\lambda_1/5a_0}-300a_0^2e^{-\lambda_1/5a_0}\right]^{\text{limits}}\left[-\frac{\lambda_2^4}{5a_0}e^{-\lambda_2/5a_0}-20a_0\lambda_2^2e^{-\lambda_2/5a_0}-200a_0^2\lambda_2e^{-\lambda_2/5a_0}-1000a_0^3e^{-\lambda_2/5a_0}\right]^{\text{limits}}\right\}.$$

and on substituting the above limits we have: $e_1=0.0055\ e$; $e_2=0.0820\ e$; $e_3=0.0187\ e$; $e_4=0.0219e$; $e_5=0.1907\ e$; $e_6=0.6792\ e$; as shown in Table I and in Fig. 1–g.

[7] F. G. Slack, Ann. d. Physik **80**, 582 (1927). The statement that there will always be $(n-m)$ regions given here is incorrect. This holds only for the special cases $k_1=0$ or $k_2=0$ where there are no intersecting parabolas for which ρ disappears. The number of regions in the general case is given by $(k_1+1)\ (k_2+1)$.

TABLE I.

n	k_1–k_2–$(m+1)$	(k_1+1) (k_2+1)	Limits for λ_1	Limits for λ_2	e_{limits}	$\bar{x}$	$\bar{z}$
1	0–0–1	1	0–∞	0–∞	e	$1.178a_0$	0
2	0–0–2	1	0–∞	0–∞	e	$4.418a_0$	0
	1–0–1	2	0–$2a_0$	0–∞	$0.0786e$	$3.825a_0$	$3.0a_0$
			$2a_0$–∞	0–∞	$0.9210e$		
3	0–0–3	1	0–∞	0–∞	e	$9.664a_0$	0
	1–0–2	2	0–$6a_0$	0–∞	$0.1213\ e$	$7.975a_0$	$4.5a_0$
			$6a_0$–∞	0–∞	$0.8787\ e$		
	2–0–1	3	0–$1.76a_0$	0–∞	$0.0296\ e$	$7.310a_0$	$9.0a_0$
			$1.76a_0$–$10.24a_0$	0–∞	$0.102\ e$		
			$10.24a_0$–∞	0–∞	$0.868\ e$		
	1–1–1	4	0–$3a_0$	0–$3a_0$	$0.0025\ e$	$9.792a_0$	0
			0–$3a_0$	$3a_0$–∞	$0.1364\ e$		
			$3a_0$–∞	0–$3a_0$	$0.1364\ e$		
			$3a_0$–∞	$3a_0$–∞	$0.716\ e$		
4	0–0–4	1	0–∞	0–∞	e	$16.91a_0$	0
	1–0–3	2	0–$12a_0$	0–∞	$0.183\ e$	$16.92a_0$	$6.0a_0$
			$12a_0$–∞	0–∞	$0.817\ e$		
	2–0–2	3	0–$5.06a_0$	0–∞	$0.038\ e$	$17.46a_0$	$12.0a_0$
			$5.06a_0$–$18.8a_0$	0–∞	$0.175\ e$		
			$18.8a_0$–∞	0–∞	$0.787\ e$		
	3–0–1	4	0–$1.664a_0$	0–∞	$0.0147\ e$	$11.46a_0$	$18.0a_0$
			$1.664a_0$–$9.176a_0$	0–∞	$0.0583\ e$		
			$9.176a_0$–$25.16a_0$	0–∞	$0.095\ e$		
			$25.16a_0$–∞	0–∞	$0.831\ e$		
	1–1–2	4	0–$8a_0$	0–$8a_0$	$0.0179\ e$	$17.48a_0$	0
			0–$8a_0$	$8a_0$–∞	$0.172\ e$		
			$8a_0$–∞	0–$8a_0$	$0.172\ e$		
			$8a_0$–∞	$8a_0$–∞	$0.638\ e$		
	2–1–1	6	0–$2.34a_0$	0–$4a_0$	$0.00178e$	$16.78a_0$	$6.0a_0$
			0–$2.34a_0$	$4a_0$–∞	$0.0595\ e$		
			$2.34a_0$–$13.66a_0$	0–$4a_0$	$0.0148\ e$		
			$2.34a_0$–$13.66a_0$	$4a_0$–∞	$0.124\ e$		
			$13.66a_0$–∞	0–$4a_0$	$0.155\ e$		
			$13.66a_0$–∞	$4a_0$–∞	$0.645\ e$		
5	0–0–5	1	0–∞	0–∞	e	$26.16a_0$	0
	1–0–4	2	0–$20a_0$	0–∞	$0.2155\ e$	$26.45a_0$	$7.5a_0$
			$20a_0$–∞	0–∞	$0.7844\ e$		
	2–0–3	3	0–$10a_0$	0–∞	$0.0918\ e$	$24.65a_0$	$15.0a_0$
			$10a_0$–$30a_0$	0–∞	$0.1409\ e$		
			$30a_0$–∞	0–∞	$0.7673\ e$		
	3–0–2	4	0–$4.68a_0$	0–∞	$0.0341\ e$	$24.84a_0$	$22.5a_0$
			$4.68a_0$–$16.53a_0$	0–∞	$0.0337\ e$		
			$16.53a_0$–$38.80a_0$	0–∞	$0.0413\ e$		
			$38.80a_0$–∞	0–∞	$0.8909\ e$		
	4–0–1	5	0–$1.625a_0$	0–∞	$0.0093\ e$	$15.72a_0$	$30.0a_0$
			$1.625a_0$–$8.730a_0$	0–∞	$0.0218\ e$		
			$8.730a_0$–$22.77a_0$	0–∞	$0.0523\ e$		
			$22.77a_0$–$46.88a_0$	0–∞	$0.2075\ e$		
			$46.88a_0$–∞	0–∞	$0.7090\ e$		
	3–1–1	8	0–$2.08a_0$	0–$5a_0$	$0.00092e$	$24.80a_0$	$15.0a_0$
			0–$2.08a_0$	$5a_0$–∞	$0.0336\ e$		
			$2.08a_0$–$11.47a_0$	0–$5a_0$	$0.0095\ e$		
			$2.08a_0$–$11.47a_0$	$5a_0$–∞	$0.0690\ e$		
			$11.47a_0$–$31.45a_0$	0–$5a_0$	$0.0182\ e$		
			$11.47a_0$–$31.45a_0$	$5a_0$–∞	$0.1064\ e$		
			$31.45a_0$–∞	0–$5a_0$	$0.1617\ e$		
			$31.45a_0$–∞	$5a_0$–∞	$0.6003\ e$		
	2–2–1	9	0–$2.930a_0$	0–$2.930a_0$	$0.00063e$	$26.85a_0$	0
			0–$2.930a_0$	$2.93a_0$–$17.07a_0$	$0.00682e$		
			0–$2.930a_0$	$17.07a_0$–∞	$0.0732\ e$		
			$2.93a_0$–$17.07a_0$	0–$2.930a_0$	$0.00682e$		
			$2.93a_0$–$17.07a_0$	$2.93a_0$–$17.07a_0$	$0.01905e$		
			$2.93a_0$–$17.07a_0$	$17.07a_0$–∞	$0.1322\ e$		
			$17.07a_0$–∞	0–$2.930a_0$	$0.0732\ e$		
			$17.07a_0$–∞	$2.93a_0$–$17.07a_0$	$0.1322\ e$		
			$17.07a_0$–∞	$17.07a_0$–∞	$0.5560\ e$		
	2–1–2	6	0–$6.34a_0$	0–$10a_0$	$0.0055\ e$	$29.25a_0$	$7.5a_0$
			0–$6.34a_0$	$10a_0$–∞	$0.0820\ e$		
			$6.34a_0$–$23.66a_0$	0–$10a_0$	$0.0187\ e$		
			$6.34a_0$–$23.66a_0$	$10a_0$–∞	$0.0219\ e$		
			$23.66a_0$–∞	0–$10a_0$	$0.1907\ e$		
			$23.66a_0$–∞	$10a_0$–∞	$0.6792\ e$		
	1–1–3	4	0–$15a_0$	0–$15a_0$	$0.0296\ e$	$27.20a_0$	0
			0–$15a_0$	$15a_0$–∞	$0.1886\ e$		
			$15a_0$–∞	0–$15a_0$	$0.1886\ e$		
			$15a_0$–∞	$15a_0$–∞	$0.5931\ e$		
6	0–0–6	1	0–∞	0–∞	e	$37.41a_0$	0
7	0–0–7	1	0–∞	0–∞	e	$50.66a_0$	0

Similar evaluations[8] have been made for all possible quantum combinations through $n=5$ and thus the configurations are given for the initial and final states resulting in several of the spectral lines of the Lyman, Balmer, and Paschen series for which the most reliable observations have been made. The results of the computations are given in Table I. In column 1 is given the total quantum number $n=(k_1+k_2+m+1)$. In the second column the values of k_1, k_2, and $(m+1)$ are given, in the third column the value of $[(k_1+1)(k_2+1)]$ or the number of regions into which the space about the nucleus is divided by the parabolas for which ρ disappears. Columns 4 and 5 give respectively the limits of the integrations over λ_1 and λ_2 in units of $a_0=0.528\times10^{-8}$ cm, while column 6 gives the results of the integration over these limits in terms of the total electronic charge e. Since the general expressions are symmetrical with respect to k_1 and k_2 results are given only for those combinations resulting in zero or positive values of (k_1-k_2).

Also in order to convey pictorially the form of the configurations we show in Fig. 1 to scale ($a_0=0.528\times10^{-8}$ cm) the various possible configurations for the total quantum number $n=5$ with the exception of the substate $k_1=k_2=0$, $(m+1)=5$ which results in a toroidal charge in a single region about the nucleus. The solid line parabolas are those for which $\rho=\psi\bar{\psi}=0$ and they are plotted to the rectangular coordinates x and z where the $+z$ direction, the axis of the λ_2 parabolas, is the positive direction of the electric field. The nucleus is at the origin. The figures represent sections in the zx plane and the values of e_{limits} given are the average electronic charge contained in the total volume obtained when the areas shown are revolved about the z axis. The value of $\bar{z}$ the average z coordinate[9] of the electronic charge as shown in each figure is computed from the general expression $\bar{z}=3/2na_0(k_1-k_2)$. This is also given in column 8 of Table I. For the states with k_1 and k_2 interchanged that is for states $k_1=0$, $k_2=1$, $(m+1)=4$; $k_1=0$, $k_2=2$, $(m+1)=3$; etc. the configurations will be identical to those shown but with the direction of the electrical field reversed.

The values of $\bar{x}$ or the average x coordinates of the charge in any plane are not so easily determined since the expression

$$\bar{x}=\iiint C\rho x\,dv=\int_0^\infty\int_0^\infty\int_0^{2\pi} C\rho(\lambda_1\lambda_2)^{1/2}\cos\phi\ \tfrac{1}{4}(\lambda_1+\lambda_2)d\lambda_1 d\lambda_2 d\phi$$

involves fractional exponents and the general integral may be expressed only as a series. For any individual quantum state however the expression may be reduced to a series with a finite number of terms of the form [10] $\int_0^\infty \lambda^P e^{-\lambda/na_0}d\lambda$ which are readily evaluated. The integration results in the common gamma function. The angle ϕ is set equal to zero and $\bar{x}$ thus is the distance from the z axis to the cylindrical shell, concentric with the z axis, which divides the

[8] Thanks are due to Messrs. Frank Burns and T. C. Butler of Vanderbilt for the evaluation of certain of these integrals.

[9] F. G. Slack, Ann. d. Physik **80**, 579 (1927).

[10] Thanks are due to Professor J. S. Morrel of Vanderbilt University.

electronic charge in half. Or as shown in Fig. 2, drawn for the state $3-1-1$ the values of $\bar{x}$ and $\bar{z}$ determine a ring which locates the average position of

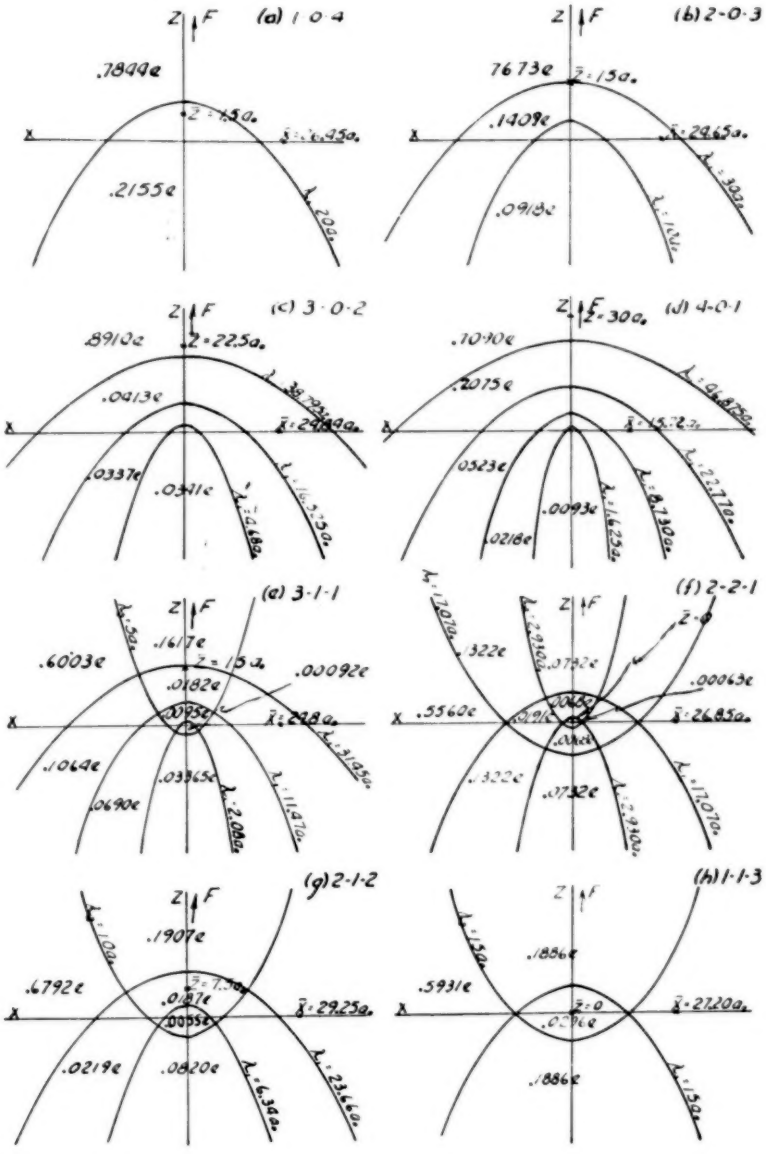

Fig. 1. Electronic configuration for quantum state $n=5$.

the electronic charge with respect to the nucleus. The values of $\bar{x}$ are given in column 7 of Table I and shown on the x axis in the figures of Fig. 1.

Attention is called to the point that for the quantum states $0-0-1$, $0-0-2$, etc. (i.e. for $k_1=k_2=0$, the circular orbits of the Bohr atom) the

values of $\bar{x}$ are not n^2a_0 as in the Bohr atom but for $n=1$, $\bar{x}=1.178a_0$, $n=2$, $\bar{x}=4.4178a_0$ and for $n=5$, $\bar{x}=26.16a_0$ etc. In general for $k_1=k_2=0$ we have

$$\bar{x}_n = \frac{(2n+1)!(2n-1)!\pi a_0}{2^{4n}\, n!\,[(n-1)!]^3}.$$

This arises from the degeneracy of the system in the case of the unperturbed atom.

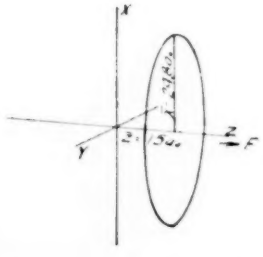

Fig. 2. Location of average electronic charge for state 3–1–1.

As stated in the introductory paragraph calculations of this type have been used by the author to explain the intensity dissymmetry found between the long and short wave components of the hydrogen canal ray light in an electric field parallel to the motion of the beam. It appears to the author that it should be possible to explain the discrepancies between the intensity ratios found by Mark and Wierl[11] and those calculated on the Schrödinger theory on the basis of impact probability computed from the above given configurations. This problem and that of polarization in hydrogen canal-ray light due to impact are now under investigation from this point of view.

[11] H. Mark and R. Wierl, Zeits. f. Physik **53,** 526 (1929); **55,** 156 (1929); **57,** 494 (1929).

A POSSIBLE ORIGIN OF THE BAND AT 2540 IN THE SPECTRUM OF MERCURY VAPOR

By R. Rollefson
University of Wisconsin, Madison

(Received March 26, 1930)

Abstract

It can be shown that the band at 2540A in the spectrum of mercury vapor can be accounted for on the basis of a molecule with low energy of dissociation, in agreement with the work of Koernicke who used this band to determine the heat of dissociation of Hg_2. Certain possibilities are suggested for explaining the high value of the heat of dissociation obtained by Mrozowski.

MUCH of the recent work on the spectrum of mercury vapor has concerned itself with the fluted bands lying between 3000 and 1850A, especially those to the short wave-length side of the resonance line 2536A. By assuming these bands to be due to Hg_2, and correlating the electronic levels involved with certain atomic levels, Mrozowski[1] has been able to obtain a value for the heat of dissociation of Hg_2 in the normal electronic state, using an extrapolation to obtain the band convergence point. The values obtained ranged between about 10 and 20 k cal/mol, depending on which band was used, but the indication was that the result should be nearer 20 than 10 since the lowest value was obtained by using a long extrapolation and hence was less reliable than the others. Using a different method, the study of the change in absorption by Hg vapor of three lines in the cadmium spark, 2144A, 2573A, and 2749A, as a function of the temperature, he obtained approximately 17 k cal/mol. These results are of a different order of magnitude from the ones obtained by Franck and Grotrian[2] (1 k cal/mol) and later by Koernicke[3] (1.4 k cal/mol). The latter investigators, however, made use of the decrease in intensity of absorption in a definite band, that at 2540, with increasing temperature. It is the purpose of this note to show that this band at 2540, which was used by Koernicke in his determination of the heat of dissociation of Hg_2, may be rather easily accounted for if we assume his small value for the energy of dissociation to be correct. We thus have two self consistent groups of phenomena which seem to contradict one another.

Considerations concerning the type of molecule one would expect to result from the union of two closed-shell atoms would seem to indicate that it should have a small energy of binding. If one considers a configuration consisting of two such atoms, attracting and repelling forces may each be expected to vary inversely as a high power of the distance between them,

[1] Mrozowski, Zeits. f. Physik **55,** 338 (1929).
[2] Franck and Grotrian, Zeits. f. techn. Physik **3,** 194 (1922).
[3] Koernicke, Zeits. f. Physik **33,** 219 (1925).

due to the high degree of symmetry of the atoms. If, then, we should plot the potential energy of the configuration as a function of the nuclear separation (following Franck) we should obtain a curve similar to I, Fig. 1. Such a sharp curvature of the potential energy curve indicates that the frequency of vibration in the zeroth vibrational state would be comparatively large, hence the energy of this lowest level might well be nearly that necessary for dissociation. In fact this ground state might be the only existing vibrational state connected with the lowest electronic level of Hg_2. A case similar to this has already been treated according to the new quantum mechanics by Peierls,[4] who also suggested the possibility of the application of his results to homopolar molecules with polarization binding. The latter is very probably what is dealt with in the case being considered, that of a molecule formed

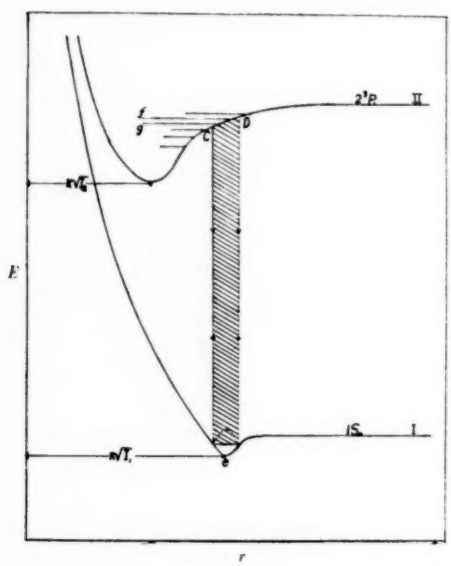

Fig. 1

by the union of two unexcited mercury atoms. Thus curve I, with only one vibrational level may be taken to represent the ground level of such a molecule.

With one atom excited, however, conditions would be somewhat changed. The polarizability and hence the binding force would be greater, and consequently the internuclear distance corresponding to equilibrium would be diminished, resulting in a potential energy curve similar to II and a smaller moment of inertia for the molecule. Applying the Franck-Condon principle for determination of the intensity of bands, we may represent the most probable transitions by the shaded area in the diagram. The number of intense bands would then be determined by the number of vibrational levels between C and D. Then, since a decrease in the moment of inertia is involved in the transition, these bands would be shaded toward shorter wave-lengths. If, for

[4] Peierls, Zeits. f. Physik **58**, 59 (1929).

instance, there were two vibrational levels *f* and *g* between *C* and *D*, we should have two bands, sharp on the long wave-length side and shaded toward the resonance line 2536, and if the energy difference between *f* and *g* were small, the two bands would be partially superposed. This is in complete agreement with what has been observed by Wood and Voss.[5] Thus the band at 2540 can be accounted for by assuming a low heat of dissociation for unexcited Hg_2, and this same band, when studied by Koernicke's method indicates that neutral Hg_2 has that low heat of dissociation.

In the light of the above it may be well to consider again the results of Mrozowski. Although the consistency of the results he obtained argues in favor of his interpretation, still it seems reasonable to assume that agencies other than Hg_2 contribute to the absorption by mercury vapor in the regions he used for determining the heat of dissociation. In the case of the line 2573 for instance, it is possible that Hg_2 is responsible for none of the absorption, but that what occurred was an interaction of radiation and impact, that is, absorption during collision, such as has already been discussed by Oldenberg,[6] or absorption by quasi-molecules as discussed by Born and Franck.[8] A possible explanation of the fact that the fluted bands indicate a large energy of dissociation may be that the bands do not involve a transition to or from the lowest electronic level of a molecule composed of two unexcited mercury atoms. For example Walter and Barratt[7] have been able to obtain the fluted band between 3000 and 2600 only when oxygen was present in the absorption tube. This band has the variation in intensity characteristic of a triatomic molecule, with no sharp edges such as one would expect in a band due to a diatomic molecule, and may be due to Hg_2O. The other bands used by Mrozowski may be due to a mercury molecule, but not necessarily the same type of molecule which gives rise to 2540.

The writer acknowledges his indebtedness to Professors C. E. Mendenhall and G. Wentzel for helpful criticism in the writing of this note.

[5] Wood and Voss, Proc. Roy. Soc. **A119,** 698 (1928).
[6] Oldenberg, Zeits. f. Physik **51,** 605 (1928).
[7] Walter and Barratt, Proc. Roy. Soc. **A122,** 201 (1929).
[8] Born and Franck, Zeits. f. Physik **31,** 411 (1925).

THE IONIZATION OF HYDROGEN BY SINGLE ELECTRON IMPACT

By Walker Bleakney
Physical Laboratory, University of Minnesota

(Received April 11, 1930)

Abstract

From an analysis of the theoretical potential energy curves for the H_2 molecule as outlined by Condon the theoretical predictions for the types of ions resulting from primary impacts with electrons are described. These predictions include the formation of H_2^+ at 15.25 volts, H^+ at 17.9 volts, H_2^+ at about 30 volts which then dissociates with several volts kinetic energy, and H_2^{++} at about 50 volts which also dissociates with kinetic energy. Using a mass spectrograph the experimental results of a study of the primary ions in hydrogen indicate the formation of H_2^+ at 15.4 ± 0.1 volts, H^+ at 18.0 ± 0.2 volts, and H^+ at 26 to 30 volts, the last having various amounts of kinetic energy.

Curves are given showing the relative number of each of these types of ions from which it appears that at the higher velocities about 92 percent of the total number of ions formed is of the H_2^+ type, 1 percent of the H^+ corresponding to the 18 volt potential, and 7 percent of the H^+ having kinetic energy. The probability of ionization for all types together as a function of the electron velocity is given by a curve, plotted to an arbitrary scale, which exhibits a well-defined maximum at 60 volts.

Introduction

THE ions produced by electron impact in hydrogen have been studied by the method of positive ray analysis so many times and by so many investigators that it might, at first sight, seem useless to try to make much more progress in this direction. As early as 1916 Dempster[1] designed a mass spectrograph with which he studied the ions produced in hydrogen by 800 volt electrons. Since that time somewhat similar experiments have been carried out by Smyth,[2] Hogness and Lunn,[3] Kallmann and Bredig,[4] Dorsch and Kallman,[5] and Brasefield.[6] The consensus of opinion of these observers is that their experiments have failed[7] to show that any ion other than H_2^+ may result from a single impact with an electron. The evidence from the experiment to be described[8] points toward a different conclusion. Moreover certain aspects of the theory of the hydrogen molecule predict several possible modes of production of the H^+ ion at a single impact.

[1] A. J. Dempster, Phil. Mag. **31,** 438 (1916).

[2] H. D. Smyth, Proc. Roy. Soc. **A105,** 116 (1924), and Phys. Rev. **25,** 452 (1925).

[3] T. R. Hogness and E. G. Lunn, Proc. Nat. Acad. Sci. **10,** 398 (1924), and Phys. Rev. **26,** 44 (1925).

[4] H. Kallmann and M. A. Bredig, Zeits. f. Physik **34,** 736 (1925), and Zeits. f. Physik **43,** 16 (1927).

[5] K. E. Dorsch and H. Kallmann, Zeits. f. Physik **44,** 565 (1927).

[6] C. J. Brasefield, Phys. Rev. **31,** 52 (1928).

[7] In their first papers both Smyth, and Hogness and Lunn (see references 2 and 3) reported H^+ as a primary process but later both reported these results as inconclusive.

[8] W. Bleakney and J. T. Tate, Phys. Rev. **35,** 658 (1930) (Abstract).

THEORY

Before the present experiment was undertaken Professor Condon drew up an outline of the results one might expect to find in making an e/m analysis of the primary ions in hydrogen. The essential ideas of this outline have been discussed by Condon,[9] and Condon and Symth,[10] and the particular points pertinent to the present experiment will be reviewed here in some detail.

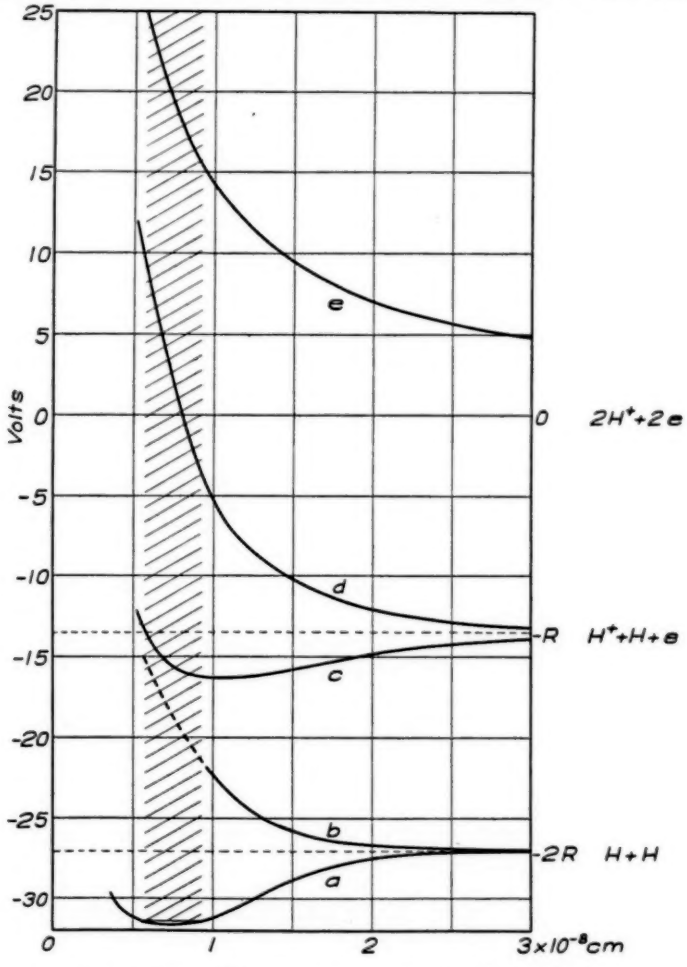

Fig. 1. Potential energy curves for the H_2 molecule.

In Fig. 1 are represented some of the theoretical potential energy curves for the hydrogen molecule. The potential energy in volts is plotted as a function of the nuclear separation in Angstrom units. Curves a and b represent the two solutions for the problem of bringing two H atoms in the normal state near each other to form an H_2 molecule as calculated by Sugiura[11] from the theory of Heitler and London.[12] Curve a has been altered slightly in order to

[9] E. U. Condon, Phys. Rev. **35,** 658 (1930) (Abstract).
[10] E. U. Condon and H. D. Smyth, Proc. Nat. Acad. Sci. **14,** 871 (1928).
[11] Y. Sugiura, Zeits. f. Physik **45,** 484 (1927).
[12] W. Heitler and F. London, Zeits. f. Physik **44,** 455 (1927).

fit the data as given by Birge and Jeppesen[13] and *b* has been lowered somewhat in the dotted region. In like manner curves *c* and *d* represent the two solutions for the problem of the formation of the H_2^+ molecular ion from a normal H atom and a proton. Curve *c* is that calculated by Burrau[14] and *d* is from the paper by Morse and Stueckelberg.[15] Curve *e* represents the potential energy of the H_2^{++} molecule due to the Coulomb force of repulsion between the two protons. The width of the shaded band corresponds to the range of nuclear separations executed by the hydrogen molecule in its lowest vibrational state.[16] The effect of rotational energy has been disregarded since it would add the same amount of energy to all the curves.

Now if a normal H_2 molecule is transformed by an electron impact from its lowest energy level on *a* to one of the states represented by the other curves it will, according to the Franck-Condon principle, suffer meanwhile little change in nuclear separation. Immediately after the transition, therefore, there is a high probability that the point representing the energy state of the molecule will lie within the shaded area. Hence, transitions are represented in this diagram by vertical or nearly vertical jumps from one state to another. Transitions from the normal to the state *b* would result in subsequent dissociation into two normal atoms each having several volts kinetic energy. This transition has no significance in the present experiment since only ions are measured. A jump to the state *c* results in the ordinary H_2^+ ion which should, according to this scheme, occur at 15.25 to 17.9 volts with various amounts of vibrational energy. An inspection of the figure shows that there is a small chance of a transition to a point on this curve which lies above the dotted line and the molecule in this state would then dissociate. Hence a small number of H^+ ions should be predicted at potentials above 17.9 volts. From 27 to 40 volts should be required to raise the molecule from its normal state to that represented by curve *d* where dissociation would occur into a normal H atom and a proton each having from 5 to 11 volts kinetic energy. Finally to strip both electrons from the H_2 molecule at a single blow should require from 46 to 56 volts and the two protons would then fly apart each with 7.5 to 12.5 volts kinetic energy. Between the last two stages there are many other transitions possible as a result of which the molecule would dissociate into a proton and an excited atom. Summarizing, then, the theory would predict the following primary reactions;

1. $H_2 \rightarrow H_2^+ + e$	15.4—17.9 volts
2. $H_2 \rightarrow H^+ + H + e$	17.9—18.0 volts
3. $H_2 \rightarrow H^+ + H + e +$ kinetic energy	27 —40 volts
4. $H_2 \rightarrow 2H^+ + 2e +$ kinetic energy	46 —56 volts.

Apparatus and Procedure

The apparatus was the same as that used for the study of mercury ions[17] and the details will therefore not be given here. In the present experiment the

[13] R. T. Birge and C. R. Jeppesen, Nature **125,** 463 (1930).
[14] Burrau, Kgl. Danske Vid. Selskal. Math-fys. Med. **7,** 14 (1927).
[15] P. M. Morse and E. C. G. Stueckelberg, Phys. Rev. **33,** 932 (1929).
[16] For the details of this theory see E. U. Condon, Phys. Rev. **32,** 858 (1928).
[17] W. Bleakney, Phys. Rev. **34,** 157 (1929) and Phys. Rev. **35,** 139 (1930).

flow method was used, the hydrogen being admitted to the system through a palladium tube. This tube was surrounded on the outside with hydrogen at atmospheric pressure and its temperature was maintained at the required value by an electric heating element. The rate of flow of the gas into the apparatus could be regulated by adjusting the rheostat controlling the heating current. The pressure of the gas in the ionization chamber was not measured but it was estimated to be in all cases in the neighborhood of 10^{-3} mm Hg. A trace of mercury vapor was allowed to remain in the apparatus for calibration purposes.

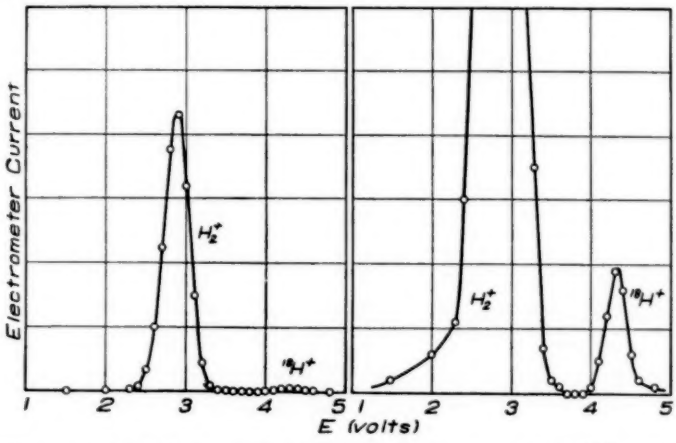

Fig. 2. A typical e/m analysis curve. Electron velocity = 150 volts. The second curve is the first magnified 40 times.

Experimental Results

Primary ions in hydrogen. Figure 2 illustrates an e/m analysis curve for hydrogen ions produced by 150 volt electrons. The symbol $^{18}H^+$ is used to designate the atomic ion which begins to appear at 18 volts. The two curves represent the same data but in the second the ordinates have been expanded forty times. These two ions have at the instant of formation very little kinetic energy compared to that given them by the analyzing fields. In Fig. 3 is shown another peak obtained when the field V_2 ordinarily used to draw out the positive ions was made 1 volt per cm negative. In this case all the ordinary ions were prevented from reaching the analyzing chamber but those having high kinetic energy reached the collector. The number, however, was small and it was necessary to increase the sensitivity of the electrometer considerably in order to detect them at all. It will be noticed that the peak is very broad compared to those in Fig. 2. The second curve in Fig. 3 represents the maximum height of this peak as a function of the electron velocity. It is evident that weak ionization sets in at about 26 volts and becomes quite strong at 30 volts. This ion will be designated by the symbol $^{30}H^+$. These results can only be interpreted as *primary* processes. No trace of secondary reactions such as the formation of H_3^+ could be found.

Critical potentials for ionization. The ionization potentials for H_2^+ and $^{18}H^+$ obtained by plotting the heights of the peaks as functions of the electron velocity in volts are shown in Fig. 4. The Hg^+ ion is included in order to

determine one point on the voltage scale assuming its ionization potential to be 10.4 volts. In this figure the curve for $^{30}H^+$ was obtained by measuring with a galvanometer the positive current reaching the plate, to which the

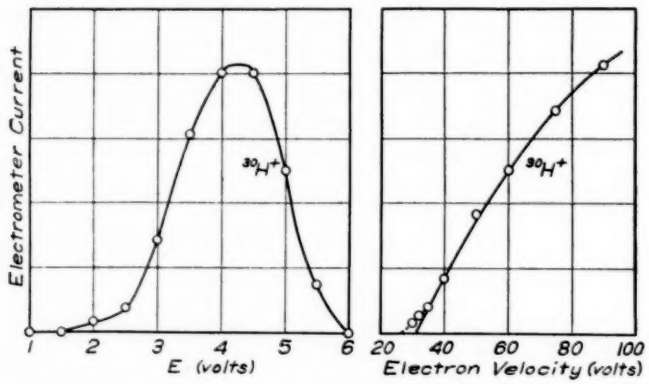

Fig. 3. A broad peak due to the initial high velocity of the ions. The second curve shows the ionization potential.

total positive ion current is ordinarily measured, against a small retarding field. This curve checks closely the one shown in Fig. 3 which was obtained in a different way. It would indicate that the critical potential for the forma-

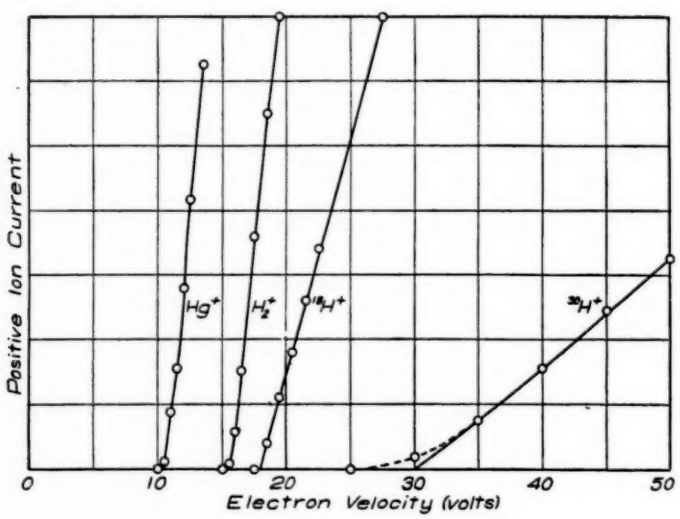

Fig. 4. Ionization potentials.

tion of this ion is about 26 volts while strong ionization of this type sets in from 30 to 35 volts. A summary of these results may be expressed in the following way.

Process	Predicted	Observed
1. $H_2 \rightarrow H_2^+ + e$	15.25 volts	15.4 ± 0.1 volts
2. $H_2 \rightarrow H + H^+ + e$	17.9	18.0 ± 0.2
3. $H_2 \rightarrow H + H^+ + e +$ kin. energy	27.	$26 \pm 1.$

These conclusions constitute a striking confirmation of the theory.

Relative numbers of the different ions. The number of $^{18}H^+$ ions relative to the number of H_2^+ ions was determined by finding the relative areas[18] under the peaks in the e/m analysis curves. Such a procedure was unsuitable, however, for determining the relative number of those ions having kinetic energy

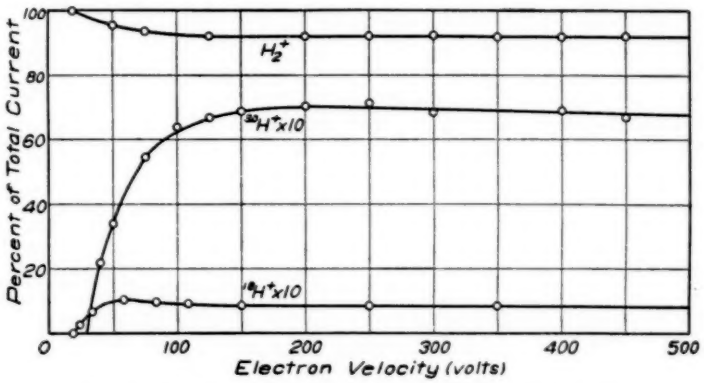

Fig. 5. Relative intensity of the different types of ions.

since only a small fraction is shot out in the direction of the analyzer. A rough estimate of their intensity was made in the following manner. The total positive ion current was measured with the galvanometer in the usual way and then the field V_2 was reversed so that only ions having kinetic energy

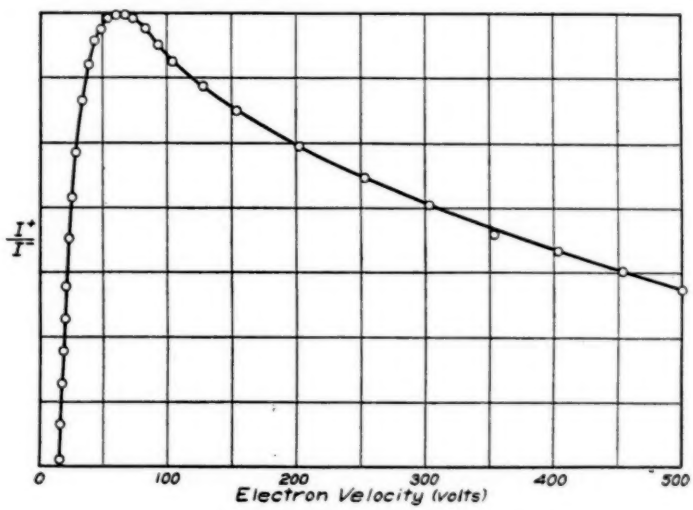

Fig. 6. Efficiency curve for hydrogen.

could reach the plate. This number reaching the plate was plotted as a function of the retarding field and the curve so obtained extrapolated to zero field. Knowing the solid angle subtended at the electron beam by the plate and assuming cylindrical symmetry the fraction of the total current due to those ions having kinetic energy was calculated. The results are shown in Fig.

[18] For a discussion of the assumption that the numbers are proportional to the areas see the second paper of reference 17.

5 where the ordinates for $^{18}H^+$ and $^{30}H^+$ have each been multiplied by ten. The curve for $^{30}H^+$ may include ions having kinetic energy as a result of some transition other than the 30 volt variety but it is believed that these are relatively very small in number.

Efficiency of ionization. Since in this experiment the pressure of the gas was not measured the efficiency of ionization could only be determined within an arbitrary constant factor. The result is given by the ratio of the electron current to the total positive ion current plotted as a function of the electron velocity. The curve, Fig. 6, shows a well-defined maximum at 60 volts. From the previous data it may be concluded that over ninety percent of the total number is made up of H_2^+ ions.

There is a marked difference between the shape of this curve and that reported by Compton and Van Voorhis[19] in that the maximum appears at a much lower electron velocity and the curve falls off more rapidly beyond this point. Qualitatively the agreement with the data of Hughes and Klein[20] is good.

Discussion

It is believed that the results of this experiment yield, at present, the most direct evidence for the existence of those repulsive forces represented by the potential energy curves for the H_2^+ ion. It will be recalled that such an energy state is contrary to the concepts of the classical theory which predicts only a force of attraction. Indirectly these results also lend support to the reality of the other repulsive curves predicted by the quantum theory.

The determinations of the critical potential for the formation of H_2^+ as made by a large number of observers[21] cluster about a mean value of about 16.0 volts. That found in this experiment, 15.4 volts, is lower than any experimentally determined value known to the writer but it is believed that the method lends itself to greater accuracy than any of the previous methods. The close agreement with the theory lends support to this view. As Condon[9] has pointed out, it is now impossible in the light of the theory and these experiments to interpret the critical potential near 30 volts which has been reported by Krüger,[22] Horton and Davies,[23] and Vencov[24] as double ionization accompanied by dissociation. In the present work a search was made for the 50 volt transition resulting in H_2^{++} but only slight evidence for its existence could be found. An effort is being extended in this laboratory to throw more light on this question with an apparatus designed to measure the velocity distribution of high velocity ions.

The author is greatly indebted to Professors E. U. Condon and John T. Tate for their many helpful suggestions.

[19] K. T. Compton and C. C. Van Voorhis, Phys. Rev. **26,** 436 (1925) and Phys. Rev. **27,** 724 (1926).

[20] A. L. Hughes and E. Klein, Phys. Rev. **23,** 450 (1924).

[21] For a compilation of these values see the paper by Hogness and Lunn, Phys. Rev. **26,** 44 (1925).

[22] T. Krüger, Ann. d. Physik **64,** 288 (1921).

[23] F. Horton and A. C. Davies, Phil. Mag. **46,** 872 (1923).

[24] S. Vencov, Comtes Rendus **189,** 27 (1929).

ELECTRON ENERGY LOSSES IN MERCURY VAPOR

By Castle W. Foard
State University of Iowa, Iowa City

(Received March 31, 1930)

Abstract

An improved magnetic spectrum method was used to determine the energy losses sustained by slow speed electrons in mercury vapor. Electron energies up to 60 volts were used, the main region of interest being from 0 to 25 volts. The energy losses detected, below that required for ionization, were; 4.9, 5.4, 6.7, 7.7, 8.8, 9.8 volts. These correspond to practically all the transitions of a valence electron from the basic $1S$ level up to each of the higher levels to $4P$. No evidence of other losses such as are observed by the photoelectric method were found. At voltages above 10.4, the ionization potential, electrons seem to be able to give up any quantity of energy in excess of that required for ionization, the higher losses being favored. A very interesting loss of 11.07 volts has been found, which has not been recorded heretofore. It begins to be resolved at about 18 volts, and grows steadily with increasing voltage in much the same manner as the 6.7 volt loss. It is thought that this loss involves the simultaneous displacement of both valence electrons from their normal levels.

THE pioneer work on inelastic impacts of electrons with mercury atoms, by Franck and Hertz,[1] showed that the energy lost by the electron is quantized. At first there appeared to be but one type of inelastic impact, that in which the loss of energy was equivalent to a drop in potential of 4.9 volts. Since that time, three other types of losses have been found by this or similar methods.[2,3,4] The photoelectric method, developed by Franck and Einsporn,[5] is also capable of giving us an insight into the phenomena of impacts. The number of critical potentials found by this latter method is quite large —eighteen, in the work referred to, and a still larger number in the later work of Jarvis.[6] Some of these critical potentials have been shown [7,8] to be due to other effects than resonance collisions: but there has persisted a discrepancy between the results of each of these methods, not only with each other, but with the results of spectroscopic study.[9,10,11,12,13]

[1] Franck and Hertz, Verh. d. Deut. Phys. Ges. **16,** 457 (1914).
[2] Mohler, Foote, and Meggers, Phys. Rev. **10,** 101 (1917).
[3] Eldridge, Phys. Rev. **20,** 456 (1922).
[4] Whitney, Phys. Rev. **34,** 923 (1929).
[5] Franck and Einsporn, Zeits. f. Physik **2,** 18 (1920).
[6] Jarvis, Phys. Rev. **27,** 808 (1926).
[7] Webb, Phys. Rev. **24,** 113 (1924).
[8] Messenger, Phys. Rev. **28,** 962 (1926).
[9] Hertz, Naturwissenschaften **11,** 778 (1923).
[10] Eldridge, Phys. Rev. **23,** 685 (1924).
[11] White, Phys. Rev. **28,** 1125 (1926).
[12] Valasek, Phys. Rev. **29,** 817 (1927).
[13] Crozier, Phys. Rev. **31,** 800 (1928).

It seemed highly desirable that the inelastic impact method, which, in the past, has given the most meager results, should be improved, with a view to determining which of the impacts involve actual quantized energy losses to the electrons. For this purpose, the method used by Whitney[4] has certain points of advantage over other methods. The electrons which have lost energy are spread out into a velocity spectrum, and can be collected, group by group, without mutual interference. This makes possible the use of greater sensitivity, in the search for the less probable types of losses. While Whitney was primarily interested in the excitation functions of the more probable impacts, his failure, under apparently favorable conditions, to detect the losses observed by the photoelectric method increased the difficulty of a reconciliation between results of the two methods.

A possible explanation of this discrepancy, as Whitney points out, would be that the types of losses which he does not find, are very improbable, except when the electron has little more than the amount of energy required for the excitation. Since Whitney's apparatus was quite insensitive to very slow electrons, we can see how these collisions involving a total loss of energy, would, under this hypothesis, have escaped detection. We therefore set about to remove this limitation by increasing the sensitivity of the Whitney method for slow speed electrons, and at the same time, to improve the resolving power. An additional end has been gained by a change of procedure which allows the energy losses to be read directly in volts from an accurate potentiometer, rather than by means of a calibration curve.

Apparatus

The apparatus is pictured in Figs. 1 and 2. Electrons evaporating from the unthoriated tungsten filament F, are attracted toward the concentric cylinder C_1, during which time they may make elastic or inelastic impacts with the atoms of mercury vapor which fills this region. A sample of the electrons arriving at the cylinder pass through the slit S_1. The second cylinder, C_2, allows us to control the speed with which the electrons emerge from S_2. In the electric field free region outside the cylinders, the electrons are spread into a velocity spectrum by means of a uniform transverse magnetic field produced by a large pair of Helmholtz coils. Electrons having some definite speed, determined by the strength of the magnetic field used, will converge at a point 180° distant from S_1, along an arc of a circle of 5 cm radius. Here they are collected by a probe wire which is shielded from stray electrons. A Compton quadrant electrometer, shunted by a radioactive leak, measures the current to the probe, which is of the order of 10^{-11} amp.

The vacuum tube was made entirely of brass, 3/8″ thick, 20 cm diameter, and 22 cm long. The only metal parts of other material were the inner (molybdenum) cylinder and the tungsten filament. Two small glass windows and a reentrant liquid air trap, used in freezing out the mercury vapor from the outside region, were carefully shielded with brass wire gauze. The vacuum was kept below 10^{-5} mm, and liquid air traps employed constantly. The mercury vapor was introduced into the impact chamber from a furnace

heated reservoir maintained at various temperatures from 90° to 118°, depending on the pressure desired. The vapor pressure, under these conditions, is hard to estimate, since diffusion through the slit S_1 and the temperature of the impact chamber play an uncertain role; from the probability of certain types of losses, the pressure seemed to be of the order of 0.1 mm.

While a number of changes have been made, the tube, as described above, is essentially of the same type as that employed by Whitney. The chief point of difference lies in the addition of the auxiliary accelerating cylinder, C_2. By means of this cylinder, the speed of the electrons may be adjusted so that any particular group may be focused on the probe wire, without changing the magnetic field.

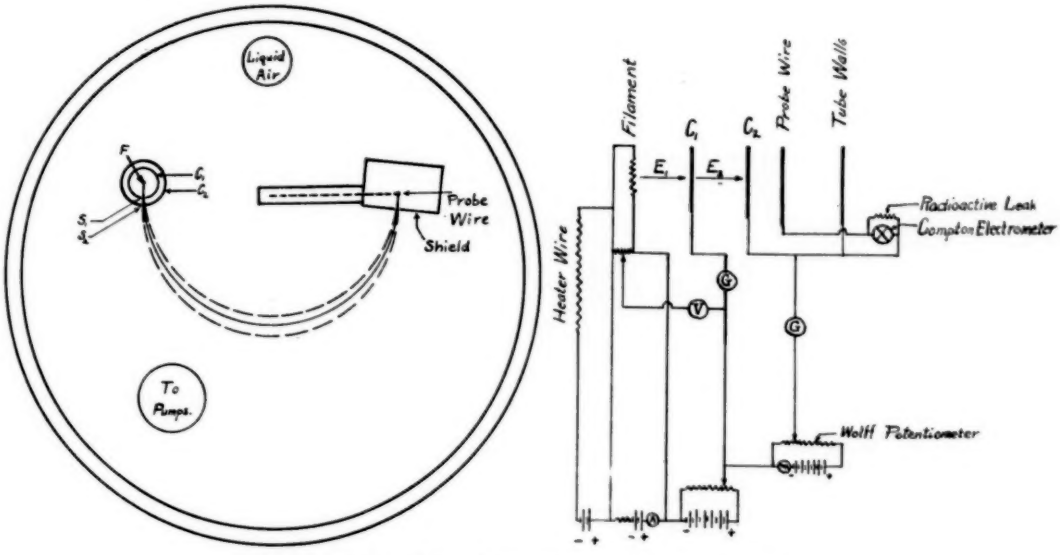

Figs. 1 and 2. Plan of apparatus and electrical circuit.

PROCEDURE

In Whitney's method, the electrons emerging from C_1 with various residual speeds, were collected, group by group, by varying the magnetic field. In the present work, the procedure was somewhat different. All of the electrons collected were made to travel the circular path to the probe, with the same speed, regardless of how much energy they had lost. This was accomplished by accelerating them enough between C_1 and C_2 to just make up for their loss in energy at impact. For example, the 6 volt curve in Fig. 4 was taken as follows. E_1, the potential on C_1, was set at 6 volts, the desired impact speed. E_2, the difference of potential between C_2 and C_1, was set at (say) 2 volts. The magnetic field was then adjusted for maximum probe current, i.e., for 8 volt electrons. E_2 was then varied from 0 to 8 volts, in convenient steps of, generally, 0.1 volt, and the data recorded directly on graph paper. Those electrons which have lost none of their initial 6 volts, will require but two volts to be brought to the probe wire: but those which

have lost 4.9 volts at an inelastic impact, will require that much more energy, or a total of 6.9 volts acceleration between the cylinders, in order to have the proper speed to be collected. The no-loss electrons then have, of course, 10.9 volts, and hence move in too large a circle to interfere. If the arbitrary two volt initial value of E_2 be neglected in plotting, the abscissas of the peaks give the values of the energy losses directly in volts, and the ordinates, approximately the relative probability of each type of impact, at a particular impact speed. The width of the peaks is due to several causes, such as velocity distribution in the original electron stream, imperfect focusing, and finite width of probe.

Fig. 3 shows the degree to which this method was successful in improving the sensitivity for slow speed electrons. The first curve is similar to that

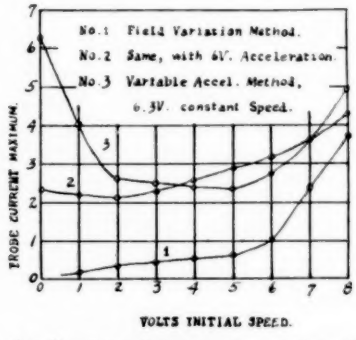

Fig. 3. Efficiency of collection of electrons as a function of their voltage.

published by Whitney, and shows the efficiency of collection of electrons, in the absence of the auxiliary cylinder. Curve 2 shows that, when this cylinder is inserted and maintained at a potential 6 volts above that of the first cylinder, the slow electrons are collected much better than before. In making curve 3, the new method of procedure was used. The total speed of collection was always 6.3 volts, but the speed with which they emerged from S_1 is varied from 0 upward. Slow electrons are still more favored than in the preceding curve, but the direct-reading characteristic of the new method is an additional advantage.

Results

Fig. 4 shows the type of curves that are obtained with electron energies below ionization. The 4.9 volt loss, which is the predominant one up to 9 volts, begins to show itself at as low as 4 volts. In that curve, it appears to be a loss of only 4.3 volts, rather than 4.9 volts. These two illusions, the detection of a loss at too low a voltage, and the apparent smallness of the loss are traceable to the rather large velocity distribution—amounting to about 1.6 V.—which is here present. Since the potential E_1 is measured with respect to the center of the emitting portion of the filament, a certain share of the electrons may well have enough more energy than the average, to be able to lose 4.86 V. After this loss, a subsequent addition of less than 4.86 V. would

be required in order to collect them at the normal speed. This effect is most prominent for the types of losses which increase most rapidly in the vicinity of their critical potentials. The occurrence of a loss by an electron which apparently does not have that much energy might also be due to impacts occurring between the two cylinders, after the electron has acquired part of the added potential E_2, though this is not considered likely.

At an impressed voltage of 5.2, an energy loss of 5.4 V. is clearly discernible, anticipated in voltage for the same reason as in the case of 4.9. A 6.7 V. loss is seen in the 6.5 volt curve, anticipated less than 4.9 was, and probably less than 5.4 would have been, had the latter not been partly obscured by the 4.9 V. peak.

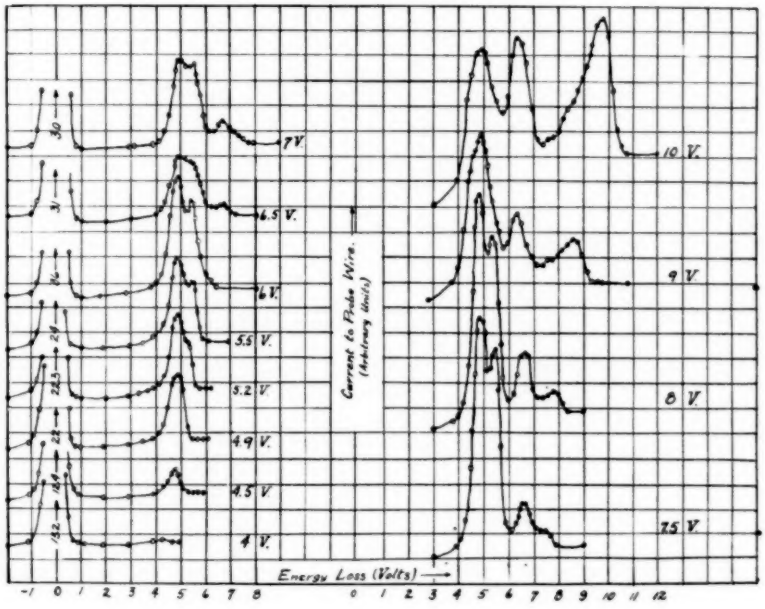

Fig. 4. Energy losses in Hg below ionization.

The failure of previous users of the inelastic impact method, to find a loss of 7.7 V., or 7.9 V., corresponding to transitions of the valence electron from the $1S$ to the $2s$ or $2S$ levels, has been a serious criticism of the completeness of the results to be obtained by this method. These levels are separated by approximately a volt on either side, from all other levels, and upward transitions to them should be easily observable, if their probability is at all large. That such a loss does occur is seen from the curves of Fig. 4, beginning with the one for 7.5 V. The probability of the loss, while always small, rises to a maximum and falls off to insignificance within two or three volts of its critical potential. The exact loss could not be determined with much accuracy, but appears to be 7.7 V., though 7.9 might also be present. It is interesting to note that Crozier[13] found that the intensity of the downward transitions from

$2s$ to $2p_{2,3}$, changed in a similar manner, while transitions from $2S$ had but one-third the probability in comparison.

The well-known loss of 8.8 V., and a loss of 9.8 V., sometimes observed, but attributed to two successive 4.9 V. losses, complete the list of losses less than that required for ionization. These may be seen better in Fig. 5, at impact speeds above ionization, because of their increased probabilities of occurrence. At 41 V., the 9.8 V. peak is at least as large as the single 4.9 V. peak, while the multiple collision peaks involving one or more 6.7 V. loss, are, quite properly, but a small fraction of the size of the single loss peak. This

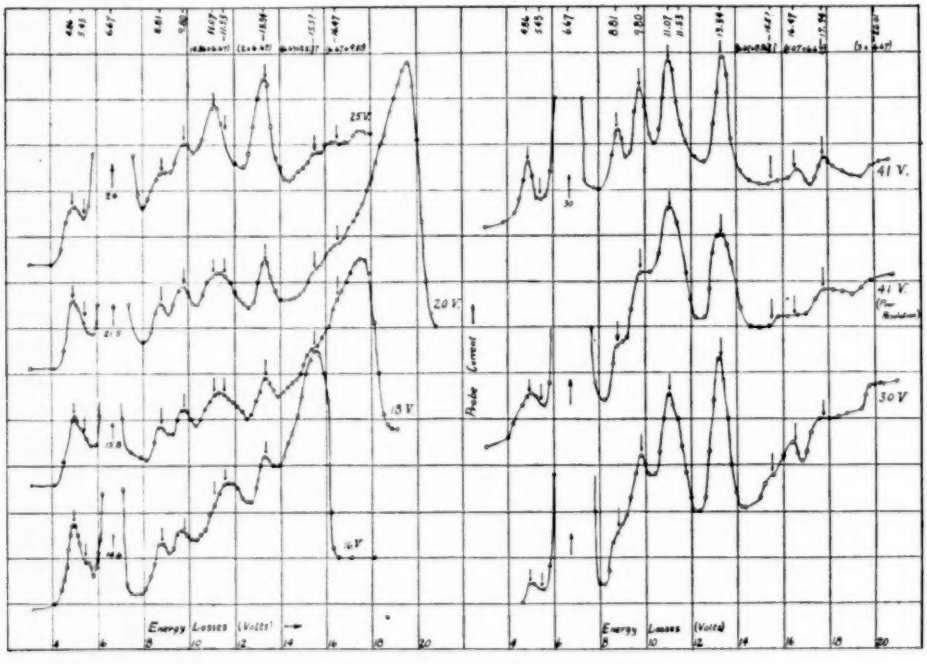

Fig. 5. Energy losses in Hg at higher electron voltages.

consideration, along with a study of the change of size of the 9.8 V. loss with change of vapor pressure, leaves little doubt of its interpretation as a single impact loss.

Ionization

In all the curves taken with impact speeds above about 10 V., the threshold current, upon which the inelastic impact peaks are superimposed, rises rapidly in the vicinity of the region indicating total energy loss. It falls again, of course, at a distance beyond the total loss value, equal to half the velocity distribution. In other words, this rather large group of electrons appears to lose any amount of their energy from about that required for ionization up to total loss, the great bulk of them being in the latter category. The absolute number of these electrons is probably a great deal less than would be inferred from the size of the peak, because of the facility of collec-

tion of slow electrons, as previously explained. It was suspected that these slow electrons might have lost their energy at reflection from the walls of one of the cylinders. To test this, the furnace was cooled to 25°C, when the slow speed peak persisted to a certain extent, while the inelastic impact peaks practically vanished. The conclusion derived from this was that a part of the effect was due to reflected electrons from the cylinder walls, but that the major portion was to be attributed to some kind of a loss involving the mercury vapor, presumably associated with ionization. Eldridge[3] came to the conclusion that, at ionization, both the impacting electron and the electron born of ionization had but a negligible amount of energy. What to do with the extra loss of energy is a moot question. Some later authors have supposed a sharing of the surplus energy by the two electrons: on this hypothesis, the current due to this source should be symmetrical about a line midway between total loss and ionizing loss; this is decidedly a different distribution than that observed here. This is, admittedly, an unsatisfactory way to leave the problem, but additional information is needed before a better interpretation can be made by this method.

Energy Losses Above Ionization

When relatively high potentials are being used, and the losses under investigation are but a fraction of the total electron energy, it becomes very advantageous to be able to use a retarding potential between the two cylinders C_1 and C_2, rather than an accelerating one, as was described in the investigation of losses near their critical potentials. Consider, for instance, the two curves in Fig. 5, marked 41 V. The upper curve was taken with a magnetic field set to collect 15.1 V. electrons to the probe wire. In order to collect the electrons which have lost no energy at impact, a retarding potential of 25.9 V. must be applied between the cylinders. As this retarding potential is reduced, which is equivalent to *increasing* the *accelerating* potential in the previous cases, electrons which have lost more and more energy are brought into focus and measured. This results in a controllable increase in the percent separation of the groups of electrons, with an accompanying increase in resolving power which is very desirable. The lower 41 V. curve was taken with a field set for 27.2 V. electrons, and hence with less retarding potential. The one-volt separation between the 8.8 and 9.8 V. losses is now but one-half the fraction of the whole path speed that it was before, and the peaks are no longer separated. With no retarding potential, the resolution was extremely bad. This improvement in resolution has been accomplished at the sacrifice of fidelity in the measurement of probabilities, in which we are not so much concerned in the present paper.

The chief point of interest in the curves of Fig. 5, is the 11.07 V. loss, which is seen to rise to an importance second only to that of the 6.7 V. loss, at this voltage. Its value may be observed very accurately, due to the presence of peaks of known value on either side of it, so that the value given is probably accurate to within 0.03 V. It makes its appearance at a potential unfavorable to its detection, because of the presence of the peak due to the

double impact loss 4.9+6.7. Rising steadily from about 18 V., where the masking peak drops rapidly, this loss becomes so prominent that, at 41 V., we even see a peak due to the double impact 11.07+6.67.

Several possible interpretations for this type of energy loss have been studied. No combination of the known losses in either the arc or the spark systems would give this value. Moreover, when the vapor pressure is changed, the size of the peak remains proportional to the single impact peaks rather than to the double impact peaks, which decrease more rapidly. It is therefore thought to involve but a single impact. If this were a *critical potential* method, a delay in the appearance of the loss until the energy of impact was somewhat above the amount required for ionization, might be interpreted as a delay in the process of ionization until some conservative force be overcome: but here, we are measuring the actual amount of the energy lost by the electron, regardless of the total energy possessed. Hence, some other type of quantized loss would have to accompany ionization, in order to account for the excess energy. According to the HgII energy values of Carroll,[14] the simultaneous ionization and spark excitation to the lowest level would involve 16.8 V. Even then, it is doubtful whether the loss would be quantized, because of the possibility of energy sharing by the two electrons, as in ordinary ionization.

The most likely interpretation so far found, seems to be that of simultaneous excitation of both valence electrons in the same atom, without ejection of either. So little is known concerning this interesting type of excitation, that a complete verification of this theory is not to be expected at this time. Sawyer[15] has classified four lines in mercury, which he attributes to such double transitions, and from them, arrives at the values of the three lowest "p'" levels.[16,17] The lowest of these has a wave number of -7860 (negative, because it lies above the ionization level), so that excitation to this level ($1S-p_3'$) would require 11.35 V. This is 0.28 V. more than that found in the present work, which is far too great a difference to be attributed to experimental error in either method. Sawyer points out, however, that this level was determined by a single line, which might have a different interpretation; the other, and higher levels have as many as three transitions observable, and hence are much less in doubt. It is possible that a reclassification of these lines, with a lower level in mind, might bring about a better agreement.

Conclusions

The energy losses observed in this work are; 4.9, 5.4, 6.7, 7.7, 8.8, 9.8, and 11.07 V.—all save the last named one being those predicted on spectroscopic grounds. The circumstances of the appearance of 7.7 both increase confidence in the data given by the inelastic impact method, and explain the

[14] Carroll, Phil. Trans. **225,** 357, A 634 (1926).
[15] Sawyer, J.O.S.A. **13,** 432 (1926). For pioneer work on p' levels see thefollowing articles.
[16] Wentzel, Phys. Zeits. **24,** 106 (1923); **25,** 182 (1924).
[17] Russell and Saunders, Astrophys. J. **61,** 8 (1925).

difficulty of detection of certain losses. Failure to detect 4.7 V. losses is attributed to the extremely large probability and rapid rise of the 4.9 V. loss, together with a rather large velocity distribution. Excitation to the $3S$ and to all of the "4" levels, involving about 9.2 and 9.5 V. losses, are thought to be even less probable than 7.7 V., and hence not detected. The unexplained losses of the photoelectric method were not observed, although they should have been, had they represented actual quantized losses of electronic energy of any appreciable probability. The energy loss at ionization is not quantized. The new loss, of 11.07 V., is thought to represent new data opening up the question of p' energy levels and simultaneous excitation of two valence electrons. The present method has not yielded spark terms, but may do so, if ionization be accomplished prior to the excitation dealt with here.

In conclusion, the author wishes to express his appreciation for the help and encouragement given him by the staff of the physics department of the University of Iowa, and especially for the constant and generous guidance of Professor J. A. Eldridge.

THE MOTION OF SLOW POSITIVE IONS IN GASES

By James S. Thompson
Ryerson Physical Laboratory, University of Chicago

(Received April 1, 1930)

Abstract

Positive caesium ions with velocities of 3.5 to 600 equivalent volts have been studied in hydrogen and helium. No absorption of the ions in the apparatus used is found for pressures below 0.01 mm of mercury. For the higher velocities this absence of absorption persisted for pressures as high as 0.05 mm of mercury. In all cases the ions were retarded in passing through the gas and there is an approximate probability distribution of ion energies about an average retarded value. The retardation in all cases is found to be proportional to the pressure. For Cs^+ ions in helium the percent loss of initial energy varies from 11.5 for 400 volt ions to 55 for ions of 3.5 volts initial energy. Similar results are found for hydrogen. Values of the constant, h, of the error curve which are characteristic of a particular distribution are given for various velocities and pressures. An interpretation of the absence of scattering and the retardation of the ions is given on the basis of elastic collisions between ion and gas molecule. It is found that no absorption of the Cs^+ ions would be expected until the pressures are high enough to give rise to multiple scattering. The data on retardation give values of the radius of the Cs^+ ion as: 1.78A in helium and 3.09A in hydrogen. The slowing up of the ions offers an explanation of the large absorption of Cs^+ in helium found by Ramsauer and Beeck. Probability considerations show that for increasing velocities the energy loss per collision found in the present experiments is less than that to be expected on the basis of elastic collisions.

The absorption of Li^+ ions has been studied by three methods for velocities of 20 to 900 equivalent volts. The coefficients of absorption, C, representing the effective absorbing cross section have been determined by two methods. The general dependence of C on the ion velocity is the same for the two types of apparatus used, but the values of C are found to depend on the dimensions of the absorbing chamber. The results have led to the interpretation of scattering in which forces other than those due to elastic collisions are effective. No general retardation of the Li^+ ions was found. Values of C found by Ramsauer and Beeck are interpreted in terms of the dimensions of their apparatus. It is concluded that no absolute significance may be attached to values of atomic radii determined from measurements of this kind.

WHEN a beam of positive ions moves through a column of gas there is in general a weakening of the bundle which may be due to a number of different processes of interaction between ion and gas molecule. Neutralization of the ions, either from the capture of a free electron or an ionization of the gas molecule, scattering or a combination of these effects will contribute to a decrease in intensity. In addition, any retardation of the ions may show itself as an absorption unless precautions are taken in the experimental method of measurement. It is customary to express any absorption of the ion bundle in the relation:

$$N = N_0 e^{-xp/760L} \qquad (1)$$

where N is the intensity of the beam after passing through a distance, x, of the gas at pressure p; N_0 the intensity of the incident ions, and L the absorption coefficient, also referred to as the mean free path under standard conditions. Writing L in terms of the radii of the ion and gas molecule,

$$\begin{aligned} L &= 1/\pi n(R_{ion} + R_{mol})^2, \text{ or} \\ C &= \pi(R_1 + R_2)^2 = 1/Ln \end{aligned} \tag{2}$$

where C may be termed the effective absorbing cross section. Most of the experiments on absorption of positive ions have yielded in effect values for L and C.

A study of the motion of hydrogen and helium ions in helium has been made by Dempster using his positive ray apparatus.[1] He found that protons with velocities corresponding to potential differences of 14 to 900 volts passed through many helium atoms without neutralization and with slight changes of velocity and direction; while 900 volt helium ions in helium were absorbed much more readily and showed a mean free path but little greater than the kinetic theory value. These were the first experiments of this kind with low velocity positive ions.

Durbin[2] and Ramsauer and Beeck[3] have studied the slow alkali metal ions in various gases and found in most cases abnormally long free paths varying up to ten times the kinetic theory value. Their experimental methods would not distinguish the three causes of absorption mentioned above.

Kennard[4] modified the method used by Durbin and Ramsauer and Beeck, and by measuring the ions of various velocities which passed through the gas column was able to detect a change in velocity as well as any weakening due to other causes. He found that for 90 volt Cs^+ ions in hydrogen there was a decrease in speed equivalent to 1.3 volts per collision, but no evidence of scattering or neutralization, for pressures up to 0.008 mm of mercury. Slowing up was also observed for 35 and 90 volt Cs^+ ions in both hydrogen and helium with only a slight weakening of the bundle due to other causes. For Cs^+ in argon no slowing up was observed but there was a rapid absorption of the bundle with pressure, which Kennard interpreted as due to neutralization.

Recently, Cox[5] has shown from experiments with Li^+ ions in mercury vapor that for gas-ion combinations which show no definite change in speed of the ion, the chief cause of absorption is scattering. The velocities were from 18 to 300 equivalent volts. For the ions of higher velocity range—10,000 to 50,000 equivalent volts—there is evidence of some scattering but the velocity losses are less than one-half of one percent.[6,7]

[1] Dempster, Phil. Mag. **7,** Series *13*, 115, (1926).
[2] Durbin, Phys. Rev. **30,** 844 (1927).
[3] Ramsauer and Beeck, Ann. d. Physik **87,** 1 (1928).
[4] Kennard, Phys. Rev. **31,** 423 (1928).
[5] Cox, Phys. Rev. **34,** 1426 (1929).
[6] G. P. Thomson, Proc. Roy. Soc. **102,** 197 (1922).
[7] Koenigsberg and Kutschewski, Ann. d. Physik **161,** 37 (1912).

Thus it appears that the entire problem of positive ion absorption is quite complex and depends not only on the gas-ion combinations, but on the velocity, gas pressure, apparatus and method used and other experimental variables. For heavy ions passing through light gases at moderate velocities the predominant effect seems to be a slowing up of the ion bundle, whereas for a light ion in a heavy gas the chief cause of absorption is due to scattering. Intermediate cases may show a combination of both effects; for example, Kennard found that for Na^+ ions with a velocity of 455 volts in hydrogen, there was a small but definite slowing up, together with an absorption probably due to scattering. As pointed out by Cox, it seems evident that the importance of any absorption process due to scattering, and, in some cases, of that due to retardation is dependent on the dimensions of the apparatus used and the method of measurement. Thus, the absorption constants usually calculated from such measurements have no absolute significance and cannot be interpreted in terms of any atomic process.

The purpose of the experiments to be described was: first, to make a more complete study of the motion of Cs^+ ions in hydrogen and helium, particularly in the region of low velocities, and, secondly, to investigate the process of absorption of a light ion in a light gas as typified by Li^+ ions in helium; and to study any dependence of this absorption on velocity.

Caesium in Hydrogen and Helium

The results obtained by Kennard for 35 and 90 volt Cs^+ ions have been obtained for 100 and 200 volt ions in helium. The apparatus used is based on Dempster's method of positive ray analysis and is shown in Fig. 1.[8] The cylinder C was removed in some experiments and a single collector mounted above the slit, S_2. The ion source contained in the furnace, A, is made positive with respect to the slit S_1, the emission current being held constant and measured with the galvanometer G. The ion beam enters the magnetic field and by varying the magnet current, is swept across the slit S_2, after traversing the gas-path S_1MMS_2. The dimensions of the path through the armature were, $3.0\times10\times112$ millimeters. The resultant intensity through S_2 is then measured by balancing the current to the collector against the ionization current from the RaE tubes shown at R. A Compton electrometer, E, adjusted to a sensitivity of 2500 divisions per volt was used as a null indicator. Helium was introduced into a reservoir by allowing it to pass slowly through a charcoal trap immersed in liquid air; after this preliminary purification the gas was admitted to the apparatus through a drying tube, a fine capillary and a second charcoal trap which was also kept at liquid air temperature. The gas was tested by observing the spectrum with a hand spectroscope, the lines showing distinctly on a dark background.

The gas enters the tube at D and is kept in circulation through the apparatus. Various pressures are established by adjusting the rate of pumping of the mercury diffusion pumps connected at O. An ionization gauge was

[8] Dempster, Phys. Rev. **11**, 316 (1918).

used in some experiments to show when steady gas pressures were attained, all final measurements being made with McLeod gauge attached at P. For a definite pressure and emission current the current through S_2 is measured as a function of the magnet current, four or five such curves being taken for a single accelerating potential.

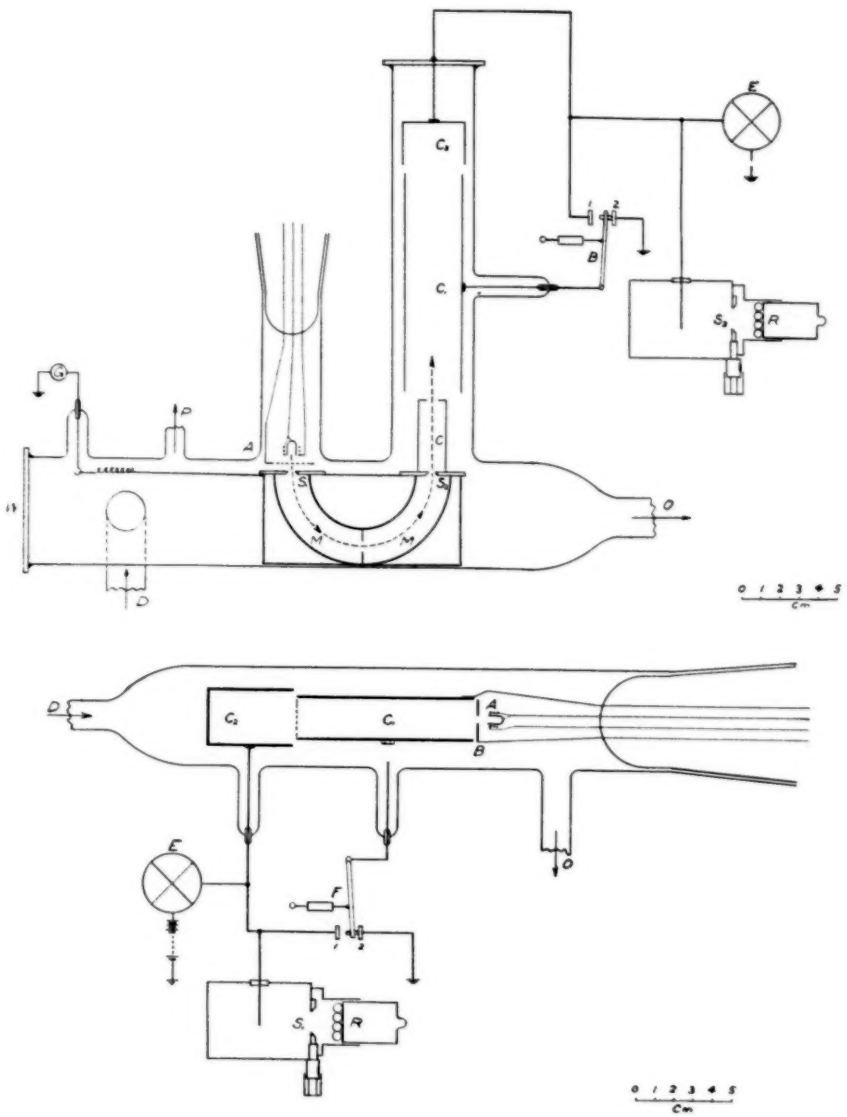

Figs. 1 and 2. Diagram of apparatus.

The type of curves obtained are the same as those of Kennard and are shown in Fig. 2. For increasing pressures the peaks of the curves are seen to be shifted in the direction of lower ion velocities, the general symmetry of the curves being retained about the shifted peak. Within the limits of

experimental variation, the areas under these curves remain constant, showing that in traversing the gas-path S_1MMS_2 all the ions of various velocities reach the collector. Kennard observed this behavior for Cs^+ ions in hydrogen and helium for 35 and 90 volts velocities. He concluded that there was a general slowing up of the Cs^+ ions, and for pressures up to 80×10^{-4} mm of mercury, due to the constancy of the areas, that there was no neutralization or scattering of the bundle.

This behavior of Cs^+ ions for the velocities used in the above method indicated the possibility of isolating a single process of interaction between ion and gas molecule and of studying this process over a range of conditions in which it was operative.

In the procedure outlined above it is essential that the emission of ions through S_1 be held constant over a considerable period of time in order that the complete curves of Fig. 3 may be obtained for several gas pressures. This difficulty together with that of obtaining sufficient intensity with low velocity ions limited the range of the method. Also in establishing the equality of the areas under the curves shown, it is difficult to determine the exact range of the base line.

Experiments were tried with the two-cylinder method shown drawn to scale in Fig. 1 and used by Cox in experiments on Li^+ ions in mercury vapor.[5] Here the ion bundle is accelerated to S_1 as before and bent through 180° in the magnetic field. The collimating slit C directs the beam up the axis of the cylinders C_1 and C_2. Measurements to detect any absorption were made by first connecting C_1 and C_2 together with the switch B in position (1); then C_1 was grounded and those ions which had travelled over the extra gas-path of length C_1 were collected and measured in C_2. Both values are determined with the balance method described. No absorption in C_1 for Cs^+ ions in helium was observed for velocities of 25 to 600 volts and pressures up to 0.013 mm of mercury. Here again the difficulty of obtaining sufficient intensity limited the range.

In order to study the behavior of Cs^+ more directly and over a range of velocities not possible with the magnetic methods described, a third tube was constructed and shown drawn to scale in Fig. 2. Tubes of similar construction have been used by Mayer,[9] Akesson[10] and Eldridge[11] in experiments on electron velocity distribution.

The source of ions was contained in the small electric furnace shown at A. The ions were accelerated to the slit B, passed through a field-free space within the nickel cylinder, C_1, 9.2 cm long and were collected in the Faraday cylinder C_2. The gas entered at D and was kept in circulation through the tube, various pressures being established by adjusting the rate of pumping of the mercury diffusion pumps connected at O. Pressures were measured with a McLeod gauge connected first at O and later, in order

[9] Mayer, Ann. d. Physik **64,** 451 (1921). Also P. Lenard; Wien's "Handbuch der Experimental Physik" XIV, 170, (1927).

[10] Akesson, Lund's Arsskrift **12,** 11 (1916).

[11] Eldridge, Phys. Rev. **20,** 456 (1922).

to insure that no pressure gradient affected the measurements, to the central tube which supports the electrode above *F*. Helium was purified as in the experiments outlined above; hydrogen was admitted through a heated platinum tube sealed into the glass line and about which was circulated commercial hydrogen at atmospheric pressure.

In experiments with a tube of this type a particularly pure source of ions was essential as no magnetic separation was possible. This source was found in the mineral pollucite which is essentially a caesium aluminum silicate containing 27 percent caesium ($H_2O.Cs_2O.\ Al_2O_3.9SiO_2$). The

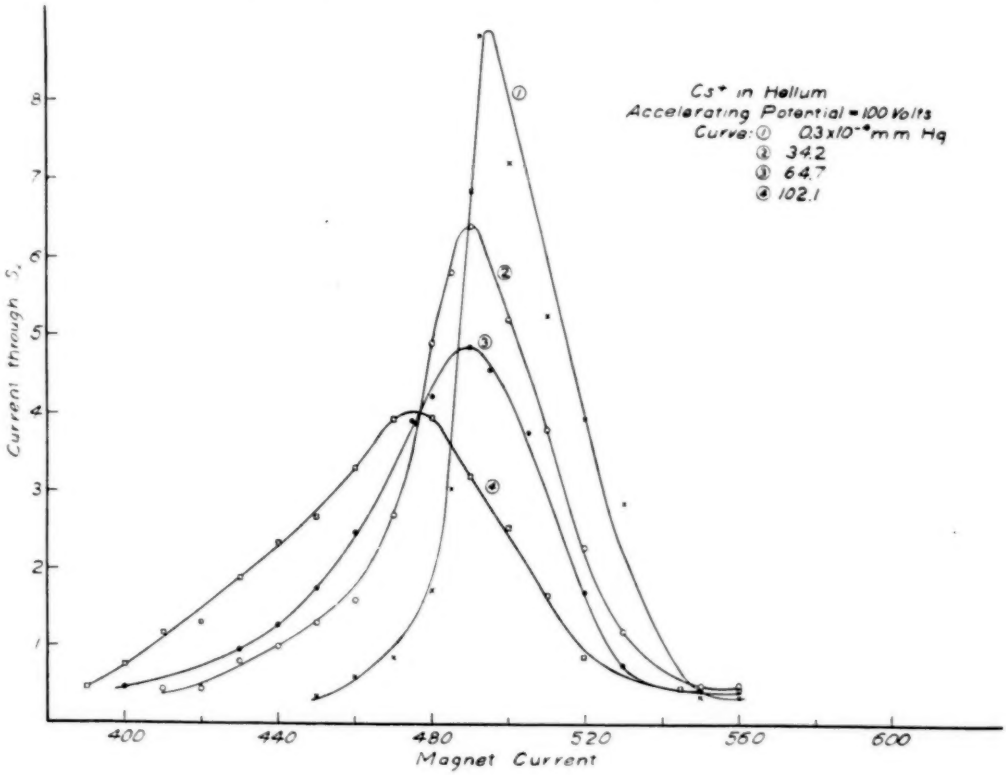

Fig. 3

mineral is powdered and packed into the small resistance-wound furnace made of steel tubing 5 mm long and about 2.5 mm inside diameter. In some instances the mineral was mixed with powdered iron to make it conducting and allow it to fuse more readily. It was found that the substance could not be fused on a platinum strip as is the case with the lithium source, spodumene. This source was prepared and always placed in the magnetic analyzing apparatus before use and examined for other ions. No emission other than Cs^+ was detected for temperatures considerably above those normally used. At a dull red heat a very strong and steady emission of Cs^+ ions was obtained. The experimental tube and source were baked out thoroughly for several hours before use.

It was thought that the process of interaction of Cs^+ ion with hydrogen and helium was one of pure retardation, but to make certain of this, experiments were first tried to detect any weakening or absorption of the ion bundle due to causes other than slowing up. For this purpose the gauze shown on the end of C_1 in Fig. 2 was removed. The central electrode supported C_1 at the center, the ground connection through the stem being removed. By connecting the switch F in position 1, the total ion current to (C_1+C_2) was observed. Then with C_1 grounded, by moving F to position 2, the ions which reached C_2 after traversing the gas-path through C_1 were measured. As in the first type of tube both currents were measured by the balanced electrometer arrangement, intensities being proportional to the slit widths, S_1. Measurements of the ratio, $C_2/(C_1+C_2)$ were taken for increasing pressures in the tube so that any weakening of the beam was detectable in a decrease in this ratio. For very low velocity ions this ratio was not equal to unity for low pressures because of the divergence of the bundle caused by the field between A and B so that some of the ions hit the wall of C_1. However, in all cases, values of the ratio were obtained for several pressures so that any real absorption could be observed.

In this way it was found that for pressures less than 0.01 mm of mercury, no appreciable absorption of the Cs^+ ions in hydrogen and helium took place for velocities of 3.5 to 600 equivalent volts. For velocities above 10 volts this absence of absorption persisted for pressures even higher than 0.03 mm of mercury. Below 10 volts and for pressures above 0.01 mm of mercury a definite weakening of the bundle set in and increased rapidly with the pressure. This absorption is probably due to the effects of multiple scattering as the number of collisions with the slow moving ions is increased, and is discussed later.

Thus for a considerable range of velocity and pressure the Cs^+ ions are not deviated appreciably from their path, making it possible to study the slowing up effect as an individual process over this range.

The arrangement used for observing the retardation of the ions is shown also in Fig. 2. The ions are accelerated as before, by applying a positive potential to A; B and C_1 are grounded as shown; the ions pass through the field-free space C_1, and are collected in the Faraday cylinder, C_2. In some experiments a grounded shield was placed around the two cylinders but this was not used in general as the ion path is well shielded as shown and the grounded cylinder provided an extra leakage path. Any retardation takes place over the gas-path, AC_2, measured from the ion source to the far end of the collector C_2 or 14.2 cm. With a constant pressure in the tube, increasing retarding potentials are placed on C_2 through the electrometer as shown. This potential is applied with respect to the gauze on C_1, which gives a more uniform distribution of the field. The current to C_2 is then observed as a function of the retarding voltage. Hence, only those ions with velocities greater than or equal to the retarding potentials will be recorded in C_2. In this way the velocity or energy distribution of the retarded ions was measured for various pressures. Curves of this type are shown in Fig. 4, which shows

the distribution for 6.4 volt Cs^+ ions in helium at the pressures given. Another set for 100 volt Cs^+ ions in hydrogen is shown in Fig. 5. In both these sets except for the lowest pressure the actual curve drawn represents the theoretical energy distribution fitted to the experimental data as explained below. The points shown were determined experimentally as described. Similar sets were taken for velocities ranging from 3.5 to 600 volts in both hydrogen and helium. Any point on these curves is proportional to the number of ions retaining energies equal to or greater than the corresponding voltages. In all such curves the distribution at low pressure was always taken as

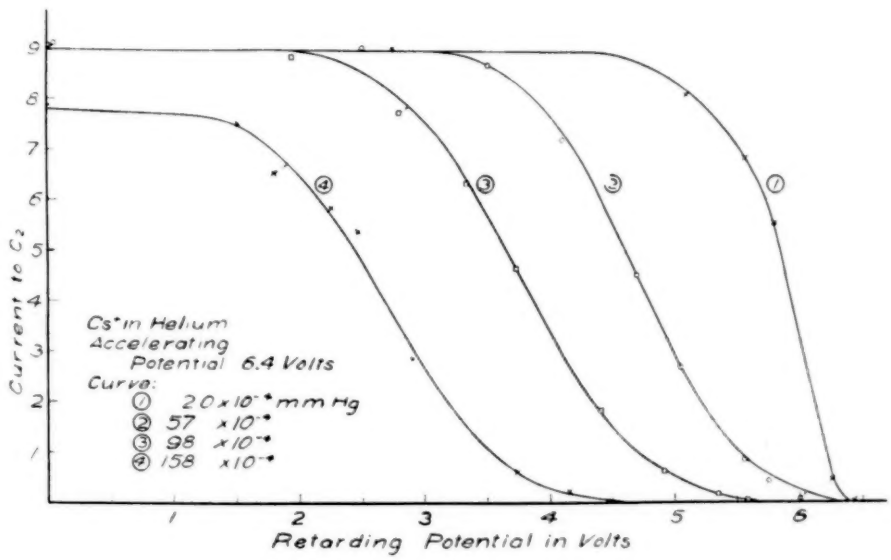

Fig. 4

a control, since here the distribution of energies should be approximately homogeneous. The points shown in the curves of Figs. 4 and 5 were not corrected for small changes in the emission current at the various pressures so that no significance is to be attached to the absolute values of the ordinates shown. As explained above, separate experiments were made to determine any change in the current to C_2 with pressure.

By integration of curves of the form

$$y = ke^{-h^2x} \tag{3}$$

it was found that the resulting curve could be fitted to the experimental points, indicating that when the ions reached the collector there was an approximate probability distribution of energies about the average retarded value. This distribution is what would be expected from probability considerations, due to some ions making more collisions, and some less than the average number in completing the path, L. Each point on the curves of Figs. 4 and 5 represents the number of ions found to retain energies equal to or greater than the corresponding voltage. For a value of the retarding voltage,

V_R, the number of ions retaining energies greater than V_R would be expected to be given by

$$I = k \int_{V_R}^{\infty} e^{-h^2V^2} dV$$

the constant, h, depending on the particular distribution. In order to obtain the value of h, which is characteristic of a particular energy distribution, we may consider the expression:

$$P = \frac{h}{\pi^{1/2}} \int_0^{V-V_0} e^{-h^2(V-V_0)^2} d(V - V_0) \tag{4}$$

for the probability that an ion will retain an energy between V_0 and V. Here V_0 is the average retarded velocity, represented in the experimental curves

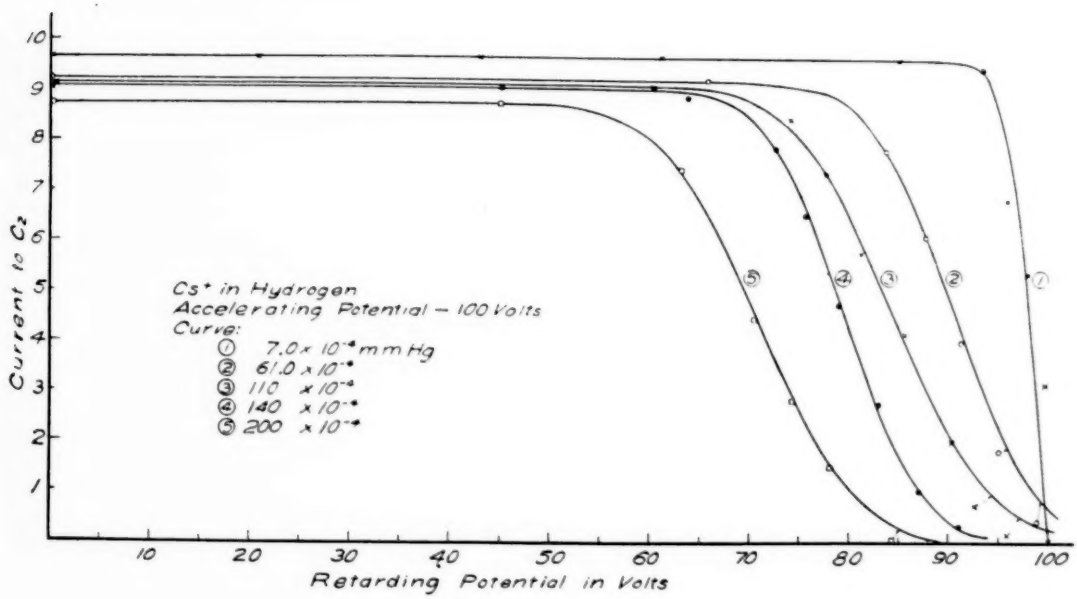

Fig. 5

(Figs. 4 and 5) by the half ordinate, and corresponding to the peak value of the error curve. The constant, h, may be conveniently found by observing the energy, V_1, at which the probability is one-fourth as indicated in Figs. 6 and 7. Setting:

$$h(V - V_0) = z$$

we then have that:

$$P = \frac{1}{\pi^{1/2}} \int_0^z e^{-z^2} dz = \tfrac{1}{4}$$

for $z = z_1 = h(V_1 - V_0)$. As, $z_1 = 0.477$, $h = 0.477/(V_1 - V_0)$.

If n is the average number of collisions, the probability of an ion making a number greater than n but less than, $n+z(2n)^{1/2}$ is:

$$\frac{1}{\pi^{1/2}}\int_0^z e^{-z^2}dz.$$

If the energy loss per collision were constant, $z(2n)^{1/2}$ would be proportional to $(V-V_0)$, or z/h. That is, we should expect h^2 to be inversely proportion-

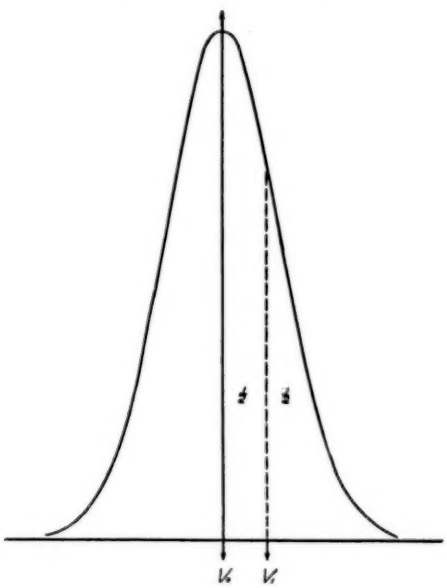

Fig. 6

al to the number of collisions, the pressure, or the average energy lost by the ions, which is (V_i-V_0), V_i being the initial velocity. Thus for a constant

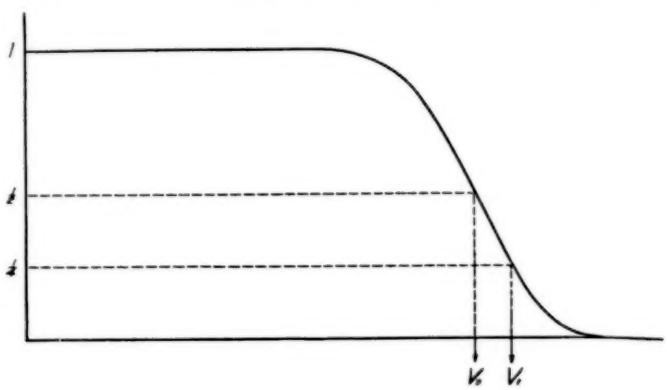

Fig. 7

energy loss per collision, $h(V_i-V_0)^{1/2}$ would be constant. If $h(V_i-V_0)^{1/2}$ is less with ions of high velocity, it signifies that the energy loss per collision is less in this case.

In the case of the 6.4 volt Cs^+ ions in helium at a pressure of 98×10^{-4} mm of mercury, the dispersion, (V_1-V_0) was 0.55 and $h=0.87$; $h(V_i-V_0)^{1/2}=1.41$. Values of h calculated from the experimental data, together with the quantity, $hV_i-V_0)^{1/2}$ are shown for various velocities and pressures in the Table I. From the values of h given in the table, the expected energy distribution may be calculated and compared with the experimental results. The theoretical curve is obtained for any particular distribution by the use of the proper h in the integral of Eq. (4). The resulting curves are shown for two initial velocities in Figs. 4 and 5 together with the experimental points. It is seen that the agreement is in general better for the low velocity ions and for the higher

TABLE I. *Cs^+ in helium.*

Initial velocity V_i	Pressure $\times10^4$ mm mercury	V_0	(V_1-V_0)	h	$h\ (V_i-V_0)^{\frac{1}{2}}$
3.5	57.0	2.24	0.31	1.54	1.73
	83.0	1.97	0.33	1.45	1.79
	110.0	1.45	0.32	1.49	2.14
	57.0	4.70	0.45	1.06	1.38
6.4	72.5	4.35	0.53	0.90	1.29
	98.0	3.75	0.55	0.87	1.41
	126.0	3.20	0.55	0.87	1.55
	158.0	2.78	0.49	0.97	1.84
9.3	52.0	6.57	0.95	0.50	0.826
	110.0	5.15	0.99	0.48	0.976
	60.0	24.40	3.05	0.157	0.372
30.0	97.0	21.80	3.00	0.159	0.455
	163.0	19.70	2.40	0.199	0.64
60.0	60.0	51.50	4.00	0.119	0.347
	116.0	45.60	4.90	0.097	0.368
	167.0	41.30	3.90	0.122	0.528
	50.0	88.00	5.70	0.084	0.291
100.0	85.0	80.50	6.60	0.072	0.318
	150.0	70.80	7.00	0.068	0.368
	88.0	170.00	13.50	0.035	0.192
200.0	168.0	151.00	14.00	0.034	0.238
	242.0	132.00	15.00	0.032	0.264
400.0	52.0	370.00	15.00	0.032	0.175
	90.0	343.00	21.00	0.023	0.174
	160.0	333.00	22.00	0.022	0.180
	220.0	293.00	27.00	0.018	0.186
590.0	76.0	570.00	16.00	0.030	0.134
	242.0	487.00	33.00	0.014	0.142
		Cs^+ in hydrogen			
	46.0	2.36	0.31	1.54	1.65
3.5	65.0	1.90	0.35	1.36	1.72
	108.0	1.17	0.33	1.45	2.21
13.5	40.0	11.40	0.60	0.79	1.14
	96.0	9.20	1.00	0.48	1.00

TABLE I. *Cs^+ in hydrogen (Continued).*

Initial velocity V_i	Pressure $\times 10^4$ mm mercury	V_0	$(V_1 - V_0)$	h	$h\,(V_i - V_0)^{1/2}$
	40.0	27.7	1.00	0.48	0.728
30.0	65.0	26.1	1.60	0.30	0.592
	100.0	23.7	2.00	0.24	0.603
	215.0	18.5	2.20	0.22	0.746
	270.0	15.5	1.70	0.28	1.060
	57.0	55.0	2.00	0.24	0.537
60.0	75.0	52.5	2.80	0.17	0.466
	160.0	44.4	3.60	0.13	0.514
	290.0	35.0	3.50	0.14	0.700
	61.0	90.5	4.50	0.11	0.340
100.0	110.0	84.4	5.34	0.089	0.352
	140.0	79.5	4.20	0.113	0.520
	220.0	71.0	5.30	0.090	0.485
	61.0	183.2	7.30	0.065	0.266
200.0	90.0	177.2	8.80	0.054	0.258
	131.0	170.0	7.50	0.064	0.350
	216.0	151.0	9.40	0.051	0.357

pressures. On the high velocity side of the curves the points were obtained with much less precision.

The values of h given in the table are seen to decrease with increasing voltage and the values of $h(V_i - V_0)^{1/2}$ are not constant as would be expected

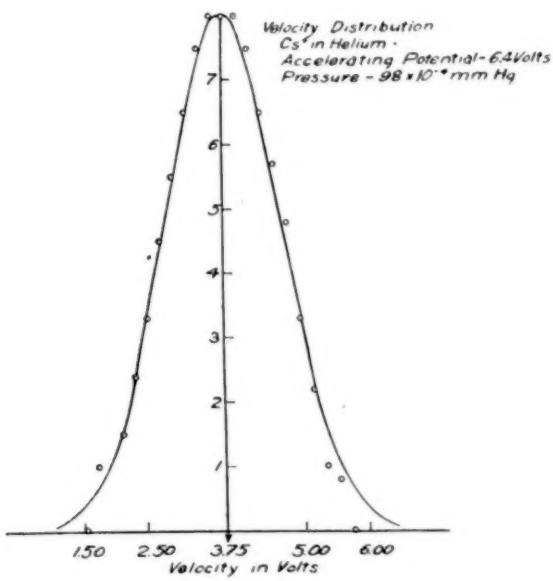

Fig. 8

if the energy loss per collision were the same for ions of all velocities. As explained above the decrease is what would be expected if the energy loss per collision decreases with the high velocity ions. In hydrogen, the consistently

larger values of h than in helium for corresponding voltages indicate that in this gas there is less loss of energy per collision.

The actual error curve distribution for the case of 6.4 volt Cs^+ ions in helium for a pressure of 98×10^{-4} mm of mercury is shown in Fig. 8. The full line represents the theoretical distribution of the velocities for curve (3) of Fig. 4. Here V_0 is 3.75 volts and V_1 is 4.30 volts; the points shown are obtained by graphical differentiation of the experimental curve.

Each of the curves in Figs. 4 and 5 represents a new distribution of energies about a most probable energy V_0 which is that corresponding to the half ordinate. The difference then between the applied potential and this half ordinate energy gives the retardation of the ions for the pressure shown. For each applied potential this retardation has been plotted as a function of the

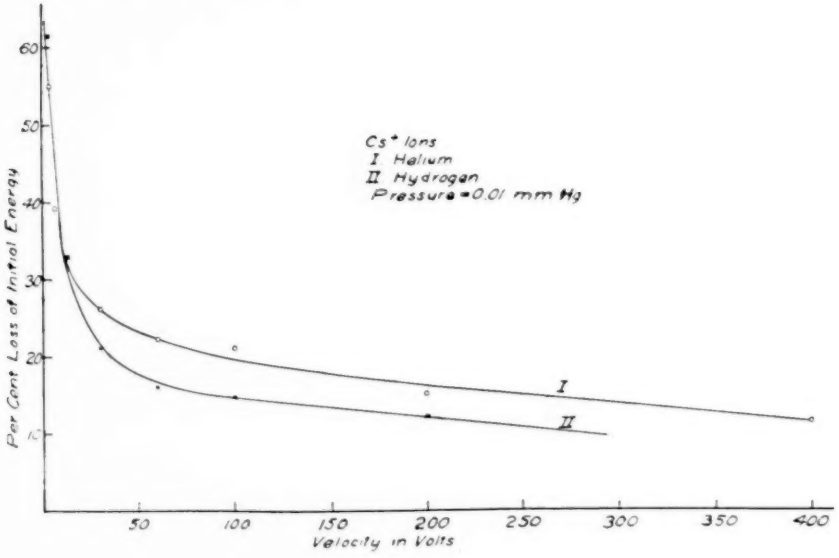

Fig. 9

pressure and is found to be linear over a wide range. This slowing up took place over the gas-path AC_2 measured from the furnace source to the far end of the collector, C_2, or 14.2 cm. From the curves the retardation for 0.01 mm of mercury was obtained since for this pressure no absorption was found. Fig. 9 shows this retardation, expressed as a percent loss of initial energy, as a function of the initial velocity in volts. Points for 600 volt ions, not shown on the curves, would fall on the lower linear portion if extended. The loss in helium is seen to be greater over most of the range as might be expected for the gas molecule of greater mass, especially if the interpretation is that of mechanical collisions. In both cases the loss decreases with increasing velocity. This is in agreement with the data cited for canal rays of 10,000 volts and more which show less than one-half of one percent loss of energy.[6,7] Below forty volts the curves rise rather rapidly and tend to merge; extending them to the axis of ordinates indicates that the maximum loss for this pressure would be about 66 percent.

These results suggest an interpretation of the results of Ramsauer and Beeck[3] for Cs^+ ions in helium that differs from their conclusions. In their experiments the apparatus used was similar to that described in connection with Fig. 1, except that the dimensions were much smaller. The method of observations was to hold the magnetic field constant and observe the weakening of the bundle for several gas pressures. Referring to Fig. 3, this is seen to be equivalent to observing the intensities along a vertical line drawn through the peak value of the lowest pressure curve used. It is evident that this method of observation would show an apparent absorption for the retarded ions. From their results, Ramsauer and Beeck calculate what is designated as the "Wirkungsquerschnitt," which is the value $1/L$ from Eq. (1), reduced to 1 mm of mercury. For Cs^+ ions in helium, they find a considerable absorption of the ions for velocities of 1 to 10 volts; for instance, reducing their values in terms of the effective cross section, C, gives a value of 11.3×10^{-1} cm^2 for ions of 9 volts velocity; or in terms of the mean free path, $L=33\times10^{-6}$

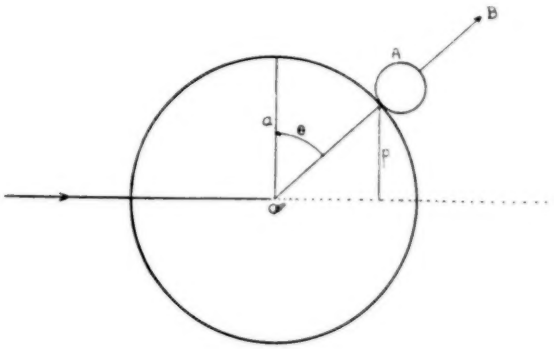

Fig. 10

cm under standard conditions. These values show a large opposing cross section of ion against molecule, whereas for the pressures used by Ramsauer and Beeck,[3] no real absorption at all was observed in the present experiments. Fig. 9 shows that 9 volt Cs^+ ions suffer a loss in velocity of about 35 percent, which, as explained above, would account for the large value of C found by Ramsauer and Beeck.[3] No relation to atomic constants can be attached to the values of C and to the various values of atomic radii calculated therefrom as they are at once seen to depend on the dimensions of the apparatus and the experimental method used. Thus the mechanism of absorption is of primary importance in the interpretation of these measurements.

It is of interest to compare the results for caesium ions with what would be expected on the basis of elastic collisions between ion and gas molecule. In Fig. 10 consider a Cs^+ ion moving forward with a velocity V among helium atoms at rest. If an elastic collision occurs with the helium atom at A, this atom is projected along OAB with a velocity, $2V\sin\theta$, provided the mass of the Cs^+ ion is very large compared to that of helium. Since the ratio is 133/4 we may take this velocity as a first approximation. The equality of momenta

in a transverse direction shows that the Cs^+ ion then receives a velocity at right angles to its direction equal to:

$$V'' = 2V \sin\theta \cdot \cos\theta \cdot 4/133.$$

The angle made by the ion with its original direction is then,

$$\phi = V''/V = 8/133 \cdot \sin\theta \cos\theta$$

since V is only slightly altered. Now the number of collisions in the range, p to $p+\Delta p$ as shown in the figure is proportional to the area presented in the direction, V, i.e., to $2\pi p \Delta p$. Since the total number of collisions is proportional to, πa^2, where a is the radius of the Cs^+ ion, we may write for the average angle of scattering,

$$\Phi = \frac{1}{\pi a^2}\frac{8}{133}\cdot\int_0^a \frac{p}{a}\left(1-\frac{p^2}{a^2}\right)^{1/2}\cdot 2\pi p\cdot dp$$

where, from Fig. 10 $\cos\theta = p/a$ and $\sin\theta = (1-p^2/a^2)^{1/2}$. This upon integration gives,

$$\Phi = \pi/133 = 0.023 \text{ radians}.$$

The maximum angle of scattering, for $\theta = 45°$, gives

$$\phi_{max} = 0.030 \text{ radians}.$$

In the apparatus used, an ion would always reach the collector unless deflected by more than 10/92 or 0.11 radians. Thus single scattering is unable to produce a weakening of the bundle. Experimentally, no weakening was observed until the pressure was made high enough to give rise to multiple scattering.

We may also calculate the energy loss to be expected on the basis of elastic collisions. In the Fig. 10 let m equal the mass of the helium atom and M the mass of the Cs^+ ion. On the basis of elastic collisions, the energy lost by the Cs^+ ion is equal to the amount gained by the helium atom, or,

$$\Delta E_0 = \tfrac{1}{2}m(2V\sin\theta)^2$$

for the loss due to a collision at angle, θ. The ratio of this loss to the initial kinetic energy of the Cs^+ ion is then,

$$\frac{\Delta E_0}{E_0} = \frac{\tfrac{1}{2}m(2V\sin\theta)^2}{\tfrac{1}{2}MV^2} = \frac{16}{133}\sin^2\theta.$$

In travelling a distance, L, the average fractional loss per collision may be written, referring to Fig. 11 as:

$$\frac{\Delta E}{E} = \frac{1}{\pi a^2 L_n}\int_0^{\pi/2}\{(2\pi a\cos\theta)(a\sin\theta d\theta)Ln\}\left(\frac{16}{133}\sin^2\theta\right) = \frac{8}{133}$$

where, $a = r_1 + r_2$, the sum of the ion and atom radii; and, n = the number of helium atoms per cc for the pressure considered.

The energy remaining after, $\pi a^2 Ln$ collisions may then be written as,

$$\left\{1 - \frac{\Delta E}{E}\right\} = \left\{1 - \frac{8}{133}\right\}^{\pi a^2 Ln}. \tag{6}$$

From Fig. 9 we may obtain a value of the percent loss of initial energy of the Cs^+ ion for the smallest velocity observed. The value for helium is 55 percent for 3.5 volt ions. In Eq. (6),

$$L = 14.2 \text{ cm}$$

$$n = 3.48 \times 10^{14} \cdots (p = 0.01 \text{ mm of mercury})$$

so that,

$$a = r_{Cs} + r_{He} = 2.88\text{A}.$$

Viscosity measurements give for the radius of the helium atom, $r_{He} = 1.10$A, so that we should expect a value for the radius of the Cs^+ ion,

$$r_{Cs} = 1.78\text{A}.$$

Herzfeld[12] gives values of r_{Cs^+} which vary from 0.83 to 2.36A depending on the method of measurement. The radius of the xenon atom obtained from

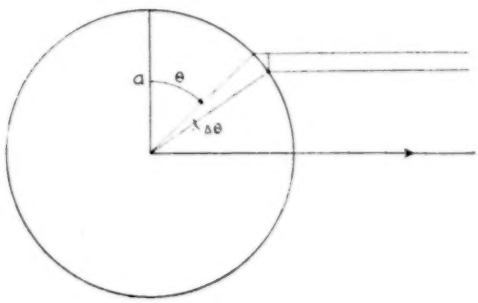

Fig. 11

viscosity measurements is 2.44A. Similar calculations for hydrogen, where $\Delta E/E = 4/133$ and the percent loss was 61.5, gave a value,

$$a = r_{Cs} + r_{H_2} = 4.55\text{A}.$$

A value for r_{H_2} from viscosity measurements quoted by Jeans as 1.36A leaves for the radius of the Cs^+ ion,

$$r_{Cs} = 3.19\text{A}.$$

For ions of greater initial energy the percent loss decreases. This disagrees with the elastic collision interpretation which would make the percent loss a constant. We must conclude that at higher velocities the interaction at a collision of a Cs^+ ion with a helium or hydrogen molecule is different from

[12] Geiger Scheel, "Handbuch der Physik," Band XXII, 386, 1926.

that considered in the kinetic theory of gases and that less energy is lost than would be the case, were the collisions elastic.

Lithium Ions in Helium.

With low velocity Li^+ ions in helium the change in the curves produced by increasing pressure was entirely different from that found in Cs^+ ions. We shall find that with the light ion, small angle scattering is the predominant phenomenon, whereas with the heavy Cs^+ ions, scattering was inappreciable in comparison with process of retardation. By using several different experimental arrangements it has been possible to establish the type of absorption that occurs over the range of velocities studied, namely 20 to 930 equivalent volts.

Method I

The apparatus used has been described in connection with the experiments with caesium and is shown drawn to scale in Figs. 1 and 2. In this method the cylinders C_1 and C_2 were replaced as before with a single Faraday cylinder, mounted above S_2. The slit S_1 varied between 1 and 2 mm and in several instances runs were taken with this slit entirely removed.

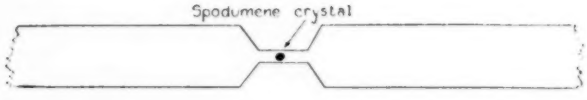

Fig. 12

In Kennard's experiments the ion sources used were the positive ion iron catalysts supplied by Kunsman. These catalysts usually emit Na^+ and K^+ to an appreciable extent together with an ion possibly arising from the insulating cement of the furnace. This necessitates the assumption that the total emission current held constant and measured with the galvanometer G, is also constant in its composition throughout the series of observations. In order to obviate this difficulty the mineral spodumene (used by Hundley[13]) was investigated for purity in emission. A small crystal, less than 0.2 mm in diameter, was melted down on the center of a constricted platinum filament as shown in Fig. 12. This strip is mounted horizontally over the slit S_1 and replaced the furnace source at A (Fig. 1). At low temperatures in vacuum this source showed a large emission of Na^+ and K^+ but continued heating at a yellow heat removed these ions to less than one-half of one percent. By treating the substance in this way a very pure source of Li_7^+ was obtained, which in many cases could be used for 100 hours or more, with good intensity and constant emission. Due to the small value of the emission current to S_1, an electrometer shunted with a high resistance replaced the galvanometer G in most of the experiments in an attempt to attain greater accuracy of observation. Since the method used depends on Eq. (1), the emission current N_0

[13] Hundley, Phys. Rev. **30**, 864 (1927).

must be constant and proportional to the actual ion current passing through S_1. The current actually recorded represents the total ion current through S_1 as well as to neighboring metal parts connected to the magnet armature. It was not possible, with this arrangement, to determine whether the actual current through the slit remained constant, but it was assumed that a constant fraction of the total emission current entered S_1. This assumption is not entirely justified as spreading of the beam may occur due to the admission of

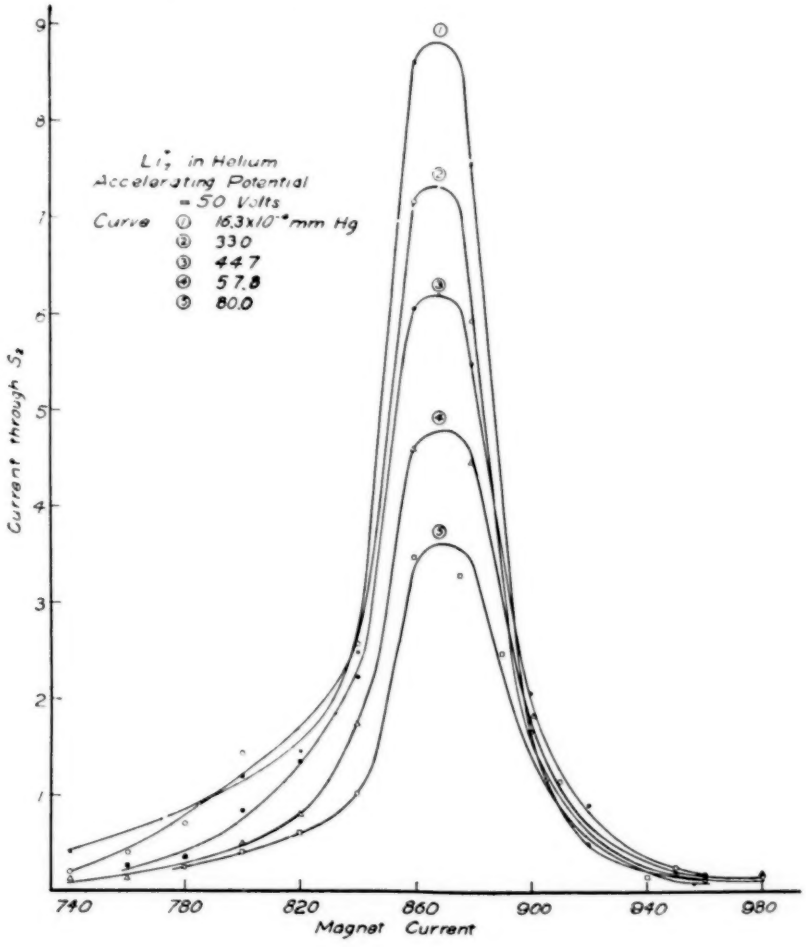

Fig. 13

gas, or the actual character of the emission from the source may change, giving a bundle of varying divergence. This indefiniteness accounts partially for the variation of the absorption coefficients obtained by this method, although no difficulty was found in getting reasonable checks.

The method of procedure is the same as that of Kennard and has been outlined above. The type of curves obtained for five different pressures with a constant accelerating potential is shown in Fig. 13 for Li^+ ions of 50 equiva-

lent volts. Sets of curves of this type were taken for velocities varying from 20 to 931 volts and for each velocity at least three such sets were obtained. From each pair of pressures of each set of curves, the value of the mean free path, L, was determined, making use of Eq. (1). The gas path was 11.2 cm in length, so that L was given by:

$$L = 11.2 \times (p_2 - p_1)/760 \times 2.30 \times \log\frac{N_1}{N_2}.$$

From Eq. (2), C is then obtained, where,

$$C = \pi(R_{Li} + R_{He})^2 = 1/Ln$$

and

$$n = 2.70 \times 10^{19}.$$

Values of C are shown as curve I, Fig. 14 for ion velocities ranging from 20 to 500 equivalent volts; a value of C for 931 volts is not shown on the curve, but

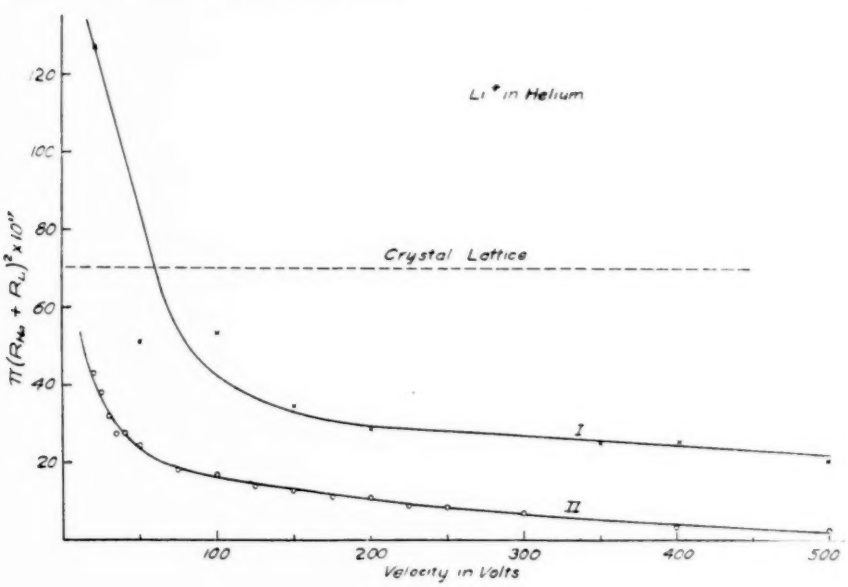

Fig. 14

has a value of 9.5×10^{-17} cm^2, and would fall on the lower linear portion if extended. Using kinetic theory values of the atomic radii as,

$$R_{He} = 1.10\times10^{-8} \text{ cm—viscosity measurements}$$

and, $R_{Li} = 0.41\times10^{-8}$ cm—crystal lattice data we find for C, $C = 70.1\times10^{-17}$ cm^2 and this value is shown as a dotted line in Fig. 14. In terms of the mean free path, the values of L found vary from about one-half the kinetic theory value at 20 volts to almost eight times this at 931 volts. Reducing Ramsauer and Beeck's values of the "Wirkungsquerschnitt" for Li^+ and helium in terms of C we find for 16 volt ions,

$$C = 42 \times 10^{-17} \text{ cm}^2.$$

This value is about one-third of that found in the present experiments which, from the curve, would give 130×10^{-17}. The difference is accounted for by the dimensions of their apparatus, which had several times the angular aperture used in the present experiments. It has been found that the rate of absorption of the lithium ions depends strongly on the dimensions of the measuring chamber, which indicates that the process is one of scattering. On this basis a considerably smaller value of C would be expected for the wider apertures used by Ramsauer and Beeck.[3] As in the experiments of Cox, the interpretation of the behavior of Li^+ in helium as due to scattering is strengthened from the results obtained with a second type of apparatus.

Method II

This method has been used by Cox and described by him in detail for the case of lithium ions in mercury vapor.[5] The experimental tube is shown in Fig. 1, where the dimensions of the various parts are drawn to scale. Measurements of C and L are based on Eqs. (1) and (2), where the length of the absorbing gas path is equal to 11.3 cm. For a given pressure, the total ion current (N_0), to C_1 and C_2 is measured by connecting these two cylinders together with the switch B in position (1). Then with B in position (2), C_1 is grounded and the value of N is measured as the ion current to C_2. This method allows a more rapid determination of N and N_0 and eliminates the problem of measuring the emission current to S_1. Values of C and L were determined from observations at three different gas pressures. In all cases the currents to C_1+C_2 and to C_2 were equal for the lowest pressures attainable (10^{-5} mm of mercury). This equality was attained by means of the collimating slit, C, placed over the emergent slit S_2, which directed the ions up the axes of the cylinders; in this way none of the ions struck the cylinder C_1 at low pressures.

The values of C determined in this way are shown plotted against the ion velocity in Fig. 14, curve II. It is seen that the general shape of this curve is identical with that obtained with Method I, but that in all cases the values of C are smaller. In both cases the values of C rise sharply for velocities below 40 volts, in the one case rising to a value over twice that calculated from kinetic theory values and in the second case approaching the crystal lattice value for low velocities. The dimensions of the absorbing paths for the two methods correspond to those used by Cox and while the actual values of C are smaller, as might be expected with the lighter gas, the same change in these values is found for the two types of apparatus. These results show that the most reasonable interpretation of the process is that of scattering in which forces other than those of elastic collisions come into play. For the large scattering apertures of Method II, a much larger cone of rays may pass over the absorbing path than for Method I, where the angular opening was several times smaller and many more of the ions were lost through deflections to the walls of the chamber. It has been shown by Dempster[5] that the rate of absorption may show a strong dependence on the dimensions of the apertures, provided some law of force other than that of elastic collisions is effective.

Experiments on the scattering of the Li^+ ions were also tried, using the apparatus shown in Fig. 2. Results obtained for several velocities confirm the conclusions reached above,—that the absorption of the ions is due to scattering and depends on the dimensions of the absorbing chamber and of the collector. Velocity distribution curves were also obtained for Li^+ in helium by the method of retarded potentials, used with Cs^+ ions. This distribution for 50 volt Li ions is shown in Fig. 15. It is seen that the shapes of these curves

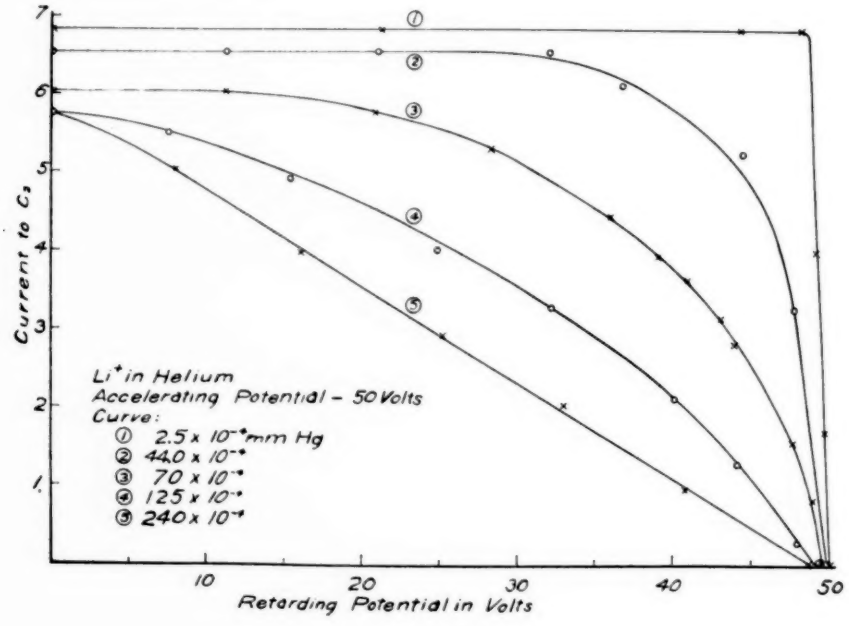

Fig. 15

are quite different from those obtained with Cs^+; they do not shift to the left as a whole and some of the ions appear to retain approximately their full initial velocity. The decrease in the number of ions of any particular velocity with pressure is probably due to a decrease in the forward component as a result of scattering, so that we have an "absorption" process which involves only a scattering of the ion bundle as distinct from retardation.

Professor A. J. Dempster suggested the experiments reported on in this paper. The writer is indebted to him for the theory of retardation of the Cs^+ ions as well as for invaluable suggestions and advice regarding experimental procedure and interpretation of results.

THE ABSORPTION COEFFICIENT FOR SLOW ELECTRONS IN GASES

By C. E. Normand
Department of Physics, University of California

(Received April, 1, 1930)

Abstract

The absorption coefficient has been measured in H_2, He, A, Ne, N_2, and CO for electrons with velocities corresponding to from 0.5 to 400 volts. As a result of the high resolving power of the apparatus fine structure was found in the curves of all the gases. A minimum in the absorption coefficient curve was found in every case at velocities between 0.7 and 1.1 $(\text{volts})^{1/2}$. A lack of agreement between the present measurements at velocities below 2 volts and recent results of Ramsauer and Kollath appears to be due to a difference of about 0.5 volts in the velocity scales of the two sets of observations.

THE absorption coefficients for slow electrons in hydrogen, helium, argon, neon, nitrogen, and carbon monoxide have been rather definitely established by the investigations of Ramsauer,[1,2] Brode,[3] and Bruche.[4,5,6] Measurements in each of these gases have been made by two or more observers. The object in redetermining the absorption coefficient curves for these gases was two-fold: first to detect any fine structure in the curves which might be brought out by the use of an apparatus having a velocity resolving power higher than had previously been used, and second to extend the measurements as far as possible into the low velocity region.

Apparatus and Method

The apparatus and method employed in this experiment were essentially the same as used by Brode in determining the absorption coefficient in gases.[3] The apparatus used in producing the electron beam was the one used by Brode in his determinations of the absorption coefficient in mercury[7] and the alkali metal vapors.[8] Except for the tungsten filament the apparatus was constructed entirely of tantalum. The electron source was a 3 mil tungsten filament placed along the axis of a cylinder 7 mm in diameter. The electrons were accelerated to the cylinder. A narrow beam of these electrons passed through a longitudinal slit 0.2 mm wide and 5 mm high in the cylinder, and was bent by a magnetic field into a circular path defined by a system of

[1] C. Ramsauer, Ann. d. Physik **64**, 513 (1921).
[2] C. Ramsauer, Ann. d. Physik **66**, 546 (1921).
[3] R. B. Brode, Phys. Rev. **25**, 636 (1925).
[4] E. Bruche, Ann. d. Physik **82**, 912 (1927).
[5] E. Bruche, Ann. d. Physik **83**, 1066 (1927).
[6] E. Bruche, Ann. d. Physik **84**, 279 (1927).
[7] R. B. Brode, Proc. Roy. Soc. **A125**, 134 (1929).
[8] R. B. Brode, Phys. Rev. **34**, 673 (1929).

four slits. The last slit of this system was 1 mm wide and 10 mm high. Electrons passing through this last slit entered a collector and were measured by a high sensitivity galvanometer placed between the collector and ground. The reading, I, of this galvanometer was taken as a measure of the intensity of the beam at the end of its path.

The initial intensity of the electron beam was taken as proportional to the total emission, M, from the slit in the cylinder which surrounded the filament. That this proportionality holds, even at low velocities, throughout the pressure range used is shown by the fact that the logarithm of the ratio of I to M is a linear function of the pressure. Fig. 1 shows several examples, taken in helium, of this linear relation. The consistency with which the points fall on a straight line is also an indication of the experimental accuracy of the determinations of the absorption coefficient at these low velocities.

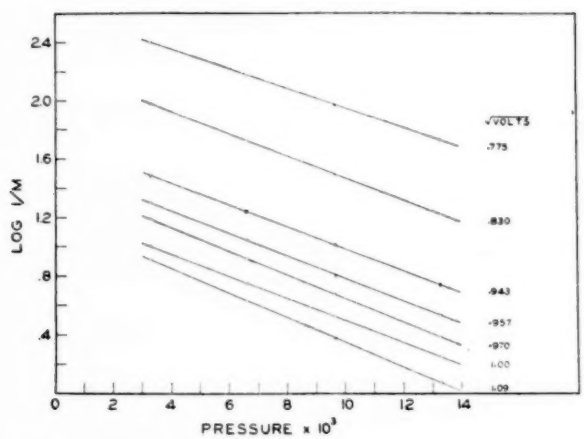

Fig. 1. Log of ratio of maximum current I at collector to total current M from slit in cylinder as a function of pressure, for low velocity beams in helium.

Due to the potential drop in the filament and the contact e.m.f. between the tantalum cylinder and the tungsten filament the applied potential will not give the true velocity of the electrons. The true velocity was determined from the magnetic field required to bend the electron beam into the circular path defined by the slit system of the apparatus. If r is the radius of this path, H the magnetic field strength in gauss, and V the energy of the electrons in equivalent volts, $H \cdot r = 3.3\, V^{\frac{1}{2}}$. Since r is a constant of the apparatus the electron velocity in root volts is proportional to the magnetic field strength or to the current, I_h, producing the magnetic field. Working with acceleration potentials of 100 volts or more, where the filament drop and the contact e.m.f. were negligible, the square root of the accelerating potential when plotted against I_h gave a straight line passing through the origin, Fig. 2. From the slope of this line the velocity corresponding to any value of I_h could be calculated. For accelerating potentials below 25 volts the influence of the filament drop and the contact e.m.f. becomes appreciable causing the points to lie above the straight line which gives the true velocity.

As a check of this method of velocity determination retarding potential curves were taken at a number of velocities between 0.5 and 1.2 volts. With a given accelerating potential I_h was varied until I was a maximum. From this value of I_h the velocity of the electrons was calculated. A retarding

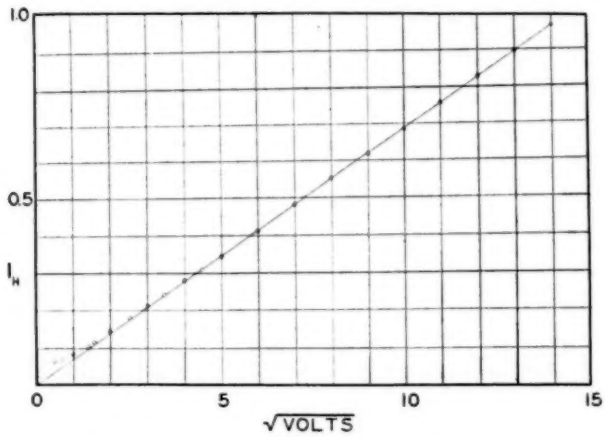

Fig. 2. Deflecting magnetic field current I_h as a function of the square root of the accelerating potential.

potential was then applied between the collector and ground and the values of I corresponding to measured increasing values of the retarding potential were recorded. The points of inflection of the curves obtained by plotting the collector current, I, against the retarding potential give the velocity of the electrons. Four of these curves are shown in Fig. 3. The vertical lines indicate the velocity as calculated from the deflecting magnetic field

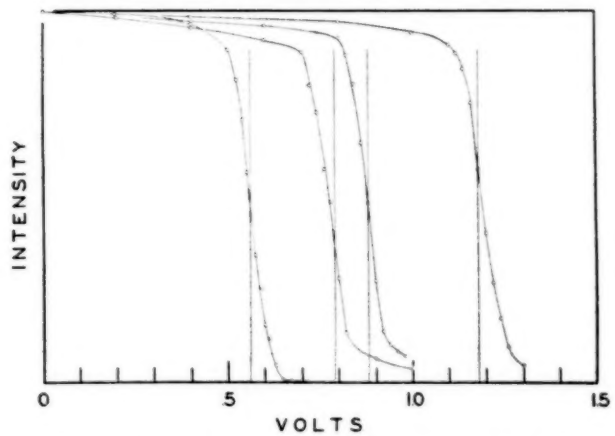

Fig. 3. Intensity of electron current arriving at collector as a function of retarding potential applied between collector and ground.

current I_h, Fig. 2. For six velocities between 0.5 and 1.2 volts the mean deviation of the values as measured by the two methods was 0.014 volts.

These retarding potential curves give also a measure of the velocity resolving power of the apparatus. The width of the half maximum of the

electron velocity distribution curves is found to be 0.035, 0.040, 0.031, 0.030 volts$^{\frac{1}{2}}$ for mean velocities equivalent to 0.56, 0.79, 0.88, 1.18 volts respectively. From the dimensions of the apparatus the maximum variation of the velocity of the electrons passing through the last slit should be about 3 percent of the mean velocity.

Results

The results are shown in Figs. 4 to 9 where the absorption coefficient, α, is plotted as a function of the electron velocity in volts$^{\frac{1}{2}}$. The previous results of Brode, and Bruche, are also given. All the observed values of α have been plotted in each case. The consistency of the results is shown by the fact that many of the points taken on different days agree within less than one percent. α is expressed in square centimeters per cubic centimeter of the gas at 0°C and a pressure of 1 mm of Hg.

Hydrogen was prepared by the electrolysis of barium hydroxide and was further purified and dried by passage over heated copper and through a phophorous pentoxide tube. The general form of the curve agrees well with the results of Bruche. A small secondary maximum in the curve appears at 2.2 volts$^{\frac{1}{2}}$, and at 1.55 volts$^{\frac{1}{2}}$ a sharp peak similar to those observed by Brode in the alkali metal vapors is superimposed on the broad maximum previously observed. A distinct minimum occurs at 1.1 volts$^{\frac{1}{2}}$ beyond which the curve rises rapidly with decreasing velocity.

Helium was purified by slow passage through a charcoal trap immersed in liquid air, the trap having been previously baked at 500°C. At the higher velocities the results are in good agreement with those of Brode. The maximum, however, occurs at a velocity lower than determined by Brode and Bruche and appears as two distinct and almost equal maxima. Beyond the second maximum is a minimum at 0.92 volts$^{\frac{1}{2}}$ and for still lower velocities the curve rises slightly.

Argon was purified by a magnesium arc. There are indications of fine structure between 4.5 and 5.5 volts$^{\frac{1}{2}}$. The minimum is at about 0.8 volts$^{\frac{1}{2}}$.

Neon, purchased as 99.5 percent pure, was used without further treatment. The value of α increases steadily to a maximum at about 5 volts$^{\frac{1}{2}}$. From here the curve drops irregularly to a final minimum at 0.85 volts$^{\frac{1}{2}}$.

Nitrogen was prepared by the decomposition of sodium azide on being heated. The curve has a small maximum at 12 volts$^{\frac{1}{2}}$, pronounced fine structure between 2 and 3 volts$^{\frac{1}{2}}$ and a very large and sharp maximum at 1.5 volts$^{\frac{1}{2}}$. A slight nick occurs at 1.2 volts$^{\frac{1}{2}}$ and a final minimum is reached at slightly below 1 volt.

Carbon monoxide was prepared by the decomposition of formic acid on being dropped into hot sulphuric acid, and was dried by passage through a phosphorous pentoxide tube. The results are in very good agreement with those of previous observers. The similarity between the CO and N_2 curves is seen to persist even in the fine structure.

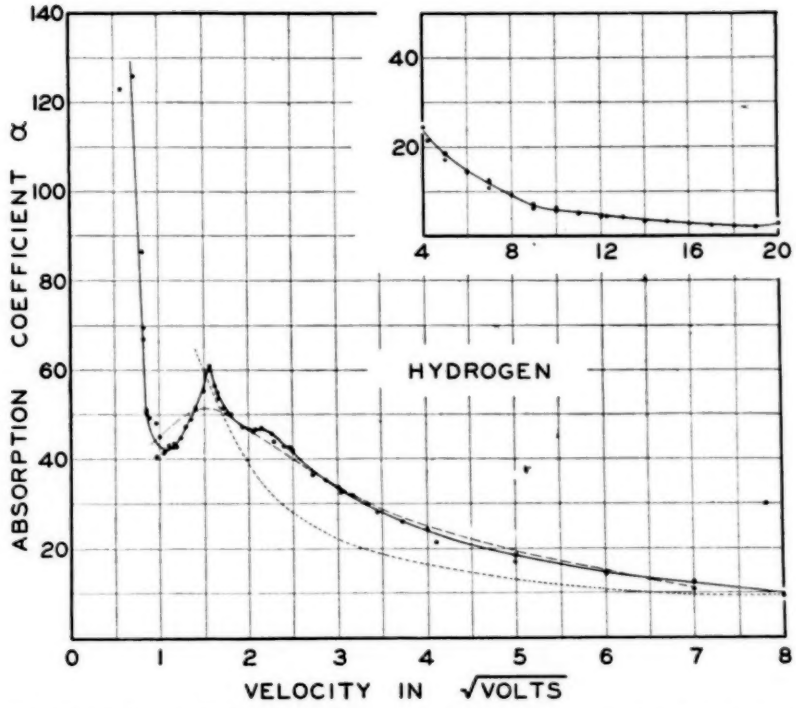

Fig. 4. The absorption coefficient α for electrons in hydrogen as a function of the velocity of the electrons.

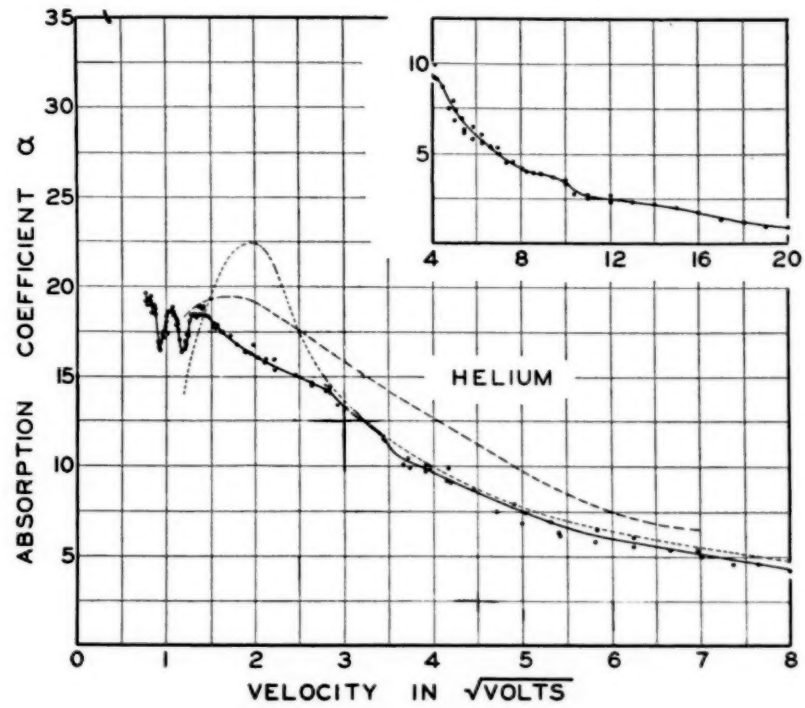

Fig. 5. The absorption coefficient α for electrons in helium as a function of the velocity of the electrons.

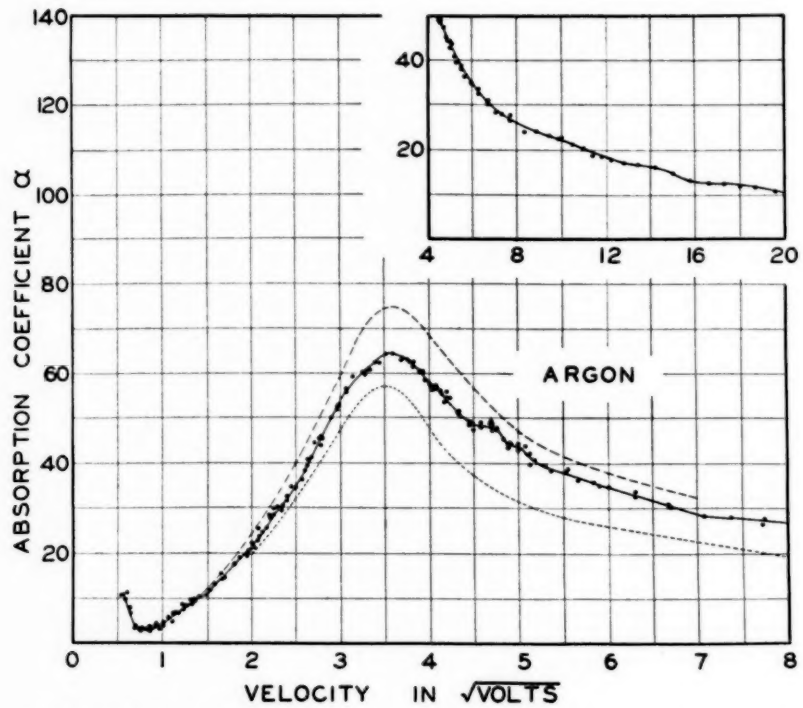

Fig. 6. The absorption coefficient α for electrons in argon as a function of the velocity of the electrons.

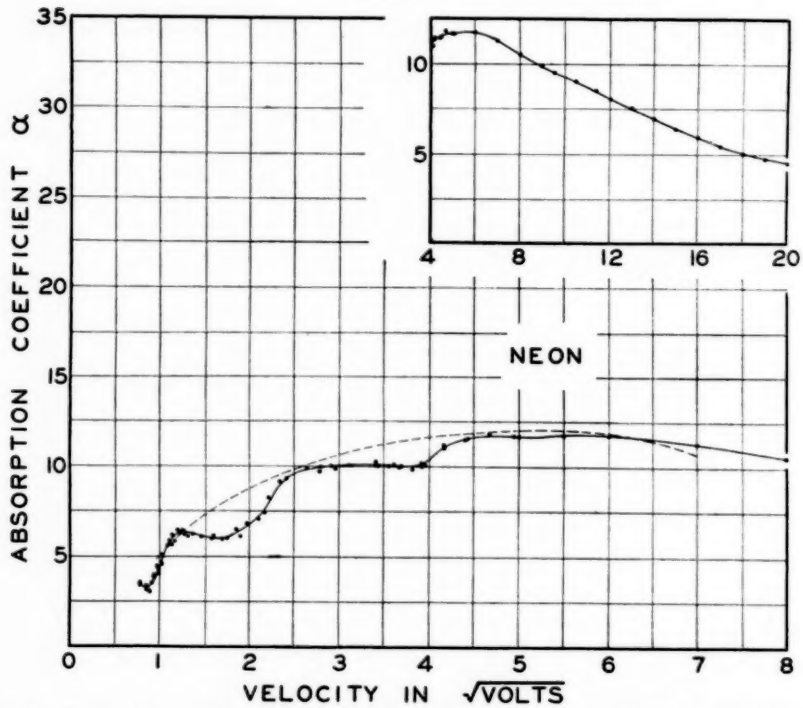

Fig. 7. The absorption coefficient α for electrons in neon as a function of the velocity of the electrons.

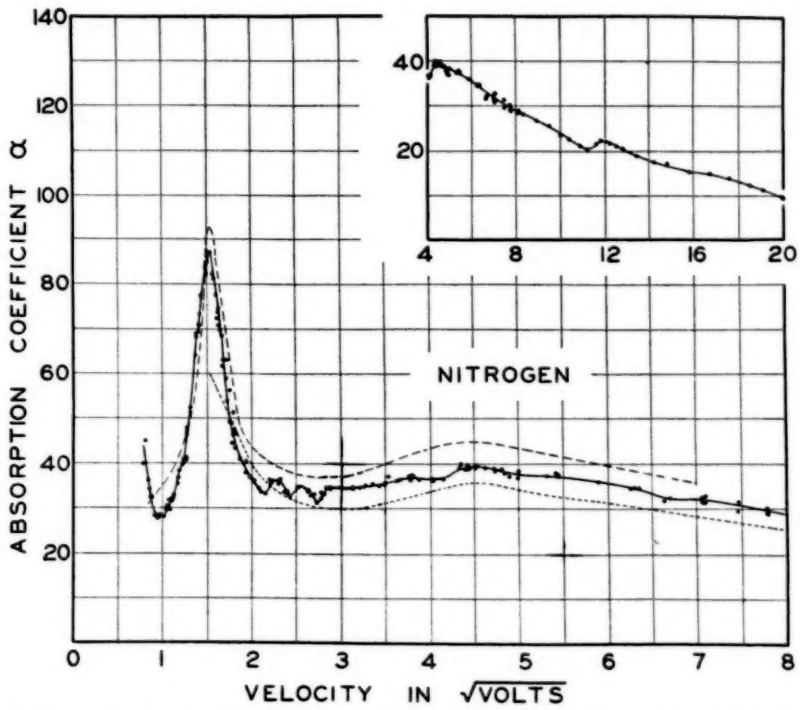

Fig. 8. The absorption coefficient α for electrons in nitrogen as a function of the velocity of the electrons.

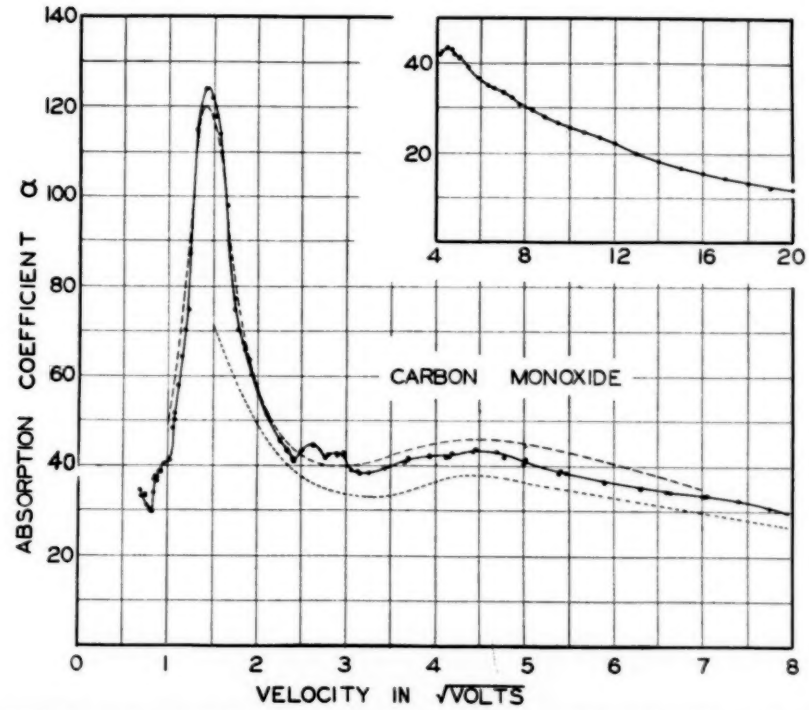

Fig. 9. The absorption coefficient α for electrons in carbon monoxide as a function of the velocity of the electrons.

Low Velocity Results

For velocities below 1 volt the intensity of the electron beam drops off very rapidly with decreasing velocity. Somewhat greater intensity and extended range toward lower velocity was obtained by applying an accelerating potential of about 1.5 to 2 volts and then retarding the electrons to the desired velocity. The values of α obtained with and without the auxiliary

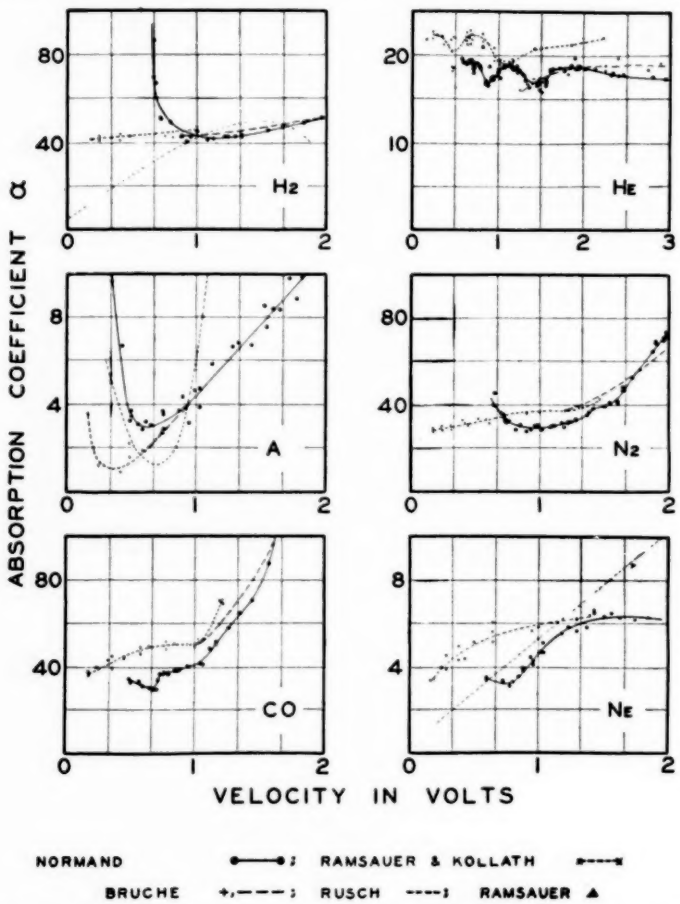

Fig. 10. The absorption coefficient α for very slow electrons in H_2, He, A, Ne, N_2, and Co as a function of the energy of the electrons in volts.

retarding potential were identical. The rapid diminution of intensity, however, rendered impossible the determination of α for velocities lower than about 0.5 volts except in the case of argon where measurements were extended to about 0.3 volts.

The results of these measurements for velocities below 2 volts, (3 volts in the case of He), are given in Fig. 10 together with the recent results of Ramsauer and Kollath,[9,10] the earlier results of Bruche,[11] and the points

[9] C. Ramsauer and R. Kollath, Ann. d. Physik **3**, 536 (1929).
[10] C. Ramsauer and R. Kollath, Ann. d. Physik **4**, 91 (1929).
[11] M. Rusch, Phys. Zeits. **26**, 748 (1925).

obtained by Ramsauer[1] in his first measurements. Here α is plotted as a function of the electron energy in equivalent volts rather than of electron velocity, volts$^{\frac{1}{2}}$. In no case is the agreement with Ramsauer and Kollath as good as might be expected from the accuracy of the measurements in each case.

A comparison of the results in the case of helium is especially interesting. The actual magnitude of the values of α given here are about 17 percent smaller than those given by Ramsauer and Kollath. Neglecting this difference in magnitude, which is of little importance, the two curves are seen to be nearly identical if Ramsauer and Kollath's velocities are increased by about 0.4 volts or if the velocities in this paper are decreased by the same amount. The agreement with the results obtained by other observers is seen to be better for the values of velocity given in this paper than for those given by Ramsauer and Kollath.

What has been said about the disagreement of the values of the velocity for helium is equally true for all the other gases measured. The magnitudes of the coefficient are in somewhat closer agreement but the volt scale is still displaced by about 0.4 to 0.6 volts. As already described, the velocity has been carefully checked throughout these measurements. Ramsauer and Kollath have also checked their velocities by both the retarding potential and the magnetic deflection method. The most probable source of the discrepency would appear to be a contact e.m.f. The thin sheet tantalum parts of the apparatus used in this experiment were spotwelded together. The apparatus was baked at 500°C for several hours and the tantalum parts were heated to a bright yellow with an induction furnace. At no time were unsteady conditions such as reported by Ramsauer and Kollath observed. The apparatus of Ramsauer and Kollath was constructed of brass and placed under an evacuated bell-jar. The unsteady conditions arising from contact e.m.f.s between the parts of the apparatus made necessary the complete dismanteling of the apparatus and the scraping of all metal surfaces at intervals of about 10 days. By this treatment steady and repeatable measurements were obtained with their apparatus.

The author wishes to express his indebtedness to Professor R. B. Brode for proposing this investigation, for his many helpful suggestions, and for his interest throughout the work.

ON THE CONCENTRATION OF METASTABLE MERCURY ATOMS

By E. Gaviola
Instituto de Fisica, La Plata University, Argentina

(Received March 26, 1930)

Abstract

The concentration of metastable atoms in presence of 3 mm nitrogen obtained using the measurements of Stuart seems to be in contradiction with a calculation given here using observations of Wood. The contradiction disappears if the different statistical weights of the levels 2^3P_1 and 2^3P_0 are taken in account. Corrected curves for the number of metastable atoms as functions of the foreign gas pressure are given for CO, H_2O, N_2, A and He which are to replace the corresponding curves of the previous paper. It is shown that the assumption of the author that by high primary light intensities the number of metastable atoms increases only with the square root of the intensity is strikingly supported by measurements of Wood.

THIS paper is a continuation of a previous one[1] by the author "On life and concentration of metastable atoms and the quenching of mercury resonance radiation." The concentration of metastable mercury atoms produced by collisions of resonance ones optically excited with nitrogen (or other foreign gas molecules) can be calculated numerically from the well-known fact that the introduction of a few mm of nitrogen into the vessel containing the mercury vapour (illuminated by a quartz mercury lamp) produces a many-fold increase in the intensity of the visible mercury lines emitted as fluorescence by the vapour. R. W. Wood[2] observed increases of the intensity of the green line 5461 ranging from 16 to 32 times. He interpreted this increase as due to the accumulation of metastable atoms when nitrogen is present and he was able to show experimentally by means of the absorption of the line 4046 that metastable atoms actually were present in large amounts. Let us now calculate numerically how many metastable atoms were present in the experiments of Wood, repeated and extended afterwards by the author.[3]

I

The green line 5461 is emitted by the 2^3S_1 level and its intensity in fluorescence which we will call J_{5461} is equal to

$$J_{5461} = A_{5461} \cdot N_s \tag{1}$$

if A_{5461} is the Einstein spontaneous transition probability and N_S the number of atoms in the level 2^3S_1. This level can be reached when mercury vapour alone is in the fluorescence vessel ("vacuum" case) practically only[3] through

[1] E. Gaviola, Phys. Rev. **34,** 1373 (1929).
[2] R. W. Wood, Phil. Mag. **50,** 761, 774 (1925); **4,** 466 (1927).
[3] E. Gaviola, Phil. Mag. **6,** 1167 (1928).

the absorption of the line 4358 of the arc on the part of the the resonance atoms in the level 2^3P_1, the number of which we call N_1^0. It is therefore possible to write

$$N_s(\text{vacuo}) = \frac{1}{c} N_1^0 \cdot I_{4358} \cdot B_{4358} \cdot \tau_s \tag{2}$$

where I_{4358} is the intensity of the line 4358 of the primary light source, B_{4358} its Einstein absorption coefficient and τ_S the mean life of the atoms N_S.

If a few mm pressure of nitrogen gas are admitted to the vessel containing the saturated mercury vapour, many resonance atoms are brought down by collisions with nitrogen molecules to the mestastable level 2^3P_0 where owing to

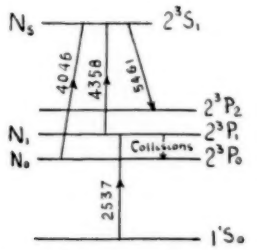

Fig. 1. Diagram of transitions.

is long life they accumulate until a concentration is obtained which, as the absorption experiments show is many times larger than the one of resonance atoms. The level 2^3S_1 is reached now practically only by the absorption of the line 4046 of the primary lamp on the part of the metastable atoms N_0 and consequently

$$N_s\,(\text{gas}) = 1/c \cdot N_0 \cdot I_{4046} \cdot B_{4046} \cdot \tau_s. \tag{3}$$

It may be thought that the admission of nitrogen might also disturb the atoms in the level 2^3S_1 diminishing their number as a result of collisions, in which case formula (3) would give too large numbers. But according to recent results of Hanle and Richter[4] it takes at least 80 mm pressure of nitrogen to produce noticeable influence upon the level 2^3S_1. Formula (3) is therefore correct for all pressures below 80 mm and as our pressures do not exceed 10 mm we can quietly use it. Combining (1) with (2) and with (3) and dividing we obtain

$$J_{5461}\,(\text{gas})/J_{5461}\,(\text{vacuo}) = N_0/N_1^0 \cdot I_{4046}/I_{4358} \cdot B_{4046}/B_{4358}.$$

This ratio was photographically measured and found to be equal to 32 in Wood's earlier experiments, therefore

$$N_0/N_1^0 = 32 \cdot I_{4358}/I_{4046} \cdot B_{4358}/B_{4046}. \tag{4}$$

Now, the ratio I_{4358}/I_{4046} of the intensities of the blue and violet lines of the arc has been repeatedly measured and found to be equal to 2. As both lines

[4] W. Hanle and E. F. Richter, Zeits. f. Physik **54**, 816 (1929).

are emitted by the same upper level, the ratio of their intensities gives at the same time the relation of the values of their corresponding Einstein emission coefficients A_{4358} and A_{4046} if that value is not falsified by absorption or reversal of the lines before they leave the mercury lamp. As that ratio is the same for the lines of the primary lamp when the discharge is magnetically deflected against the wall of the tube as for the secondary fluorescence light in the case of "vacuo" when practically no reabsorption can take place, one can write with confidence

$$A_{4358}/A_{4046} = 2 = I_{4358}/I_{4046}. \tag{5}$$

Between the coefficients A and B there is a relation

$$A = B \cdot 2h\nu^3/c^2 \cdot q_1/q_2 \tag{6}$$

where q_1 and q_2 are the statistical weights of the lower and upper levels respectively. The statistical weights of the levels 2^3P_0, 2^3P_1 and 2^3S_1 are 1, 3 and 3, therefore for 4358 $q_1/q_2 = 1$ and for 4046 $q_1/q_2 = 1/3$. We can then write

$$A_{4358}/A_{4046} = 2 = B_{4358}/B_{4046} \cdot (\nu_{4358}/\nu_{4046})^3 \cdot \tfrac{1}{3}$$

and since $(\nu_{4358}/\nu_{4046})^3 = 0.8$ we obtain

$$B_{4358}/B_{4046} = 7.5.$$

Introducing the now known numerical values in formula (4) we have finally

$$N_0/N_1^0 = 32 \times 2 \times 7.5 = 480. \tag{7}$$

That means that when a few mm of nitrogen are present in the tube the number of metastable atoms is 480 times larger than the number of resonance atoms when no nitrogen is present. This last number can be easily obtained numerically if the intensity of the primary line 2537.5 is known. N_1^0 is for instance equal to one if 10^7 light quants are absorbed per second in the volume element considered (since the life of 2^3P_1 is 10^{-7} sec.).

II

In a former paper of mine on the same subject[1] I have made a numerical calculation of the ratio N_0/N_1^0 as a function of the foreign gas pressure for different gases (and among them for nitrogen) using the measurements of Stuart for the quenching of resonance radiation and some other experimental data. Now, Fig. 5 of that paper indicates that for a pressure of about 3 mm of nitrogen (which was the pressure used by Wood to obtain a 32 fold increase of the green line) the ratio N_0/N_1^0 ought to be about 1200. This number is nearly three times larger than the one obtained above. It is therefore necessary to solve this contradiction. This we shall here do. The values of my former paper were all calculated neglecting the fact of the different statistical weights of the levels 2^3P_1 and 2^3P_0.[5] If we take this fact into account, none of the previous formulas is changed but the value α which

[5] Dr. H. Beutler kindly called my attention to this point.

indicates the ratio N_0/N_1 for the case of thermal equilibrium and is given by the formula

$$\alpha = q_0/q_1 \cdot e^{w/kT} \tag{8}$$

where q_0 and q_1 are the statistical weights of the levels 2^3P_0 and 2^3P_1 respectively and w their energy difference, this value α becomes three times smaller than it was assumed to be in the previous paper because $q_0/q_1 = 1/3$. For the same reason the constants b and E_0 of Table I of that paper are three times too small. If we recalculate now the curves for $N_0/N_1{}^0$ as a function of

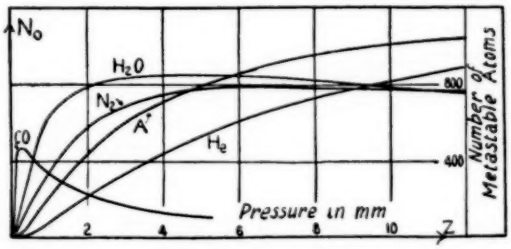

Fig. 2. Number of metastable atoms as a function of the foreign gas pressure if 10^7 quanta are absorbed per second.

the pressure of foreign gases using three times larger values for b and E_0 and a three times smaller α we obtain the curves reproduced in Figs. 2 and 3 which are to take the place of Figs. 5 and 6 of the previous paper. We see in Fig. 2 that the number $N_0/N_1{}^0$ for about 3 mm nitrogen pressure has reduced itself to about 700. This number is still larger than the one obtained independently in the first part of this paper but we have to remember that the number 480 corresponds to the experimental conditions of Wood while the number 700

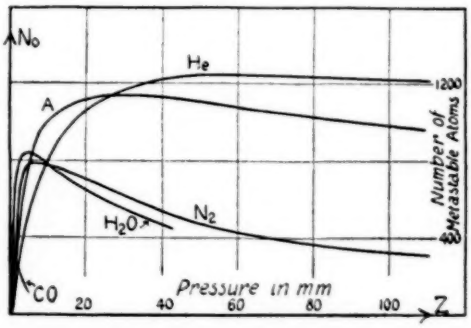

Fig. 3. Number of metastable atoms as a function of the foreign gas pressure for $N_1{}^0 = 1$ (10^7 quanta absorbed per second).

to those of Stuart. The main difference between the experimental conditions of both observers was that Wood used a considerably larger primary light intensity. As I have shown in the previous paper N_0 increases for large primary light intensities not proportional to the intensity itself but to the

square root of it, while N_1^0 grows on linearly. The relation N_0/N_1^0 must therefore become smaller for large intensities, as in the case of Wood. An interesting confirmation of this result is given by the measurements of Wood himself. In his earlier experiments[6] he obtained as said above a 32 fold increase of the green line by the admission of nitrogen. After that he increased his primary light intensity considerably by pressing the arc discharge against the wall with a magnetic field. The increase of the green line was now at best only 15 fold.[7] The ratio N_0/N_1^0 had decreased therefore (compare formulas (4) and (7)) to 225. Since the decrease of N_0/N_1^0 for large intensities is due to collisions between two metastable atoms which destroy both of them (one is excited to a higher level, the other becomes normal) the above result is a striking hint at the fact that the probabity of such collisions (collision-section) must be rather large.

[6] R. W. Wood, Phil. Mag. **50**, 761 (1925).
[7] R. W. Wood, Phil. Mag. **4**, 485 (1927).

THE MOST PROBABLE 1930 VALUES OF THE ELECTRON AND RELATED CONSTANTS

By Robert A. Millikan
Norman Bridge Laboratory of Physics, California Institute, Pasadena

(Received April 8, 1930)

Abstract

The conclusions are reached that: (1) No such empirical oil-drop formula as that suggested by H. A. Wilson can be valid, (2) It is highly improbable that the spectroscopic fine structure constant can be a whole number—either 136 or 137, (3) The most probable 1930 values of e, N, and h, are the same as in 1917, corrections due merely to new determinations of the velocity of light and the absolute value of the ohm being alone needed. These values so corrected are

$$e=(4.770\pm0.005)\times10^{-10} \quad h=(6.547\pm0.011)\times10^{-27} \quad N=(6.064\pm0.01)\times10^{23}.$$

(4) If Lewis and Adam's theoretical equation is considered valid the probable errors are much smaller than the foregoing estimates.

THE first purpose of this paper is to comment on Professor H. A. Wilson's "Note on the Value of the Electric Charge,"[1] in which he concludes that "the oil-drop experiments do not definitely exclude" a value of e one percent higher than 4.774×10^{-10}; the second purpose is to express an individual 1930 judgment, with the reasons therefor, as to the best values of these constants in view of all that has been done to date in the way of their exact evaluation; the third purpose is briefly to discuss the mutual restrictions which the theorists and the experimentalists impose upon each other; and the fourth is to present evidence bearing on Eddington's contention that the spectroscopic fine-structure constant is a whole number.

I. Oil-Drop Method's Precision

If there were nothing more to the oil-drop work than the finding of some empirical equation that would reproduce the experimental data published in my 1917 paper,[2] then the statement quoted above might have some justification; but the experimental facts are, first, that Professor Wilson's empirical equation merely fits the relatively *short portion* of the oil-drop curve which corresponds to these data, and shoots above a considerable number of *observed points* farther down on the curve, that is, corresponding to smaller values of $1/pa$, then runs into the axis at a point much higher than these observed points permit; second, that it departs very largely from the *observed curve* at its upper end, that is, for large values for $1/pa$. For not only has the complete oil-drop curve from very low to very high values of $1/pa$ been worked out empirically so that we know by experiment

[1] H. A. Wilson, Phys. Rev. **34**, 1493 (1929).
[2] R. A. Millikan, Phil. Mag. **34**, 1 (1917).

that no such equation as that given by Professor Wilson is valid, but also—and this is more important—in view of a group of papers, some by myself,[3] partly experimental and partly theoretical, and a masterly one by Epstein,[4] *we now know precisely why Stoke's law of fall breaks down*, and why the law of fall embodied in the oil-drop equation takes its place.

I shall later in the paper have reason to insist that the theorist is bound to build his theories so that they do not collide head on with experimental facts; but at this point my insistance is that the experimentalist is not justified in setting up an empirical equation which makes Nature behave in a way which established and well verified theory tells him that she cannot behave. With this my comment upon Professor Wilson's paper is ended, and possibly no further remarks on e, h, and N would be needed had not Professor Zwicky's recent work on the secondary or block-structure of crystals gone far toward clearing the atmosphere surrounding these constants since Birge's masterly review[5] of last July appeared. This may perhaps justify the following brief historical review and new appraisal of where these constants now seem to me to stand.

II. Changes in e, h, and N in Fourteen Years

Fourteen years ago, at the conclusion of seven years of work on the experimental evaluation of these three constants, the electron, the Avogadro number, and Planck's quantum of action, the following were published as the most reliable values then attainable:[2]

$$\begin{aligned} e &= 4.774 \pm .005 \times 10^{-10} \\ h &= 6.547 \pm .006 \times 10^{-27} \\ N &= 6.062 \pm .006 \times 10^{-23} \end{aligned} \tag{1}$$

and these values have been incorporated into most of the tables and texts compiled since that time; but quite recently some uncertainty has arisen, and there has been a widespread discussion of these constants, stimulated, in the first instance, by Eddington's theoretical suggestion as to what ought to be the value of the spectroscopic fine-structure constant, and in the second place by the more recent experimental work of Bäcklin,[6] Wadlund,[7] and Bearden[8] on the comparison of x-ray wave-lengths as determined by ruled gratings and by crystals. After this discussion, the following is where the matter now stands from the viewpoint of an experimentalist,—that is, the man who is engaged in making the measurements themselves and who has the feeling and the judgment that possibly only the observer can have about the relative reliability of the readings involved.

[3] R. A. Millikan, Phys. Rev. **21,** 67 (January 1923); also **21,** 217 (March 1923); also **22,** 1 (July 1923).

[4] P. S. Epstein, Phys. Rev. **23,** 710 (June 1924).

[5] Raymond T. Birge, Phys. Rev. Supplement **1,** 1 (1929).

[6] E. Bäcklin, "Absolute Wellenlängenbestimmungen der Röntgenstrahlen," Uppsala Dissertation, 1928.

[7] A. P. R. Wadlund, Proc. Nat. Acad. Sci. **14,** 588 (1928), and Phys. Rev. **32,** 841 (1928).

As to the electron, I think it is generally agreed that the oil-drop method still remains the chief, if not the sole, reliance of the physicist, so far as directness, reliability, and precision are concerned, in arriving at its value. I had myself hoped, and expected, that the comparison of wave-lengths as determined by ruled gratings and by crystals would lead to greater precision in the fixing of both N and e, but I now feel sure that both (1) the experimental results obtained by this method, and (2) Zwicky's theoretical work (Proc. Nat. Acad. March, 1930) on the secondary structure of crystals, show that this method cannot have anything like the reliability which we had hoped that it would show, and therefore that all of the methods which depend upon crystal grating-space, as computed from density and N, had better be left out of the accounting.

No new work has been done by the oil-drop method that is comparable in elaborateness nor precision with that published in 1917, but the fundamental constants entering into that method, such as the velocity of light and the value of the ohm, have been redetermined within that period, so that *the 1917 data, treated precisely as it was then treated, but combined with Michelson's new value of the velocity of light, namely, 2.99796 instead of 2.999, and the absolute value of the ohm* (my international volts thus are raised 1 part in 2000 to reduce them to absolute volts) *yields*

$$e = (\mathbf{4.770 \pm .005}) \times \mathbf{10^{-10}} \text{ absolute electrostatic units}^{9} \qquad (2)$$

in place of $(4.774 \pm .005) \times 10^{-10}$. *The foregoing is, then, merely the old oil-drop value of e* brought up to date by inserting new values of the velocity of light and the value of the ohm.

This value of the electron is also that at which Birge finally arrives as a result of his survey of the whole field of fundamental constants. It is true that he reanalyzes for himself my individual oil-drop readings and weights them so that he gets from them the value 4.768 ± 0.005 in place of my value

[8] J. A. Bearden, Proc. Nat. Acad. Sci. **15,** 528 (1920).

[9] The following quotation is made from an article published in Science on May 10, 1929:

"The reason I have not heretofore made the foregoing readjustment in my value of e is, first, that it is of no particular significance any way, since it is in any case within the limits of my estimated uncertainty; and, second, that I have until recently doubted its legitimacy.

"In the presentation of the best values of widely used physical constants I have heretofore questioned the wisdom, or even the correctness, of making a differentiation between so-called international units and absolute units before a suitably authorized international commission had recognized that difference, since otherwise such differentiation would rest merely upon some individual's *estimate* of the superior reliability of some particular new determination or determinations over the weighted mean of the whole series of determinations used by the international commission which in 1908 and 1911 fixed upon the international units. However, Professor Raymond T. Birge has called my attention to the fact that in view primarily of the close agreement between new determinations of the absolute value of the ohm by F. E. Smith (*Phil. Trans.*, 1914) and Grüneisen and Giebe (*Ann. d. Physik*, 1920), the compilers of tables have actually recently begun to make the foregoing differentiation. It is because of this fact and because of Michelson's undoubted new precision in the measurement of the velocity of light that I have thought it worth while to begin herewith to recognize the effect of these changes upon the value of e."

4.770 ± 0.005, a result that is so much nearer mine than my experimental uncertainty that I am quite content—indeed gratified—but I may perhaps be pardoned for still preferring my own graphical weightings, since I thought at the time, and still think, that I got the best obtainable results in that way from my data. The person who makes the measurements certainly has a slight advantage in weighting over the person who does not, and the *graphical method by which I got at my final estimated uncertainty* is, I think, in the hands of the experimenter himself more dependable than least squares. A glance at the 1917 paper will show that I used least squares only to exhibit how well my observed points were distributed about my final graphically chosen *line*. Birge actually chooses for his final value my own foregoing value, 4.770, instead of 4.768, because he attaches enough weight to Wadlund's work to induce him to push the latter value up by 2 parts in 5000. Wadlund's work, however, must now, I think, be thrown entirely out of account, both because Bearden's repetition of it yielded a full percent of divergence from it and because Zwicky's theoretical block-structure work indicates that the method itself involves up to a percent of uncertainty.

The photoelectric evaluation of h, as reported in this same 1917 article, was $(6.56 \pm 0.03)10^{-27}$, but *it was definitely stated in that article* that the value of this constant derived from the Bohr equation

$$R_\infty = \frac{2\pi^2 e^5}{h^3 c^2 e/m} \tag{3}$$

was in my judgment the most reliable value then obtainable, the value then resulting from inserting in the foregoing equation $e = 4.774$ and $e/m = 1.767$ was as given in that paper

$$h = (6.547 \pm 0.01) \times 10^{-27} \tag{4}$$

Birge, from his recently published survey, comes to precisely this 1917 value with practically the same estimated error, namely, 0.008, so that these fourteen years have not changed at all the final result as to h. The reason that h remains unchanged while my e suffers a slight decrease is that the new work done by Babcock[10] and Houston[11] changes e/m as spectroscopically determined to 1.761, while the value used in the 1917 computations was 1.767, and this change just balances the foregoing change in e. The present numerical equation is

$$h = \left[\frac{2\pi^2(4.770 \times 10^{-10})^5}{109737.42(2.99796 \times 10^{10})^2(1.761 \times 10^7)}\right]^{1/3} = 6.5471 \times 10^{-27} \text{erg. sec.} \tag{5}$$

The Avogadro number Birge estimates as 6.064 ± 0.006 in place of the 1917 value, namely, 6.062 ± 0.006. In view of the estimated error in both cases the difference of course has no significance whatever. The reason the agreement is so good is that new work on the electro-chemical equivalent

[10] Babcock, Phys. Rev. **33**, 268 (1929).
[11] Houston, Phys. Rev. **30**, 608 (1927).

leads Birge to choose to modify the Faraday constant in such a way as nearly to offset the influence of the slight change in e on the value of N.

So far, then, as the foregoing estimates by both Dr. Birge and myself are to be depended upon, the last fourteen years have introduced no change into the values of e, h, and N as experimentally determined, save the insignificant one in e due to new precision in the velocity of light and the value of the ohm.

III. Theoretical Relationships

What, then is to be said of the demands that the theorists have made upon the relations of these constants? This is a very important and a very interesting question. There are two such relations to be considered, one brought forward by Lewis and Adams[12] in 1914 and one by Eddington[13] in 1929. With respect to the first, I have nothing to add to Birge's comments, except to emphasize them. Lewis and Adams, from their theory of ultimate rational units arrive at the following relation between h, c, and e:

$$\frac{hc}{2\pi e^2} = 8\pi\left(\frac{8\pi^5}{15}\right)^{1/3}. \tag{6}$$

It will be seen that the right side of this equation involves no physical measurements whatever. It has the value 137.348. The left side, which is Eddington's spectroscopic fine-structure constant $1/\alpha$, contains three physically measured quantities, and if the values $e=4.770\times10^{-10}$, $h=6.547\times10^{-27}$, and $c=2.99796\times10^{10}$ be inserted, *it yields 137.29 in exceedingly close agreement with the right side.*

This Lewis and Adams theoretical relationship is introduced here merely to emphasize the fact that if it is correct, then without recourse to any experiment at all the spectroscopic fine-structure constant—the left side of the foregoing equation—cannot possibly be a whole number, as contended by Eddington. Also, the remarkable agreement of the left side with the demands of the right side lends rather extraordinary experimental credentials to the Lewis and Adams relationship, although I believe that in other particulars it has not behaved itself so well.

But, turning next to experiment alone, what has it to say as to Eddington's suggestion that the spectroscopic constant $1/\alpha$ ought to be a whole number? The number he originally suggested was 136, but, as Birge pointed out, this suggestion was in irreconcilable conflict, first, with the oil-drop results on e; second, independently of e, it was in conflict with Houston's and Babcock's determinations of the spectroscopic value of e/m; and, third, it collided with Lewis and Adams' equation. The combined weight of this attack was so great that Eddington's suggestion could not possibly be entertained, provided the principle be admitted that the theorist cannot be permitted to ignore the facts in building his theories.

Quite recently, however, Eddington has changed the theoretical value of his fine-structure constant, still keeping it a whole number, but now

[12] G. N. Lewis and E. Q. Adams, Phys. Rev. **3**, 92 (1914).

[13] A. S. Eddington, Proc. Roy. Soc. **A122**, 358 (1929).

making it 137[14] instead of 136. This might perhaps remove the clash with my experimental oil-drop work, for if h were kept at 6.547 and e pushed up to 4.775—a change only a trifle outside the limits of my estimated experimental uncertainty—$1/\alpha$ would come down from 137.29 to 137. But quite independently of the oil-drop work on e, Eddington would still be in what appears to be an irreconcilable clash with the spectroscopic measurements on e/m and the following series of measurements on the ratio of h/e. To see this, write with Birge the spectroscopic equation in the following form:

$$R_\infty = \frac{\alpha^2}{2}\left(\frac{e}{h}\right)\frac{1}{e/m}.$$

This fits perfectly with $1/\alpha = 137.29$, $e = 4.770$, $h = 6.547$, and $e/m = 1.761$.

If, then, α^2 is to be pushed up the 0.42% necessary to make $1/\alpha$ equal to 137, then if e/h remains constant, e/m, spectroscopically determined, must go up 0.42%. But e/m, spectroscopically determined, and it is this mode of evaluation which obviously must be used for substitution in a spectroscopic equation, is now known to about one part in a thousand, for not only are both Babcock's and Houston's published determinations extraordinarily precise, but Houston and his associates inform me that the new independent determination that they are now making appears to check with the other two. If, then, there is no flexibility in e/m, the factor e/h must go down 0.42% or h/e up 0.42% to match the 0.42% rise in α^2.

Now h/e has been determined by four different methods, none of which involve the properties of crystals: (1) the photoelectric method; (2) the ionizing potential method; (3) the c_2, or Wien displacement-law method; and (4) the σ, or Stefan-Boltzmann-law method. *Not one of these methods will permit h/e to go up 0.42%.* The best result to date by the photoelectric method—which involves simply the equation $h\nu = eV$—is probably my 1916 value of h/e for sodium; for the length of the line, the slope of which gives h/e, was several times greater than that used by other observers, and in addition the currents were large and stopping potentials accurately determined. The value of h as published both in my 1916[15] and 1917[16] papers, and in "The Electron"[17] (1917) was $(6.56 \pm 0.03) \times 10^{-27}$, and this remains the value when absolute units, Michelson's new c, and $e = 4.770$ are used. Lukirsky and Prilezaev's recent determination[18] made with the metals Al, Zn, Sn, Ni, Cd, Cu, and Pt yields a mean 6.543×10^{-27}, and there has just appeared a paper by Olpin[19] which yields $h = 6.541 \times 10^{-27}$ "significant to three figures." I shall take the mean of these three, 6.560 and 6.543 and 6.541 namely 6.548, as the most probable value of h which combines with $e = 4.770$ to make the best photoelectric value of h/e.

[14] A. S. Eddington, Proc. Roy. Soc. **A126,** 696 (1930).
[15] Millikan, Phys. Rev. **7,** 373 (1916).
[16] Millikan, Phil. Mag. **34,** 14 (1917).
[17] Millikan, "The Electron" (1917), p. 227.
[18] Lukirsky and Prilezaev, Zeits. f. Physik **49,** 236(1928).
[19] A. R. Olpin, Phys. Rev. **35,** 670 (1930).

The ionizing potential method, also involving merely $h\nu = eV$ is most accurately used by Lawrence,[20] who gets, corresponding to $e = 4.770$, the value $h = 6.560 \pm 0.015$.

I have nothing to add to Birge's estimates of h/e from the Wien Displacement Law method which corresponds to $h = 6.548 \pm 0.015$. The equation here is $c_2 = hc/k$ where k is determined from, and is proportional to e, so that h/e has here the same error as c_2 and $c_2 = 1.432 \pm 0.003$ cm deg.

The Stefan-Boltzmann Law method does not yield h/e directly, but it does give, through Planck's equation, $h/k^{4/3} \propto /\sigma^{1/3}$ and although the variation in the experimental values of σ is large, since the error in $h/k^{4/3}$, or $h/e^{4/3}$, is only one-third that in σ, I am willing to accept Birge's estimate that the probable error in the value of h corresponding to $e = 4.770$ as given by this method is $h = (6.539 \pm 0.010) \times 10^{-27}$.

The mean of the values 6.548, 6.560, 6.548, and 6.539 by these four methods is 6.549, which is very close to my 1917 value 6.547, and *the foregoing analysis shows how extraordinarily unlikely it is that h/e can go up the 0.42% necessary to permit $1/\alpha$ to be 137*, as Eddington wishes it to be, so that even when the theoretical evidence from Lewis and Adam's equation is entirely discarded the *experimental situation alone* renders it highly improbable that Eddington's conclusion can be correct.

If, however, the experimental credentials which have thus far developed for Lewis and Adam's relation are considered significant, then the values of e, h, and N are probably considerably more accurately known than the foregoing estimates of probable experimental error indicate. If both Eqs. (5) and (6) are to be considered correct, then, since (5) is of the form $h/e^{5/8} \propto 1/e/m$, and (6) of the form $h/e^2 = \text{constant}$, when I compare them with the experimental limits of error of h/e I find that the possible range of variation in e, h, and e/m is very small indeed, and I should then write the most probable values of e, h, and e/m as follows:

$$e = (4.769 \pm 0.001) \times 10^{-10}$$

$$h = (6.547 \pm 0.001) \times 10^{-27}$$

$$e/m = (1.7595 \pm 0.001) \times 10^{7}.$$

It will be interesting to see whether new experimental work can check this prediction as to the value of e/m.

However, in view of the theoretical uncertainty in Lewis and Adams' relation, I think it safer not to depend at all upon it, and hence to continue to write, as representing the best 1930 experimental situation, the 1917 values merely corrected for volts and for speed of light, namely,

$$\boldsymbol{e = (4.770 \pm 0.005) \times 10^{-10}}$$

$$\boldsymbol{h = (6.547 \pm 0.010) \times 10^{-27}}$$

$$\boldsymbol{N = (6.064 \pm 0.006) \times 10^{23}}.$$

[20] E. O. Lawrence, Phys. Rev. **28**, 947 (1926).

THE UNIFORM POSITIVE COLUMN OF AN ELECTRIC DISCHARGE IN MERCURY VAPOR

By Thomas J. Killian
The Massachusetts Institute of Technology, Cambridge, Mass.
and
The Research Laboratory, General Electric Co., Schenectady

(Received January 11, 1930)

Abstract

Uniform positive column of an electric discharge in mercury vapor. The uniform positive column was studied in a long circular cylindrical tube by means of the Langmuir probe electrode method. Measurements were made of the space potentials, random electron current densities, and the electron temperatures along the axis and across a diameter of the tube at vapor pressures ranging from 0.27 baryes to 7.13 baryes. *The mobility of the electrons* was obtained and the results interpreted in terms of the mean free path of the electrons by Langevin's expression for mobility. ($\mu = 0.75e\lambda/m\bar{v}$) These mean free paths were in fair agreement with those obtained in angular scattering experiments by other investigators. *The rate of generation of positive ions* per electron was obtained from measurements of the positive ion current to the walls and the total number of electrons per unit length of tube. With the probabilities of ionization for electrons of various velocities obtained by other observers, it is found that at vapor pressures above 1.4 baryes the ionization is accounted for by the direct impacts with neutral atoms of electrons whose velocity distribution is Maxwellian. At lower vapor pressures it seems necessary to assume the presence of a larger number of higher speed electrons than is present in a Maxwellian distribution. The ratio of the concentrations of electrons at any two points on a diameter satisfies the Boltzmann equation. As the temperature of the electrons is lowered from 38,000°K to 19,900°K by raising the pressure of the mercury vapor the energy delivered to the walls by the recombination of positive ions and electrons decreases from 48 percent to 14 percent of the total input. Since less than 0.03 percent is lost through elastic collisions of electrons and atoms the remainder of the energy goes into excitation.

I. Introduction

THE electrical conditions in an ionized gas are completely determined when the densities of the electrons and ions and their distributions of velocities are known at every point within the discharge. The velocity distributions must of course be known both in direction and magnitude. From the densities of the electrons, negative ions and positive ions, n_e, n_n, and n_p respectively, the variation of the electric field can be obtained by means of Poisson's equation. A single integration of this equation gives the field at any point while a double integration the potential at the point. The currents to and the potentials of the various electrodes and walls of the tube furnish the boundary conditions necessary for the complete solution. The current densities of the electrons and ions, I_e, I_n, and I_p, can be determined in any direction at any point from the densities of the electrons and ions and the laws of their distribution of velocities. It is not difficult to understand why

the behavior of some discharges is so complicated since any of the variables may vary in time as well as in space.

In order to gain a general idea of the mechanism of gaseous discharges an investigation should be made of the simplest sort of discharge. In the positive column conditions are primarily dependent upon the pressure and nature of the gas and the current carried by the discharge and not upon the nature and position of the electrodes and the walls of the tube. If, furthermore, the positive column be studied in a long circular cylindrical tube, conditions will not only be constant along its length but in the absence of any transverse magnetic field there will also be radial symmetry. The uniform positive column of a mercury arc was studied in such a tube by means of the Langmuir probe electrode method.[1,2,3]

The most common type of velocity distribution occurring in nature is the random type known as the Maxwellian distribution. It has been found from an analysis of the volt-ampere characteristics of small electrodes placed in the positive column of a discharge that the free electrons move with a Maxwellian distribution of velocities in nearly random directions.[1,2,4] A small electrode, placed in the discharge, will repel electrons from its neighborhood and collect positive ions when it is negatively charged. Electrons with energies greater than Ve, where V is the potential of the collector below that of the space and e the charge of an electron, can, however, reach the collector. As the potential of the collector is increased a greater number of the more slowly moving electrons will be collected. Since these electrons have a Maxwellian distribution of velocities the ratio of their concentrations in two regions differing in potential by an amount V is given by the Boltzmann equation

$$n'/n = \epsilon^{Ve/kT} \tag{1}$$

where k is the Boltzmann constant and T the temperature of the electrons. Since the velocity distribution is not affected by a retarding field the random current densities are in the same ratio as the electron concentrations. It is thus seen that the logarithm of the electron current to a small collector varies linearly with the voltage of the collector and that the rate of change of the logarithm of the electron current with respect to the voltage is e/kT, where e/k is 11,600 degrees per volt and T is the temperature of the electrons in degrees absolute. This relation is only true when the collector is negative with respect to the space. If the field is an accelerating one the current increases more slowly and according to different laws.[3] Thus there is a transition at space potential. If the probe is a small one the break may be sharp enough to fix the space potential as in Fig. 5. When the collector is at space potential there is no sheath about it and its presence does not affect the discharge. Hence the random electron current, I_e, can be obtained by dividing

[1] I. Langmuir, Jour. Frank. Inst. **196,** 751 (1923).
[2] I. Langmuir and H. Mott-Smith, Gen. Elec. Rev. **27,** 449, 538, 616, 762, 810 (1924).
[3] H. Mott-Smith and I. Langmuir, Phys. Rev. **28,** 727 (1926).
[4] I. Langmuir, Phys. Rev. **26,** 585 (1925).

the electron current to the collector at this point by the area of the collector. According to kinetic theory the density of electrons in terms of their temperature and random current is given by

$$n_e = \frac{4I_e}{ev} = \left(\frac{2\pi m}{kT}\right)^{1/2} \frac{I_c}{e} = 4.03 \times 10^{13} \frac{I_c}{T^{1/2}} \tag{2}$$

where I_c is in amperes per cm^2. There is a second method of finding the space potential which consists in analysing the electron current to a collector when it exerts an accelerating field.[2,3]

Since the fields existing in the positive column are very small the density of positive ions is very nearly equal to that of the electrons, but due to their much higher mobility the electron current is from 200 to 400 times the positive ion current.

The positive ions do not appear to have a Maxwellian distribution of velocities but seem to obtain their velocities from the fields they move through after being formed.[5] Therefore the positive ion current to a collector is a measure of the number of positive ions formed per second in a region drained by the collector and surrounded by a surface of maximum potential. This surface will be somewhat blurred due to the thermal energy of the positive ions which is probably very nearly equal to that of the gas molecules.

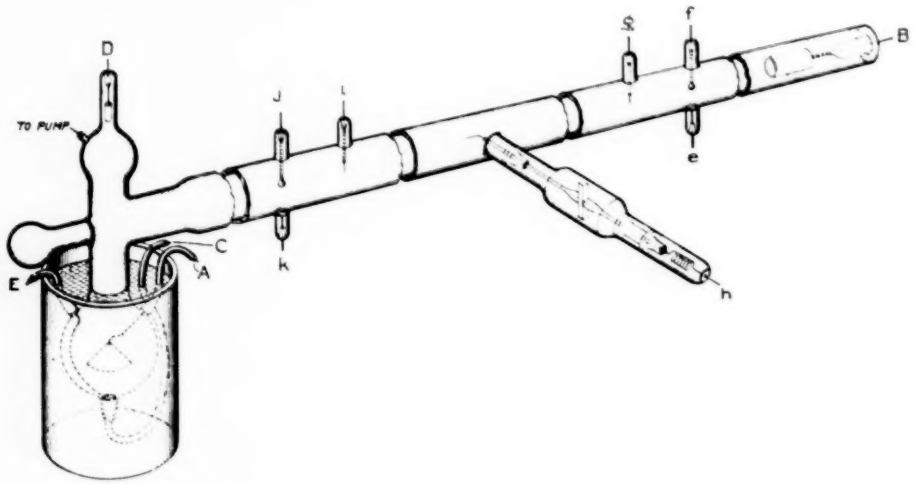

Fig. 1. Mercury vapor tube with various collectors.

II. Method

The tube used in the experiments is represented in Fig. 1. The long cylindrical portion in which the positive column was studied is 6.2 cm in diameter and 140 cm long. Anode A, which is above the pool of mercury which served as a cathode, is cone-shaped to prevent the blast of mercury from the cathode spot from affecting the pressure in the tube. Anode B consists of an

[5] L. Tonks and I. Langmuir, Phys. Rev. **34**, 876 (1929).

open molybdenum cylinder 5.1 cm long and 3.18 cm in diameter. Probe wires *i* and *g*, 61.1 cm apart, are 3 mil tungsten wires of area 0.0311 cm² each. The nickel collectors *f* and *j*, 7.6 cm respectively from *g* and *i* are approximately spherical and of area 1.22 cm² and 1.15 cm² respectively. The disks *e* and *k* bent to conform with the curvature of the walls and fitting closely against them are each of area 1.99 cm². The movable collector *h* consists of a 4 mil tungsten wire of 0.061 cm² area.* It can be moved by magnetic control across a diameter of the tube and also be turned to make any angle with the axis of the tube. In the present experiments it was kept parallel to the axis of the tube.

Before any experiments were made the electrodes were heated by means of a high-frequency coil and the tube allowed to run several days with a large current while being exposed to the radiation of several radiant heaters in order to drive out any water vapor or other occluded gases which might be present. Throughout all of the experiments the tube was being constantly exhausted by means of a two-stage Langmuir condensation pump and the vacuum was always such that a distinct click might be heard when the mercury was slowly raised in the McLeod gauge. The vapor pressure of the mercury in the tube was controlled by means of a water bath about the cathode bulb. When the temperature of the bath was above that of the room, mercury was prevented from condensing in the tube by means of small heating coils on each of the appendices and by exposing the whole tube to the radiant heaters.

In order to insure stable operation resistances were places in series with *A* and with *B*. In all of the runs the current to *A* was held between 4 and 5 amperes. Sometimes a small current was drawn to *D* but the effect of this upon the stability was negligible. Complete voltage current characteristics were taken of each of the collectors at various vapor pressures. At each of these vapor pressures complete characteristics were made with *h* at different points across the tube.

Large rectangular coils, placed above and below the tube, furnished a means of obtaining a transverse magnetic field. The effects of this transverse field upon the positive column were studied and will be reported in a later paper. In the present experiments the current through the coils was only such as to cancel the effect of the earth's field.

III. Experimental Results

Complete runs were made with the water bath about the cathode at 1.4°C, 18.6°C and 38.6°C. Using the methods of Langmuir and Mott-Smith[2] the random electron currents, electron densities and temperatures, and the

* After these experiments and others involving much higher current densities had been carried out, it was found that the probe wire *h* had been sputtered so that it varied from 0.0028 inches in diameter at one end to 0.004 inches at the bend into the glass tube. Since the experiments which would cause the most severe sputtering were performed after most of the runs reported here were made it is believed that the area of this probe wire was very close to 0.061 cm² when these runs were made.

space potentials were obtained from the semi-log plots of the electron current to the collector and the voltage of the collector for the probe wires i, g and h. Due probably to the small thickness of the sheaths about the probe wires better results were obtained by this method of analysis than from an analysis of the electron currents to the probe wires when they exert an accelerating field and the current to them is limited by orbital motion. In most of these runs the drift current through the tube, i_z, was held at 5 amperes. With smaller currents the agreement of the results obtained by each of the methods was very good. In each case the electron current to the collector was found by adding to the observed current the positive ion current to the collector at this voltage. This positive ion current was found by extrapolating to higher

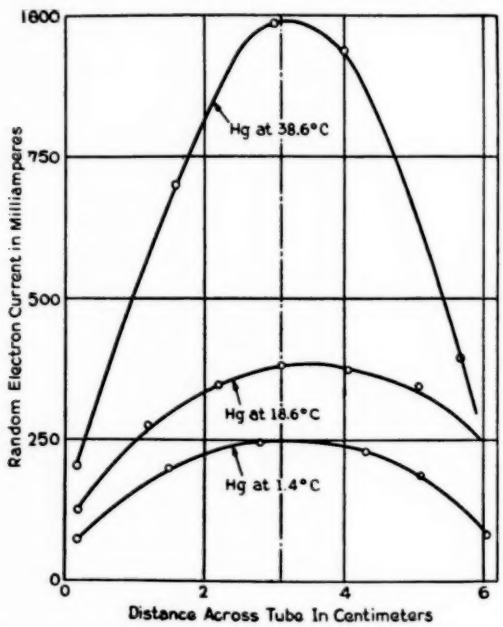

Fig. 2. Variation of the random electron current across the tube at different vapor pressures. Drift current, 5 amperes.

voltages the positive ion currents obtained at voltages so low that practically no electrons were collected.[2]

The vapor pressure of mercury was found from the data of Knudsen[6] and also that of Poindexter.[7] Since he has taken Knudsen's values at 0°C the values are very similar in the range here considered.

The positive ion current densities to the walls of the tube were obtained by plotting $(i_+)^{1/2}$ against $\nu^{1/2}$ where i_+ is the positive ion current to one of the disk-shaped collectors and $\nu = V^{3/2}\,[1+0.0247(T/V)^{1/2}]$. Here V is the voltage of the collector below that of the space and T is a factor which takes into account the initial velocities of the positive ions on entering the sheath and is about 10,000. If the positive ions had a Maxwellian distribution, T

[6] Knudsen, Ann. d. Physik **29,** 179 (1909).
[7] F. E. Poindexter, Phys. Rev. **26,** 859 (1925).

would correspond to their temperature in degrees absolute. Values of the shape factor equal to 1.36 ± 0.17 agreeing fairly well with the values Langmuir and Mott-Smith[8] found were obtained over a thirty-fold range in vapor pressure.

In Fig. 2 the variation of the random electron current across the tube is represented as measured by h. It is seen that there is a large variation

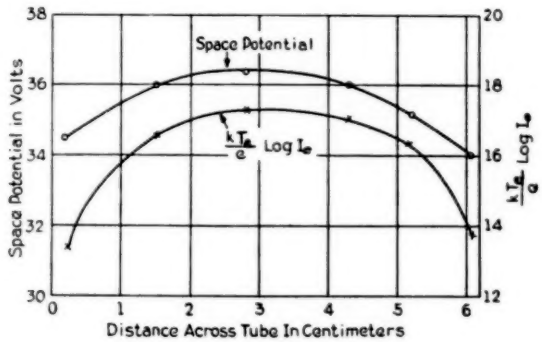

Fig. 3. Comparison of space potential with $kT_e/e \log I_e$. Cathode bulb at 1.4°C. p, 0.264 baryes.

in this random current. In Figs. 3 and 4 are the space potentials at these points. The electrons move in a retarding field in going from the axis of tube toward the walls. If their density at any point is determined by the the Boltzmann equation the space potential curve should be identical with that of the variation of $kT_e/e \log I_e$ across the tube. It is seen that this is very

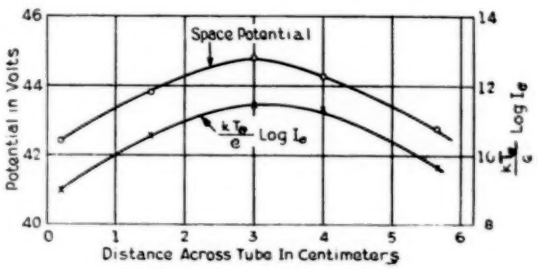

Fig. 4. Comparison of space potential curve with $kT_e/e \log I_e$. Cathode bulb at 38.6°C. p, 7.13 baryes.

nearly true at 38.6°C. Except for the points near the walls the agreement at 1.4°C is also within the experimental error. Also the semi-log plots of the voltage-current characteristics taken at different points along the diameter should lie on the same straight line as far as the space potential, where a break occurs. This is seen to be the case in Fig. 5. Here the cathode bulb was at 38.6°C where the best results were obtained.

[8] I. Langmuir and H. Mott-Smith, Gen. Elec. Rev. **27** 541 (1924).

IV. Mobility of the Electrons

If the density of electrons at a distance r from the axis is n_e the total number of electrons per unit length of tube is

$$N_e = 2\pi \int_0^R n_e r dr \tag{3}$$

where R is the radius of the tube. If v_x is the average drift velocity of the electrons toward the anode the total electron drift current is

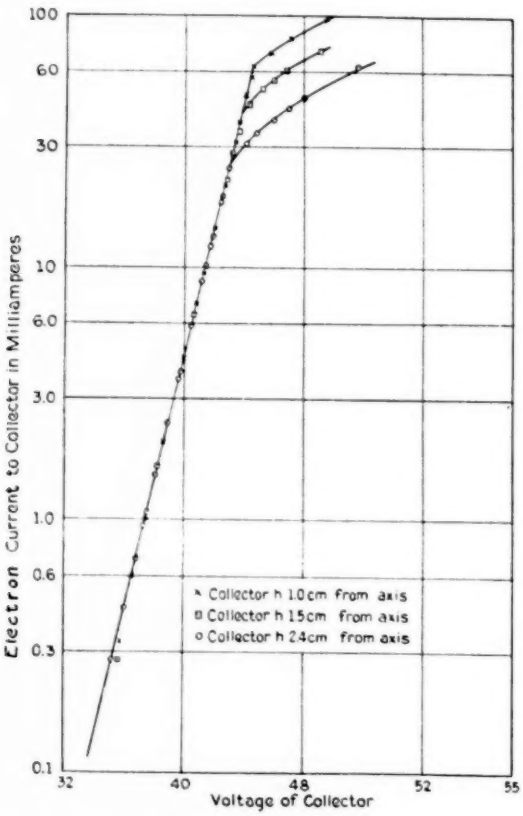

Fig. 5. Semi-logarithmic plot of the electron current to h against its voltage for various positions of h. Temperature of cathode bulb, 38.6°C. Drift current, 5 amperes.

$$i_- = N_e e v_x. \tag{4}$$

Since the current carried by electrons is 300 or 400 times that carried by positive ions the current to the anode B, i_x, can be assumed to be equal to the electron drift current. The mobility of the electrons is given by

$$\mu_- = \frac{v_x}{X} = \frac{i_x}{N_e e X} \tag{5}$$

where X is the longitudinal potential gradient. Assuming the speed gained between successive collisions to be small compared with the average speed of the electrons Langevin[9] has derived an expression for the mobility of electrons given by

$$\mu_- = 0.75 e\lambda / m\bar{v} \tag{6}$$

where λ is the mean free path of the electrons in the gas, m the mass of an electron and $\bar{v}$ the average speed.

Since $\bar{v} = (8kT/\pi m)^{1/2}$ it is possible to combine Eqs. (5) and (6) and obtain

$$\lambda = \frac{(8kTm)^{1/2} i_x}{0.75(\pi)^{1/2} N_e e^2 X} = 2.94 \times 10^9 \frac{i_x T^{1/2}}{N_e X} \tag{7}$$

where T is the temperature of the electrons in degrees absolute, i_x the drift current in amperes and X the longitudinal voltage gradient. N_e was obtained by a graphical integration of Eq. (3), n_e being found by means of Eq. (2). In Column 4 of Table I are the values of the mean free path of electrons in mercury vapor for three different vapor pressures. In reducing to λ_1, the mean free path at 1 barye and 20°C, it was assumed that the temperature of the gas molecules was 50°C. The kinetic theory value of the mean free path (i.e. $4(2)^{1/2}$ times the mean free path of gas molecules) is usually taken to be about 20 cm at this temperature and pressure.[10] Since, however, the mean free path is dependent upon the velocity of the electrons this value cannot be expected to apply very accurately.

TABLE I

Temperature of Cathode Bulb °C	Pressure of Hg baryes	T_e °K	λ from Eq. (7) cm	λ_1 cm	λ_1' from Eq. (8) cm
1.4	0.27	38,000	27.6	6.78	12.9
18.6	1.38	27,500	5.7	7.14	9.6
38.6	7.13	19,900	1.46	9.45	8.3

The angular scattering of low-velocity electrons in mercury vapor has been studied by various investigators whose results can be interpreted in terms of the mean free path of the electron.[11,12,13,14] A comparison of the temperature of the electrons in Table I, Column 3, and λ_1 in Column 5 seems to show that as the velocity of the electrons is increased there is a small increase in the effective diameter of the molecules. Minkowski[11] seems to have observed this Ramsauer effect for electrons whose velocities were less than an equivalent volt. Beuthe,[13] using the Ramsauer method, studied the absorption of low-velocity electrons and found that as the velocity decreased

[9] Langevin, Ann. de Chemie et de Physique 81, **5,** 245 (1905).
[10] S. Dushman, Hochvakuumtechnik, 1926.
[11] R. Minkowski, Zeits. f. Physik **18,** 258 (1923).
[12] L. R. Maxwell, Proc. Nat. Acad. Sci. **12,** 509 (1926).
[13] H. Beuthe, Ann. d. Physik **84,** 949 (1928).
[14] T. J. Jones, Phys. Rev. **32,** 459 (1928).

the absorption increased to a maximum at about 3 volts and then fell off to about 1/6 of this maximum value at 1 volt. Jones[14] using the Ramsauer and another method could find no evidence of this effect in mercury vapor. The results he obtained by his second method are very close to those obtained by Maxwell.[12] If the mean free path of an electron is given as a function of its velocity, i.e. $\lambda\ (v)$, then the mean free path of electrons with a Maxwellian distribution of velocities at a temperature T is given by

$$\lambda' = 4\pi\left(\frac{m}{2\pi kT}\right)^{3/2}\int_0^\infty \epsilon^{-mv^2/2kT}v^2\lambda(v)dv. \tag{8}$$

Using the values of $\lambda\ (v)$ as found by Maxwell[12] and reducing the mean free paths found from Eq. (8) to the mean free path, λ'_1, at 1 barye and 20°C it is seen by a comparison of these values in Column 6 with those in Column 5 that the two vastly different methods of obtaining the mean free path give results in fair quantitative agreement, although the free paths as obtained by each method vary differently with the temperature of the electrons.

One of the assumptions made in the derivation of Eq. (6) is that the speed gained between collisions is small compared with the average speed of the electrons. This is not true at the lower vapor pressures. The average distance the electrons move in the direction of the electric field between collisions, as Compton[15] has shown is given by

$$s = \mu_- E\lambda/\bar{v} = 0.75\lambda^2 eX/m\bar{v}^2. \tag{9}$$

The average energy gained between collisions is therefore $\Delta U = Xs$ and since $\bar{v}^2 = 0.849\ c^2$ and $eU = \frac{1}{2}mc^2$ the average energy gained between collisions is

$$\Delta U = 0.441\lambda^2X^2/U. \tag{10}$$

This varies from 1.5 percent of the average energy of the electrons when the cathode bulb is at 38.6°C to 12 percent when it is at 1.4°C. However, the degree of the agreement between the values of λ_1 and λ'_1 is an indication of the extent to which the simple classical kinetic theory considerations, which underlie the Langevin mobility equation and the calculation of the free path, are applicable to this case.

V. Rate of Generation of Positive Ions

a. Experimental. If I_+ is the positive ion current density to the walls, the total positive ion current to the walls per unit length of tube is $2\pi RI_+$ and since the recombination of positive ions with electrons is negligible within the positive column, the number of ionizing collisions per electron per second is given by

$$\alpha = 2\pi RI_+/eN_e. \tag{11}$$

The values of α as obtained from Eq. (11) are in row 8 of Table II.

b. Theoretical. Consider unit length of tube containing N_e electrons with a Maxwellian distribution of velocities corresponding to a temperature T. Let the gas in the tube have a pressure p and temperature T_g. An electron of

[15] K. T. Compton, Phys. Rev. **22**, 333 (1923).

velocity v has an energy of V volts where $\frac{1}{2}mv^2 = Ve$. The probability, P, of such an electron making an ionizing collision in going unit distance is dependent only upon the velocity of the electron and the nature and density of the gas. For an electron of velocity v the probability is given by $P = P'(n/n') = P'(pT'_g/p'T_g)$ where P' is the probability of an ionizing collision per cm path at pressure p' and temperature T'_g. These probabilities have been studied for different gases including mercury vapor by Compton and Van Voorhis[16] and for mercury vapor by Jones[17] and by von Hippel.[18]

The probability that an electron of velocity v will make an ionizing collision in one second is Pv. The number of electrons whose velocities lie between v and $v+dv$ is

$$N_e f(v)dv = 4\pi N_e \left(\frac{m}{2\pi kT}\right)^{3/2} v^2 \epsilon^{-mv^2/2kT} dv. \tag{12}$$

Hence, the number of positive ions formed per second by electrons whose velocities are between v and $v+dv$ is given by

$$N_e P f(v) v dv = 4\pi N_e \left(\frac{m}{2\pi kT}\right)^{3/2} P v^3 \epsilon^{-mv^2/2kT} dv. \tag{13}$$

If v be replaced by $(2Ve/m)^{1/2}$ the number of positive ions formed per second by electrons whose energies lie between V and $V+dV$ is found to be

$$N_e P F(V) dV = 8\pi N_e \left(\frac{m}{2\pi kT}\right)^{3/2} \frac{e^2}{m^2} P V \epsilon^{-eV/kT} dV. \tag{14}$$

In the case of mercury it has been found that the probability of ionization for electrons of less than 30 volts, varies linearly with the difference between the energy of the impinging electron and that required to ionize. Thus if V is less than V_i, P is zero but if V is greater than V_i but less than $3V_i$ we may write $P = \beta(V - V_i)$. Since, however, very few electrons have energies greater than $3V_i$ the total number of positive ions formed per second per cm is approximately

$$\nu_p = 8\pi N_e \left(\frac{m}{2\pi kT}\right)^{3/2} \frac{e^2}{m^2} \beta \int_{V_i}^{\infty} (V - V_i) V \epsilon^{-eV/kT} dV. \tag{15}$$

Integrating this expression and dividing by the total number of electrons per unit length of tube, the number of positive ions formed per second by each electron is found to be

$$\alpha' = \beta \left(\frac{8kT}{\pi m}\right)^{1/2} \epsilon^{-eV_i/kT} \left(V_i + \frac{2kT}{e}\right)$$

$$= 6.24 \times 10^5 \beta T^{1/2} \epsilon^{-eV_i/kT} \left(V_i + \frac{2kT}{e}\right) \tag{16}$$

[16] K. T. Compton and C. C. Van Voorhis, Phys. Rev. **26**, 436 (1925); **27**, 724 (1926).
[17] T. J. Jones, Phys. Rev. **29**, 822 (1927).
[18] A. von Hippel, Ann. d. Physik **87**, 1035 (1928).

In order to find out how much Eq. (16) is in error due to the fact that Eq. (15) is integrated to infinity, Eq. (15) may be integrated from $3V_i$ to infinity and the contribution to α' of electrons whose energies are greater than $3V_i$ found. This contribution, α'_1, divided by α' gives the maximum relative error made in assuming that the expression for the probability holds to infinity. It is found that

$$\frac{\alpha_1'}{\alpha'}=\epsilon^{-2V_ie/kT}\left\{\frac{(6eV_i^2/kT)+5V_i+(2kT/e)}{V_i+(2kT/e)}\right\}. \tag{17}$$

Since $V_i=10.4$ volts, α'_1/α' varies from 0.00018 for T equal to 20,000°K to 0.033 for T equal to 40,000°K. Thus the error made in integrating Eq. (15) from V_i to infinity is small.

From the work of Compton and Van Voorhis[16] β is given by $0.20\ p/T_g$ while from that of Jones[17] it is equal to $0.28\ p/T_g$ where p is in baryes and T_g in degrees Kelvin. The values of α' as found by substituting these two values of β in Eq. (16) are in row 9 of Table II. It is seen that at higher vapor pressures the ionization within the positive column may be accounted for by the impacts with neutral atoms of electrons whose velocity distribution is Maxwellian. However at 1.4°C it would appear that only about 40 percent of the positive ions are produced by these electrons. At this low pressure with the mean free path of the electrons several times the diameter of the tube there is probably very little cumulative ionization.

A more acceptable explanation of the relatively large values of α found at low pressures as compared with the calculated values, is to assume that the excess ionization is due to "high-speed" electrons, not belonging to the Maxwellian group considered above. At 0.27 baryes the random current is only 4.3 times the drift current so that there are probably present more "high-speed" electrons than there would be if the electrons were moving in random directions with a Maxwellian distribution corresponding to 38,000°K.

In the experiments of Compton and Van Voorhis[16] and also in those of Jones[17] a measured current of electrons of a given speed was passed through an ionizing chamber and the number of positive ions produced measured. For electrons whose energies lay between 10 and 30 volts the effect of the fields necessary to collect the positive ions was less in the arrangement of Jones than in that of Compton and Van Voorhis.

When an electron ionizes an atom it will not only lose an amount of energy corresponding to the ionization potential but will in general divide its energy with the new electron formed. Then the average energy of the two electrons is half of the surplus energy. The impinging electron and that formed by ionization will be considered secondary electrons. The total surplus energy delivered per second to these secondary electrons is given by

$$W'=8\pi N_e\left(\frac{m}{2\pi kT}\right)^{3/2}\frac{e^3}{m^2}\int_{V_i}^{\infty}PV(V-V_i)\epsilon^{-eV/kT}dV. \tag{18}$$

To find the average energy transferred per ionizing collision Eq. (18) is divided by the number of ionizing collisions per second and the average energy of the secondary electrons is found to be

$$\bar{V}=\frac{kT}{e}\left\{\frac{eV_i+3kT}{eV_i+2kT}\right\}. \tag{19}$$

If $\bar{V}_e$ is the average energy of the primary electrons ($e\bar{V}_e=3kT/2$) the following results are obtained

$T=0$	$\bar{V}=0.667\bar{V}_e$
$T=10{,}000°\text{K}$	$\bar{V}=0.714\bar{V}_e$
$T=40{,}000°\text{K}$	$\bar{V}=0.797\bar{V}_e$
$T\rightarrow\infty$	$\bar{V}\rightarrow\bar{V}_e$

The secondary electrons would have a Maxwellian distribution of velocities if the probability of ionization were independent of the energy of the impinging electron. However, since this probability increases with the energy of the electrons there exists among the secondaries a surplus of higher-speed electrons and a deficiency of the lower-speed ones. Since the rate at which a Maxwellian distribution is reëstablished among the electrons decreases with decreasing vapor pressures[19] the discrepancies between the values of α and α' at 0.27 baryes may in part be due to this surplus of higher-speed electrons at this pressure.

TABLE II. *Summary of results. Diameter of tube =6.2 cm.*

1. Bulb temperature	°C	1.4	18.6	38.6
2. Pressure of Hg vapor	baryes	0.27	1.38	7.13
3. Drift current	amperes	5.0	5.0	5.0
4. Longitudinal potential gradient (X)	volts cm^{-1}	0.0932	0.196	0.311
5. Electron temperature (T)	°K	38,000	27,500	19,900
6. $2\pi\int_0^R n_e r\,dr$	N_e	11.1×10^{11}	21.8×10^{11}	45.7×10^{11}
7. Positive ion current density to the walls of tube (I_+)	milliamps cm^{-2}	0.356	0.45	0.505
8. Rate of production of positive ions per electron from Eq. (11)	α	41,000	25,800	13,800
9. Rate of production of positive ions per electron from Eq. (16)				
$\beta=0.20\ p_0/T_0$	α'	14,600	16,900	12,600
$\beta=0.28\ p_0/T_0$		20,400	23,600	17,600
10. Random electron current in the direction of the axis ($2\pi\int_0^R I_e r\,dr$)	amperes	21.5	35.8	64

* Tonks and Langmuir[5] derive an expression for α for a cylindrical mercury discharge at low pressures gives by $\alpha=703.1\ T_e^{1/2}/R$. The values of α obtained by means of this expression are: at 1.4°C, 44,200; at 18.6°C, 37,500; at 38.6°C, 32,000.

VI. ENERGY BALANCE

The power input per unit length of tube is

$$W=Xi_z \tag{20}$$

[19] A. F. Dittmer, Phys. Rev. **28,** 507 (1926).

where X is as before the longitudinal potential gradient and i_z the drift current in the tube. Part of this energy is delivered to the walls by the recombination of positive ions and electrons, by the absorption of radiation and by the diffusion of metastable atoms to the walls and part goes into radiation which escapes from the tube. The total energy delivered to the walls by the recombination of a positive ion and an electron is the sum of the energy of recombination and the energies of the combining electron and positive ion. Since the electrons are moving in a retarding field their average energy expressed in volts is $2k\,T/e$. Therefore the total energy delivered to the walls per second by recombination is

$$W_r = 2\pi R I_+ (V_i + 2kT/e + \overline{V}_p) \tag{21}$$

where $\overline{V}_p$ is the average energy of the positive ions. The positive ions acquire most of their energy in the sheath close to the walls. The potential of the walls must be such as to make the current of electrons equal to that of the positive ions. It is therefore that at which zero current flows to a small collector against the walls such as e or k. The potential of a point on the axis opposite e or k can be found from the longitudinal gradient and the space potentials at i or g. Thus the difference between the potentials of points on the axis and the walls opposite can be found. Combining this with the results obtained by means of collector h as given in Figs. 3 and 4 the total variation of potential across a diameter of the tube can be found. Since the temperature of the electrons is constant the rate of production of positive ions at any point is proportional to the electron density. The energy acquired by a positive ion from the time it is formed until it recombines at the walls is equal to the difference between the potentials at the point where it was formed and that at which it recombined. At very low vapor pressures when the probability of a collision is very small it will deliver all this energy to the walls. However, even if it does make collisions and lose energy to gas molecules they in turn will deliver it to the walls. As a first approximation the longitudinal potential gradient may be neglected and the average energy delivered to the walls due to the fields the positive ions move in is given by

$$\overline{V}_p = \frac{2\pi\alpha \int_0^R n_e V_r r\,dr}{2\pi\alpha \int_0^R n_e r\,dr} = \frac{2\pi \int_0^R n_e V_r r\,dr}{N_e} \tag{22}$$

where V_r is the difference between the potentials at r and R and n_e is the electron density at r. $\overline{V}_p$ was obtained graphically from Eq. (22) and found to vary from 7.3 volts at 38.6°C to 14.5 volts at 1.4°C. The fraction of the power input delivered to the walls ($F_r = W_r/W$) by the recombining ions and electrons is in the fourth column of Table III. It is seen that this fraction increases rapidly with the temperature of the electrons.

By multiplying the frequency of collisions between electrons and gas molecules by the average loss of energy per electron per elastic collision the energy lost by the electrons per second through elastic collisions can be found.

When the energy of electrons is much greater than that of the gas molecules Compton[15] has shown that the average fraction of energy lost at an elastic collision is $2m_e/M$. Using the values of mean free paths as found from Eq. (7) and given in column 4 of Table I, the fraction, F_e, of the power input delivered by the electrons to the gas molecules by elastic collisions was found. It is seen from column 5 of Table III that this energy is very small and may be neglected.

TABLE III. *Fraction of power input delivered to the walls by the recombination of positive ions and electrons. Arc current = 5 amperes.*

Temp. of cathode bulb °C	Temp. of electrons T °K	Power input per unit length W watts	Fraction to walls F_r	Fraction to gas molecules by elastic impacts F_e
1.4	38,000	0.466	0.483	2.8×10^{-5}
18.6	27,500	0.98	0.233	4.0×10^{-5}
38.6	19,900	1.55	0.136	2.5×10^{-4}

In order to obtain a rough idea of the efficiency of excitation it may be assumed that the remainder of the energy input goes into raising the mercury atoms from the normal 1^1S_0 to the 2^3P_1 state, which excitation requires 4.9 volts. This state is between the two metastable states 2^3P_0 at 4.66 volts and 2^3P_2 at 5.43 volts. Making this assumption the average number of resonance collisions per electron per second, α_r, and per atom per second, a_r, can be found. These values are given in the third and fourth columns of Table IV. Using the values of the mean free path found by means of Eq. (7) the probability of ionization, P'_i, and that of resonance, P'_r, can be obtained. These values are given in the fifth and sixth columns of Table IV.

TABLE IV

Temp. of cathode bulb °C	Temp. of electrons °K	Number of resonance collisions per electron per second α_r	Number of resonance collisions per atom per second a_r	Probability of ionization on collision P_i'	Probability of excitation on collision P_r'
1.4	38,000	2.78×10^5	1690	0.0091	0.063
18.6	27,500	4.41×10^5	1030	0.0014	0.024
38.6	19,900	3.74×10^5	354	0.00023	0.0062

Few data are available on the probability of excitation on collision in mercury vapor. Sponer[20] found the average efficiency to be about 0.004 for the excitation of mercury atoms by electrons of from 5 to 6 volts energy. Using a different value for the total number of impacts made by the electrons Hertz[21] recalculated her results and obtained 0.03 for the average efficiency.

VII. DISCUSSION OF RESULTS

The free electrons in the uniform positive column move in nearly random directions with a Maxwellian distribution of velocities. This distribution

[20] H. Sponer, Zeits. f. Physik **7,** 185 (1921).
[21] G. Hertz, Zeits. f. Physik **32,** 298 (1925).

is being continually disturbed by the loss of higher-speed electrons to the walls and by excitation and ionization. This continuous loss of energy by the electrons is supplied to the drift current by the longitudinal field and in some manner is transferred to the electrons so that they keep their Maxwellian distribution. No satisfactory explanation of the mechanism by which this distribution is maintained has yet been offered. There is evidence that it may be due to oscillations.[22,23] In any event it has been shown that the temperature corresponding to this distribution of velocities is one of the most important characteristics of the discharge. It determines the ionization and excitation efficiencies of the electrons. Furthermore, since the electrons have a Maxwellian distribution of velocities their concentrations satisfy the Boltzmann equation.

The mobility of the electrons was measured and by means of the Langevin equation the results were interpreted in terms of the mean free path of the electrons. Over a twenty-five fold range of vapor pressures the mean free paths found in this way, when reduced to the values at 1 barye and 20°C, were within 30 percent of each other. It was true even when the mean free path appeared to be five or six times the diameter of the tube. This is probably because the electrons make specular reflections at the walls. Their momentum is unchanged except for the component perpendicular to the walls, which is reversed.

The rate of production of positive ions seems to be accounted for by direct impacts with neutral atoms of the higher-speed electrons of the Maxwellian group when the vapor pressure is greater than 1.4 baryes. At 0.27 baryes only about one half of the ionization can be accounted for in this way. The small ratio of the random to the drift current probably accounts for the additional high-speed electrons.

It is seen that as the temperature of the electrons is lowered from 38,000° K to 19,900°K by raising the pressure the percentage of the energy delivered to the walls by the recombination of positive ions and electrons decreases from 48 to 14.

There are several sources of error in this work which are difficult to eliminate. The space potentials are probably accurate to within two-tenths of a volt. The random electron currents may be in error due to the fact that some electrons are reflected when the collector is at space potential. However, the results of Farnsworth[24] show that this coefficient of reflection must be very small under these conditions. The electron temperatures in the tube were usually within 1500°K of each other as measured by any collector during a run. It is therefore believed that the probable error is within five percent.

The author wishes to express his appreciation for the many suggestions and kind assistance of Dr. I. Langmuir and Dr. L. Tonks of the Research Laboratory of the General Electric Company at Schenectady where this work was done. He is also grateful for the considerable aid rendered by Professor K. T. Compton of Princeton University.

[22] I. Langmuir, Proc. Nat. Acad. Sci. **14,** 627 (1928).
[23] L. Tonks and I. Langmuir, Phys. Rev. **33,** 195 (1929).
[24] H. E. Farnsworth, Phys. Rev. **25,** 41 (1925).

ABSORPTION OF RESONANCE RADIATION IN MERCURY VAPOR

By Ancil R. Thomas
Valparaiso University, Valparaiso, Indiana

(Received April 8, 1930)

Abstract

The theories of absorption in mercury vapor of mercury resonance light of wave-length 2536.7A as formulated by Malinowski and H. A. Wilson are briefly reviewed. It is well established that the absorption coefficient for resonance radiation increases as the number of absorbing atoms decreases. This is probably due to a Doppler effect in the radiating vapor. To diminish the influence of the Doppler effect a jet of mercury vapor was used, and the resonance radiation coming from it was investigated. A series of measurements of the absorption coefficient of this light is given. The maximum atomic absorption coefficient observed is 10.22×10^{-13}, nine times as large as any previously observed. It is shown that Malinowski's assumptions are not in accord with the observed effects.

Introduction

A NUMBER of people[1,2,3,4,5,6] have investigated the properties of mercury resonance light of wave-length 2536.7A since it was first discovered by R. W. Wood.[7] The writer[8] assisted in one such investigation in which the atomic absorption coefficient was measured. The atomic absorption coefficient, γ, is defined by the equation

$$I = I_0 e^{-\gamma n_a} \tag{1}$$

where I_0 is the intensity of the light as it enters the cell, I the intensity as it leaves it and n_a is the number of absorbing atoms per cm^2 of the cell. As the number of absorbing atoms changed from 1.35×10^{12} to 87.6×10^{12} per cm^2 of the absorption cell the atomic absorption coefficient changed from 11.2×10^{-14} to 2.53×10^{-14}. Several investigators have observed this variation in the absorption coefficient. The cause appears to be the non-homogeneity of the resonance line for in the case of a perfectly homogeneous radiation γ should be constant. Consequently, the values of γ are to be regarded only as average values for the atoms involved.

[1] A. v. Malinowski, Ann. d. Physik **44,** 935 (1914).
[2] C. Füchtbauer, G. Joos, and O. Dinkelacker, Ann. d. Physik **71,** 222 (1923).
[3] W. Orthmann, Ann. d. Physik **78,** 601 (1925).
[4] F. Goos and H. Meyer, Zeits. f. Physik **35,** 803 (1926).
[5] M. Schein, Ann. d. Physik **85,** 257 (1928).
[6] P. Kunze, Ann. d. Physik **85,** 1013 (1928).
[7] R. W. Wood, Phil. Mag. **23,** 696 (1912).
[8] A. L. Hughes and A. R. Thomas, Phys. Rev. **30,** 466 (1927).

Former Theories

The Doppler effect predominates among the various effects[9] proposed to account for the width of spectrum lines, particularly when the pressure is low, as it is in mercury vapor at room temperature. It has been shown that the visibility in interference patterns[10,11] is the same as one would expect if the entire width were due to the Doppler effect.

The shift in wave-length $\delta\lambda$ due to the Doppler effect is given by

$$\frac{\delta\lambda}{\lambda}=\frac{v}{c} \tag{2}$$

from which we get that

$$v = \frac{c\delta\lambda}{\lambda} = \beta\delta\lambda \tag{3}$$

where β is a constant. The number of atoms with any particular component of velocity along the line of emission is given by the formula from kinetic theory,

$$dn = Ke^{-v^2/\alpha^2}dv. \tag{4}$$

The intensity, dI, of the light at any particular wave-length, separated from the center of the line by a wave-length difference $\delta\lambda$, is proportional to the

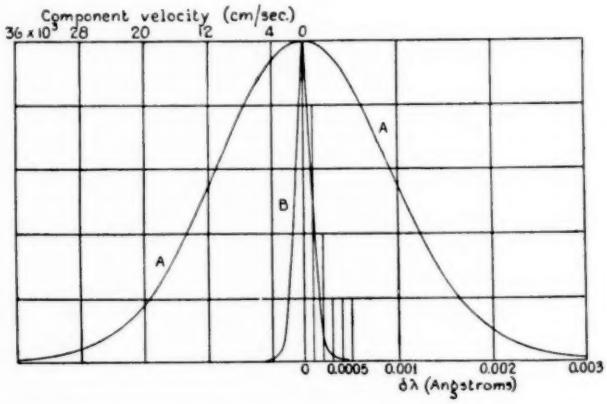

Fig. 1. Distribution of energy in the resonance line. Curve A shows the distribution in the ordinary resonance line, curve B, the distribution in the line used in this experiment.

number of atoms, dn, which have the proper component of velocity, v, to give this wave-length. We then have that

$$dI \propto dn \propto e^{-v^2/\alpha^2}dv \propto e^{-(\beta\delta\lambda)^2/\alpha^2}d(\delta\lambda) \tag{5}$$

[9] Rayleigh, Phil. Mag. **29,** 274 (1915).
[10] A. A. Michelson, Astrophys. J. **3,** 251 (1896).
[11] Buisson and Fabry, Jour. d. Physique **2,** 442 (1912).

where v and also $\delta\lambda$ varies from $-\infty$ to $+\infty$. This distribution is shown graphically in Fig. 1, curve A, when the emitting vapor is at a temperature of 293°K.

Malinowski[1], assuming this line form, has worked out an expression for I/I_0 in terms of n_a (see Eq. (1)). He also assumes that the ability of the atoms in an infinitely thin layer to absorb light of any particular wave-length will be given by

$$k_v = k_0 e^{-v^2/a^2} \tag{6}$$

where k_0 represents the ability of the atoms to absorb the very center of the line. This equation results from assuming that an atom in the absorption cell can absorb light only near the wave-length which it, itself, can emit, and also that this band over which it can absorb light is very narrow with respect to the entire line. (If, in accordance with the strict quantum theory, we suppose that the correspondence between $\delta\lambda$ and v must be exact it is evident that there can be no absorption for as we narrow down the velocity range in which an atom must be in order to absorb light of a particular wave-length the number of atoms available for such absorption approaches zero.[12]) On these assumptions Malinowski shows that the absorption coefficient for the very center of the line is the square root of two times the observed value for a cell which is infinitely thin. The atomic absorption coefficient for the very center of the line should, then, also be the square root of two times the observed value for a very thin cell. A reasonable extrapolation of the values secured by Hughes and Thomas gives $\gamma = 12 \times 10^{-14}$ for an infinitely thin layer of vapor and $\gamma_0 = 17 \times 10^{-14}$. If his ideas are correct, it is evident that, if the importance of the Doppler effect could be reduced greatly, the observed atomic absorption coefficient should approach γ_0, that is, the square root of two times the former value observed for an infinitely thin layer of atoms. Also the coefficient should remain constant for all cell thicknesses.

H. A. Wilson[13] has also proposed a theory which is applicable in this case. He assumed that the atom absorbs as a simple linear oscillator, the equation of motion of which may be taken to be

$$n\ddot{x} + k\dot{x} + \mu x = Fe \tag{7}$$

where m is the mass of the vibrating particle, k the viscous resistance to the motion at unit velocity, μ a constant, F the electric intensity in the light at the atom, which may be taken as equal to $F_0 \cos pt$, e the charge on the particle and x the displacement of the particle. From this he deduces that

$$\gamma = \frac{\gamma_0}{1 + (4m^2/k^2)q^2} \tag{8}$$

where γ_0 is the atomic absorption coefficient for exact resonance, γ that for a departure from exact resonance given by a frequency difference q (which

[12] A. L. Hughes and A. R. Thomas, Phys. Rev. **30,** 472 (1927).
[13] H. A. Wilson, Proc. Roy. Soc. **A118,** 362 (1928).

corresponds to $\delta\lambda$ as used above). He then assumed that the energy distribution in the incident line was given by $Ae^{-\beta^2 q^2}$ which is the form appropriate for a Doppler effect but does not demand this explanation for the finite width of the line. With this added he shows that

$$\gamma_0 = \frac{1}{(n_a)^{1/2}} \left(\log \frac{I_0}{I} \right) \frac{m}{\beta k} \tag{9}$$

when n_a is not too small. Wilson showed that this fitted Hughes and Thomas' results when n_a was greater than about 10^{13}. It is implied in the derivation of Eq. (8) that the emission line is broader than the absorption line.

Both theories predict that if the width of the resonance line could be reduced the observed absorption coefficient should increase and Malinowski's work specifies the amount of this increase. Also according to Malinowski the absorption coefficient should not change with cell thickness. An experimental test of these predictions is described on the following pages.

Distribution of Energy in Incident Light

The most feasible method of reducing the width of the resonance line which presented itself was to use a jet of mercury vapor as a source of resonance light. If the light is taken out at right angles to the jet the component velocities of the atoms in the line of emission will be quite small. The jet was diaphragmed so that five degrees was the maximum angle that any atom's path could make with the line of centers of the diaphragms. The distribution of energy in the radiation from such a jet was computed and the results plotted graphically in Fig. 1, curve *B*. While this distribution curve cannot be represented accurately by a curve of the form e^{-v^2/α^2}, we may, however, find a curve of this form which is roughly superposable on the distribution curve, and so find a value for the "most probable velocity," α, in a direction perpendicular to the jet. This turns out to be about one tenth of the value of the most probable velocity in isotropic mercury vapor at room temperature. This means that laterally its effective temperature as measured by the component velocity of the atoms is about 0.31 times its real temperature, that is 90°K.

Apparatus and Procedure

The source of light was a vertical quartz mercury arc. It was kept cool by circulating distilled water around it. Ice was kept in the water most of the time to prevent heating. The current for the arc was supplied by a generator floating across a bank of storage batteries. A preliminary test showed that about four amperes through the arc gave the greatest amount of light from the resonance lamp. The central part of the arc was deflected to the front of the tube by an electro-magnet excited by the same current that was used in the arc. Under these circumstances the arc ran very steadily. No fluctuations could be noticed in the course of an entire day's work.

The light from this arc was focused into a resonance lamp constructed of Pyrex glass shown in Fig. 2. *A* is a cross section, *B* is a vertical section.

Light, not absorbed in the jet, continued into the horn, H_1, (see Fig. 2*A*) where it was lost by multiple reflection. The resonance light taken out through the window, W, had the horn H_2 as a background so that any stray light returning from H_1 could not get out in the same direction as the resonance light. The most careful tests made showed no light of this sort whatever. An intensity much less than one percent of the resonance light could have been detected. The jet (see Fig. 2*B*) was diaphragmed as shown, the upper diaphragm being merely a slight constriction in the tube. The walls of the tube were cooled with solid CO_2 as was the reentrant tube, R, on which the mercury in the jet condensed. A heater, T, to increase the strength of the jet was not used as the jet proved to be quite strong enough without it.

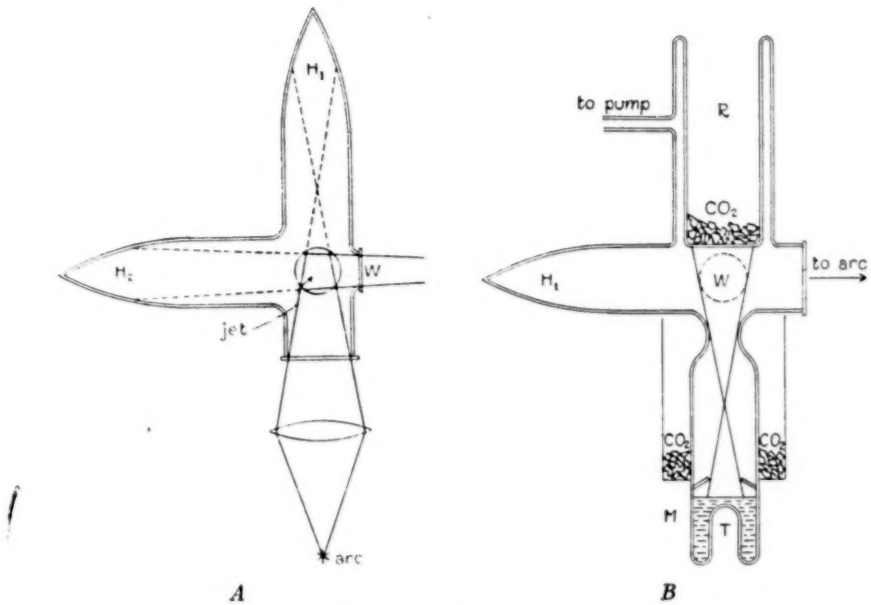

A *B*

Fig. 2. The resonance lamp used. *A* is a cross section, *B*, a vertical section.

Moreover the amount of stray vapor, the atoms of which were moving at random, was greatly increased by heating the mercury. In the final experiment practically the whole of the lamp was surrounded by solid CO_2 in order to diminish the amount of stray vapor as much as possible. In a former unpublished investigation[14] with potassium a method for securing quite strong jets was developed. A diaphragm was placed very near the liquid metal surface, M, and the walls of the tube were kept cool as close down to this diaphragm as possible. By this method it was possible to secure jets several times as strong as is possible with the metal in the bottom of just a straight tube with no diaphragm near the surface of the liquid metal.

The remainder of the apparatus was arranged as in Fig. 3. The resonance light passed through the absorption cell C, on through a quartz lens L, a

[14] Done with L. C. Van Atta.

variable rotating shutter S, and into a photoelectric cell. The active material in the photoelectric cell was aluminum. It was filled with helium to about one mm pressure after the surface had been sensitized by a discharge through hydrogen as is done in making an alkali hydride surface. A potential of 200 volts was used on the cell. The sensitivity to mercury resonance radiation was about seventy five times that of the untreated vacuum cell. The absorption cell, C, consisted of a glass tube 1.622 cm long to which quartz windows were sealed. A side tube contained a drop of mercury. The pressure in the cell and thus the number of absorbing atoms was controlled by cooling the side tube. The absorption cell was fixed so that it could be shifted

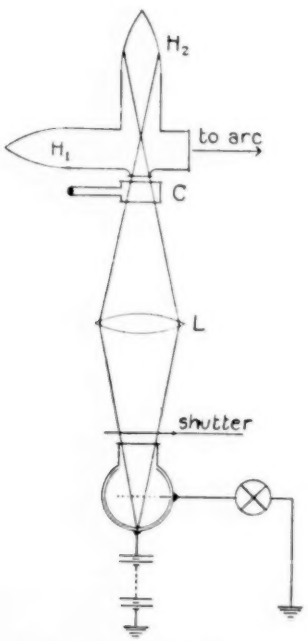

Fig. 3. Arrangement of the apparatus.

out of the beam and the electrometer current secured without the cell. The transmission of the cell was approximately matched by the variable rotating shutter and the actual transmission secured by interpolation. The mercury was all frozen out of the cell and its transmission secured by the same method as well as by comparing it with a previously calibrated screen. The transmission was 0.69. Calling the amount of light getting through the cell with the side tube cooled by solid CO_2 I_0, and the amount at any other temperature I then the fraction transmitted by the vapor will be I/I_0.

Results

The experimental values for I/I_0 are shown in Fig. 4 plotted against the temperature of the side tube. A smooth curve was drawn through the experimental points and values read off this for purposes of computation. These

values are listed in Table I. The temperatures of the side tube are listed in column one and the corresponding values for I/I_0 in column two. The next column gives the values of the natural logarithms of I_0/I.

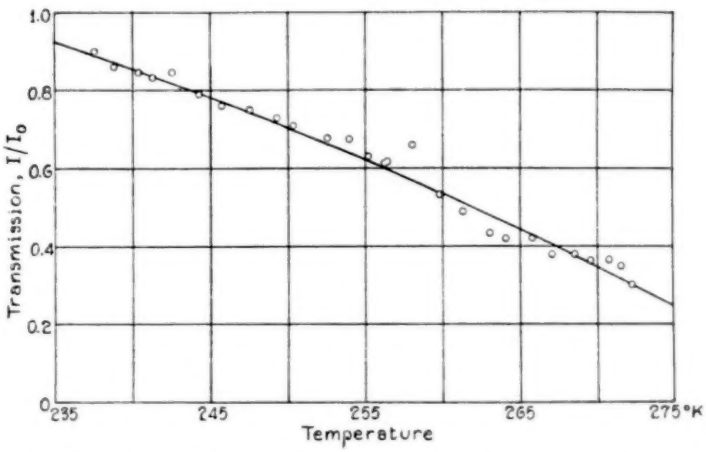

Fig. 4. Ratio of transmitted to incident radiation for various temperatures of mercury vapor.

To determine the atomic absorption coefficient we have to calculate the number of atoms involved in the absorption in each case. This must be calculated from the pressure. The fourth column gives the pressures of the

TABLE I.

Temp. °K	I/I_0	$\log I_0/I$	p in side tube in mm	p in cell in mm	n_a	γ
235	0.915	0.0888	1.45×10^{-6}	1.62×10^{-6}	8.71×10^{10}	10.22×10^{-13}
240	0.862	0.1484	3.09	3.41	18.36	8.08
245	0.792	0.2332	6.30	6.89	34.06	6.29
250	0.715	0.3355	12.3	13.3	71.63	4.68
255	0.628	0.4652	23.2	24.9	133.8	3.48
260	0.538	0.6200	42.8	45.4	244.4	2.54
265	0.444	0.8118	76.2	80.1	431.0	1.88
270	0.344	1.0671	133.	139.	745.3	1.43
275	0.240	1.4271	228.	235.	1266.	1.13

mercury vapor in the side tube for the corresponding temperatures recorded in the first column. The vapor pressures of mercury at different temperatures given in the International Critical Tables were used in this computation. As the same absorption cell was used which Hughes and the writer used in their former investigation the relations deduced at that time can be used. The pressure, p, in the absorption cell and the pressure, p_m, in the side tube are connected by the relation

$$\frac{p}{p_m} = \left(\frac{T}{T_m}\right)^{1/2} \tag{10}$$

where T and T_m are the temperatures of the absorption cell and the side tube respectively. The pressures in the absorption cell, as corrected by this equation, which takes care of thermal transpiration, are listed in column five.

The number of absorbing atoms, n_a, per cm^2 of the cell is connected with the pressure, p, by the equation

$$n_a = (5.38 \times 10^{16})p. \tag{11}$$

The values of n_a are listed in column six. The atomic absorption coefficient, γ, is calculated according to Eq. (1) and listed in column seven. This is an average value for all the atoms present in the absorption cell although it is not absolutely certain that they are all active in absorbing the light.

The atomic absorption coefficient which, according to Malinowski's theory, should have been almost constant for all values of n_a, is shown plotted against n_a in Fig. 5, curve A, along with the values of the atomic

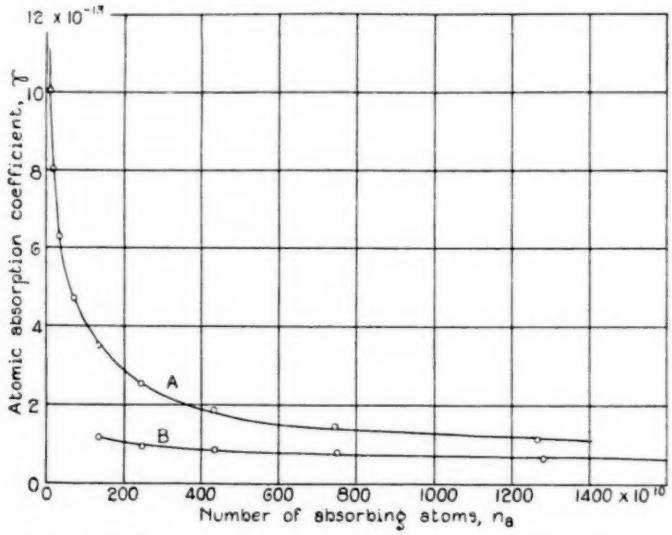

Fig. 5. Variation of the atomic absorption coefficient with the number of absorbing atoms. A is the curve secured in this experiment, B, that secured by Hughes and Thomas.

absorption coefficient from the previous work, curve B. The coefficient is definitely not a constant and it is certainly several times greater than the square root of two times any possible extrapolation of the former curve to an infinitely thin cell.

TABLE II.

n_a	$\frac{1}{(n_a)^{1/2}} \log_e \frac{I_0}{I}$	$\frac{(n_a+6\times10^{10})^{1/2}}{n_a} \log_e \frac{I_0}{I}$
8.71×10^{10}	3.01×10^{-7}	3.91×10^{-7}
18.36	3.46	3.99
34.06	3.83	4.13
71.63	3.96	4.13
133.8	4.02	4.11
244.4	3.97	4.01
431.0	3.91	3.94
745.3	3.91	3.92
1266.	4.01	4.02

According to H. A. Wilson's theory, $1/(n_a)^{\frac{1}{2}} \log I_0/I$ should be constant for values of n_a which are not too small. These values are tabulated in Table II column 2. It is seen that they are practically constant for values of n_a greater than about 50×10^{10}. Wilson also proposed an empirical expression which is constant for all values of n_a and by means of which γ for an infinitely thin cell can be deduced. It is

$$\frac{(n_a + K)^{1/2}}{n_a} \log_e \frac{I_0}{I} = C. \tag{12}$$

It is seen that it goes over into the theoretical relation when n_a is large. Values of C are tabulated in Table II, column 3. From it γ for the infinitely thin cell is given by $C/K^{\frac{1}{2}}$ which for this case is 16.33×10^{-13}. This is thirteen times greater than the value secured (1.25×10^{-13}) when the same relation is applied to the results of Hughes and Thomas and about sixty per-cent greater than the maximum experimental value obtained in this experiment, (viz. 10.22×10^{-13}).

Discussion

As the light from the jet is much more absorbable than that from an ordinary resonance lamp the distribution of energy in the line must be very different from the ordinary distribution, certainly the line must be much more homogeneous, probably as homogeneous as light from a discharge tube cooled in liquid air (disregarding, for the moment, the fact that actually all the atoms would be condensed). It would seem from this that the Doppler effect controls emission for no other effect presents itself which will be affected by the jet sufficiently to explain, even qualitatively, the observed effects. It is evident that Malinowski's assumption that the absorption and emission lines have the same width is not justified for we do not get his predicted results. A consideration of these results points to the conclusion that the emission line must be wider than the absorption line, otherwise the absorption coefficient would not increase rapidly as the number of atoms, n_a, diminishes. Since there are good reasons, already mentioned, for believing that the width of the emission line is determined by the Doppler effect, we must, therefore, conclude that, because the absorption line is apparently narrower than the emission line, the width of the absorption line is not controlled by the Doppler effect. It appears, since H. A. Wilson's theory applies to these results, that we may consider the mercury atoms, as far as absorption goes, behaving like simple linear oscillators. It does not seem possible, at present, to interpret the results of these absorption experiments in such a way as to give a satisfactory and consistent picture of the processes involved in emission and absorption of resonance radiation.

The above work was done at Washington University, St. Louis, Mo. The writer wishes to thank Dr. A. L. Hughes for especial assistance and advice given during the course of the experiment. Also he wishes to thank Mr. C. A. Reinhart, instrument maker, for help in the construction of apparatus.

THE DISPERSION FORMULA AND RAMAN EFFECT FOR THE SYMMETRICAL TOP

By Morris Muskat
The Gulf Companies, Pittsburgh, Pa.

(Received March 28, 1930)

Abstract

Schroedinger's theory of dispersion is applied to the symmetrical top. The dipole of the top is assumed to lie along the axis of symmetry, and the wave-length of the incident light to be large as compared with the dimensions of the top. An explicit expression is derived for the index of refraction of a gas composed of symmetrical tops, as a function of the frequency of the incident light. As the perturbed eigenfunction is a linear function of only 3 unperturbed eigenfunctions, the dispersion formula, for a given state, consists of only 2 terms.

The moments for the Raman effect transitions for the symmetrical top are also computed. Simple closed expressions are obtained, again because of the simplicity of the perturbed eigenfunctions. The polarization of the Raman variations is computed with the result that the unshifted lines are unpolarized whereas for the shifted lines: $|m_x|^2/|m_z|^2=4/3$.

THE importance of the symmetrical top for the interpretation of molecular spectra makes it of interest to derive the dispersion formula and Raman effect intensities for this mechanical system. Kronig and Rabi,[1] Reiche and Rademacher,[2] Manneback,[3] and Condon,[4] have developed the theory of the unperturbed state of the top, and its Stark and Zeeman effects. However, explicit expressions have not been yet given for the interaction of the top with time varying fields.

As a mechanical system, the top is defined by the fact that two of its moments of inertia are equal to A, and are unequal to the moment of inertia, C, about the axis of symmetry. It is considered as a rigid system. A dipole, of moment μ, lies along the axis of symmetry and interacts with a small periodic field, $E_0 \cos 2\pi\nu t$, directed along the Z axis, fixed in space.

The wave mechanical treatment of dispersion and Raman transitions is well known, being given originally by Schroedinger.[5] This treatment in which the dispersion phenomena are considered as pulsating Stark effects, is valid if the wave-length of the incident light is large as compared to the dimensions of the atomic or molecular system; the application made here will also assume that we are dealing with relatively long wave-lengths.

[1] Kronig and Rabi, Phys. Rev. **29,** 262 (1927).
[2] Reiche and Rademacher, Zeits. f. Physik **39,** 444 (1926); **41,** 453 (1927).
[3] Manneback, Phys. Zeits. **28,** 72 (1927).
[4] Condon, Phys. Rev. **30,** 781 (1927).
[5] Schroedinger, Ann. d. Physik **81,** 109 (1926).

The Dispersion Forumula

We may begin with the well-known expression for the "partial density" to be associated with two states, j and j', of the system perturbed by the radiation:

$$\psi_j\psi_{j'} = e^{2\pi i/h(W_{j'}-W_j)t}\left[u_ju_{j'}^* + e^{2\pi i\nu t}\left\{u_{j'}^*\sum_r c_{jr}^+u_r + u_j\sum_r c^{*-}_{j'r}u_r^*\right\}\right.$$
$$\left. + e^{-2\pi i\nu t}\left\{u_{j'}^*\sum_r c^-_{jr}u_r + u_j\sum_r c^{*+}_{j'r}u_r^*\right\}\right]. \tag{1}$$

In this equation, W_j is the eigenvalue of the unperturbed j state, and u_j is the corresponding unperturbed eigenfunction. The c_{jr} are proportional to the matrix elements of that part of the potential energy of the system that is due to the perturbing field. The * indicates the complex conjugate. If we refer the top to the Eulerian angles θ, ϕ, and χ, the c_{jr} in our case are given by:

$$c_{jr}^{\pm} = \frac{-\mu E_0 AC^{1/2}}{2(W_j - W_r \pm h\nu)}\int_0^{2\pi}\int_0^{2\pi}\int_0^{\pi} u_ju_r^*\cos\theta\sin\theta d\theta d\phi d\chi$$
$$\equiv \frac{-\mu E_0 z_{jr}}{2(W_j - W_r \mp h\nu)}. \tag{2}$$

Following Manneback, the eigenfunctions u_j may be expressed as:

$$u_j \equiv u_{jnm} = e^{i(n\chi+m\phi)}y_{jnm}(x), \tag{3}$$

where n, m are quantum numbers associated with χ and ϕ, $x=\cos\theta$, and the y_{jnm} are an orthogonal set of functions satisfying the equation:

$$\frac{d}{dx}\left[(1-x^2)\frac{dy_{jnm}}{dx}\right] - \frac{m^2 - 2mnx + n^2}{1-x^2}y_{jnm} + j(j+1)y_{jnm} = 0. \tag{4}$$

n and m are integral and range independently from $-\infty$ to $+\infty$; j is integral and $\geqq |n|, |m|$. Furthermore, the y_{jnm} satisfy a recurrence relation of the form:

$$xy_{jnm} = A(jnm)y_{j+1,nm} + B(jnm)y_{jnm} + C(jnm)y_{j-1,nm}. \tag{5}$$

It follows, then, that in our case the c_{jr} vanish unless the values of n and m are the same for both states j and r. They also vanish unless $|j-r|\leqq 1$.

When in Eq. (1) we set $j'=j$, we have the "density" determining the dispersion produced by the (jnm) state. The form of (3) and the above remarks about the c_{jr} permit us to rewrite Eq. (1) in the form:

$$\psi_j\psi_j^* = u_ju_j^* + 2\cos 2\pi\nu t\left[u_j^*\sum_r u_r(c_{jr}^+ + c_{jr}^-)\right]. \tag{6}$$

In this equation the values of n and m are the same in all the terms and hence are omitted from the subscripts. The dispersion moments are now:

$$m(jnm) = m_z = \mu\int\cos\theta\psi_j\psi_j^*d\tau. \tag{7}$$

The moments $m_x = \mu \int \sin\Phi \sin\theta \psi_j \psi_j^* d\tau$ and $m_y = -\mu \int \cos\Phi \sin\theta \psi_j \psi_j^* d\tau$ are obviously zero. Introducing the matrix elements z_{jr}, defined in Eq. (2), we get for the time varying part of m_z in which alone we are interested:

$$m(jnm) = 2\mu^2 E_0 \cos 2\pi\nu t \sum_r z_{jr}^2 \frac{(W_j - W_r)}{h^2\nu^2 - (W_j - W_r)^2}. \tag{8}$$

Now it may be shown from the formulae given by Manneback that the coefficients in Eq. (5) have the following values:

$$A(j,n,m) = \frac{1}{j+1}\left(\frac{\{(j+1)^2 - m^2\}\{(j+1)^2 - n^2\}}{(2j+1)(2j+3)}\right)^{1/2};$$

$$B(jnm) = \frac{mn}{j(j+1)} \tag{9}$$

$$C(jnm) = A(j-1,n,m).$$

These give the explicit values of the only non-vanishing matrix elements z_{jr}, which are, clearly:

$$z_{j,j+1} = A(jnm);\ z_{j,j} = B(jnm);\ z_{j,j-1} = C(jnm). \tag{10}$$

Recalling that the eigenvalues of the symmetrical top are given by:

$$\frac{8\pi^2 A}{h^2} W_{jnm} = j(j+1) + \left(\frac{A}{C} - 1\right)n^2, \tag{11}$$

and setting $\eta = -8\pi^2 A\nu/h$, we finally get for m_z:

$$m_z = \frac{32\pi^2\mu^2 A E_0}{h^2(2j+1)} \cos 2\pi\nu t \left[\frac{\{(j+1)^2 - n^2\}\{(j+1)^2 - m^2\}}{(j+1)(2j+3)\{4(j+1)^2 - \eta^2\}} - \frac{(j^2 - n^2)(j^2 - m^2)}{j(2j-1)(4j^2 - \eta^2)}\right]. \tag{12}$$

As the state (j, n) has a $2j+1$ fold degeneracy in the quantum number m, we must use for our dispersion formula the average of m_z over m, i.e. the value: $\bar{m}_z = (1/2j+1)\Sigma_{m=-j}^{m=+j} m_z$. And noting that $\Sigma m^2 = j(j+1)(2j+1)/3$, where $|m| \leqq j$, we get:

$$\bar{m}_z = \frac{32\pi^2\mu^2 A E_0}{3h^2(2j+1)} \cos 2\pi\nu t \left[\frac{(j+1)^2 - n^2}{4(j+1)^2 - \eta^2} - \frac{(j^2 - n^2)}{4j^2 - \eta^2}\right]. \tag{13}$$

For the state: $j = 0$, we must use:

$$\bar{m}_z = m_z = \frac{32\pi^2\mu^2 A E_0 \cos 2\pi\nu t}{3h^2(4 - \eta^2)}. \tag{13a}$$

We therefore have the result that the index of refraction, r, for a gas in which there are N molecules, of the type of the symmetrical top, per unit volume, and all of which are in the (j, n) state, is given by:

$$\frac{r^2-1}{r^2+2} \leqq \frac{r^2-1}{3} \leqq \frac{2}{3}(r-1) = \frac{128\pi^3\mu^2 A N}{9h^2(2j+1)}\left[\frac{(j+1)^2-n^2}{4(j+1)^2-\eta^2} - \frac{j^2-n^2}{4j^2-\eta^2}\right]. \quad (14)$$

For an ensemble of molecules with a thermal equilibrium distribution the index of refraction will be:

$$r^2 - 1 = \frac{128\pi^3\mu^2 A N}{3h^2} \frac{\left[\frac{1}{4-\eta^2} + \sum_{-\infty}^{+\infty} n \sum_{|n|}^{\infty} j\left\{\frac{(j+1)^2-n^2}{4(j+1)^2-\eta^2} - \frac{j^2-n^2}{4j^2-\eta^2}\right\} e^{-W_{jn}/kT}\right]}{\sum_{-\infty}^{+\infty} n \sum_{|n|}^{\infty} j(2j+1)e^{-W_{jn}/kT}} \quad (14a)$$

If we denote $h/8\pi^2 A$ by ν_k, and if we put in the value of W_{jnm} from Eq. (11), (14a) may be rewritten as:

$$r^2 - 1 = \frac{\frac{256\pi^3\mu^2 N A}{3h^2} \sum_{-\infty}^{+\infty} n \sum_{0}^{\infty} p \left\{\frac{(|n|+p)^2-n^2}{4(|n|+p)^2-(\nu/\nu_k)^2}\right\} \sin h - \frac{h\nu_k}{kT}(|n|+p)\, e^{-h\nu_k/kT\{(A/C-1)n^2+(|n|+p)^2\}}}{\sum_{-\infty}^{+\infty} n \sum_{0}^{\infty} p(2|n|+2p+1) \exp - \left\{\left(\frac{A}{c}-1\right)n^2 + \{|n|+p)(|n|+p+1)\}\frac{h\nu_k}{kT}\right.} \quad (15)$$

These formulae are simply special cases of the Kramers-Heisenberg general dispersion formula. And as is to be expected, the two terms in (14) are those corresponding to the only two possible transitions, involving radiation, from the (jnm) state of the unperturbed top.

The Raman Transitions

To get the intensities of the Raman effect radiations we must compute the moments:

$$m_z = \mu \int \cos\theta \psi_{jnm} \psi^*_{j'n'm'} d\tau \quad (16)$$

$$m_x \pm i m_y = \mp \mu i \int \sin\theta e^{\pm i\phi} \psi_{jnm} \psi^*_{j'n'm'} d\tau. \quad (17)$$

From (1), (3) and our remarks about the c_{jr} we immediately get the following selection rules:

$$\left.\begin{aligned} m_z(jnm; j'n'm') &= 0, \text{ unless: } n' = n;\ m' = m. \\ m_x + i m_y(jnm; j'n'm') &= 0, \text{ unless: } n' = n;\ m' = m+1. \\ m_x - i m_y(jnm; j'n'm') &= 0, \text{ unless: } n' = n;\ m' = m-1. \end{aligned}\right\} \quad (18)$$

We may now express the form of the moments as:

$$m(jnm; j'n'm') = \mu e^{2\pi i/h(W_{j'}-W_j)t}\left[q_{jj'} + e^{2\pi i\nu t}\left\{\sum_r (\overset{+}{c}_{jr} q_{rj'} + \overset{-}{c}_{j'r} q_{jr})\right\} + e^{-2\pi i\nu t}\left\{\sum_r (\overset{-}{c}_{jr} q_{rj'} + \overset{+}{c}_{j'r} q_{jr})\right\}\right] \quad (19)$$

where for m_z, $q_{jj'}=z_{jj'}$, as defined in Eq. (2); and for $m=m_x\pm im_y$, $q_{jj'}=\mp if\sin\theta e^{\pm i\phi}u_j u_{j'}^* d\tau$. The problem that remains is that of obtaining the values of the $q_{jj'}$ and putting them into Eq. (19).

From Eqs. (2) and (10) we see that the only non-vanishing moments m_z are: $m_z(j;j\pm 2)$ and $m_z(j;j\pm 1)$. Upon putting into (19) the values of the matrix elements as given in Eqs. (9) and (10), we get for these moments:

$$m_z(j;j+2)=\frac{-8\pi^2\mu^2E_0Ae^{+2\pi i/h(W_{j+2,n}-W_{j,n})t}}{h^2(j+1)(j+2)(2j+3)}\left(\frac{\{(j+2)^2-n^2\}\{(j+2)^2-m^2\}\{(j+1)^2-n^2\}\{(j+1)^2-m^2)}{(2j+1)(2j+5)}\right)^{1/2}$$
$$\left[\frac{e^{2\pi ivt}}{\{\eta-2(j+1)\}\{2(j+2)-\eta\}}-\frac{e^{-2\pi ivt}}{\{2(j+2)+\eta\}\{2(j+1)+\eta\}}\right] \tag{20}$$

$$m_z(j;j+1)=\frac{\mu e^{2\pi i/h(W_{j+1,n}-W_{j,n})t}}{j+1}\left(\frac{\{(j+1)^2-m^2\}\{(j+1)^2-n^2\}}{(2j+1)(2j+3)}\right)^{1/2}$$
$$\left[1-\frac{16\pi^2\mu E_0Amn}{h^2j(j+2)}\left\{\frac{e^{2\pi ivt}}{\eta\{\eta-2(j+1)\}}+\frac{e^{-2\pi ivt}}{\eta\{\eta+2(j+1)\}}\right\}\right]. \tag{21}$$

$m_z(j;j-2)$ is to be obtained from $m_z(j;j+2)$ by replacing j by $j-2$ and taking the conjugate; and similarly we get $m_z(j;j-1)$ from $m_z(j;j+1)$ by replacing j by $j-1$ and taking the conjugate.

To evaluate the matrices $q_{jj'}$ from $m_x\pm im_y$ we have to compute integrals of the form: $\int_0^\pi \sin^2\theta\, y_{jnm}y_{jn'm}d\theta$. For this purpose we make use of the results of Reiche and Rademacher. If we compare the present notation with theirs we find that we have the following relation for the integrals in question:

$$4\pi^2AC^{1/2}\int_0^\pi \sin^2\theta\, y_{jnm}y_{j'n'm'}d\theta=2L_{\substack{a,b,l\\a',b',l'}}/(J_{abl}J_{a'b'l'})^{1/2} \tag{22}$$

where the $L_{abl,a'b'l'}$ and J_{abl} are integrals evaluated by Reiche and Rademacher, the latter being normalization integrals. The parameters a, b, l, are defined by:

$$a=|m+n|\,;\ b=|m-n|\,;\ l=j-\frac{a+b}{2}\,.$$

In addition to the selection rules of Eq. (18) we must take account of the four following cases possible for the change: $|m'-m|=1$.

a) $\Delta a=+1$; $\Delta b=+1$; *b*) $\Delta a=+1$; $\Delta b=-1$; *c*) $\Delta a=-1$; $\Delta b=+1$; *d*) $\Delta a=-1$; $\Delta b=-1$.

The Δ_s refer to the difference of the value of the parameter between the primed and unprimed states. Different integrals $L_{a,b,l,a'b'l'}$ must be used for these four cases. It turns out, however, that all four cases give the same final result, so that here only case *a* will be considered.

For this case, we have, according to Reiche and Rademacher:

$$L^{abl}_{a+1,b+1,l'} = 0 \text{ for } l' < l-2 \text{ and } l' > l. \tag{23}$$

The non-vanishing integrals have the values:

$$\begin{aligned}
&L^{a,b,l}_{a+1,b+1,l} /(J_{a,b,l}J_{a+1,b+1,l})^{1/2} \\
&= \frac{1}{2l+a+b+2}\left(\frac{(l+a+1)(l+b+1)(l+a+b+1)(l+a+b+2)}{(2l+a+b+1)(2l+a+b+3)}\right)^{1/2} \\
&L^{a,b,l}_{a+1,b+1,l-1} /(J_{a,b,l}J_{a+1,b+1,l-1})^{1/2} \\
&= \frac{(b-a)(l(a+b+l+1))^{1/2}}{(2l+a+b)(2l+a+b+2)} \\
&L^{a,b,l}_{a+1,b+1,l-2} /(J_{a,b,l}J_{a+1,b+1,l-1})^{1/2} \\
&= \frac{1}{(2l+a+b)}\left(\frac{l(l-1)(l+b)(l+a)}{(2l+a+b-1)(2l+a+b+1)}\right)^{1/2}.
\end{aligned} \tag{24}$$

In these formulae, the following values of the parameters are to be used:

For: $m'=m+1$, $a=n+m$, $b=m-n$, $l=j-m$.

For: $m'=m-1$, $a=-n-m$, $b=n-m$, $l=j+m$.

When these substitutions are made in the values of the integrals and finally in Eq. (17), the results are the following:

$$\left.\begin{aligned}
m_x \pm im_y &= \frac{\pm 8\pi^2\mu^2 iAE_0 e^{2\pi i/h(W_{j+2,n}-W_{j,n})t}}{h^2(j+1)(j+2)(2j+3)}\left(\frac{\{(j+2)^2-n^2\}\{(j+1)^2-n^2\}\{(i+1)^2-m^2\}}{(2j+1)(2j+5)}\right)^{1/2} \\
&\quad\cdot((j+m+3)(j\pm m+2))^{1/2}\left\{\frac{e^{2\pi i\nu t}}{\{\eta-2(j+1)\}\{2(j+2)-\eta\}}-\frac{e^{-2\pi i\nu t}}{\{\eta+2(j+1)\}\{\eta+2(j+2)\}}\right\} \\
m_x \pm im_y &= \frac{\mp i\mu e^{2\pi i/h(W_{j+1,n}-W_{jn})t}}{(j+1)}\left(\frac{\{(j+1)\to n^2\}(j\pm m+2)(j\pm m+1)}{(2j+1)(2j+3)}\right)^{1/2} \\
&\quad\left[1\mp\frac{8\pi^2\mu AE_0}{h^2j(i+2)}n(j\pm 2m)\left\{\frac{e^{2\pi i\nu t}}{\eta\{\eta-2(j+1)\}}+\frac{e^{-2\pi i\nu t}}{\eta\{\eta+2(j+1)\}}\right\}\right] \\
m_x \pm im_y &= \frac{\pm 8\pi^2\mu^2 iAE_0 e^{2\pi i/h(W_{j-2,n}-W_{j,n})}}{h^2j(j-1)(2j-1)}\left(\frac{\{(j-1)^2-n^2\}(i^2-n^2)(j^2-m^2)(j\mp m-1)(j\mp m-2)}{(2j-3)(2j+1)}\right)^{1/2} \\
&\quad\left[\frac{e^{2\pi i\nu t}}{(2j+\eta)\{2(j-1)+\eta\}}+\frac{e^{-2\pi i\nu t}}{\{2j-\eta\}\{2(j-1)-\eta\}}\right],
\end{aligned}\right\} \tag{25}$$

The value for $j'=j-1$, is to be obtained from that for $j'=j+1$ by replacing in the expression for the latter j by $-j-1$.

As in the case of m_z, all the moments $m_x \pm im_y$ vanish for which $|j-j'| \geqq 3$. It should be noted that as $m_x-im_y=0$, for $m'=m+1$, $m_x+im_y=2m_x=2im_y$; and as $m_x+im_y=0$, for $m'=m-1$, $m_x-im_y=2m_x=-2im_y$.

Formally, we can express the general moment $m(jnm;\, k'n'm')$ as:

$$m(j;\, k) = m(\nu_{jk})e^{2\pi i\nu_{jk}t} + m(\nu+\nu_{jk})e^{2\pi i(\nu+\nu_{jk})t} + m(\nu-\nu_{jk})e^{-2\pi i(\nu-\nu_{jk})t} \tag{26}$$

where $m(\nu)$ is the moment oscillating with the frequency ν, and $\nu_{jk} = (W_k-W_j)/h$. To get the intensities of transitions for these particular

frequencies, we must pick out from the general expression of Eq. (26) the "partial moments" oscillating with that frequency. We thus see immediately that all the $m(\nu_{jk})$ vanish for $|\Delta j| = 2$. This simply means that there is no "unshifted" Raman lines for such transitions; and this is to be expected, since there are no spontaneous transitions for the unperturbed top, for which $|\Delta j| = 2$. To get the total intensities we must know the squares of the resultant moments, given by:

$$R(\nu) = |m_x(\nu)|^2 + |m_y(\nu)|^2 + |m_z(\nu)|^2 \tag{27}$$

From the previous equations we find that:

$$\left.\begin{aligned}
\overset{j'=j+2}{R(\nu+\nu_{j,j+2})} &= \frac{64\pi^4\mu^4A^2E_0^2\{(j+2)^2-n^2\}\{(j+1)^2-n^2\}\{(j+1)^2-m^2\}}{h^4(j+1)^2(2j+3)^2(j+2)(2j+1)\{\eta-2(j+1)\}^2\{2(j+2)-\eta\}^2} \\
\overset{j'=j+1}{R(\nu+\nu_{j,j+1})} &= \frac{64\pi^4\mu^4A^2E_0^2n^2\{(j+1)^2-n^2\}(j^4+3j^3+2j^2-2j^2m^2+9m^2+3m^4)}{h^4(j+1)^2j^2(2j+1)(2j+3)(j+2)^2\eta^2\{\eta-2(j+1)\}^2} \\
R(\nu_{j,j+1}) &= \frac{\mu^2\{(j+1)^2-n^2\}}{(2j+1)(j+1)} \\
\overset{j'=j-2}{R(\nu+\nu_{j,j-2})} &= \frac{64\pi^4A^2E_0^2\mu^4\{(j-1)^2-n^2\}(j^2-n^2)(j^2-m^2)}{h^4j^2(j-1)(2j-1)^2(2j+1)(2j+\eta)^2\{2(j-1)+\eta\}^2}.
\end{aligned}\right\} \tag{28}$$

In the above, the values of R are not listed for the Raman lines of frequency $\nu-\nu_{jk}$. But these may be obtained from those given by replacing η by $-\eta$ wherever it occurs. It may be noted that the values of R for the unshifted lines are independent of m; this is in agreement with the observation of Reiche and Rademacher that none of the squared moments of the unperturbed top depend on m.

We have finally to sum the given values of R over m, since the unperturbed top is degenerate with respect to m. Using the value of

$$\sum_{|m|\leq j} m^4 = \frac{j}{15}(j+1)(2j+1)(3j^2+3j-1)$$

we get

$$\left.\begin{aligned}
\overset{j'=j+2}{I(\nu+\nu_{j,j+2})} &\equiv \sum_{|m|\leq j} R(\nu+\nu_{j,j+2}) \\
&= \frac{64\pi^4\mu^4A^2E_0^2\{(j+2)^2-n^2\}\{(j+1)^2-n^2\}}{3h^4(j+1)(j+2)(2j+3)\{\eta-2(j+1)\}^2\{2(j+2)-\eta\}^2} \\
\overset{j'=j+1}{I(\nu+\nu_{jj+1})} &= \frac{448\pi^4\mu^4A^2E_0^2n^2\{(j+1)^2-n^2\}}{15h^4j(j+1)(j+2)\eta^2\{\eta-2(j+1)\}^2} \\
I(\nu_{j,j+1}) &= \frac{\mu^2\{(j+1)^2-n^2\}}{(j+1)} \\
I(\nu+\nu_{j,j-2}) &= \frac{64\pi^4\mu^4E_0^2\{(j-1)^2-n^2\}(j^2-n^2)}{3h^4j(j-1)(2j-1)(2j+\eta)^2\{2(j-1)+\eta\}^2}.
\end{aligned}\right\} \tag{29}$$

For $j'=j-1$, we replace the values of j in the expression for I for $j'=j+1$ by $-j-1$ and change the sign. Again, the values for I for $\nu-\nu_{jk}$ are to be obtained from the above by replacing η by $-\eta$, wherever it occurs.

These formulae permit a computation of the intensities of any Raman line emitted or absorbed by a gas whose molecules are of the type of symmetrical tops.

It is of interest to note that in none of these formulae for the Raman moments or for the dispersion by a single state, does the moment of inertia C enter. This might be expected, however, since as observed by Manneback, C does not enter in the corresponding formulae of the Stark effect, and our dispersion theory deals essentially with a pulsating Stark effect. But to formally remove the effect of the moment of inertia C we must make $n=0$. This makes the top equivalent to the three dimensional rotator. And in fact, putting $n=0$, in our dispersion formulae reduces them to those derived by Debye[6] for the rotator. When we put in $n=0$ in the expression for the Raman moments we see that there will be no Raman lines, with the shift in frequency, for the transitions occurring in the unperturbed state of the rotator; on the other hand, there will be the shifted Raman lines for the transitions that violate the selection rule of the unperturbed rotator, and which are induced by the incident light. This fact may be considered as a special case of the same rule which has been shown by a number of authors to hold in the rotational fine structure of the Raman spectra of diatomic molecules.

Finally we may compute from Eqs. (20), (21), and (25) the polarization of the Raman radiations. The result is that for the unshifted lines we get:

$$|m_x|^2 = |m_y|^2 = |m_z|^2 . \tag{30}$$

For the shifted lines, however, we do get a polarization, given by:

$$|m_x|^2 = |m_y|^2 = \tfrac{3}{4}|m_z|^2. \tag{30a}$$

The writer is indebted to Dr. A. E. Ruark for the opportunity of discussing with him questions arising in this problem.

[6] Debye; Polar Molecules, p. 165.

THE LOCATION OF THE ELECTROMOTIVE FORCE IN THE PHOTOVOLTAIC CELL

By W. Norwood Lowry
Department of Physics, Cornell University

(Received April 8, 1930)

Abstract

1. A method was developed to utilize a 4-element vacuum tube to measure small potential differences.

2. The so called photovoltaic e.m.f. appears to be a modification of the electrolyte with light, there being no indication of any effect due to the direct illumination of the electrode or the boundary region between the electrode and the electrolyte.

3. In certain types of experiments with these cells, current measurements cannot be regarded as a quantity proportional to e.m.f.

4. The e.m.f. of the photovoltaic cell increases with the concentration of the electrolyte.

Introduction

IT IS well known that when two similar electrodes are placed in a suitable electrolyte and one of the electrodes is illuminated while the other is kept in the dark, an e.m.f. is produced. Goldmann[1] attributed the phenomena to a photoelectric effect arising from the illumination of the boundary between the electrode and the electrolyte. Grumbach[2] introduced near one electrode of a dark cell a small amount of previously irradiated electrolyte and obtained an effect, thus showing that the e.m.f. produced was due, at least in part, to a change or modification of the electrolyte with light.

Murdock[3] devised a means whereby the electrolyte flowed by the electrode in such a way that the electrolyte could be irradiated before, while, or after flowing by the electrode, and like Grumbach found the effect largely due to some change in the electrolyte. But in addition having found that the steady state current increased suddenly when the electrode first entered the edge of the illuminated region, he was led to believe that there might be some effect superimposed upon that due to photo-chemical change, when the boundary between the electrode and the electrolyte was irradiated.

Subsequent workers[4,5] have felt that certain variations in their results might arise from an effect other than the photochemical change of the electrolyte.

The original purpose of this present work was to devise a means of finding some of these variations if they existed, and, if found, to study them.

[1] A. Goldmann, Ann. d. Physik **27,** 449 (1908).
[2] A. Grumbach, Comptes Rendus **176,** 88 (1923).
[3] C. C. Murdock, Proc. Nat. Acad. Sci. **12,** 504 (1926).
[4] W. Rule, Proc. Nat. Acad. Sci. **14,** 272 (1928).
[5] H. W. Russell, Phys. Rev. **32,** 667 (1928).

Apparatus and General Discussion

The apparatus used in the first part of this investigation has been patterned after that of Murdock,[6] but with some modifications. Briefly, platinum electrodes in the form of long narrow strips were sputtered diametrically opposite on the outside of a pyrex test tube 18×150 mm. Pyrex was used as it was found less likely to crack than the soft glass test tubes, when copper wires were soldered to the top of the platinum films. The sputtered films were about 130×6 mm. After the Cu wires were soldered, the test tubes were covered with bakelite lacquer down to about 8 mm from the end of the film. This left the electrode itself exposed, with dimensions of about 8×6 mm. The rest of the platinum film served only as a conducting lead to the soldered wire. Except for very thin electrodes the platinum leads were the same density as the electrodes, as it was found that cells made in this way stood up over longer periods than those previously used,[3] due to the tendency of the bakelite lacquer (used to insulate the lead from the electrolyte) to chip off from the glass with the thicker films, and that higher resistance was not objectionable, in making e.m.f. measurements.

Considerable care was taken with the sputtering process, a special sputtering jar being designed so as to eliminate as far as practicable the occlusion of undesirable gases in the films. A G.E. 10 kv, 100 m.a. D.C. generator was used, which permitted very close control of current and voltage while sputtering. The test tubes were first thoroughly cleaned. After sputtering they were aged slowly by heating to a temperature ranging between 300–360°C for several hours; then they were slowly cooled, lacquered, dried in air, and baked at 135°C. Of the 32 cells made in this way, only a few were found, when first tried, to have a dark e.m.f. of such a magnitude as to prohibit their use.

The test tube was slipped over a vertical brass tube covered with felt so as to hold the test tube snugly, but permit of its rotation about the brass tube. A small rectangular window was cut in the lower end of the brass tube, and a beam of light, caused to pass down the brass tube, was reflected through the window by means of a mirror placed at a 45° angle just behind it. By turning the test tube, the electrode, which was slightly smaller than the window, could be brought directly in front of the window, or on either side of it, through a range of more than 180°, and by a suitable scale and index the position of the electrode in respect to the window could be determined. The test tube was placed in a cylindrical glass bottle (painted black to exclude external light) containing the electrolyte, rhodamine B in absolute alcohol. The mouth of the bottle was just large enough to give about 2 mm clearance around the test tube, in order to reduce evaporation. This bottle was mounted on a rotator, driven by a synchronous motor through a reduction gear, assuring constant speed of rotation. The bottle with its electrolyte thus rotated concentrically about the test tube with its electrodes.

[6] C. C. Murdock and D. W. Murdock, Trans. of the Faraday Soc. **23**, part 5, 593 (1927).

Filters were used to vary the intensity of illumination. They consisted of photographic plates exposed for different lengths of time and developed in the usual manner. The transmission of the filters as well as the electrodes was measured photometrically. In every case the light passed through a water cell to remove the infra red radiation.

All concentrations of electrolyte are given as percent of rhodamine B by weight in absolute alcohol.

Using a similar cell, Murdock obtained the curve previously published[3] by plotting the current against the position of the electrode in respect to the window. The current was measured by a high sensitivity galvanometer in series with a suitable resistance, after a steady state had been obtained. He pointed out that his results were in agreement with Grumbach's,[2] but that the change in slope of the curve at the points where the electrode began to be directly illuminated indicated that some effect other than photochemical change might exist. He also showed that the effect was dependent

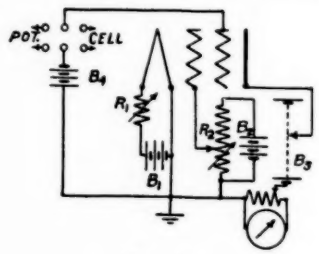

FIG. 1

upon the shape of the electrode and that polarization[6] played an important rôle.

It was felt that the actual e.m.f. produced might not be directly proportional to the residual current that he measured. Therefore it was decided to utilize a potential measuring instrument, that would not draw current.

A Compton type quadrant electrometer was used in the major part of the work, but on account of its long period another device was developed. This consisted of a specially constructed 4-element vacuum tube, built by Osram in Berlin, connected as shown in Fig. 1. The purpose of this tube was to act as a voltage amplifier for the small potentials measured, and by means of the 4th element or "space charge grid" to effectively prevent current being drawn from the source. The filament is surrounded by a helical "space charge grid," which is enclosed by a second helical control grid, with a lead brought out through an amber bushing in the top of the tube. The cylindrical plate is just outside of the control grid. The 4 elements are nearly concentric. B_1, B_2 and B_3 are storage batteries of 6, 6, and 24 volts respectively. B_4 consists of 3 standard cells, which were used because of the necessity to maintain a constant negative bias in series with the e.m.f. to be measured. Plug type resistance boxes were used for R_1 and R_2 to eliminate variable contact resistance. A highly insulated mercury contact switch was used to quickly connect either the potentiometer or cell circuits

to the measuring system. A galvanometer having a sensitivity of 25,000 megohms was connected in the plate circuit through an Ayrton shunt and an auxiliary resistance to critically damp it.

In operation the control grid was made more negative than its floating potential to prohibit electron current. The space charge grid was made positive (from 2 to 3 volts) in respect to the filament in order to shield the control grid from positive ions. An extremely hard tube, operation of filament at 40 percent of normal temperature, and low plate potential (18 to 22 volts) all contributed to reduce positive ion current. Leakage was reduced by precautions in the insulation of the control grid lead coming out through the top of the tube, and the use of ceresine wax to insulate every lead and piece of apparatus in the circuit. A galvanometer having a sensitivity of 25,000 megohms used at a distance of 3 meters from the scale showed no trace of a deflection when connected in series with the control grid circuit. It should indicate any current greater than 10^{-13} amperes.

E.m.f. measurements were made by noting the change in plate current when the source of potential was connected in series with the standard cells so as to make the control grid more negative.

Sensitivity could be varied by changing R_1, R_2, B_3 or B_4. After proper adjustments were once made R_1 and R_2 were the only controls needed. The system was used with a sensitivity between 3000 and 4000 mm per volt, although 5200 mm per volt was obtained. With suitable amplification higher sensitivities should be possible.

For very small values the e.m.f. was found to be nearly linear with scale deflections.

The advantages of the system lie in the short period of the galvanometer, and freedom from the usual electrometer adjustments.

The disadvantages may be summed up as follows:

1. It was difficult to make comparative measurements over long periods of time due to slight fluctuations in battery voltages.
2. Changes in room temperature changed the constants of the circuit.
3. The tube was found to be photoelectric. (This was taken care of by covering the tube with a metal shield and grounding it.)
4. Special precautions had to be taken against leakage currents.
5. The system was extremely sensitive to high tension discharges or arcs.
6. The filament of the tube had to be burned several hours before using the system.

Experimental

The electrolyte rotating with the bottle had a small region illuminated as it passed in front of the window. The test tube was adjusted vertically while assembling so that the front electrode was symmetrically placed in front of the window. By moving the test tube about the axis of the brass tube, the horizontal position of the electrode in respect to the window could be altered, and thus the electrolyte could be irradiated before, while in contact with, or after passing by the electrode. This arrangement per-

mitted a study of the effect when the boundary region between the electrode and electrolyte was illuminated, as well as the condition when the electrode was displaced from the window so that the effect was produced by the previously irradiated electrolyte flowing by the electrode. The scale which indicated the position of the electrode in respect to the window was arranged to read in millimeters displacement.

There were four variable factors: (1) speed of rotation of electrolyte; (2) thickness of sputtered films; (3) intensity of illuminaton; and (4) con-

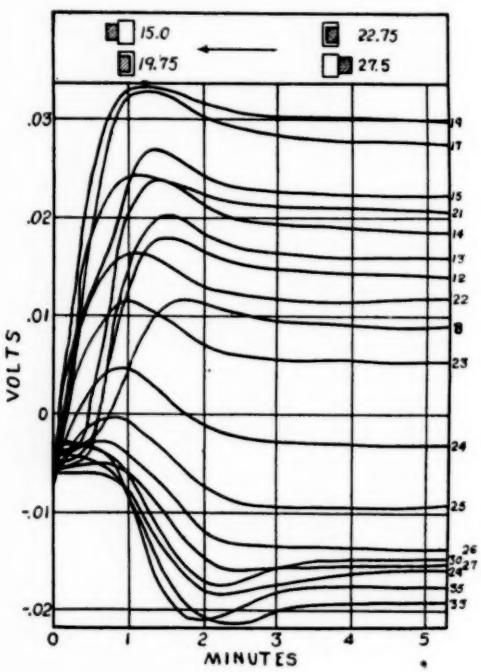

FIG. 2

Opposite electrodes	
Electrode transmission	35 percent
Speed of rotation	20.8 r.p.m.
Concentration of electrolyte	2.19 percent
Method of measurement	4-element vacuum tube system

In this experiment a square electrolyte bottle was used.

centration of rhodamine B in the electrolyte. In order to make a thorough study of the effect many sets of data were obtained in which three of these factors were held constant and the fourth varied.

Two distinct types of cell were used in this part of the work. (1) The electrodes were arranged opposite each other, and were of the same length. (2) The back electrode, while opposite, was from 3 to 4 cm above the front one. Hereafter the former will be referred to as a cell with "opposite" electrodes, and the latter as one with "staggered" electrodes. With staggered electrodes the irradiated material from the window should stream around

an annulus the height of the window, and should not come in contact with the back electrode, except for vertical diffusion.

The following curves show a few results which are representative of many sets of data taken. The white rectangles represent the window and the shaded ones the electrode, and the numbers the scale readings for the positions shown. The arrows indicate the direction in which the electrolyte flowed by the window.

Fig. 2 is a set of curves showing the relation between e.m.f. and time for various positions of the electrode in respect to the window. The numbers along the right hand side of the curve represent the positions of the electrode, the scale being laid off so that each unit represented a movement of 1 mm in respect to the window.

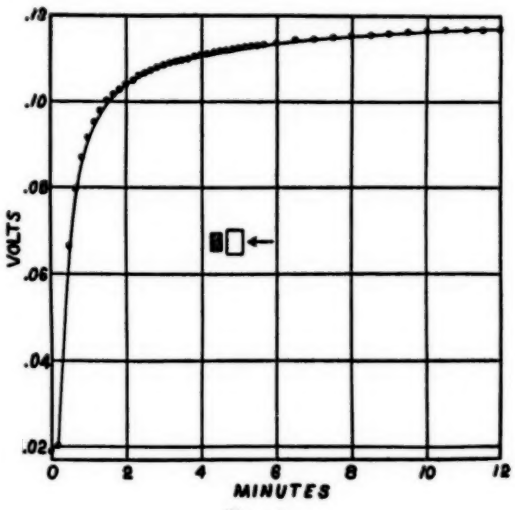

FIG. 3

Staggered electrodes	
Electrode transmission	11 percent
Speed of rotation	49.5 r.p.m.
Concentration of electrolyte	2.19 percent
Method of measurement	4-element vacuum tube

The cell was allowed to rotate in the dark until only a small dark e.m.f. was present; then time was measured from the beginning of illumination. This procedure was repeated for each curve. These shown are only part of the total number of time curves thus studied. No attempt has been made to indicate the points, as the curves were drawn free hand through practically all of them.

They show that after a time a steady state value of e.m.f. is obtained for each position of the electrode. The shape of the curves can be accounted for. If the electrode is at the left of the window, a certain time will elapse before the irradiated material will be carried around to the electrode. When it reaches this point, there will be a sudden rise in the e.m.f. Later some of the material will be carried around to the back electrode giving a differential

effect, and causing a decrease in the e.m.f. As one would expect, the maximum effect is found when the electrode is part way across the window and moving from left to right, because, as the electrode more nearly covers the window, the intensity of illumination is decreased by the electrode itself. When the electrode is at the left of the window the effect grows smaller since diffusion carries away some of the changed material. When the electrode is at the right of the window the back electrode receives the modified material first, which accounts for the negative e.m.f., and which of course is much smaller on account of diffusion as stated above. It is interesting to note that as the electrode approaches the window in either direction

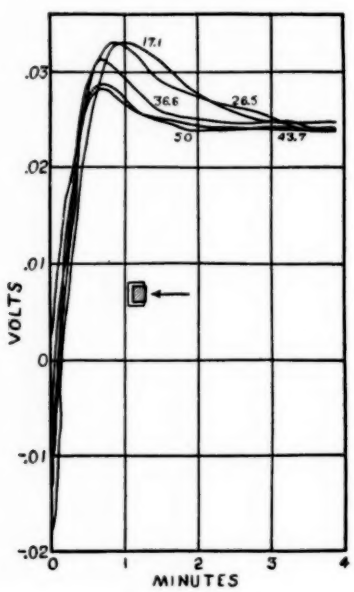

FIG. 4

Opposite electrodes	
Electrode transmission	35 percent
Concentration of electrolyte	2.19 percent
Method of measurement	4-element vacuum tube system

the maximum effect for each curve, which is either a positive or a negative e.m.f., occurs sooner. This represents the time required for the largest amount of changed material to reach the front electrode. It will also be observed that the steady state e.m.f. occurs in a shorter time as the electrode approaches the window. This latter fact was observed in all subsequent experiments.

Fig. 3 represents a curve similar to those in Fig. 2 except "staggered" electrodes were used. The approximate position of the electrode is shown by the diagram, and the arrow shows the direction of flow of the electrolyte. As might be expected, no maximum is found, but the e.m.f. builds up to the steady state value.

Fig. 4 shows a set of e.m.f.—time curves for varying speeds of rotation. The diagram shows the position of the electrode in respect to the window for all curves, and the arrow shows the direction of flow of electrolyte. Numbers on curves represent speeds of rotation. These curves show that the steady state of e.m.f. is independent of speed, within the limits tried. It is also seen that the maximum point is reached in shorter time as the speed increases; this result would be expected from the discussion of Fig. 2. The curves were drawn free hand through practically all of the points.

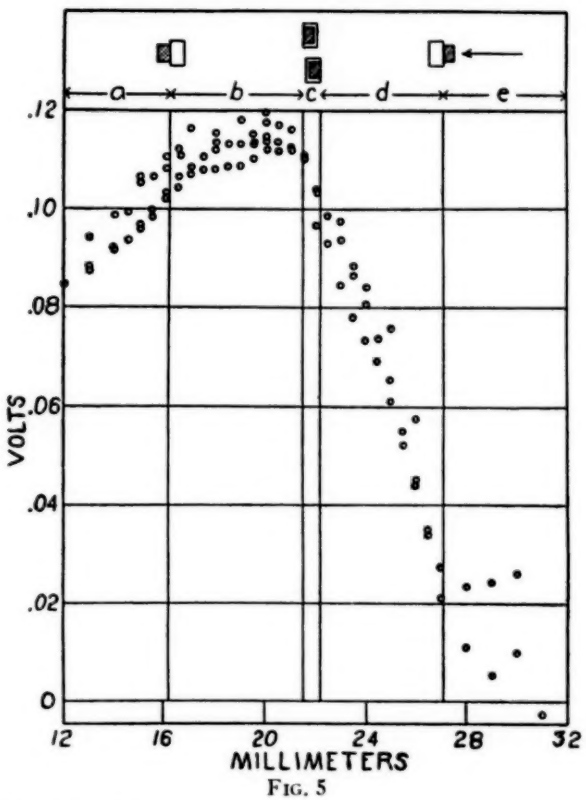

FIG. 5

Opposite electrodes	
Electrode transmission	9 percent
Speed of rotation	21.6 r.p.m.
Concentration of electrolyte	2.46 percent
Method of measurement	4-element vacuum tube system

Fig. 5 shows the relationship between e.m.f. and position of electrode in respect to window. Each point was taken after a steady state e.m.f. had been reached. The points were not taken on consecutive electrode positions, but at random positions over different parts of the scale. The variations are small when it is considered that the time for taking these data was several hours, and that the voltages used for controlling the vacuum tube system were bound to fluctuate some in this period. The diagrams at the top show the positions of the electrode and the vertical lines on the curve

indicate these positions. This arrangement is similar to that of Murdock,[3] the regions *a*, *b*, *c*, *d*, and *e* representing respectively: electrolyte illuminated before passing electrode; electrode partially illuminated; electrode completely illuminated; electrode partially illuminated; and electrolyte illuminated after passing electrode. The arrow shows the direction of flow of the electrolyte.

Fig. 6 shows two curves plotted with positions of electrode in respect to e.m.f. Curve *B* was obtained by reversing the direction of rotation of the electrolyte from that in *A*, the lettered arrows indicating the respective directions of electrolyte rotation. In this case data were taken for consecu-

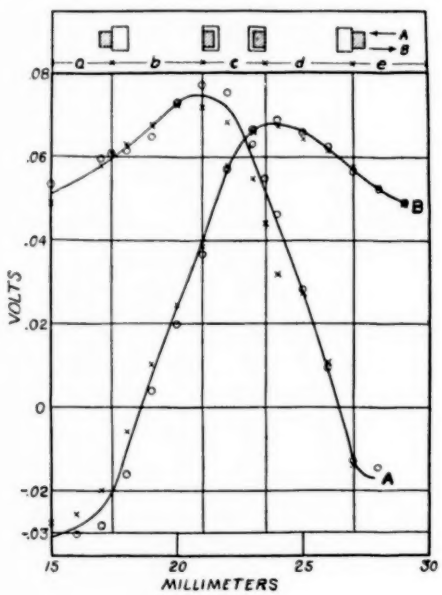

FIG. 6

Opposite electrodes	
Electrode transmission	14.5 percent
Speed of rotation	19.9 r.p.m.
Concentration of electrolyte	2.46 percent
Method of measurement	Compton electrometer

tive electrode positions, and as a check were again taken consecutively back over the scale. The circles represent increasing scale readings for electrode positions, and the crosses, the return or decreasing scale readings. The symmetry of the two curves is quite marked. Murdock[3] was unable to obtain this symmetry when making current measurements, which failure he attributed to the shape of the electrode.

Fig. 7 is another group of curves taken in a similar manner to those in Fig. 6. In this case the intensity of illumination was varied by filters, the other factors being kept constant. Curves *A*, *B*, and *C* represent intensities of 3 percent, 17 percent, and 100 percent respectively. The circles and crosses again have the same meaning as in Fig. 6.

Discussion

If there is an e.m.f., due to the illumination of the electrode or the boundary between the electrode and the electrolyte, measurable with the instruments used, superimposed upon that due to a photo-chemical change

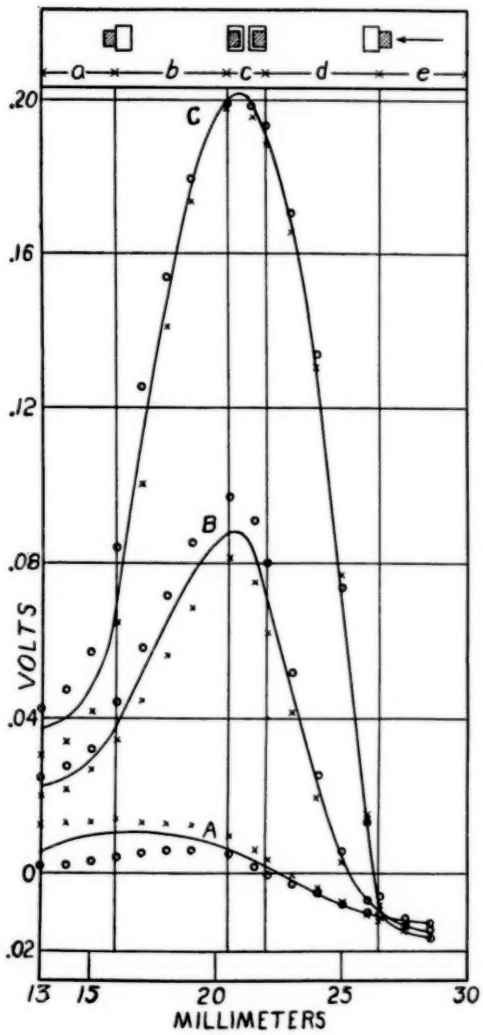

Fig. 7

Opposite electrodes	
Electrode transmission	24 percent
Speed of rotation	14.9 r.p.m.
Concentration of electrolyte	4.2 percent
Method of measurement	Compton electrometer

of the electrolyte, one would expect to find an abrupt change of slope on going from a dark to an illuminated region. A study of Figs. 5, 6 and 7 reveals no such change. Many similar sets of data were taken in which one

of the four factors before mentioned was varied and in every case a smooth curve resulted in going from region "*a*" to region "*b*."

This regularity leads to the viewpoint that the phenomenon is due entirely to the modification of the electrolyte with light, and that the effect follows the laws of the concentration cell theory. If one calls the original material A and the modified material due to light, B, then the e.m.f. will depend upon the difference in concentrations of B at the two electrodes, and this has been shown to be a function of $\log C_1/C_2$, where C_1 and C_2 are the concentrations of B at the electrodes.

In these cells the concentration of material B should be some function of three variable factors: (1) the intensity of the light; (2) time of illumination; and (3) the concentration of material A. According to the concentration cell theory, one would expect the effect to increase with these three factors. Rule[4] has shown that the e.m.f. is a function of the intensity and time of illumination. In an earlier experiment[7] by him and independently by Mrs. Junkins,[8] it was found that a maximum effect occurred for a particular concentration of material A, and any further increase in concentration of material A gave a decreased effect.

From the results in the rotational experiments of the present work in which concentrations were varied, and from the concentration cell theory, it was felt that the effect must increase with the concentration of material A. Accordingly ten rhodamine B solutions of varying strengths were made up in small bottles, and in turn were slipped over a test tube with the electrode placed directly in front of the window and the electrolyte at rest. Fig. 8 shows the results where e.m.f. was plotted against time, the numbers on the right hand side of the curves being percent concentrations of rhodamine B. It is seen that the effect increases with the concentration. It was later found that the solution became saturated a little above 8 percent. While care was used in making up the solutions, the concentrations were not afterward checked gravimetrically, as in the case of the former experiments with the rotating electrolyte, and may be slightly in error. In Fig. 9 the data were secured by subtracting the dark e.m.f.'s observed at the beginning of each time curve from the values obtained after ten minutes irradiation. It is quite evident that there is no maximum value for any particular concentration below saturation. Goldmann,[1] while making current measurements, found no maximum sensitivity for any particular concentration. In Rule's experiment[7] using fluorescein, e.m.f. was measured against concentration, but the electrode was illuminated through the electrolyte. For very dilute solutions not much light would be absorbed in the outer layers of the electrolyte, but on increasing the concentration more and more light would be absorbed. Hence there would be a particular concentration for any given intensity of illumination where the intensity of light near the electrode (and therefore material B) would be a maximum. Mrs. Junkins[8] illuminated the

[7] W. Rule, Phil. Mag. **1**, 532 (1926).
[8] R. Y. Junkins, Phys. Rev. **18**, 402 (1921), May 1929.

electrolyte through a semi-transparent electrode, as in the present work, but used current measurements as an indication of the effect with concentration, and found that for rhodamine B the maximum value occurred near 3 percent. Subsequent workers[3,5] used this value, believing it to give a maximum effect. Probably the current measurement was affected by polarization, and the rate of diffusion of polarizing material, which constitutes a quantity proportional to the current measured, must have attained a maximum value at 3 percent concentration.

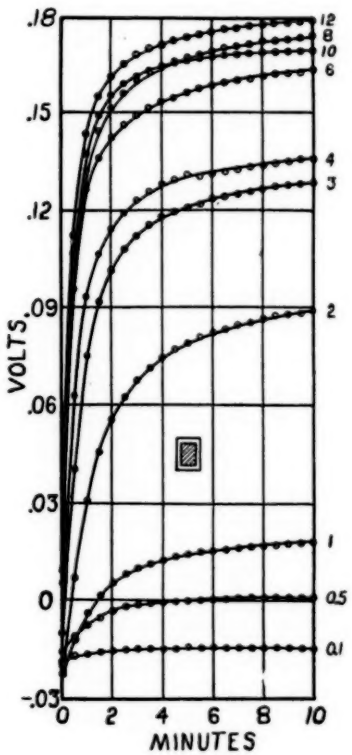

FIG. 8

In Figs. 5, 6, and 7 it will be observed that in region "*e*" the values of e.m.f. fluctuate. This is probably due to the fact that the effect is small, and that some light gets to the electrode by scattering and reflection, even though the electrode is at the right of the window, and in this position the back electrode begins to receive some of the irradiated material first. Diffusion also carries some of the new material to the front electrode against the direction of rotation. The fluctuation was observed in all of the data taken. It was also found that a greater length of time was always necessary to reach a steady state condition in this region. This effect was more marked in those curves where the intensity of light or the concentration of electrolyte was very small.

Rule,[4] using uranine, found at the beginning and end of illumination a small e.m.f. opposite in sign from the major effect. Russell,[5] working with rhodamine, did not actually observe a reversal, but found that the values of e.m.f., for a short interval of time after illumination began, departed somewhat from the theory he had developed, leading him to believe that some effect similar to the one found by Rule might be superimposed upon that due to photo-chemical change. Grumbach[2] also observed reversals.

Such an effect would not be compatible with the theory that an e.m.f. due to a pure concentration cell was the only one present, so a careful investigation was deemed advisable. In getting the data for Figs. 8 and 9, readings at the exact beginning and end of illumination were noted for each concentration, but no such effect was observed. Several different types of cell holders were used with rhodamine B and uranine at different concentra-

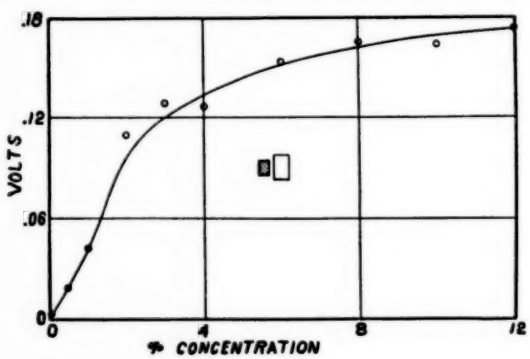

FIG. 9

tions. No reversal was found either at the beginning or end of illumination, even when a cell was made up and used in exact accordance with the method of Rule,[4] though the growth-time curves were found to agree consistently with his.

REMARKS

In all of the rotational experiments, in which e.m.f. was plotted against position of electrode in respect to the window, no break in the slope of the curve was found when the electrode first entered the illuminated region. As stated before, in the case of current measurements such a break has been observed. Contradictory to the results of another investigator, no reversal of e.m.f. was observed at the beginning or end of illumination in taking the growth-time curves of a cell. Both of these small effects had been previously interpreted as due to the illumination of the electrode or a region very close to it, and had been thought to be superimposed upon the main effect arising from a photo-chemical change of the electrolyte. The results of the present work thus lead to the viewpoint that there is no auxiliary effect produced by directly irradiating the electrode.

The failure to find a break in the curve when the electrode first entered the illuminated region can be attributed to the fact that e.m.f., instead of

current measurements were made. Likewise the discrepancy between the results of the present work and that of Mrs. Junkins, in which sensitivity of the effect with inceasing concentrations was studied, can be explained in the same way. Therefore, it is inferred that current measurements are not satisfactory for studying some of the phenomena occurring in this type of cell, especially in these particular cases mentioned where it was evidently assumed that the current was proportional to the e.m.f. A possible explanation might be that this disagreement in results was linked with some peculiarity of the polarization present in current measurements.

The author wishes to express his appreciation to Professor C. C. Murdock, who suggested the original problem and contributed many suggestions and valuable criticism during its progress. Also to Professors Ernest Merritt and R. C. Gibbs in particular, and to other members of the Physics staff in general, who made helpful suggestions in regard to the work.

THE VISCOSITY OF COMPRESSED GASES

By James H. Boyd, Jr.†
Department of Chemical Engineering, Massachusetts Institute of Technology

(Received April 7, 1930)

Abstract

New data and a new theory for the viscosity of compressed gases are presented. Data for nitrogen, hydrogen and a mixture of these gases are given, in the calculation of which, the "end effects" are not neglected as has been done in the past. Previous viscosity data are of doubtful validity owing to neglect of this factor. The theory is based on an analogy between the kinetic pressure and viscosity of a gas and is derived using an equation of state of the Lorentz type. Allowance is made for the difference between the viscosity and compressibility covolumes. The theory is substantiated experimentally and further confirmed by the recalculation of other data on the variation of Reynolds' criterion with the pressure, which is here shown to be constant. The mixture data offer a direct opportunity of comparing the Lorentz and linear rules for the calculation of the covolume of a mixture from the covolumes of the components and such comparison indicates that the Lorentz rule is not to be preferred. The substantiation of the new theory is the first direct proof of the validity of the separate treatment of the kinetic and cohesive pressures in the equation of state.

I. Introduction

THE viscosity coefficient of a gas is defined as the time rate of the net transfer of momentum across an imaginary, plane unit-surface in the interior of a flowing gas when there is a unit velocity gradient normal to the plane surface and normal also to the direction of gas flow. The statement is often encountered that the viscosity of gases is independent of the pressure. At atmospheric pressure and less this is substantially true and is confirmed experimentally but for high pressures theory predicts and experiment concurs in giving greater values of the gas viscosity.

A number of theories of the viscosity at high gas densities have been advanced and Meyer,[1] Brillouin[2] and Batschinski[3] have attempted solutions of this problem. Far more significant are the investigations of Jäger,[4] H. B. Phillips[5] and Dubief[6] who employed equations of state of the van der Waal type in their derivations. H. B. Phillips' paper is of particular interest in view of certain generalizations made concerning the effect of intermolcular forces on gas properties.

† Research Assistant, Research Laboratory of applied chemistry.

[1] Meyer, Kinetic Theory of Gases, 2 Ed., Eng. Trans., Longmans, Green and Co., 1899.

[2] Brillouin, Lecon sur la Viscosite, II, p. 132, Villiers, Paris, 1907.

[3] Batschinski, see Bingham, Fluidity and Plasticity, pp. 142–152, McGraw Hill, New York, 1922.

[4] Jäger, Wien. Sitz. Ber. **150,** 2A, 15 (1896); **108,** 2A, 447 (1899).

[5] H. B. Phillips, J. Math. and Phys., M. I. T. **1,** 42 (1921).

[6] Dubief, J. de Phys. et Rad. **7,** 402 (1926); Compte Rendus **180,** 1164 (1925); **182,** 688 (1926).

In the experimental field Warburg and von Babo[7] and P. Phillips[8] determined the viscosity of gaseous carbon dioxide at pressures exceeding one hundred atmospheres and for several temperatures. Wildhagen,[9] in his study of the flow of compressed air, measured the viscosity of air at room temperature for pressures up to two hundred atmospheres. All of the writers cited used some form of the transpiration method. In all of these investigations end effects were neglected.

The transpiration method of determining viscosity coefficients is that most readily adapted to use at high pressures. This method is based on Poiseuille's law for isothermal viscous flow which may be expressed

$$\Delta p = \frac{k_c M}{\rho} \mu \tag{1}$$

where Δp is the pressure drop in centimeters of mercury at 0°C, occasioned by the flow of M grams per second of an incompressible fluid of viscosity μ and density ρ through a tube of circular section whose dimensions determine the value of k_c. The density and viscosity are in c.g.s. units and k_c equals $8L/13.596\ g\pi r^4$* where L and r are the length and radius respectively in centimeters of the tube and g is the gravitational acceleration. When Eq. (1) is integrated assuming the ideal gas laws and an isothermal expansion there results

$$p_1^2 - p_2^2 = 2RTk_cM\mu \tag{2}$$

Here p_1 and p_2 are the upstream and downstream pressures respectively, R the gas constant and T the absolute temperature.

Neither of these equations may be applied directly to experimental data as they neglect "end effects" which are caused by losses in the kinetic energy of the fluid due to changes in the cross-section of the path of flow. As a result the observed pressure difference is greater than it would be were there no such loss. Accordingly Eqs. (1) and (2) should be modified as otherwise the calculated values of the viscosity coefficients would be high. End effects are discussed by Brillouin,[10] Fisher,[11] Rapp,[12] Bingham,[13] Benton,[14] Walker, Lewis and McAdams,[15] and by Trautz and Weizel.[16] The majority of these writers agree, on reducing their results, that the proper form for the end correction is

[7] Warburg and von Babo, Ann. d. Physik **17,** 390 (1882).

[8] P. Phillips, Proc. Roy. Soc. Lon. **87a,** 48 (1912).

[9] Wildhagen, Z. Angew. Math. u. Mech. **3,** 181 (1923).

* The coefficient of slip is negligible and has been omitted here.

[10] Brillouin, reference 2, pp. 117–124.

[11] Fisher, Phys. Rev. **32,** 216 (1911).

[12] Rapp, Phys. Rev. **2,** 263 (1913).

[13] Bingham, Fluidity and Plasticity, p. 17.

[14] Benton, J. Ind. Eng. Chem. **11,** 623 (1919).

[15] Walker, Lewis and McAdams, Principles of Chemical Engineering, p. 90, 2nd Ed., McGraw Hill, New York, 1927.

[16] Trautz and Weizel, Ann. d. Physik **48,** 799 (1915).

$$\Delta p_e = \frac{k_e M^2}{\rho} \tag{3}$$

where Δp_e is the end effect pressure drop and k_e is the end effect constant. Eqs. (1) and (2) accordingly become

$$\Delta p = \frac{k_c M \mu}{\rho} + \frac{k_e M^2}{\rho} \tag{4}$$

$$p_1^2 - p_2^2 = 2RT(k_c M \mu + k_e M^2) \tag{5}$$

It is of interest to consider the effect of a change in density of a given gas on the magnitude of the end correction when the latter is negligible at atmospheric pressure. Assume that the pressure drop due to the viscous action of the gas is relatively small and constant and that the viscosity is independent of the density. Eq. (4) is sufficient for this estimate since at the higher pressures the gas density is substantially constant throughout the apparatus. For these conditions M/ρ is constant and therefore the end correction, $k_e M^2/\rho$, is linear in density. For density variations of several hundred-fold the end correction may well be of the order of ten to twenty percent. This approximation shows that all previous high pressure investigations are of questionable quantitative significance in view of the neglect of end effects.

II. The Experimental Method

The transpiration method was used in this investigation and consisted in measuring the pressure drop occasioned by the isothermal flow of a gas of known density at a measured rate through a metal capillary whose constants, k_c and k_e, were determined by direct calibration. This necessitated relatively large amounts of the gases and so precluded the use of highly purified materials. Hydrogen and nitrogen of the highest commercial purity obtainable were used in these experiments.

The capillary used in these experiments was a steel tube about a meter long and roughly 0.025 cm in internal diameter. It was immersed in a stirred water bath thermostat whose temperature was read from calibrated thermometers fully immersed. The temperature variation seldom exceeded 0.2°C and generally was within 0.1°C which was adequate for these experiments. The calibration of the capillary for k_c and k_e will be described later. A metal capillary was used to insure isothermal flow.

The pressure-drop measurements were made with a new type of high pressure manometer. In principle, the instrument consisted of a mercury filled manometer whose arms were of widely different diameters thus giving practically the entire pressure differential in the smaller arm. The change of the mercury level in the smaller arm was detected by successively making and breaking an electrical circuit by means of a platinum tipped screw rod which was insulated from the body of this apparatus. The relative travel of the rod was determined by measuring the distance between its upper end and

a fixed reference plane by means of a micrometer depth gauge. A galvanometer indicated the completion of the circuit through which a feeble current flowed whose source was a thermocouple immersed in ice and water. This very feeble current was desirable to minimize arcing on breaking the circuit. The pressure differential was calculated from the difference between the flow and zero or no-flow readings. In this calculation corrections were made for the drop in mercury level in the larger arm, the gas density, and the temperature variation of the mercury density.

The gas density was computed from the temperature and pressure of the gas flowing. Pressures were measured with a dead weight piston gauge of the type developed by Keyes[17] and his coworkers. The gas temperature was taken to be that of the bath and the density was calculated from these data using Bartlett's[18] compressibility factors. No attempt was made to

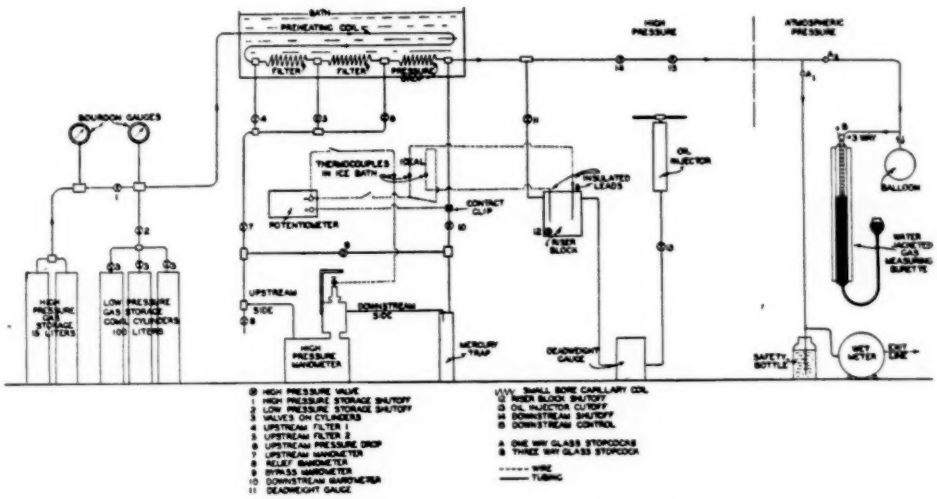

Fig. 1. Diagrammatic sketch of viscosity apparatus.

correct the gas density for the water vapor present since its concentration was very low as has been shown by Bartlett.[19]

The transpiration rate was determined by expanding the compressed gas and passing it into an exhausted rubber balloon for an observed time interval measured with a calibrated, split-second stop watch. The gas was then drawn into a water jacketed burette and measured at known temperature and pressure. From these data and the gas composition the transpiration rate was calculated.

The gas mixture was made up in a small holder, allowed to stand for several hours, compressed and then analyzed. The same method of compression was used for the pure gases to obtain pressures exceeding 150 atmospheres.

[17] Keyes, and Dewey, J. Opt. Soc. Am. and Rev. Sci. Instr. **14**, 491 (1927).
[18] Bartlett, J.A.C.S. **49**, 687 (1927); **49**, 1955 (1927).
[19] Bartlett, Cupples and Tremearne, J.A.C.S. **50**, 1275 (1928).

The apparatus is shown diagrammatically in Fig. 1. The gas flowed from the storage cylinders through a preheating coil of relatively large capillary tubing and then through two fine steel capillaries employed as dust filters before entering the pressure drop capillary. These capillaries were all immersed in the bath. On leaving the pressure-drop capillary the gas passed through a needle control valve and was reduced to atmospheric pressure. Care was taken that steady viscous flow was maintained during experiments.

The capillary constant k_c was determined by low pressure transpiration experiments which were calculated by Eq. (5) inspection of which shows that $(p_1^2-p_2^2)/M$ is linear in M. Actually Eq. (5) ignores the effect of the acceleration of the gas in the capillary but since the data plotted by the

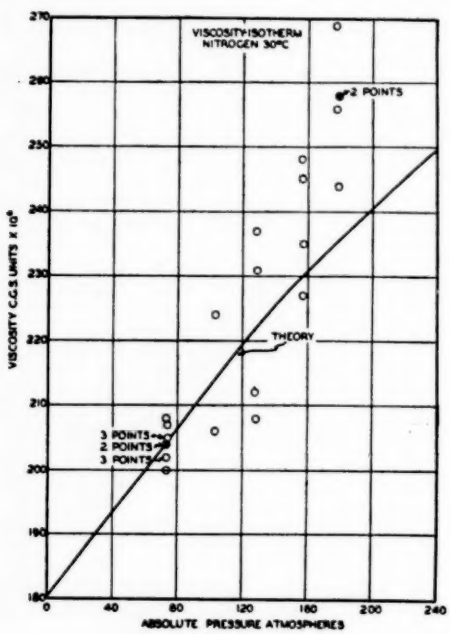

Fig. 2.

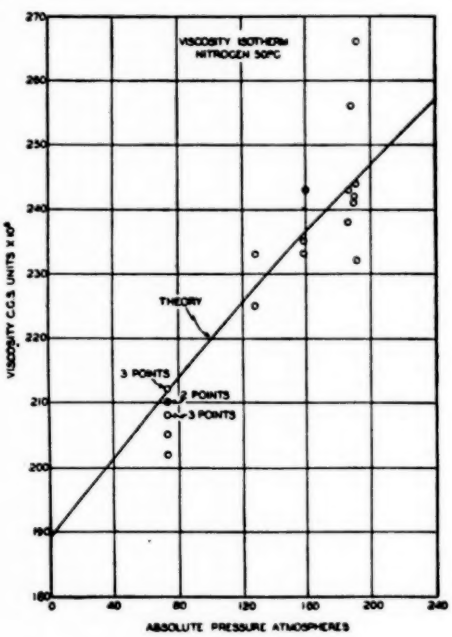

Fig. 3.

above method were linear the value of k_c was readily calculated on obtaining the intercept by extrapolation to zero gas flow. A very satisfactory check was given by an alternative method based on the determination of the volume of the capillary. This latter procedure required the weight, length and average external diameter of the tubing and further necessitated the determination of the density of the steel in the tubing. From these data k_c was calculated. The excellent agreement of the results obtained by these two separate methods gave great confidence in the validity of the transpiration method for this calibration. The distention of the capillary by changes in temperature and pressure which, if appreciable, would affect the value of the constant, was found to be negligible for the ranges of temperature and pressure employed here. A supplementary transpiration calibration for k_c

was required because of a very slight rusting of the interior walls of the capillary. This rusting was due to the condensation of small amounts of water vapor from the compressed gas which occurred on increasing the pressure in the capillary above that in the supply cylinder from which the gas was drawn. This was avoided in subsequent experiments by performing them in the order of their descending pressures. After establishing this procedure check transpiration calibration experiments showed the value of k_c to be unchanged.

The constant k_c was determined by means of high pressure transpiration experiments which were calculated with Eq. (4) which is linear in $\Delta p \cdot \rho / M$ versus M. The slope of such a plot gave the value of k_c. Here the use of

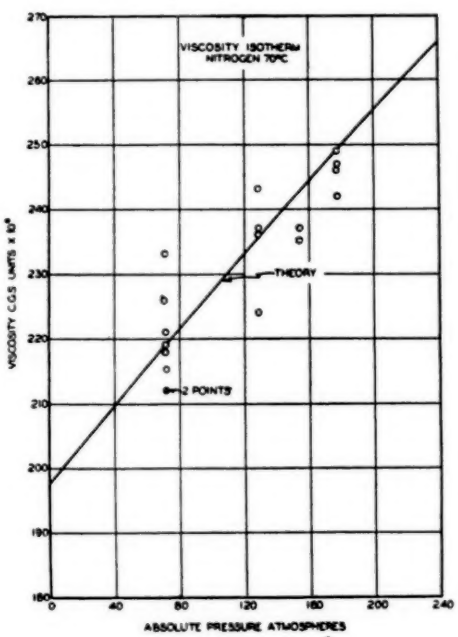

Fig. 4.

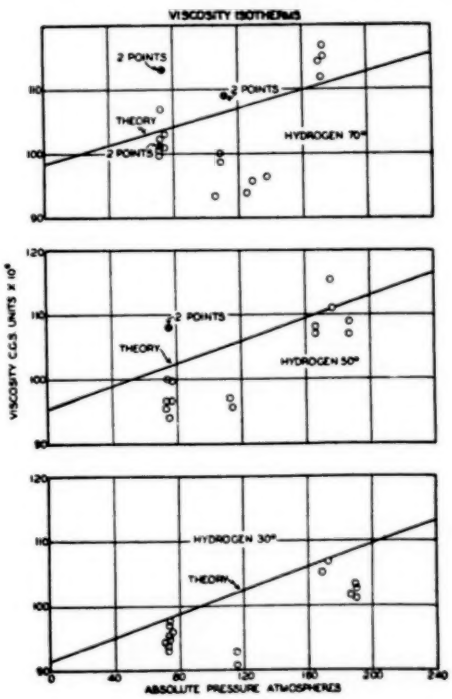

Fig. 5.

Eq. (4) simplified the calculations and was valid because at high pressures the gas density was substantially constant throughout the apparatus. This constancy of the density required that the linear velocity of flow in the capillary also be constant, and thus the acceleration effect previously mentioned was eliminated in the high pressure experiments. Experiments with nitrogen were made proving that the constant is independent of the temperature and pressure ranges covered here. Further experiments with hydrogen checked the value so determined and showed it to be independent of the gas employed. The magnitude of k_c exceeds that predicted from theory but this is believed due to a divergence between the actual experimental conditions and those postulated in the theoretical derivations. In any case this does not invalidate the results reported here.

In the high pressure experiments the system was brought under pressure by permitting the gas to flow through the capillaries to the *downstream* side of the differential manometer, under the mercury seal and into the upstream side. When the pressure was equalized throughout the system the by-pass valve and then the upstream valve were opened. The zero reading was then made after which the screw rod was run up the riser well to a point above the approximate mercury level expected in the experiment. Gas flow at the desired rate was obtained with the downstream control valve. The by-pass valve was then closed and twenty minutes allowed to insure a steady flow

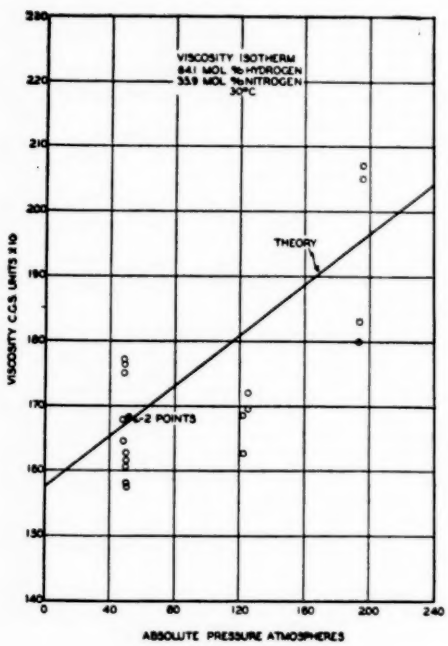

Fig. 6.

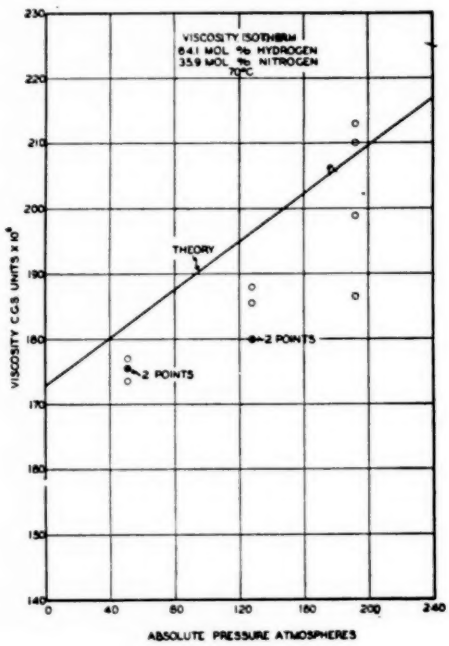

Fig. 7.

before manometer readings were taken. In each case the mercury approached its equilibrium position from below thus tending to introduce a compensation of errors. The gas was then passed into the balloon during an observed time interval after which manometer readings were again made and the average of the initial and final readings was taken for computation. The pressure was next measured by means of the dead weight piston gauge. The bath temperatures were noted during each experiment. The volume of the gas in the balloon was then determined at atmospheric pressure and room temperature. These data permitted the calculation of the viscosity coefficients.

III. Experimental Results

Viscosity coefficients for nitrogen and hydrogen were obtained at 30°, 50° and 70°C for pressures from 75 to 180 atmospheres. Similar data were obtained for a mixture containing 64.1 mol percent of hydrogen and 35.9

TABLE I. *Viscosity data, nitrogen.*

30°C		50°C		70°C	
Absolute Pressure Atm.	Viscosity c.g.s. units $\times 10^6$	Absolute Pressure Atm.	Viscosity c.g.s. units $\times 10^6$	Absolute Pressure Atm.	Viscosity c.g.s. units $\times 10^6$
178.8	258	191.0	232	176.9	246
178.8	244	191.0	266	176.9	242
177.6	258	189.8	242	176.9	247
177.6	256	189.8	244	176.9	249
176.9	269	188.0	241	154.1	237
176.9	276	188.0	256	154.1	235
156.8	235	185.5	238	127.5	224
156.8	227	185.5	243	127.5	236
156.2	245	158.7	243	126.7	243
156.2	248	158.5	235	126.7	237
128.4	231	158.5	233	71.5	219
128.4	237	128.4	225	71.5	221
128.4	208	128.4	233	71.5	215
128.4	212	73.2	208	71.5	212
103.6	224	73.2	212	71.5	218
103.6	206	73.0	210	71.5	212
74.3	207	72.9	212	70.4	226
74.1	205	72.7	205	70.4	233
73.7	202	72.7	208		
73.5	200	72.4	208		
73.5	202	72.4	210		
73.5	204	72.1	212		
73.5	205	72.1	203		
73.5	205				
73.3	204				
73.0	208				
73.0	202				

TABLE II. *Viscosity data, hydrogen.*

30°C		50°C		70°C	
Absolute Pressure Atm.	Viscosity c.g.s. unit $\times 10^6$	Absolute Pressure Atm.	Viscosity c.g.s. units $\times 10^6$	Absolute Pressure Atm.	Viscosity c.g.s. units $\times 10^6$
191.7	102.5	186.8	107.0	173.4	115.0
191.7	101.2	186.8	109.0	172.8	116.8
189.8	103.4	176.1	111.0	172.1	112.7
188.0	101.6	175.5	115.6	171.7	115.8
172.8	106.2	165.7	107.7	138.5	98.4
169.1	105.2	164.8	107.8	128.7	96.7
116.3	92.8	113.8	95.7	125.6	94.8
115.9	90.8	113.2	96.8	112.5	109.0
104.0	98.7	76.9	99.7	112.1	109.0
103.3	102.0	76.7	96.7	108.7	100.0
74.7	95.8	75.7	108.0	107.6	98.8
74.2	97.7	75.7	108.0	105.8	93.5
74.0	95.6	75.0	94.2	74.7	103.0
73.6	94.8	75.0	100.0	74.6	101.0
73.6	97.6	73.5	96.6	73.7	113.7
73.6	94.6	73.4	95.5	73.5	113.7
73.5	93.0			72.7	101.3
73.3	94.7			72.7	101.4
				72.0	102.4
				71.7	107.0
				71.5	101.6
				71.2	99.5

TABLE III. *Viscosity data.*
64.1% Hydrogen—35.9% Nitrogen

30°C		70°C	
Absolute Pressure Atm.	Viscosity c.g.s. units $\times 10^6$	Absolute Pressure Atm.	Viscosity c.g.s. units $\times 10^6$
195.9	205	192.4	187
195.9	207	192.4	199
194.4	183	192.1	210
194.4	180	192.1	213
124.9	172	128.4	188
124.9	170	128.4	180
122.2	163	127.8	186
122.2	168	127.8	180
50.4	168	51.0	176
50.4	168	51.0	173
50.2	163	50.7	175
50.2	161	50.7	177
50.1	158		
50.1	158		
49.2	177		
49.2	160		
48.7	175		
48.7	176		
48.0	164		
48.0	168		

mol percent of nitrogen at 30° and 70°C for a somewhat greater pressure range.

The new viscosity data are presented in Tables I to III and are shown graphically in Figs. 2 to 7 inclusive.

IV. A NEW VISCOSITY THEORY

In the theory of the equation of state it has been customary to regard the hydrostatic pressure as the net effect of a kinetic (distending) pressure and of a cohesive pressure. The kinetic pressure of a gas is defined as the time rate of the transfer of momentum across an imaginary plane unit surface in the interior of the gas. The viscosity coefficient is, by definition, the time rate of the *net* transfer of momentum in a flowing gas across a similar unit plane when there is a unit velocity gradient normal to the plane surface and normal also to the direction of gas flow. Thus the viscosity and kinetic pressure are similar phenomena whose origin is in the molecular motion and therefore it is logical that the kinetic pressure and the viscosity may be treated by the same analytical method.

Of the quantitative equations of state that of Beattie and Bridgeman[20] has had marked success in reproducing the observed pressures of a number of gases for wide ranges of temperature and pressure. Application of this equation to the computation[21] of the specific heat and Joule-Thomson coefficients of compressed air has shown good agreement between theory and experiment. The derivation of the equation is based on the two main assump-

[20] Beattie and Bridgeman, Proc. Am. Acad. Sci. **63**, 229 (1928).
[21] Bridgeman, Phys. Rev. **34**, 527 (1929).

tions that the kinetic and cohesive pressures may be treated separately and that the law of intermolecular force be such that it diminish rapidly with distance.

Their evaluation of the kinetic pressure is of interest here. The kinetic pressure of a perfect gas is calculated on the basis of a rectilinear free path, but the existence of intermolecular forces, as in a real gas, alters the linearity of the free path and increases the molecular migration in the gas interior. H. B. Phillips[22] on general considerations has pointed out this is so regardless of the nature and law of such forces and, further, that this is independent of the size of the molecules. Beattie and Bridgeman employ a slight modification of H. B. Phillips' method of calculating the kinetic pressure of a real gas and obtain

$$P_a = \bar{\rho}RT(1 + r) = P_i(1 + r) \tag{6}$$

where P_a and P_i are the pressures of the actual and ideal gases respectively, $\bar{\rho}$ is the density, R the gas constant, T the absolute temperature, and r the fractional increase in the molecular migration relative to an ideal gas owing to the intermolecular forces. Further, r is a function of the density and covolume

$$r = B_0\bar{\rho}(1 - b\bar{\rho}) \tag{7}$$

where B_o is the covolume in liters per mol, b a characteristic constant of the gas and the density is in mols per liter. These authors also correct the kinetic pressure to allow for the change in the time of molecular encounter with temperature and the complete expression for the kinetic pressure now is

$$P_a = P_i(1 + r)(1 - \epsilon) \tag{8}$$

where ϵ is the encounter factor and equals $c\bar{\rho}/T^3$, c being another characteristic constant of the gas. Eq. (8) is of the form first derived by Lorentz in his calculation of the kinetic pressure.

In adapting this equation to viscosity theory the viscosity coefficients are substituted for the kinetic pressure terms. It is well known that for isothermal pressure changes at low densities the viscosity of a gas is independent of the density. Thus the viscosity of a real gas at low densities is substantially that of a perfect gas, μ_o. For high densities the viscosity coefficient of a real gas, μ, corresponds to P_a. In the equation of state the covolume, B_o, is obtained from compressibility data. Among others, Jeans[23] and Keyes[24] have remarked that the compressibility covolume differs from that obtained from viscosity data. Therefore it is consistent and desirable in a viscosity theory to use the viscosity covolume, B_o' and further the relative density effect on the viscosity covolume should be the same as for the compressibility covolume and in addition the time of encounter factor

[22] H. B. Phillips, reference 5.

[23] Jeans, The Dynamical Theory of Gases, pp. 282, 326, 4 Ed., University Press, Cambridge, 1925.

should be identical for both the kinetic pressure and viscosity. The viscosity equation is then

$$\mu = \mu_0(1 + r)(1 - \epsilon). \tag{9}$$

The constants b and c are the same as before and are derived from compressibility data. The term B_0' is evaluated from the relation given by Keyes[25] which on reducing to units employed here is

$$B_0' = \left(\frac{3.159 \times 10^{-7}(M_w^{1/2})}{D}\right)^{3/2} \tag{10}$$

where M_w is the molecular weight and D is a constant in Sutherland's equation

$$\mu_0 = \frac{DT^{1/2}}{1 + C/T}. \tag{11}$$

The relation cited for the calculation of the viscosity covolume requires that the covolume be independent of the temperature which is true for gases obeying Sutherland's Law.

So far the theory has been implicitly limited to pure gases but as Beattie and Bridgeman's equation of state has been found valid[26] for mixtures the viscosity theory is readily extended to this case also, provided that μ_0 for the mixture be known. The constants B_0', b and c for the mixture are calculated from those for the components by the rule of linear combination, where

$$\begin{aligned} B_0'_{mix} &= \Sigma(B_{01}' X_1) \\ b_{mix} &= \Sigma(b_1 X_1) \\ c_{mix} &= \Sigma(c_1 X_1), \end{aligned} \tag{12}$$

and X_1 is the mol fraction of component (1) in the mixture. The viscosity theory is now complete.

The theory derived here is based on the analogous treatment of the kinetic pressure and viscosity of a real gas and uses a viscosity covolume instead of a compressibility covolume which, it is assumed, density changes affect in exactly the same way. The viscosity covolume, $\underline{Bo}'$, is calculated from the constants in Sutherland's equation and so it is assumed to be independent of the temperature. The time of encounter factor should be the same in the two cases. By a suitable combination of the constants of the components the theory is applicable to mixtures.

V. Discussion of Results

Examination of the tabulated results shows that the data prove beyond question that, at high densities, the viscosity of a gas is not independent of

[24] Keyes, Z. Phys. Chem. Cohen Fest Band, 709 (1927).
[25] Keyes, Chem. Rev. **6**, 210 (1929).
[26] Beattie, J. Am. Chem. Soc. **51**, 19 (1929).

the density. The maximum relative increase in the viscosity observed for nitrogen is 25 percent, for hydrogen is 10 percent and for the mixture is 20 percent. The increase in viscosity is not as great as might have been expected on the basis of previous work which however is believed to be of gravely questionable validity in view of the neglect of end effects.

The absolute accuracy of the calculated coefficients is not all that could be desired. Errors in the computed values of the viscosity and in the constants, k_c and k_ϵ, are due to errors of observation and the presence of impurities in the gases used. This latter factor is significant in the case of hydrogen as its viscosity at low pressures and its density are both extremely sensitive to traces of impurities. This source of error is not significant for nitrogen and the mixture. The method of calculation is of itself not conducive to accuracy since it involves the taking of differences and so the error in the calculated viscosities is generally greater than that of the observations.

TABLE IV. *Comparison of theory with experiment for nitrogen.*
B_0 compressibility = 0.05046 Beattie and Bridgeman
B_0' viscosity = 0.0421*

Pressure Atm.	No. of Experimental Points	Observed Mean	Viscosity Coefficients c.g.s. units $\times 10^6$ Viscosity Covolume	Compr. Covolume
		30°C		
1	—	181*	—	—
73	11	204	204	212
103.6	2	215	214	220
128.4	4	222	222	237
156.8	4	240	229	248
176.9	6	260	235	257
		50°C		
1	—	189.5*	—	—
73	10	209	212	220
128.4	2	229	228	244
158.5	3	237	236	256
188	8	246	244	267
		70°C		
1	—	198*	—	—
71.5	8	219.5	219	224
126.7	4	235	236	242
154.1	2	236	243	252
176.9	4	246	249	259

* Calculated from Sutherland's constants derived by least squares by Dr. F. G. Keyes after a critical survey of the literature and transmitted to the author in a private communication. The values of these constants were

	C	$D \times 10^6$
Nitrogen	101.3	1.386
Hydrogen	35.8	0.588

The new data afford a test of the theory derived above which is graphically shown in Figs. 2 to 7. The time of encounter factor was neglected in all calculations as for the least favorable case, lowest temperature and highest density, the correction is less than one percent for nitrogen and is much less for hydrogen. Numerical comparison of the mean observed and calculated viscosity coefficients for nitrogen are given in Table IV. Both viscosity and compressibility covolumes were used in computing the viscosities.

In general there is excellent agreement between experiment and theory when the viscosity covolume is used, but with the compressibility covolume there is a progressively greater difference between the observed and calculated values. The evidence is decidedly in favor of the new theory using the viscosity covolume and the three discrepancies between theory and fact are all attributed to experimental error. In the 30° isotherm two thirds of the maximum pressure is attained without introducing a trend in the comparison and the disagreement is attributed to experimental error. The discrepancy in the 70° isotherm occurs at a point where but two experimental values were available so the disagreement here is not regarded as serious.

A numerical comparison for the hydrogen data is not given as the graphical comparison shows reasonably good agreement in view of the sensitivity of the hydrogen density and low pressure viscosity to traces of impurities. The hydrogen data are of a confirmatory nature.

The mixture data are of especial interest in that they are believed to be the first data of this nature and they afford the opportunity of a direct comparison of the linear and Lorentz[27] rules for the calculation of the covolume of a mixture from those of the components. This comparison is particularly significant in view of the appreciable difference in magnitude of the covolumes of the components. The Lorentz rule of combination for a binary mixture is

$$B'_{0\ mix} = B'_{01}X^2 + B'_{012}(1 - X_1)X_1 + B'_{02}(1 - X_1)^2 \tag{13}$$

where X_1 is the mol fraction of component one and

$$B'_{012} = \left[\tfrac{1}{2}(B'_{01})^{1/3} + \tfrac{1}{2}(B'_{02})^{1/3}\right]^3 \tag{14}$$

The calculated and observed values are given in Table V. A slight but not significant trend in favor of the Lorentz rule is shown. The highly desirable

TABLE V. *Comparison of the Lorentz and linear rules for mixtures.*
64.1% Hydrogen—35.9% Nitrogen
30°C

Pressure Atm.	No. of Exper. Points	Viscosity Coefficients c.g.s. units $\times 10^6$ Mean Obs.	Calc. Lorentz	Calc. Linear
1	—	158*	—	—
49.4	8	166.4	167.0	167.3
123.5	4	168.1	181.5	182.0
195.	4	193.1	195.5	196.0
		70°C		
1	—	173*	—	—
51	4	175.3	181.8	182.0
128	4	183.5	196.7	197.3
192	4	202	207.9	208.5

* By interpolation from data of Kleint, Landolt-Bornstein-Roth Tabellen, 5 Ed., Berlin 1923.

[27] Lorentz, Wied. Ann. **12**, 127, 660 (1881).

simplicity of the linear rule leads to its recommendation here. A plot of the theoretical (using the linear rule) and observed values gives good agreement as shown in Fig. 7.

Further confirmation of the theory is obtained by a recalculation of Wildhagen's[28] data which purport to show a variation of Reynolds' criterion with the pressure. This quantity is defined by the equation

$$M/r\mu = \text{constant} \tag{15}$$

and the variation claimed above is in contradiction with a vast amount of experimental evidence which has shown that the value of the criterion is independent of the fluid employed.

Viscosities were computed with the new viscosity theory and values of Reynolds' criterion recalculated for Wildhagen's data. The results are given in Table VI and yield a constant for Reynold's criterion which is strong evidence in support of the new viscosity theory. The chief source of error in

TABLE VI. *Recalculations of Wildhagen's values for Reynold's criterion for compressed air.*

Pressure Atm.	40	80	120	160	200
		Values of viscosity coefficients $\times 10^6$			
Wildhagen (Mean of *A* and *B*)	195	224	235	268	321
Calculated from Viscosity Theory	192	205	218	230	242
		Reynold's criterion			
Wildhagen (Mean of *A* and *B*)	2000	1835	1910	1763	1526
Calculated from Viscosity Theory	2030	2010	2060	2050	2025

Wildhagen's results lies in the neglect of end effects and may attain the order of thirty percent at high densities. The magnitude of the end effects in the cases of Warburg and von Babo[29] and of P. Phillips[30] is not easy to estimate but is believed to be of the order of at least ten per cent on the basis of previous considerations.

The author wishes to acknowledge his appreciation of the financial aid given him by the Research Laboratory of Applied Chemistry and the committee on Graduate Courses and Scholarships of the Massachusetts Institute of Technology. He is particularly grateful to Dr. T. E. Warren for his assistance and to Dr. J. A. Beattie for his many helpful suggestions. Further, the author wishes to thank Drs. W. K. Lewis, F. G. Keyes and P. K. Frolich for their advice and criticism.

[28] Wildhagen, reference 9.
[29] Warburg and von Babo, reference 7.
[30] P. Phillips, reference 8

LETTERS TO THE EDITOR

Prompt publication of brief reports of important discoveries in physics may be secured by addressing them to this department. Closing dates for this department are, for the first issue of the month, the twenty-eighth of the preceding month; for the second issue, the thirteenth of the month. The Board of Editors does not hold itself responsible for the opinions expressed by the correspondents.

A New System of Bands in Carbon Monoxide

A new system of CO bands have been obtained when a trace of CO was excited in a long atomic hydrogen tube. Under the best conditions of the experiment, the spectrum of CO showed features that are usually obtained when a trace of CO is excited in the presence of the inert gases.

Under low dispersion, the new bands resemble the third positive group and its two associated groups, $5B$ and $3A$. Each band apparently contains six heads and in addition shows the complex structure that is typical of the above mentioned multiple-headed bands of CO. Because of this striking resemblance it was suspected that the final level of these new bands coincides with the final level of the third positive group and its two associated groups. Only three of the new bands have been found and the separations of similar heads show that they correspond to transitions from an initial level (that may be called "e") to the $v=1$, 2, and 3 levels associated with the "a" level. A rough measurement of these heads has been made and they have been found to have wavelengths 2518A, 2630A and 2750A, yielding a value of ν_e for the initial level of 88954 cm^{-1}. This value depends of course on the assumption that the upper level is the zero vibrational state.

The failure of these bands to appear under ordinary conditions shows that the initial level must be either a metastable quintet state or a triplet or singlet state. It has not been possible to excite the Cameron bands in the present conditions and this, together with the fact that the Cameron bands have been obtained only very weakly under the best conditions that have been found, shows that intercombinations are very improbable. Until further evidence is available it seems that the most probable identity of the new "e" level is as a metastable quintet state.

JOSEPH KAPLAN

University of California,
Los Angeles, California,
April 25, 1930.

Boundary Conditions in Wave Mechanics

In the April 15 issue of this Journal[1] H. A. Wilson attempts to construct a Schrödinger equation whose solutions shall be known and represent the case of an electron approaching a potential barrier. He neglects to state the interpretation of his procedure explicitly; there are two possible, the second of which is probably the one intended, and I discuss the first only as a basis for the second.

The first interpretation depends on the assumption that any function $F(x,E)$ (x=coordinate, E=total energy of the electron) is the solution of some problem in wave mechanics. The assumption is obviously false, but a proof of its falsity will clarify the discussion of the second interpretation. It is true that a differential equation,

$$\phi''+k^2(E-V)\phi=0 \qquad (1)$$

can always be found such that $\phi=F(x, E)$ is a solution for any value of E. While this is superficially identical with the Schrödinger equation, it usually differs from the latter in the fundamental fact that V, the potential energy, depends on E, the total energy of the electron. The fact that V is independent of E is one of the fundamental postulates of the Schrödinger theory, hence

[1] Wilson, Phys. Rev. **35**, 948 (1930).

only those functions $F(x, E)$ which yield a V independent of E can be considered as solutions of a wave-equation.

The alternative interpretation suppose that V in Eq. (1) is really independent of E, but dependent on another parameter (call it W) which happens to be numerically equal to E; but then $F(x, E)$ is not in general a solution of (1), but only if $E=W$. The original goal (the construction of a wave-equation, all of whose solutions shall be known) has thus been missed. To put it in another way, $F(x, E_1)$ and $F(x, E_2)$ are solutions of two different wave-equations, corresponding to two physical systems which differ in both their potential and total energies. In order to obtain a complete set of solutions for any one physical problem (single value of the parameter W) it will be necessary to find a function $\phi(x, E, W)$.

This function may satisfy the condition $\phi(x, E, E)=F(x, E)$, but there are other solutions which do not, since electrons may move in either of two directions along the x-axis. The conclusion is that Wilson has not found a complete set of characteristic functions for a given system, but rather one particular function for each of a large number of systems. This seriously restricts the generality of his results.

Turning to these, the only one I shall discuss is the conclusion that electrons are not reflected by a potential barrier if their total energy is greater than the maximum value of the potential energy. From the foregoing remarks it follows that this is true for only one particular value of E, and it becomes of interest to find the physical reason for the distinction enjoyed by this particular value of E. This becomes apparent on an examination of Figs. (2) and (3) reference 1, which represent the potential energy, i.e., qualitatively the index of refraction of the de Broglie waves. It is seen that the optical problem analogous to this dynamical one is that of an etalon consisting of one very thin plate placed at a distance of $\frac{1}{4}$ wave-length in front of a much thicker plate. Elementary optical considerations show that such an etalon will not reflect any light but will transmit all of it. If the wave-length of the incident light be changed (variation of E) keeping the separation between the plates constant (fixed W) this situation will change, and for some other wave-length, the reflection will be complete, the transmission zero.

CARL ECKART

University of Chicago,
April 29, 1930.

Photographic Record of First Order Diffraction of Hydrogen Atoms by a Lithium Fluoride Crystal

I have recently obtained a photographic record of the diffraction pattern resulting from the reflection of a beam of monatomic hydrogen atoms from a crystal of lithium fluoride.

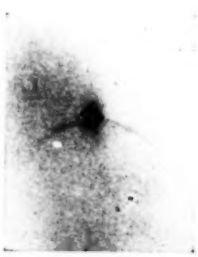

The atom beam, which was of nearly circular cross section, was incident upon the crystal at an angle of 30° from grazing and the plane of incidence made an angle of 45° with the cleaved edges. In this position rows of similar ions run parallel and perpendicular to the plane of incidence with a spacing between two consecutive rows of 2.835A. The reflected atoms were recorded on a plane surface coated with MoO_3 which was placed perpendicular to the plane of incidence and parallel to the incident beam.

The atoms of the beam were moving with the velocities of thermal agitation in equilibrium at a temperature of about 200°C. Their deBroglie wave-length $\lambda=h/mv$ had a distribution corresponding to the Maxwellian velocity distribution with the most probable wave-length equal to 0.89A.

A diffraction pattern appeared on the plate reproduced in the figure which satisfies the cross grating formulae

$$\cos\theta_0-\cos\theta=n\lambda/d$$

$$\cos\phi_0-\cos\phi=m\lambda/d$$

where θ and ϕ are, respectively, the angles between any beam and the parallel and perpendicular rows of ions on the surface of the

crystal. The subscript 0 refers to the incident beam. The beams corresponding to $n=0$, $m=\pm 1$ were the most intense and are reproduced quite clearly. They appear in the figure as the parabolic intersection of the detecting plate with the cone $\theta=\theta_0$. The positions of calculated maxima of intensity corresponding to $\lambda=0.89$A are opposite the white-dots and agree well with the observed maxima.

The beams corresponding to $m=0$, $n=\pm 1$ were possibly visible on the original plate but were too faint to reproduce. The maximum corresponding to $n=+1$ is calculated to be at the upper dot but that corresponding to $n=-1$ lies below the plane of the crystal.

THOMAS H. JOHNSON

Bartol Research Foundation,
April 23, 1930.

BOOK REVIEWS

Photo-Processes in Gaseous and Liquid Systems, R. O. GRIFFITH AND A. MCKEOWN. Pp. 690. figs. 52. Longmans, Green and Co., London and N. Y., 1929. Price $8.50.

The authors have brought together in one volume two subjects which have usually been dealt with separately: spectroscopy and photochemistry. Their purpose in presenting the former as an introduction to experimental photochemistry will be generally recognized and approved. The importance of such a ground-work is evident in that the entire first half of the book is concerned with the nature of radiation, series and band spectra, the application of the quantum theory to atomic structure, excitation, spectral absorption of atoms, life of the excited state, molecular spectra, fluorescence and chemiluminescence. This material has been treated not only with all the clarity which is essential in presenting the fundamental principles to chemists, but with a directness and simplicity that may recommend itself to any one interested primarily in this field.

The second half of the book deals with photochemical processes and presents a very careful review of the most important literature. The authors have been generous in their treatment of the views and hypotheses which have been put forward in support of various reaction mechanisms. One chapter is devoted to photochemical reactions in general, two to Einstein's law and photochemical reaction mechanisms, one to the hydrogen-chlorine and carbon monoxide-chlorine reactions, one to photo-sensitization and one to photochemical catalysis and inhibition, temperature coefficient and after effects. An appendix of four and a half pages is devoted to chemical effects of X-rays, alpha-particles and electrons, which affords a brief summary of the field and serves to show that the three quite different agents of chemical activation have common ground in ionization at one stage of the process.

S. C. LIND

Jetziger Stand der grundlegenden Kenntnisse der Thermoelektrizität. C. B. BENEDICKS. Special reprint of 42 pages from volume VIII of Ergebnisse der exakten Naturwissenschaften, Julius Springer, Berlin, 1929.

It is so unusual that the Physical Review should be asked to write a review of one of the single articles in the series of the "Ergebnisse" that one looks for some special feature in the situation in explanation, and indeed on reading the article one feels that only special considerations could account for its publication in the series at all. It is well known that in 1916 Benedicks discovered certain thermoelectric phenomena which he claimed rounded out the classical scheme of thermoelectric effects embraced in the Seebeck, Peltier, and Thomson effects, and also that this claim has been received with considerable sceptism, and that the concensus of opinion has been unfavorable. Benedicks has always defended his ideas. In the last few years several papers by other authors have appeared not unfavorable to Benedicks views, and this has apparently impressed the editors of the Ergebnisse as lending sufficient interest to the whole subject to justify an invitation to Benedicks to expound from the beginning his whole argument, which he does. It seems to me unfortunate that this new exposition by Benedicks embraces very little new material, and in fact does not discuss at all recent developments which entirely alter the significance of his whole point of view. For example, the relation between Benedicks' "phoretic" theory of conduction in metals and his thermoelectric ideas is expounded. If the ideas of the phoretic theory are to be taken seriously today, one has a right to expect some discussion of the connection between them and the wave mechanics picture of conduction, but wave mechanics is not mentioned.

Perhaps the briefest characterization of Benedicks' position is that he does not accept as correct the law of Magnus, which states that the thermal e.m.f. of a couple depends only on the temperatures of the two junctions, and not on the details of the temperature distribution in the two homogeneous branches. Benedicks fails to recognize that as a general statement applied to solid metals this "law" of Magnus is reduced to a purely academic position in view

of our new knowledge of thermoelectric phenomena in single crystals (as I stated in a paper in 1926), because it is now recognized that there may be thermoelectric currents in a single crystal of a non-cubic metal in which there are temperature differences. It follows that in any ordinary bar or wire of a non-cubic metal in which the size of the individual grains is appreciable, the law of Magnus would not be expected to hold. If I understand Benedicks' position correctly, he would say that this is not the sort of thing he understands by his effect, but he would expect the e.m.f. in an infinitely thin single crystal rod to depend on the manner of temperature distribution along the rod. It follows, therefore, that Benedicks' experiments should now be performed with material so chosen as to rule out this newly recognized possibility, but Benedicks' gives no consideration at all to this sort of thing. It is perhaps significant that he found by far his largest effects in graphite, which is non-cubic.

Benedicks' other experimental evidence leaves me personally unconvinced. I still am confident that an experiment which I made some time ago with liquid mercury to show the non-existence of his effect in mercury constitutes a valid objection, and I have since then tried without success to duplicate his experiment on the temperature difference between two ends of a long wire of constantan carrying a current. (This experiment has not been published.) Finally there is the fact that it has not been possible to find numerical magnitudes for any properties of metals connected with the new effect, neither has it been possible to introduce the constants of the new effect into any thermodynamic discussion or to show their quantitative connection with other phenomena.

The reader cannot but be pleased with the undogmatic attitude of Benedicks in describing his measurements and his ideas. Should any one else be predisposed to examine this subject by independent experiment, he should be fully conscious of the enormous difficulty of eliminating or correcting for all extraneous effects, such as those arising from stresses inevitably associated with temperature gradients in solids, and getting a clean cut proof of the existence of the effect.

P. W. BRIDGMAN

La Théorie de la Relativité et la Mecanique Céleste, Tome II, JEAN CHAZY. 258 pp. Gauthier-Villars et Cie, Paris, 1930. Price fr 60.

This is the second volume of the work of this author on the theory of relativity and celestial mechanics.

In the first volume the author has assumed the Schwarzschild line element as the starting point for investigating the problems of celestial mechanics, and has given from this basis a discussion of the motions of the planets and the curvature of light in passing the sun. The volume includes a detailed chapter on the calculations of Le Verrier and Newcomb on the motions of the planets.

In the present volume, the author presents an exposition of the fundamental principles of general relativity, and proceeding from this basis obtains the results of particular interest for celestial mechanics. These include a derivation of the Schwarzschild line element and the line element inside a fluid sphere, approximate methods for the solution of gravitational problems, a treatment of the effect of the rotation of the attracting mass on the motion of a particle, a discussion of the problem of n bodies with application to the motion of the planets, a treatment of the motion of the moon, and a discussion of the cosmological line elements of Einstein and de Sitter.

RICHARD C. TOLMAN